A Novel Approach in Formulation of an Extended Release Gastroretentive Delivery System of Metformin Hydrochloride

By

MRS. ROSY PRIYADARSHINI
M. Pharm

THESIS SUBMITTED FOR THE AWARD OF
DOCTOR OF PHILOSOPHY (PHARMACY)

DEPARTMENT OF PHARMACEUTICAL TECHNOLOGY
FACULTY COUNCIL OF ENGINEERING & TECHNOLOGY
JADAVPUR UNIVERSITY
KOLKATA, INDIA

2019

JADAVPUR UNIVERSITY
KOLKATA-700032, INDIA

INDEX NO – 184/13/P

Title of the thesis: "A novel approach in formulation of an extended release gastroretentive delivery system of metformin hydrochloride"

Name, Designation and Institution of Supervisors:

(a) Prof. (Dr.) L. K. Ghosh
Professor
Department of Pharmaceutical Technology
Jadavpur University,
Jadavpur
Kolkata-700 032
(b) Dr. Gouranga Nandi
Assistant Professor
Department of Pharmaceutical Technology
University of North Bengal
Darjeeling-734013

List of Publications:

(i) **Rosy Priyadarshini**, Gouranga Nandi, Abhijit Changder, Sailee Chowdhury, Sudipta Chakraborty, Lakshmi Kanta Ghosh. (2016). Gastroretentive extended release of metformin from methacrylamide-*g*-gellan and tamarind seed gum composite matrix. *Carbohydrate Polymers*, *137*, 100 – 110. (Elsevier – Science Direct Journal; impact factor: **4.074**).

(ii) Gouranga Nandi, Poushali Patra., **Rosy Priyadarshini**., Santanu Kaity & Lakshmi Kanta Ghosh (2015). Synthesis, characterization and evaluation of methacrylamide grafted gellan as sustained release tablet matrix. *International Journal of Biological Macromolecules, 72*, 965-974. **(Impact factor: 3.096; 5 yr impact factor: 3.227)**

List of Patents: Nil

List of presentation in national/ international conference:

(i) Presented a poster in the National Seminar on "Current Perspective of Nano-Technology for Drug Delivery" on "Floating cum Mucoadhesive Gastro retentive Extended Release Tablet of Metformin Based on Methalcrylamide G-Gellan and Tamarind seed Gum Composite Matrix" (**PT-020**) organized by College of Pharmaceutical Sciences, Puri on 19th February 2016.

(ii) Presented a poster in the 3rd Pharm. Tech IAPST International Conference on "Molecular Mechnism of Diseases And Novel Therapeutic Approaches" on "In Vitro Drug Release Study of Metformin Hydrochloride from Extended Release Tablet Formulation Using Neem Gum as Binder" (**P-42**) organized by Centurion University, Bhubaneswar from 19th to 20th January 2019.

DEDICATED

TO

MY BELOVED PARENTS

AND

MY FAMILY

ACKNOWLEDGEMENTS

I take this opportunity to humbly acknowledge the contributions of my principal supervisor, Prof. (Dr.) L. K. Ghosh, an eminent pharmaceutical scientist, in completion of this piece of work. His constant encouragements, guidance and generous help were the driving forces. I express my heartfelt gratitude and thankfulness to him and hope to continuously get his attention, love and guidance throughout my life and career. Next, I would like to express my deep sense of gratitude to my joint supervisor Dr. Gouranga Nandi for his active help, unstinted support and appropriate guidance without which it would have been well-nigh impossible for me to complete this work. I feel extreme pleasure in expressing my deep sense of gratitude for his constructive and valuable suggestions, active co-operation and constant encouragement throughout this investigation.

I am thankful to All India Council for Technical Education, New Delhi for giving opportunity to carry out Ph D curriculum and necessary grant.I place on record, my thanks to Jadavpur University and Department of Pharmaceutical Technology authorities to allow me to use their material and instrumental facilities, specially UGC-DSA laboratory in the Department of Pharmaceutical Technology, Jadavpur University. I place on record my thankfulness to Department of Metallurgy, Jadavpur University, for giving their instrumental facilities.

I am also thankful to East India Pharmaceutical Works Pvt. Ltd., Kolkata, India for providing Metformin HCl required for this study. I would like to thank seniors and juniors of the Pharmaceutics Research Laboratory-II, Dept. of Pharm. Tech., Jadavpur University specially Moumita Das Kirtyania, Koushik Sengupta, Debjani Sarkar, Abhijit Changder, Poushali Patra, Prasenjit Hudati, Asoke Mukherjee, Mahanaam, Sanchita Das Bhowmik, Pabitra Mondal for their co-operation and help. I place my sincere pranam to the feet of my parents who sacrifice a lot for my upbringing.

I would like to express my gratitude towards Metallurgical Department, Jadavpur University for their kind co-operation to carry out the FTIR evaluation studies.

At last, but not the least, I express my sincere regards and thanks to all my family members for their constant encouragement, inspiration and support without which I would not have been able to complete my work successfully.

(Rosy Priyadarshini)

CERTIFICATE FROM THE SUPERVISORS

This is to certify that the thesis entitled **"A novel approach in formulation of an extended release gastroretentive delivery system of metformin hydrochloride"** submitted by **Mrs. Rosy Priyadarshini**, who got her name registered on …….. for the award of **Ph. D. (Pharmacy)** degree of Jadavpur University is absolutely based upon her own work under the supervision of **Prof. (Dr.) L. K. Ghosh,** Professor and Former Head, Department of Pharmaceutical Technology, Jadavpur University, and **Dr. Gouranga Nandi**, Associate Professor, BCDA College of Pharmacy and Technology, Kolkata-700127 and that neither her thesis nor any part of the thesis has been submitted for any degree/ diploma or any other academic award anywhere before.

1.…… 2. ……

Prof. (Dr.) L. K. Ghosh

Signature of Sole Supervisor

Dr. Gouranga Nandi

Signature of Joint Supervisor

Preface

Metformin HCl is an orally administered biguanide widely used in the management of type-2 diabetes. It is slowly and incompletely absorbed from the stomach and proximal small intestine. The absolute bioavailability is reported to be 50–60% with relatively short plasma elimination half-life of approximately 2 h. This has raised the interest in developing extended-release formulations of metformin. Due to its narrow absorption window, it would be beneficial to develop gastroretentive device through which the gastric residence could be prolonged to release the drug at the absorbing site in a controlled manner for the entire period of drug release from the extended release products to maximize the bioavailability as well as therapeutic benefit along with better patient compliance.

Use of various natural polysaccharides as rate modulator in extended release drug delivery devices is a current trend because of their biocompatibility, low cost, free availability and biodegradability. Gellan, an anionic deacylated exocellular polysaccharide produced by a pure culture of *Pseudomonas elodea* with a tetrasaccharide repeating unit of one α-L- rhamnose, one β-D-glucuronic acid and two β-D-glucose residues, has been used in several types of dosage forms such as stomach-specific controlled release beads, interpenetrating hydrogel microsphere, tablets. However, rapid solubility in water, substantial swelling and rapid erosion of gellan are some of the limitations to make it an ideal matrix material for extended release. One of the powerful methods to modify the various physical,

chemical and functional properties of polysaccharides is graft co-polymerization in which polymers are grafted onto polysaccharides backbone. Graft co-polymerization introduces hydrophobicity and steric bulkiness which considerably protect the matrix and carbohydrate backbone from rapid dissolution and erosion, and provides extended release of drugs. Therefore, firstly, methacrylamide has been grafted onto gellan backbone in order to synthesis gellan graft copolymer and the copolymer has been characterized. The copolymer obtained has been found to possess significant hydrophobicity and capacity to form a rigid erosion proof matrix. However, the matrix is less continuous due to poor gelation. On the other hand, native natural hydrophilic polysaccharides are capable of forming intensively continuous matrix due to high degree of swelling that ensures drug release in more sustained manner but advance erosion is the their main limiting factor. Incorporation of natural hydrophilic polysaccharide into hydrophobic matrix of graft-copolymer is another approach to improve desired functional properties like swelling, drug release kinetic and stability. This composite blending yields a continuous soft but rigid erosion proof hydrated matrix after absorbing water from gastrointestinal fluid, followed by extended drug release over a significantly long period of time.

Tamarind seed gum (TSG) is an excellent natural hydrophilic polysaccharide obtained from the endosperm of *Tamarindus indica* Linn (family Leguminosae) having branched structure consisting of a main chain of β-D (1→4) linked glucopyranosyl units, with a side chain consisting of a single xylopyranosyl unit attached to every second, third and fourth D-glucopyranosyl unit through an α-D

(1→6) linkage. One D-galacotopyranosyl units is attached to one of the xylopyranosyl unit through a β-D (1→2) linkage. It is widely used as a thickening, stabilizing, emulsifying, mucoadhesive and gelling agent in various pharmaceutical formulations due to possessing of high thermal and chemical stability, non-carcinogenicity, biocompatibility, mucoadhesivity, non-toxicity and high drug holding capacity. Numerous oral sustained release gastroretentive drug delivery systems viz., buoyant systems mucoadhesive systems, expandable or swellable systems, high density systems etc. have been reported. Recently, the combined floatation–mucoadhesion approaches for gastroretention have gained importance as these devices exhibit a better gastroretention by virtue of their buoyancy and bio-adhesion properties. Sodium bicarbonate (SBC) has been widely reported as buoyancy contributor in different buoyant systems. Further, TSG has been reported as excellent natural mucoadhesive. Therefore, incorporation of TSG in the matrix of polymethacrylamide-*g*-gellan would impart sustained release as well as mucoadhesion property which can be combined with buoyancy to achieve better gastroretention.

In this study, a novel buoyant-mucoadhesive extended release tablet formulation of metformin HCl based on a hydrophobic polymethacrylamide-g-gellan copolymer and hydrophilic TSG composite matrix has been developed, which is not reported earlier. In this study, SBC and TSG have been used as buoyancy contributor and release modulator-cum-mucoadhesive, respectively. A 2^3 full factorial design was adopted to evaluate the influence of independent factors

on the responses (dependent variables) using Design-Expert software (version 9.0.4.1, Stat-Ease Inc., Minneapolis, USA). Tablets were prepared employing wet granulation method and evaluated for *in vitro* drug release, buoyancy, ex-vivo mucoadhesion, hydration kinetic, viscoelastic property and surface morphology. Compatibility between drug and excipients was checked by DSC, FTIR and XRD analysis. The formulation was numerically optimized to obtain USP-reference release profile, minimum buoyancy lag time and maximum mucoadhesive strength.

In the chapter-I of this thesis, introduction to oral drug delivery systems has been discussed. In chapter-II controlled release drug delivery systems, in chapter-III, gastroretentive delivery systems, have been discussed. The chapter-IV includes a review of the previous works reported towards the gastroretentive approaches for extended release of metformin hydrochloride. The chapter-V and VI include drug profiles and excipients profiles respectively. Experimental works have been presented in chapter-VII including experimental design, preparation of floating-mucoadhesive tablets and their evaluations along with statistical analysis and optimization. Chapter-VIII contains the summary and conclusion of the present study.

CONTENTS

CHAPTER I

CHAPTER II

CHAPTER III

CHAPTER-IV

CHAPTER-V

CHAPTER-VI

CHAPTER-VII

CHAPTER-VIII

CHAPTER-I

INTRODUCTION

1.1 INTRODUCTION

A drug delivery system is a therapeutic system which contains one or more drugs and releases the drug (s) to the proper site in the body to produce the maximum simultaneous safety, effectiveness and reliability [1]. The delivery devices are expected to be capable of presenting the drug in its active form at right site, at right time, at right rate and over a right period of time. There are different types of pharmaceutical dosage forms or delivery systems broadly subdivided into two groups:

1. Peroral drug delivery systems (tablets, capsules, solutions, suspensions, emulsions etc.)

2. Non-oral drug delivery systems (TDDS, aerosol, injections, implants, etc.)

Peroral drug delivery systems are the commonest mode of drug administration. Some advantages are there:

- ❖ It is safer.
- ❖ More convenient.
- ❖ Does not need assistance.
- ❖ Noninvasive, often painless.
- ❖ The medicament needs not to be sterile so it is cheaper.

1.2 LIMITATIONS OF ORAL ROUTE

1. Action is not so prompt compared to i.v. or i.m. routes.

2. Unpalatable drugs are difficult to administer. They need coating or encapsulation.

3. May cause nausea and vomiting.

4. Cannot be used for uncooperative, unconscious, vomiting patients.

5. Certain drugs are not absorbed from oral route (streptomycin).

6. Some drugs are destroyed in gastric juice (proteins or peptide drug).

7. Poor bioavailability of the drugs with first pass effect.

Inspite of these limitations, peroral delivery systems are the commonest, convenient and potential drug delivery system till the date. The peroral delivery systems are broadly subdivided into two categories:

- Conventional Peroral Dosage Forms
- Novel Peroral Dosage Forms

1.3 CONVENTIONAL PERORAL DOSAGE FORMS

Conventional peroral dosage forms such as tablets, capsules, suspensions, solutions, emulsions, etc. release their active ingredients into an absorption pool immediately in the g.i.tract. A conventional oral dosage form produces a bell-shaped drug-blood-level vs time profile that indicates that this type of dosage form cannot maintain drug blood level or drug concentration at site of action within the therapeutic range for extended period of time. The short duration of action is due to the inability of conventional dosage form to control temporal delivery of the drug. One attempt may be made to maintain drug conc. either in the blood or at the site of action in the therapeutic range for longer period of time by administering a high initial doseto attain a high initial plasma conc. This approach obviously is undesirable and unsuitable. An alternate approach is to administer the drug repetitively using a constant dosing interval, as in multiple dose therapy. In this case, the drug-blood-level reached and the time required to reach that level depend on the dose and dosing interval. There are several potential problems in multiple dosing [2]:

1. If the dosing interval is not appropriate for the biological half-life of the drug, large “peaks” and “valleys” in the drug blood level may result. For examples, drugs with short half-lives require frequent dosing to maintain constant therapeutic level.

2. The drug blood level may not be within the therapeutic range at sufficiently early time, an important consideration for certain disease states.

3. Patient non-compliance with the multiple dosing regimens can result in failure of this approach. To overcome these problems different novel oral controlled release dosage forms have been designed. In the next chapter these types of dosage forms have been outlined.

1.4 REFERENCES

1. Jens T. Carstensen, In "Modern Pharmaceutics" 3rd ed., rev. and expanded (Gilbert S. Banker, Chreistopher T. Rhodes eds), Marcel Dekker, New York (1996), p.16.

2. James Wells, In "Pharmaceutics The Science of Dosage form design", 2nd ed., (M.E. Aulton ed.) 2002, Churchill Livingstone.

CHAPTER-II

CONTROLLED RELEASE DRUG DELIVERY SYSTEMS

2.1 INTRODUCTION

The goal of any drug delivery system is to provide a therapeutic amount of drug to the proper site in the body to promptly achieve and then maintain the desired drug concentration. This idealized objective points to the two aspects most important to drug delivery, namely, spatial placement and temporal delivery of a drug. Spatial placement relates to targeting of a drug to a specific organ or tissue, while temporal delivery refers to controlling the rate of drug delivery to target tissue. An appropriately designed sustained release drug delivery system can be a major advance towards solving these two problems. The bulk of research has been directed at oral dosage forms that satisfy the temporal aspect of drug delivery, but many of the newer approaches under investigation may allow for spatial placement as well. Controlled drug delivery can be defined as delivery of the drug at a predetermined rate and/or to a location according to the needs of the body and disease states for a definite time period [1].

2.1.1 Terminology

Over the years, there have been several attempts to classify long acting oral dosage forms. This terminology problem is compounded because various indexing and abstracting services have also not adopted any uniform language when indexing such dosage forms. There are four major groups in these types of preparations [2].

2.1.1.1 Delayed release systems

These systems are either those that use repetitive, intermittent dosing of a drug from one or more immediate-release units incorporated into a single dosage form or an enteric delayed release system. Examples of delayed-release systems include repeat-

action-tablets and capsules, and enteric-coated tablets where timed release is achieved by a barrier coating.

2.1.1.2 Extended release systems

Extended release systems include any dosage form that maintains therapeutic blood or tissue level of the drug for a prolonged period. If the system can provide some actual therapeutic control, whether this is temporal or spatial or both, of drug release in the body, it is considered a controlled delivery system. This explains why extended release is not equivalent to controlled release.

2.1.1.3 Site specific release systems

Drug action can be localized by spatial placement of a controlled release system (usually rate-controlled) adjacent to or in the diseased tissue or organ [3].

2.1.1.4 Receptor targeting release systems

These delivery systems utilize carriers or chemical derivatives to delivery drugs to a particular ‘target’ receptor.

2.1.2 Requirements of a controlled drug delivery system

A controlled drug delivery system must fulfill one or several of the following requirements.

(a) Extend drug action at a predetermined rate by maintaining a relatively constant, effective drug level in the body with concomitant minimization of undesirable side effects that may be associated with a saw-tooth kinetic pattern of conventional release.

(b) Localize drug action by placing a controlled delivery system (usually rate-controlled) adjacent to or in a diseased tissue or organ.

(c) Target drug action by using carriers or chemical derivatives to deliver a drug to a particular target cell type.

(d) Provide a physiologically / therapeutically based drug release system. In other words, the amount and the rate of drug release are determined by the physiological/ therapeutic needs of the body.

2.1.3 Rationale for controlled release delivery systems

The basic logic for controlled release delivery systems is to alter the pharmacokinetic and pharmacodynamics of pharmacologically active chemical moieties by using novel drug delivery systems or by modifying the molecular structure or physiological parameters inherent in a selected route of administration.

It is desirable that the duration of drug action becomes more a design property of a rate-controlled dosage form and less or not at all a property of the drug molecule's inherent kinetic properties. Thus, optimal design of a controlled release system necessitates a thorough understanding of the pharmacokinetic and pharmacodynamics of the drug.

2.1.4 Objectives and potential advantages of controlled release systems [4]

- To reduce dosing frequency.
- To provide more constant therapeutic drug level.
- To obtain more uniform pharmacological response, or in other words, less potentiation or reduction in drug activity with chronic use.
- To reduce total amount of drug used.
- To reduce inconvenience to the patient and increase compliance.

- To avoid night time dosing.
- To reduce gastrointestinal irritation.
- To reduce both local and systemic side effects.
- To reduce fluctuations in circulating drug levels and minimization of drug accumulation in body tissues with chronic dosing.
- To allow the use of drug with low therapeutic index.

2.1.5 Possible disadvantages of controlled release systems

- Possibilities of dose dumping.
- Reduced potential for accurate dose adjustment.
- Increased potential for first pass metabolism.
- Possible reduction in systemic availability.
- Drug release profile restricted to residence time in gastrointestinal tract.
- Difficulty or impossibility of quick stoppage of pharmacological action of drugs, when serious poisoning or intolerance occurs.
- Little or no efficacy of dosage forms if the drug is not absorbed by intestinal mucosa [5].
- Greater cost than conventional dosage forms [5].

2.2 DRUG PROPERTIES INFLUENCING THE DESIGN OF CONTROLLED RELEASE DRUG DELIVERY SYSTEMS

To establish a basis for discussion of drug property influencing the controlled release product design, it is worthwhile focusing attention on the two principal elements of the system –

(a) Behavior of the drug in the drug delivery system.

(b) Behavior of the drug in the body.

The first of these two elements concerns itself with the way in which the drug properties can influence the release characteristics from the drug delivery systems. Under normal circumstance with a non-controlled release product, the rate limiting step in drug availability is usually absorption of drug across a biological membrane such as gastro intestinal wall. In a controlled release product on the other hand, one generally aims for release of drug from the dosage form as the rate limiting step so that the availability of drug is controlled by the kinetics of drug release rather than absorption.

The second element, behavior of the drug in body, is an extremely complex picture, involving the rate of the drug during its transit to the target area as well as its fate while in the biophase. The drug potentially interacts with a variety of substances leading to undesired drug loss as well as desired drug absorption. This undesired drug loss as well as desired drug absorption is a function of the structure and hence the property of the drug as well as the type of the delivery system in which it is housed.

2.2.1 Physicochemical properties of a drug influencing the drug product design and performance

These properties at times prohibit placement of the drug in a prolonged release form, restrict the route of the drug administration and significantly modify drug performance for one reason or another. The properties are as follows:

2.2.1.1 Dose size [6]:

Erikson has stated that drugs with a single oral dose larger than 0.5 gm are poor candidates for oral controlled release products since the absorption mechanism will, in most cases; generate a substantial volume of the product, depending on the density of the drug, duration of intended prolongation and type of sustaining mechanism. However a compromise between the dose size and the efficacy should always be sought.

2.2.1.2 Aqueous solubility:

Extremes in aqueous solubility are undesirable in the preparation of a controlled release product. The principal reason for this restriction centers on the dissolution rate of the drug. Aqueous solubility of a drug exercises its control on the absorption process in two ways.

- By its influence on the dissolution rate of a compound which establishes the drug concentration in solution and hence the driving force for the tissue permeation, and
- By its effect on the ability of the drug to penetrate tissue, which is determined in part by its proportional to its solubility, the aqueous solubility of the drug could be used as a first approximation to its dissolution rate. It has been reported that the drug with water solubility less than 0.1 mg/ml are appropriate to have reduced physiological availability in conventional oral dosage forms [7]. Drugs with greater water solubility are equally difficult to incorporate a sustained release system [8].

2.2.1.3 Partition coefficient [9]*:*

It has been shown that a parabolic relationship exists between partition coefficient and membrane permeation extremes. In partitioning behavior, one expects low rates of drug flux and at some intermediate partition coefficient, there should be a maximum

rate of permeation in general, drugs with extremely high partition coefficient will readily penetrate into body membranes producing an accumulation in body tissues with subsequent slow elimination.

2.2.1.4 Drug stability:

The extent of drug loss through hydrolysis or metabolism in the stomach and intestine is proportional to the residence time in these organs and the apparent rate of degradation. Since most oral sustained release systems are designed to release their contents over much of the length of the gastrointestinal tract, drugs which are unstable in the environment of the intestine would be unsuitable to be formulated into such delivery system [10]. Interestingly placement of a labile drug in a sustained release form often improves the bioavailability.

2.2.1.5 Protein binding:

Mane drugs bind to plasma proteins with a concomitant influence on the duration of drug action. This drug-protein complex serves as a depot for the drug producing a prolonged release.

Charged compounds would be expected to have a greater potential for binding than uncharged compounds. The presence of the drug molecules of a hydrophobic chain that is capable of stabilizing the drug-protein complex will make binding especially favorable.

2.2.1.6 pKa:

The pH partition hypothesis states that the uncharged form of a drug species will be preferentially absorbed through many body tissues. The release of ionizable drug from a sustained release product should be programmed in accordance with variation in pH of the different segments of the GI tract so that the amount of preferentially absorbed

uncharged species and the plasma level of the drug would be approximately constant throughout the time course of the drug.

2.2.1.7 Particle size:

The density of the core is very important in controlling the transit time in the GI tract. Increasing density is the most important factor promoting the retention of pellets in the microvilli. It has been reported that the coated heavy pellets containing barium sulphate of density 1.6 significantly increased the average transit time in ileostomy subjects compared to coated light pellets containing hard paraffin of density 1.0 [11, 12]. The average transit times were 7 and 2 hours for light and heavy pellets respectively. Subsequently it has been shown that the GI transit time for unmediated, non-disintegrating, hard paraffin tablets was far less reproducible than that of the small pellets [13].

2.2.1.8 Molecular size:

The ability of a drug to diffuse through membranes, its so-called diffusivity can be influenced by its molecular size as shown by the following equation.

$$\text{Log } D = - S_V \text{ Log } V + K_V = - S_M \text{ Log } M + K_M$$

Where D is diffusivity, M is molecular weight, V is molecular volume and S_V, S_M, K_V, and K_M are constants. Molecular size of a drug is an important that must be considered if a polymeric membrane is relied upon in the controlled release mechanism.

2.2.2 Biological factors

The design of controlled release product should be based on a comprehensive picture of the drug disposition. Each pharmacokinetic property and biological response parameter has a useful range for the design of controlled release products

and outside the range, sustained release product design becomes difficult or impossible.

2.2.2.1 Absorption:

Drugs that are slowly absorbed or absorbed with a variable absorption rate are candidates for a sustained release system. For oral dosage forms, the lower limit on the absorption rate constant is in the range of 0.25 $hour^{-1}$, assuming a GI transit time of 10 – 12 hours.

2.2.2.2 Distribution:

For design of controlled release products, one of the important pharmacokinetic parameters to be considered is the apparent volume of distribution. The apparent volume of distribution influences the concentration and amount of drug either circulating in the blood or in the target tissues. It can influence the elimination kinetics of the drug. Thus the drugs with high apparent volume of distribution are poor candidates for controlled release.

2.2.2.3 Metabolism:

Controlled release systems for the drugs that are extensively metabolized is possible as long as the rate of metabolism is neither too great nor the metabolism is variable with GI transit or other routes. Thus a controlled release product can be as long as the metabolism remains predictable and can be incorporated in the design of these products.

2.2.2.4 Biological half life:

The rate of elimination of a drug is quantitatively described by its biological half life, $t_{1/2}$. The half life of a drug is related to its apparent volume of distribution V and its systemic clearance.

$$t_{1/2} = 0.693\ V/Cl_s = 0.693V.\ AUC/\ dose$$

The systemic clearance, Cl_s is equal to the ratio of an intravenously administered dose to the total area under the drug blood level versus time curve AUC. A drug with a short half-life requires frequently dosing and this makes it is desirable candidate for a sustained release formulation. On the other hand, a drug with a long half-life is dosed at greater time intervals and thus there is less need for a sustained release system. It is difficult to define precise upper and lower limits for the value of the half-life of a drug that best suits it for sustained release formulation. In general, however, a drug with a half-life of less than 2 hours should probably not be used. Since such systems will require unacceptably large release rates and large doses. At the other extreme, a drug with a half-life of greater than 8 hours should also probably not be used. In most instances, formulation of such a drug into a sustained release system is generally unnecessary [14].

2.2.2.5 Side effects:

For some drugs, the incidence of side effects in addition to toxicity is believed to be related to their plasma concentration. A sustained release system can, at times, minimize side effects for a particular drug by controlling its plasma concentration and utilizing less total drug ever the time course of therapy. The technique of controlled release has been more widely used to lower the incidence of side effects and appears to be beneficial.

2.2.2.6 Margin of safety of the drug:

For every patent drug whose therapeutic concentration range is narrow, the value of Therapeutic Index (TI) is small. In general, the large value of TI, the safer the drug. Drugs with very small values of TI are usually poor candidates for formulation into

sustained release products primarily because of technological limitations of precise control over release rates.

2.3 TECHNIQUES OF OBTAINING CONTROLLED RELEASE SYSTEMS

There are three broad categories of obtaining controlled or sustained release systems.

2.3.1 The Biological Methods

These methods have limited applications and are only used by physicians. These approaches consist of administering two drugs in order to modify the biological fate of one of them. For example, oral penicillin is rapidly excreted by the kidney. This effect of penicillin is extended by the administration of probenacid, which interferes with the renal excretion of penicillin. Therefore, penicillin remains in the body providing prolonged action.

2.3.2 The Chemical Methods

The chemical methods of preparing sustained or controlled release drug delivery systems are based on the promise that a drug is first released at some target site within the body and then continues to be released slowly.

Two approaches have been used to achieve this goal:

2.3.2.1 The analogue approach:

This method is rarely identified as an approach to sustained or controlled release of drug delivery systems. Synthesis of analogues may alter the solubility, partitioning characteristics, distribution, metabolism, excretion, etc.

2.3.2.2 The prodrug approach:

This method involves the chemical modification of a compound in order to form a complex that regenerates the active molecule when exposed to body fluids. As an example, one can mention most of the actual sustained release steroids, generating the active molecule through the in vivo hydrolysis of the ester or the ether. The rate of hydrolysis determines the duration of action.

2.3.3 The Pharmaceutical Methods

These methods are based on proving a slow release of the active compound through the dosage form itself. These methods may involve the dissolution and /or diffusion of the drug through the delivery system matrix, the ion exchange, resins etc.

2.3.3.1 Classification of controlled release systems [15, 16]:

This classification is based on mechanism that controls release of incorporated drug.

2.3.3.1.1 Monolithic Devices (Matrix Systems):

In a monolithic device, the therapeutic agent is intimately mixed in a rate controlling polymer and release occurs by diffusion of the agent from the device. There are two types of devices. In one, the active agent is dissolved in the polymer, whereas in the other, the active agent is dispersed in the polymer.

Although the release of the active agent from the monolithic systems does not proceed by zero-order kinetics, it is the simplest and most convenient way to achieve prolonged release of an active agent. Such devices can be conveniently prepared by using simple polymer fabrication techniques involving a physical blending of the drug with a polymer matrix, followed by compression molding, injection molding, extrusion, calendaring, or solvent casting.

2.3.3.1.2 The Reservoir Devices (Membrane Devices):

In a reservoir device, the drug is contained in a core that is surrounded by a rate-controlling membrane. Transport of the material in the core through the surrounding nonporous, homogenous polymer film occurs by dissolution at one interface of the membrane and then diffusion down a gradient in the thermodynamic activity.

If the thermodynamic activity of the drug in the reservoir remains constant, if there is no change in the rate-limiting membrane characteristics and if infinite sink conditions are maintained at the downstream side of the membrane, rate of drug release will be constant and can be predictable from knowledge of membrane permeability and device configuration. Examples of these devices are –

- Membranes [17]
- Capsules [18]
- Microcapsules [19, 20]
- Liposomes [21]
- Hollow fibres [22]

2.3.3.1.3 Solvent Controlled Devices:

These devices release drugs as a consequence of controlled penetration of a solvent into device. Although nonaqueous solvent can be used, clearly only water is of importance in controlled release application for human applications. Based on two general mechanisms, osmosis and swelling, there are two types of devices.

2.3.3.1.3.1 Osmotically controlled devices:

In this device, an osmotic agent is contained within a rigid housing and is separated from an active agent compartment by a movable partition. One wall of the rigid housing is a semipermeable membrane so that when the pump is exposed to an aqueous environment, water will be driven osmotically across the membrane; the

increased volume within the osmotic compartment will force the active agent out of the device through the delivery orifice.

2.3.3.1.3.2 Swelling controlled devices:

The drug is homogeneously dispersed in a glassy polymer. Because glassy polymers are essentially impermeable, the drug is immobilized in the matrix and no diffusion through the solid polymer phase takes place when such a monolithic device is placed in an aqueous environment, water begins to penetrate the matrix and swelling takes place. As a consequence of the swelling process, chain relaxation takes place, and the incorporated drug begins to diffuse from the swollen layers.

2.3.3.1.4 Chemically Controlled Devices:

In a chemically controlled device, rate of drug release from the polymer is controlled by a chemical reaction that can be hydrolytic or enzymatic cleavage of a labile bond, ionization or protonation.

2.3.3.2 Oral controlled release drug delivery systems:

The oral route has been the preferred route for drug administration in general because it offers more flexibility in dosage form design is relatively safe. The major techniques used in formulating oral drug delivery systems are as follows:

2.3.3.2.1 Enteric Coating:

The coating is intended to protect either the stomach from unwanted effects of the drug or the drug from degradation in gastric environment.

2.3.3.2.2 Beads or Spheres:

The spansules contain beads or spheres of the drug that are coated with a material that differs in thickness form beads, determining the time at which the drug will be released.

2.3.3.2.3 Enteric Coated Beads in Capsules:

This system combines the two previous mentioned strategies. The rate of drug release depends partially on the emptying rate of the beads from the stomach.

2.3.3.2.4 Mixed Release Granules:

This method uses granules as by the preparation of compressed tablets. Two or more sets of granules are used. One set, which carries the immediate release component of the drug, is prepared in the usual manner. The second set contains drug that either coated with slowly digestible or poorly soluble materials or mixed with solution retarding additives.

2.3.3.2.5 Erosion Core with Initial dose:

In this method, the sustaining component is formulated as a non-disintegrating tablet that essentially maintains its geometric shape through the GI tract. The initial dose may be contained in a press or pan coated outer shell. Most of these systems are designed as a cylinder more than as a sphere. Erosion on a sphere does decrease total surface in significant way ($4\pi r^2$), while erosion on a cylinder with a large diameter to height ratio does not affect too much release rate.

2.3.3.2.6 Matrix Tablets:

A matrix tablet is a tablet in which the drug is embedded in a nondissolving material. Upon ingestion, the drug leaches out by diffusion, leaving behind the inner, porous matrix, which is excreted.

2.3.3.2.7 Ion Exchange:

The mechanism of ion exchange can be considered as a chemical reaction of the type –

$$RSO_3^- DH^+ \rightarrow RSO_3^- Na + DH$$

Sulfonic acid type cationic exchange resin

This type of resin slowly releases the drug by exchanging with ions as H^+ etc. The rate of the release is dependent on the concentration of ions present in the GI tract.

2.3.3.2.8 Complexation:

The preparation of complexes or salts of active drugs that are slightly soluble in the GI fluids gives sustained action. For example, therapeutically active amine drugs form insoluble complexes with tannic acid.

2.3.3.2.9 Microencapsulation:

In the microencapsulation technology, particles of drug powder or solutions are coated with a thin coating of polymer behaving as semipermeable membrane. There are several methods for preparation of microcapsules.

2.3.3.2.10 The Osmotic Pump:

This is the most recent method for sustained release. It consists of a core tablet and a semipermeable coating with a laser drilled hole, through which drug releases. The system operates on the principle of osmotic pressure. The GI fluids permeate the semipermeable membrane, dissolve the drug in the core and the osmotic pressure forces or pump the drug solution out of the delivery orifice.

2.4 NEWER APPROACHES IN OBTAINING CONTROLLED RELEASE DRUG DELIVERY SYSTEMS

Various potential developments and new approaches have recently been introduced to overcome the problems associated with oral drug administration.

1. Development of a viable drug delivery system, which is capable of administering a drug at a preprogrammed rate for the duration, required for an optimal efficacy.

2. For prolongation of the gastrointestinal residence time, the delivery system developed can reside at the vicinity of absorption site for sufficiently long time to deliver the entire dose.

3. For drugs subjecting to an extensive hepatic “first pass elimination”, preventive measures have been developed to minimize the extent of hepatic “first pass” metabolism.

2.4.1 Novel Peroral Drug Delivery Systems

There are a number of novel drug delivery systems, which could be utilized for the controlled delivery of drug in the alimentary canal. They can be outlined as follows:

a. Osmotic pressure controlled drug delivery systems.

b. Hydrodynamic pressure controlled drug delivery systems.

c. Membrane diffusion controlled drug delivery systems

(i) Microporous Membrane-coated tablets

(ii) Solubility Membrane-controlled solid dosage forms

(iii) Enteric Controlled Release Tablets

d. Multi-laminated sustained release tablets

e. pH-independent controlled release granules

f. Polymer coated drug-resin preparations

g. Thixotropic bilayer tablets

2.4.2 Prolongation of Gastrointestinal Transit Time

All of the controlled release drug delivery systems discussed so far will have only limited utilization in the oral controlled administration of drugs if the system

cannot remain in the vicinity of the absorption site for life-time of the drug delivery system. The alimentary canal transit time for an indigestible object can vary from 8 to 62 hours. However, 40% of human beings were found to excrete the object within 24 hours. Therefore, the majority of controlled release drug products designed for oral administration have a limited residence time in the vicinity of absorption sites 2 – 3 hours as pointed out by Hofmann *et al* [23]. So most of the long acting drug products require a dosing schedule of twice a day.

Several approaches have recently been developed to extend the gastrointestinal transit time by sustaining the residence time of the delivery systems in the stomach:

(i) Intragastric Floating drug delivery systems

(ii) Gastro-Inflatable drug delivery system

(iii) Intragastric osmotic-controlled drug delivery system

(iv) Intra-rumen controlled release drug delivery system

(v) Bioadhesive oral drug delivery system

2.4.3 Overcoming Hepatic First Pass Elimination

There are a few approaches, which have been undertaken to overcome this problem.

- Physical approaches
- Chemical approaches
- Buccal and sublingual drug administration
- Transmucosal sustained release troches
- Oral sustained release microcapsules
- Rectal drug administration

2.5 REFERENCES:

1. Remington's Pharmaceutical Science, 17 ed., (A. R. Gennaro *et al* Eds.), Mack Publishing Co., Pennsylvania, (1985), page 939.

2. Controlled Drug Delivery Fundamentals and Applications, 2nd ed., Edited by J. R. Robinson, V. H. L. Lee, Marcel Dekker, Inc.

3. Remington's Pharmaceutical Science, 17 ed., (A. R. Gennaro *et al* Eds.), Mack Publishing Co., Pennsylvania, (1985), page 940.

4. Welling PG, *Drug Dev. Ind. Pharm.*, **9**:1 185 (1983).

5. Salsa T, Veiga F and Pina ME, *Drug Dev. Ind. Pharm.*, **25(9)**: 929 – 938(1997).

6. Erikson, In "The Theory and Practice of Industrial Pharmacy", (L. Lachman, H. A. Lieberman and J. L. Kanig eds.), Lea & Febiger, Philadelphia, p. 408 – 437 (1970).

7. Fincher JH, *J. Pharm. Sci*., **57**: 1825 (1968).

8. Ballard BE, In "Sustained and Controlled Release Drug Delivery System", (J. R. Robinson ed.), Mercel Dekker, P 76-106 (1978).

9. Fujita J, Iwasa J and Hansch C, *J. Amer. Chem. Soc*., **85**: 5175 (1964).

10. Beerman B, Halstrom K and Rosen A, *Clin. Pharmacol. Ther*, **13**: 212 (1972).

11. Bechgaard H and Antonsin O, In "F. I. P. Abstracts", 37th International Congress of Pharmaceutical Science, The Hague, September p. 69 (1977).

12. Bechgaard B and Ladefoged K, J. *Pharm. Pharmacol*., **30**: 690 (1978).

13. Bechgaard H and Ladefoged K, *J. Pharm. Pharmacol*., **33**: 791 (1981).

14. Remington's Pharmaceutical Science, 17 ed., (A. R. Gennaro et al Eds.), Mack Publishing Co., Pennsylvania, (1985), page 1650.

15. Langer R, *Chem. Eng. Common*., **6**:1. (1980).

16. Langer R and Folkman J, *Nature*, **262**: 797 (1976).

17. Baker RW and Lonsdale HK, In "Controlled Release of Biologically Active Agents, In "Advances in Experimental Biology and Medicine", (A. C. Tanquary and R. E. Lacey eds.), Vol 47, Plenum Press, New York, P. 15 (1974).

18. Paul DR, In "Controlled Release of Polymeric Formulations", (D. R. Paul and F.W. Harris eds.), American Chemical Society, Washington, 1976, P.1.

19. Chang TMS, In "Artificial Cells", (C.C.Thomas ed.), Springfield, Illinois, (1972).

20. Microencapsulation Process and Application, (J.E.Vandegaer ed.), Plenum Press, New York, (1974).

21. Thies E, *Polymer Plast. Technol. Eng*., 5:1 (1975).

22. Goodson JM, Haffajee A and Soeransky SS, *J.Clin.Periodontology*, **6**:83 (1979).

23. Hinton JM, Lennard-Jones JE and Young AC, *Gut,* **10**:842 (1969).

CHAPTER-III

GASTRORETENTIVE DRUG DELIVERY SYSTEMS

3.1 INTRODUCTION

Effort to develop efficient gastroretentive drug delivery systems had been started from about 1990 following the discovery of *Helicobacter pylori* by Warren and Marshall, with the intention of delivering anti-*H.pylori* drugs locally in the stomach over a prolonged period of time to eradicate the bacteria more efficiently in the treatment of *H.pylori* mediated gastric ulcer [1]. Later this strategy has been tried to develop rate-controlled oral dosage form to achieve increased bioavailability and predictable and reproducible plasma drug conc. vs. time profile and other pharmacokinetic parameters from the delivery systems [2]. The rate and extent of drug absorption depend on the physicochemical characteristics of the drug molecule, the physiological environment of the absorption site and the residential time of the delivery device at the absorption site. Therefore uniform drug release following absorption of a particular drug can be obtained only when the drug can be made available at the absorption site from a particular environment throughout the whole period of drug release from the delivery system. But this faces difficulty due to highly variable nature of the gastric emptying rate and the existence of different pH region along the g.i. tract. This type of difficulties can be overcome by lodging the delivery device in the stomach for the entire period of drug release. But prior to design and develop gastroretentive delivery device it is necessary to consider the physiological aspects of stomach. In the following sections of this chapter we will focus the physiology of stomach and different approaches towards gastric retention with some special cases for eradication of *H.pylori*.

3.2 PHYSIOLOGIC CONSIDERATION

The intrinsic properties of the drug molecule and the target environment for delivery are the major determining factors in bioavailability of the drug. Factors such as pH,

enzymes, nature and volume of secretions, residence time, and effective absorbing surface area of the site of delivery play an important role in drug liberation and absorption. In stomach there are several types of cells that secrete up to 2–3 liters of gastric juice daily. For example, goblet cells secrete mucus, parietal cells secrete hydrochloric acid, and chief cells secrete pepsinogen. The contraction forces of the stomach churn the chyme and mix it thoroughly with the gastric juice. The average length of the stomach is about 0.2 meter, and the apparent absorbing surface area is about $0.1m^2$. A brief survey of relevant physiological features that pose challenge to the development of an effective gastroretentive delivery system is presented below [3].

3.2.1 Gastric pH

The gastric pH is not constant rather it is influenced by various factors like diet, disease, presence of gases, fatty acids, and other fermentation products [4]. In addition, the gastric pH exhibits intra-as well as inter-subject variation. This variation in pH may significantly influence the performance of orally administered drugs. Radiotelemetry, a noninvasive device, has successfully been used to measure the gastrointestinal pH in human. It has been reported that the mean value of gastric pH in fasted healthy subjects is 1.1±0.15 [5-7].On the contrary, the mean gastric pH in fed state in healthy males has been reported to be 3.6±0.4, and the pH returns to basal level in about 2 to 4 hours. However, in fasted state, basal gastric secretion in women is slightly lower than that of in men. Gastric pH may be influenced by age, pathological conditions and drugs. About 20% of the elderly people exhibit either diminished (hypochlorhydria) or no gastric acid secretion (achlorhydria) leading to basal pH value over 5.0.Pathological conditions such as pernicious anemia and AIDS may significantly reduce gastric acid secretion leading to elevated gastric pH In addition, drugs like H_2 receptor antagonists and proton pump inhibitors significantly reduce

gastric acid secretion. The pH in the proximal duodenum may rise as high as 4 pH units from the stomach. This increase in pH is caused by the bicarbonate secreted by the pancreas and the duodenal mucosa that neutralize the acidic chyme peristalsed from the stomach. The mean pH value in fasted duodenum has been reported to be 5.8±0.3 in healthy subjects while the fasted small intestine has been observed to have a mean pH of 6.0±0.14. Passing from jejunum through the mid small intestine and ileum, pH rises from about 6.6 to 7.5. Gastric pH is an important consideration in selecting a drug substance, excipients, and drug carrier(s) for designing intragastric delivery systems [3].

3.2.2 Gastrointestinal Motility and Transit Time [3]

Based on fasted and fed states of the stomach, two distinct patterns of gastrointestinal motility and secretions have been identified. In the fasting state, the stomach usually contains saliva, mucus, and cellular debris. The fasted state is associated with some cyclic contractile events commonly known as migrating myoelectric complex (MMC). Liquid components easily pass through the partially constricted sphincter. On the contrary, the large undigested materials are retained by an ‘‘antral-sieveing’’ process and are retropulsed into the main body of stomach and remain in the fed state. In the fed state, gastric contractions move the contents towards the antrum and the pyloric sphincter. Usually a series of interdigestive events take place in the stomach. However, feeding disrupts this cycle causing a period of irregular contractile pattern. The MMC, which governs the gastrointestinal motility pattern, has been described as an alternating cycles of activity and quiescence. Apparently there are four consecutive phases of activity in the MMC:

Phase I: It is a quiescent period lasting from 30 to 60 minutes with no contractions.

Phase II: It consists of intermittent contractions that gradually increase in intensity as the phase progresses, and it lasts about 20 to 40 minutes. Gastric discharge of fluid and very small particles begins later in this phase.

Phase III: This is a short period of intense distal and proximal gastric contractions (4–5 contractions per minute) lasting about 10 to 20 minutes; these contractions, also known as ‘‘house-keeper wave’’ sweep gastric contents down the small intestine.

Phase IV: This is a short transitory period of about 0 to 5 minutes, and the contractions dissipate between the last part of phase III and quiescence of phase I. A simplified schematic representation of the motility pattern, frequency of contraction forces during each phase, and average time period for each period is shown in **Figure 1.**

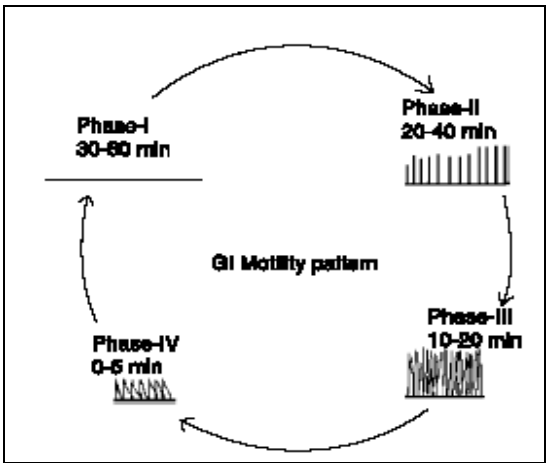

Figure 1: Schematic representation of interdigestive motility pattern (adapted from Ref [3])

The different phases originating in the foregut continue to the terminal ileum cycle in about 2 hours. Therefore, when one phase III reaches the terminal ileum, another begins in the stomach and duodenum. As mentioned before, feeding disrupts this cycle resulting in a period of irregular contractile activity, which may last for many hours (i.e., 3 to 4 hours). Thus frequent feeding may prolong gastric retention time.

3.3 FACTORS AFFECTING GASTRIC RETENTION [2, 8]

There are several factors that can affect gastric emptying (and hence GRT) of an oral dosage forms. These are discussed below:

1. **Density**- Density of the dosage form should be less than 1.0 gm/ ml for floating and high density systems should have density of about 2.5 gm/ml for efficient gastric retention.
2. **Size and Shape** – Dosage form units with a diameter of more than 7.5mm are reported to have an increased GRT compared with those with a diameter of 9.9mm. Tetrahedron and ring shaped devices with a flexural modulus of 48 and 22.5 kilo pound per sq.inch. are reported to have better GRT = 90-100% retention at 24 hours compared with other shapes.
3. **Single or multiple unit formulation**- Multiple unit dosage forms show a more predictable floating profile and permit larger margin of safety against dosage forms failure compared with single unit dosage forms.
4. **Fed and unfed state**- under fasting conditions, the g.i. motility is characterized by periods of strong motor activity or the migrating myoelectric complex (MMC) that occurs every 1.5 to 2.0 hours. The MMC sweeps undigested materials from the stomach and, if the timing of administration of the formulation coincides with that of the MMC, the GRT of the unit can be expected to be very short. However, in the fed state, MMC is delayed and GRT is considerably longer.
5. **Nature of meal**- Feeding of indigestible polymer of fatty acid salts can change the motility pattern of the stomach to fed state, thus decreasing the gastric emptying rate and prolonging gastric retention.
6. **Caloric content of food-** GRT can be increased by 4-10 hours with a meal that is high in proteins and fats.

7. **Frequency of feed**- The GRT can increase over 400 mins when successive meals are given compared with a single meal due to the low frequency of MMC.
8. **Gende**r- Mean ambulatory GRT in males is less compared with their age and race matched female counterparts, regardless of the weight, height and body surface.
9. **Age**- Elderly people, especially those over 70 years have a significantly longer GRT.
10. **Posture**- GRT varies between supine and upright ambulatory states of the patient.
11. **Concomitant intake of drugs**- The drugs such as anti-cholinergic (Atropine sulphate, Propanthelin), opiates (codeine) increase the GRT by decreasing peristalsis, whereas prokinetic drugs like cisapride, metoclopramide decrease GRT.
12. **Biological factors**- Diabetes or Chron's disease affect the GRT of the dosage forms.

3.4 DEVICES DEVELOPED AS PLATFORM FOR GASTRIC RETENTION [1]

A. High Density systems

B. Floating systems

   1. Hydrodynamically Balanced system- HBS™
   2. Gas generating systems
   3. Raft forming systems
   4. Low density core systems

C. Unfoldable , Extendible and Expandable systems

D. Super porous hydrogels

E. Mucoadhesive systems

F. Magnetic systems

3.4.A High Density Systems

High-density devices utilize weight as a retention mechanism. As the density of the device is larger than that of gastric juice, the device settles down to the bottom of the stomach, as shown in **Figure 2**. For veterinary applications, the high-density devices are made of heavy materials such as steel cylinders or steel balls. Such devices work well in ruminants, but obviously cannot be applied to humans. There are limits to the density of oral dosage forms for humans, as well as to the size of oral dosage forms based on a high-density mechanism.

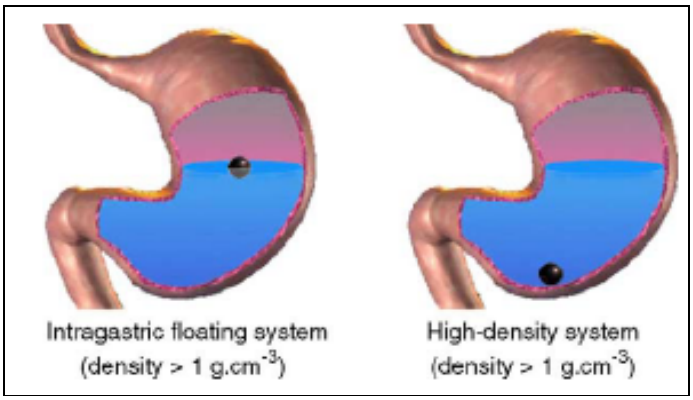

Figure 2: Schematic localization of an intra-gastric floating system and a high density system in stomach

3.4.B Floating Systems

The main concept here is to use devices in which density is lower than that of water so that the devices can float on top of the gastric fluid. This is expected to prolong the gastric residence time and thus increase the bioavailability of drugs that are mainly absorbed in the upper part of the GI tract. The devices may acquire low density after

administration to the stomach or possess low density from the beginning. There are various types of floating systems that are discussed below:

3.4.B.1. Hydrodynamically Balanced System (HBS™)

A hydrodynamically balanced system (HBS) was the first formulation that used the floating property of a device with density lower than that of water. HBS is simply a capsule containing a mixture of drug, gel-forming hydrophilic polymers (e.g.,hydroxy-propyl methyl cellulose), and such other excipients as hydrophobic fatty materials (e.g., stearates). Upon contact with gastric fluid after oral ingestion, the capsule shell dissolves and the drug-hydrocolloid mixture absorbs water swells to create a soft gelatinous outside surface barrier. Since the relative integrity of the overall shape is maintained, the density of the system at this stage becomes <1, mainly because of the presence of a dry mass in the center as well as the presence of stearates, which slow down the penetration of water to the inside. As the hydrated outer layer is eroded, a new gelatinous layer is formed. During this process, the drug in the hydrated layer is thought to be released by diffusion. (**Figure 3**)

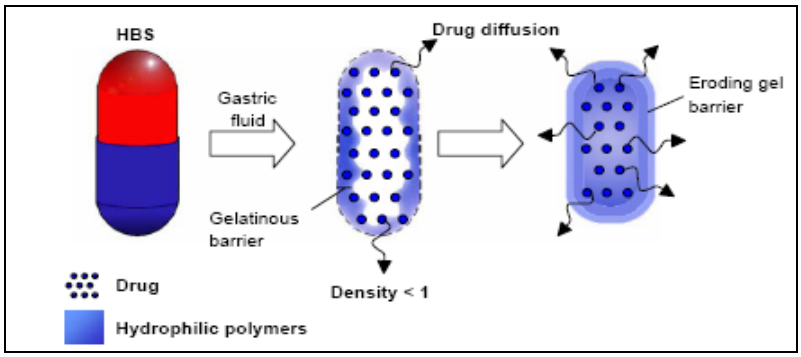

Figure 3: HBS System [1]

3.4.B.2. Gas-generating systems

The gas-generating floating systems lower density by generating gas bubbles in the matrix. Usually CO_2 is generated from sodium bicarbonate at an acidic pH. For this reason, acids such as citric or tartaric acid are included in the formulation. The system

may be composed of single- or multi-layers in various geometries such as membranes or spheres. The gas-generating unit can be incorporated in any of the multiple-layers. Alternatively, the gas-generating unit can be loaded inside microparticles such as ion-exchange resin beads coated with a semipermeable membrane. On contact with gastric acid, CO_2 is released, which causes floatation of the device. (**Figure 4 & 5**)

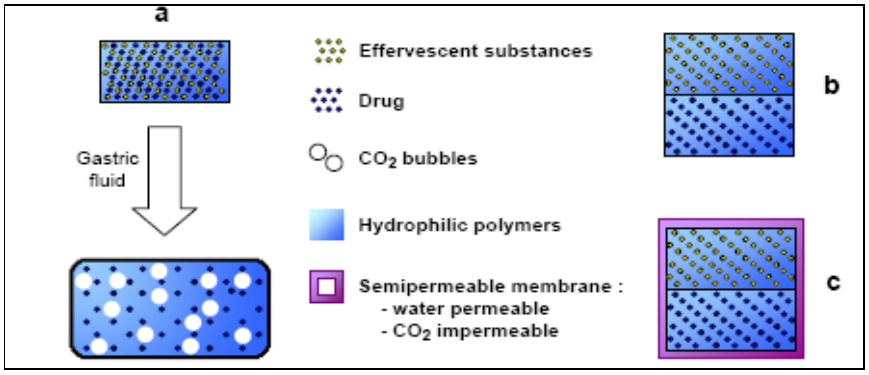

Figure 4: Gas-generating system (a) monolayer system (b) bilayer without semipermeable membrane (c) bilayer with semipermeable membrane

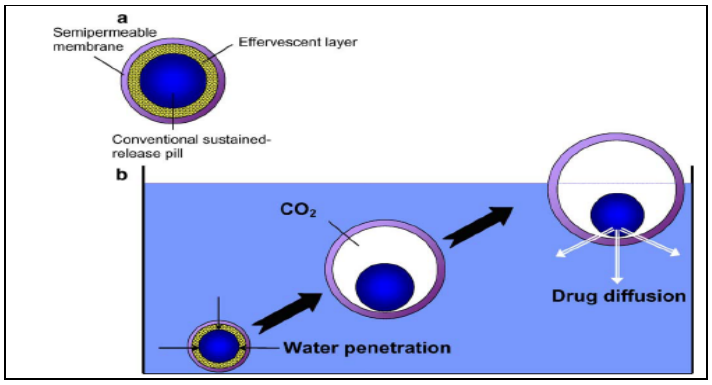

Figure 5: Schematic representation of floating pill

3.4.B.3. Raft Forming System

It is a gel-forming solution (e.g., sodium alginate solution containing carbonates or bicarbonates) swells and forms a viscous cohesive gel containing entrapped CO_2 bubbles (**Figure 6**) on contact with gastric fluid. Raft forming systems produce a layer on the top of the gastric fluid. Usually antacids such as aluminium hydroxide or calcium carbonate are incorporated in raft forming systems to reduce gastric acidity.

A marketed raft forming system is Liquid Gaviscon® (GlaxoSmithkline) used in the treatment of gastroesophageal reflux.

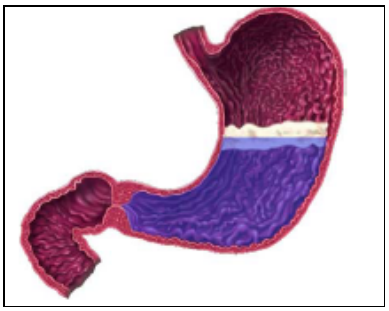

Figure 6: Schematic illustration of the barrier formed by a raft forming system

3.4. B. 4. Low-density Core System

In this type of system, the core materials are made of low-density materials such as empty hard gelatin capsules, polystyrene foams, pop-rice grains, or concave-moulded tablet shells. By proving a buoyant property from the beginning, the device is thought to have a better chance to stay afloat in gastric juice. The external surface of the low density materials are coated with drugs and subsequently with a variety of polymers, such as cellulose acetate phthalate or ethyl cellulose, to control drug release characteristics. Low-density systems can also be produced using hydrogel matrices, such as agar, carrageenan, and alginic acid, which contain light mineral oil. The presence of entrapped oil air provides the buoyancy effect. Hollow microspheres (microballoons) are also included in this type of system. (**Figure7**)

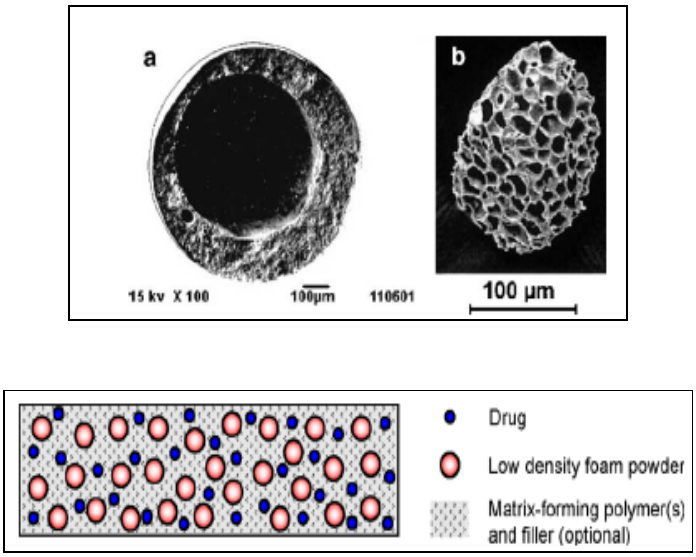

Figure 7: (a) micriballoon (b) foam particles (below) low density, floating matrix tablet

3.4.C Unfoldable, Extendible or Expandable Systems

3.4.C.1. Systems unfolding in the Stomach

Systems that unfold in the stomach have one or more noncontinuous compressible retention arms. The retention arms are initially folded to make the whole system smaller, with the arms folded, the system can be fit into gelatin capsules or the folded arms can be fixed by a gelatin band. In the stomach, the compressed or folded retention arms are expanded to make the whole system too large to resist gastric transit. This system is made of biodegradable or erodable polymer. (**Figure 8**)

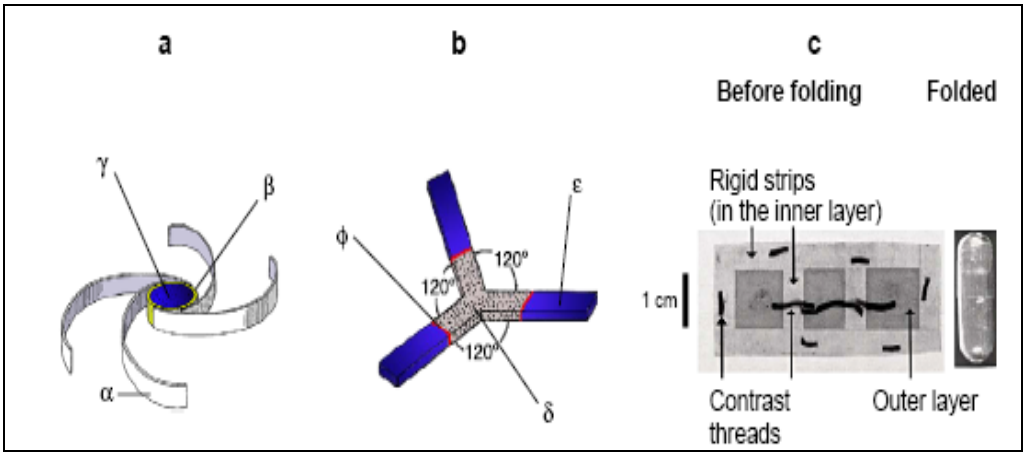

Figure 8: unfoldable system: (a) α: retention arms, β: receptacle, γ: controlled release tablet (b) δ: shape memory material, ε: erodable material, Φ: component connecting δ and ε (c) gastroretentive dosage form before and after folding

3.4.C.2. Systems Extending to Complex Geometric Shapes

Studies have shown that devices that extend in the stomach to certain geometric shapes can prolong gastric retention time. The geometric shapes include lobules, disc, ring, and tetrahedron. Since these devices should be small in the beginning for easy swallowing, they have to be compressible to a small size and expandable to a size large enough to prevent emptying through the pylorus. (**Figure 9**)

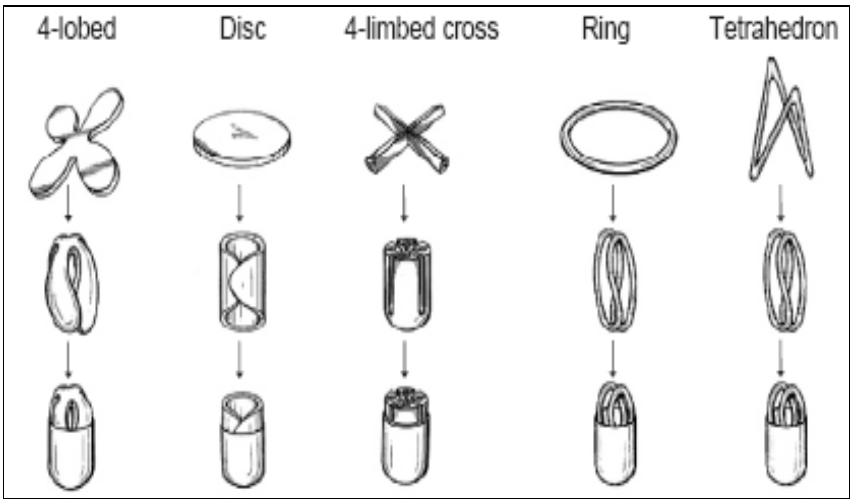

Figure 9: Different geometric forms of unfoldable systems

3.4.C.3. System Expanding to Larger Size

These small devices expand in the stomach to a size too large to pass through the pylorus. The devices are made of biodegradable or erodable polymers. Usually these systems contain swellable component such as hydrophilic colloids, osmotic expanding agents (sugars, salts), swellable resins or solidified or liquefied gas at ambient temperature. The liquefied or solidified gas in a compartment will vapourize at physiological temperature to produce gas that inflates the device from a collapsed state to an expanded state. Gases that have a boiling point lower than 37°C can be used. Examples of such gases are diethyl ether (b.p. 34.6°C), methyl formate (b.p.31.5°C) etc. (**Figure 10**)

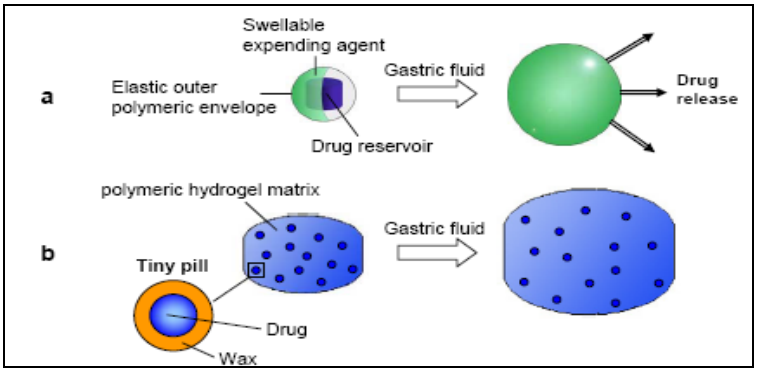

Figure 10: Swellable system

3.4.D Superporous Hydrogel system

Superporous hydrogel swells upon contact with gastric fluid. The extent of swelling of superporous hydrogel is enormously higher than conventional gel. Swelling factor of superporous hydrogel is >1000 whereas, in case of other gel it is 2 to 50. The main difference between hydrogel and superporous hydrogel is pore size. The size of the pores between polymer chains of conventional gel are within molecular dimensions (a few nanometer), but the size of the pores in superporous hydrogel is larger than 100

nm, usually in the range of several hundred micrometer. Superporous hydrogels swell to eqillibrium size within a minute due to rapid water uptake by capillary wetting through numerous interconnected open pores. (**Figure 11**)

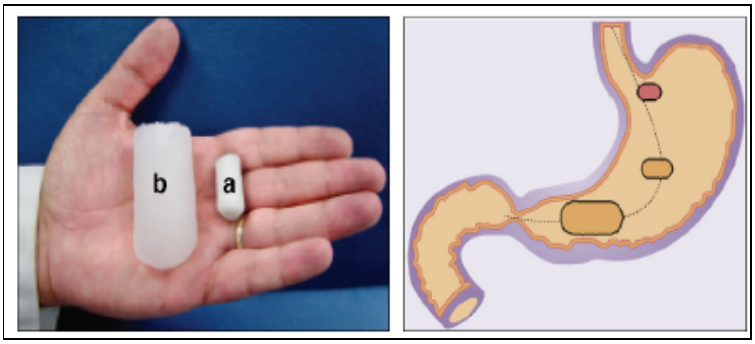

Figure 11: (a)Superporous hydrogel in dry (left), (b) water-swollen state, (on the right) transit of superporous hydrogel

3.4.E Mucoadhesive Systems

These systems can stick to the mucosal surface of the gastric tissue and remain in the stomach for a prolonged period of time. Different theories are suggested to explain the mechanisms of bioadhesion. Firstly, the electronic theory proposes attractive electrostatic forces between the glycoprotein mucin network and the bioadhesive material. Secondly, the adsorption theory suggests that bioadhesion is due to secondary forces such as Vander Waals forces and hydrogen bonding. The wetting theory is based on the ability of bioadhesive polymers to spread and develop intimate contact with the mucus layers, and finally, the diffusion theory proposes physical entanglement of mucin strands and the flexible polymer chains, or an interpenetration of mucin strands into the porous structure of the polymer substrate. Materials commonly used for bioadhesion are poly (acrylic acid) (Carbopol, polycarbophil), chitosan, Gantrez (Polymethyl vinyl ether/maleic anhydride copolymers), cholestyramine, tragacanth, sodium alginate, HPMC, sephadex, sucralfate,

polyethylene glycol, dextran, poly (alkyl cyanoacrylate) and polylactic acid. Even though some of these polymers are effective at producing bioadhesion, it is very difficult to maintain it effectively because of the rapid turnover of mucus in the gastrointestinal tract. Furthermore, the stomach content is highly hydrated, decreasing the bioadhesiveness of polymers.

3.4. F Magnetic Systems

Magnetic systems are usually constructed from a hydrophilic matrix tablet containing a small internal magnet (e.g., magnesium ferrite). An extracorporeal magnet is placed and fixed over the position of the stomach to control GI transit of the dosage form.

3.5 Advantages of GRDDS [2, 8]

1. Sustained release: usually, the GI transit time of most drug products is approximately 8-12 hours. For this reason peroral sustained release DDS cannot be designed over 12 hours. But gastric retention approaches can be tried for 24 hour sustained drug release (Once-daily formulation).

2. Predictable drug release and plasma drug conc. vs. time profile: The plasma drug conc. vs. time profile from a dosage form depends on the drug release kinetics of the dosage form. But due to highly variable nature of gastric emptying rate the release kinetic varies greatly and thus leads to a very unpredictable plasma drug conc. Profile. Localization of the delivery systems in the stomach for the entire period of drug release can provide an environment for consistent and uniform drug release and can help to achieve a more predictable plasma drug conc. vs. time profile.

3. Site specific drug delivery: A floating dosage form is a feasible approach especially for the drugs such as furosemide and riboflavin which have narrow absorption window in the upper small intestine and for the drugs which are primarily

absorbed from the stomach. FDDS present these drugs at its main absorption site and bioavailability increases.

4. Local action in the stomach: sometimes local action of some drugs in the stomach is desirable for the prolonged period of time, especially for the eradication of *Helicobacter pylori*, which is now believed to be the causative organism for chronic gastritis. Peptic ulcer and stomach cancer. Although the bacterium is highly sensitive to most antibiotics, its eradication from patients requires high conc. Of drug be maintained within the gastric mucosa for a long duration, which is more difficult systemically, but it can be achieved more easily by releasing drugs locally in the stomach for a long period of time. Thus it can be expected that local delivery of anti *H. pylori*-drugs through GRDDS may result in complete removal of the organism. Antacids can also be incorporated in GRDDS to reduce hyperacidity in the stomach.

5. Enhanced bioavailability: There are some drugs such as chlordiazepoxide, diazepam, cinnarizine, which are poorly soluble at intestinal pH and dissolution is the main rate limiting step in the absorption from the intestine, which leads to wastage of drug and their poor bioavailability. It has been found that FDDS enhances the bioavailability of these drugs.

6. GRDDS can be explored to deliver the drugs (e.g., captopril) orally that are degraded at intestinal pH.

3.6 LIMITATION OF GRDDS [2]

1. FDDS requires a sufficiently high level of fluid in the stomach for the system to float therein to work efficiently. This limitation can be overcome by coating the system with bioadhesive polymers, thereby enabling them to adhere to mucous lining of the stomach wall. Alternatively, the dosage forms may be administered with a glass of water (200-250 ml).

2. GRDDS are not feasible for those drugs that have low solubility or stability problems in gastric fluid.

3. Drugs such as Nifedipine which are well absorbed along the entire GI tract and which undergoes significant first-pass metabolism, may not be desirable candidates for GRDDS since the slow gastric emptying may lead to reduced systemic bioavailability.

4. The drugs that are irritant gastric mucosa are not feasible candidates for GRDDS.

3.7 EVALUATION OF GRDDS

The parameters that need to be evaluated in gastroretentive formulations include in vitro floating lag time, floating duration, dissolution profiles, specific gravity, content uniformity, hardness, and friability in case of solid dosage forms (tablets) [2]. In the case of multiparticulate dosage forms, differential scanning calorimetry (DSC), particle size analysis, flow properties, surface morphology, and mechanical properties are also performed. In case of mucoadhesives, bioadhesion test is to be performed[8].The tests for floating ability and drug release are generally performed in simulated gastric fluid at 37˚C. Gastric retention capacity of the dosage form should be evaluated in animal and human model by γ-scintigraphy [9] or Roentgenography [10].

3.8 MARKETED GRDD PRODUCTS

- **Valrelease®**- an HBS (Floating capsule of Diazepam) [11]
- **Madopar®-** an HBS (combination of levodopa and benserazide)[12]
- **Liquid Gaviscon®-** a raft forming solution (aluminium hydroxide)[13]
- **Alginate Flot-Coat®-** a raft forming system (antacid preparation)[14]
- **Topalkan®-**a raft forming system (antacid preparation)[15]

3.9 REFERENCES

1. P.L. Bardonnet , V. Faivre , W.J. Pugh , J.C. Piffaretti , F. Falson , "Gastroretentive dosage forms: Overview and special case of Helicobacter pylori", *Journal of Controlled Release* 111 (2006) 1 – 18

2. Brahma N. Singh, Kwon H. Kim, "Floating drug delivery systems: an approach to oral controlled drug delivery via gastric retention", *Journal of Controlled Release* 63 (2000) 235–259

3. R. Talukder and R. Fassihi, " Gastroretentive Delivery Systems: A Mini Review", *Drug Development and Industrial Pharmacy*, Vol. 30, No. 10, pp. 1019–1028, (2004)

4. Rubinstein.A, "Microbially controlled drug delivery to the colon", *Biopharm. Drug Dispos*. (1990), 11, 465–475.

5. Dressman. J.B., Berardi, R.R.; Dermentzoglou, L.C.; Russell, T.L.; Schmaltz, S.P.; Barnett, J.L.; Jarvenpaa, K.M., "Upper gastrointestinal (GI) pH in young, healthy men and women", *Pharm. Res*.(1990), 7, 756–761.

6. Russell, T.L.; Berardi, R.R.; Barnett, J.L.; Dermentzoglou, L.C.; Jarvenpaa, K.M.; Schmaltz, S.P.; Dressman, J.B., " Upper gastrointestinal pH in seventy-nine healthy, elderly, North American men and women." *Pharm. Res*. (1993), 10 (2), 187– 196.

7. Lui, C.Y.; Amidon, G.L.; Berardi, R.R.; Fleisher, D.; Youngberg, C.; Dressman, J.B, " Comparison of Gastrointestinal pH in dog and humans: implications on the use of the beagle dog as a model for oral absorption in humans", *J. Pharm. Sci*. (1986), 75, 271–274.

8. Shweta Arora, Javed Ali, Alka Ahuja, Roop K. Khar and Sanjula Baboota, "Floating Drug Delivery Systems: A Review", *AAPS PharmSciTech* (2005); 6 (3) Article 47

9. J. Timmermans, B. Van Gansbeke, A.J. Moes, "Assessing by gamma scintigraphy the in vivo buoyancy of dosage forms having known size and floating force profiles as a function of time",Proc. 5th Int. Conf. Pharm. Technol., vol. I, APGI, Paris, (1989), 42–51.

10. Y. Kawashima, T. Niwa, H. Takeuchi, T. Hino, Y. Ito, "Preparation of multiple unit hollow microspheres (microballoons) with acrylic resin containing tranilast and their drug release characteristics (in vitro) and floating behavior (invivo)", *J. Control. Release* 16 (1991) 279–290.

11. Sheth PR, Tossounian J. " The hydrodynamically balanced systems (HBS): a novel drug delivery system for oral use". *Drug Dev Ind Pharm*. (1984);10:313Y339.

12. Erni W, Held K. "The hydrodynamically balanced system: a novel principle of controlled drug release". *Eur Neurol.* (1987);27:215Y275.

13. Washington N, Washington C, Wilson CG, Davis SS. "What is liquid Graviscon? A comparison of our international formulations." *Int J Pharm*. (1986);34:105Y109.

14. Fabregas JL, Claramunt J, Cucala J, Pous R, Siles A., "In vitro testing of an antacid formulation with prolonged gastric residence time (Almagate flot coat)." *Drug Dev Ind Pharm*. (1994); 20:1199Y1212.

15. Degtiareva H, Bogdanov A, Kahtib Z, etal. "The use of third generation antacid preparations for the treatment of patients with nonulcerous dyspeosia and peptic ulcer complicated by reflux esophagus [in Chinese]." Liakrs' ka sprava. (1994); 5-6:119Y122.

CHAPTER-IV

LITERATURE REVIEW

Ali et al [1] reported a hydrodynamically balanced system (HBS) of metformin as a single unit floating capsule. Various grades of low-density polymers were used for the formulation of this system. These were prepared by physical blending of metformin and the polymers in varying ratios. The formulation was optimized on the basis of in vitro buoyancy and in vitro release in simulated fed state gastric fluid (citrate phosphate buffer pH 3.0). Effect of various release modifiers was studied to ensure the delivery of drug from the HBS capsules over a prolonged period. Capsules prepared with HPMC K4M and ethyl cellulose gave the best in vitro percentage release and was taken as the optimized formulation. By fitting the data into zero order, first order and Higuchi model it was concluded that the release followed zero order release, as the correlation coefficient (R^2 value) was higher for zero order release. In vivo studies were carried out in rabbits to assess the buoyancy, as well as the pharmacokinetic parameters of the formulation using gamma scintigraphy. The formulation remained buoyant during 5 h of study in rabbits. The comparative pharmacokinetic study was performed by administration of the optimized HBS capsules and immediate release capsules, both with radiolabeled metformin, using gamma counter. There was an increase in AUC in optimized HBS capsules of metformin when compared with immediate release formulation.

Boldhane et al [2] reported formulation and optimization of floating tablets of metformin HCl which was prepared using sodium alginate, sodium carboxymethylcellulose as a gelling agent, and release modifiers, respectively.

Eudragit NE 30 D was used as sustained release polymer to control the initial burst release. 3^2 full factorial design was applied to optimize the formulation. The optimization study using a 3^2 full factorial design revealed that the amount of sodium alginate and sodium carboxymethylcellulose had a significant effect on $t_{50\%}$, $t_{90\%}$, floating lag time and f_2.

The objective of the investigation reported by Nath et al [3] was to design a sustained release floating microcapsules of Metformin HCl using two polymers of different permeability characteristics Cellulose acetate butyrate (MW of 16,000) and Eudragit RL100 (MW of 150,000) using the oil-in-oil emulsion solvent evaporation method. Polymers were used separately and in combination (1:1) to prepare different microcapsules using acetone as organic phase. In all batches of microcapsules, the total polymer concentration was kept constant (10%w/w). No significant differences in drug loading in microcapsules made from different polymer were noted. Drug loaded microcapsules were found to float on 0.1M HCl for more than 8 hour. FT-IR study showed no drug polymer interaction. SEM study clearly revealed the smoothness of the spherically shaped particles. All the prepared microcapsules showed higher amount of drug release in phosphate buffer (pH 6.8) as compared to the release in 0.1M HCl (pH 1.2). Evaluation of the release data revealed that microcapsules prepared from RL100, Cellulose acetate butyrate and combination of both the polymers exhibit Higuchi spherical matrix release, followed by first order and zero-order release kinetics. Finally, the drug loaded floating microcapsules were found to be safe, economical and would

overcome the drawbacks associated with the drug in conventional tablet form, by reducing plasma drug fluctuations.

Gastroretentive floating drug delivery systems (GFDDS) of metformin hydrochloride, an have been reported by Raju et al [4]. Hydroxy propyl methyl cellulose (HPMCK4M) and carbopol 934P were used as polymers and sodium bicarbonate as gas generating agent to reduce floating lag time. Tablets were prepared by wet granulation method. Floating tablets were evaluated for hardness, friability, weight variation, drug content, floating properties and in vitro release pattern. The in vitro drug release followed first order kinetics and drug release was found to be diffusion controlled.

Yellanki et al [5] reported development of optimized mucoadhesive microcapsules of antihyperglycemic agent drug Metformin. Alginate microcapsules coated with mucoadhesive natural or synthetic polymers were prepared by Orifice-Ionic Gelation technique utilizing calcium chloride as a cross linking agent. The effect of type (natural or synthetic) and concentration of coating polymers and concentration of alginate on formulation was investigated. Prepared microcapsules were evaluated for drug content, entrapment efficiency, shape, size, in vitro mucoadhesion and in vitro release. The microcapsules obtained were found spherical and free flowing. The microcapsules coated with mucoadhesive polymer Carbopol exhibited good mucoadhesive property in the in vitro mucoadhesion test and also showed high percentage drug entrapment efficiency. The in vitro release study

indicates that carbopol as coating polymer containing formulations showed controlled drug release up to 10 h from microcapsules.

Rajab et al [6] optimized the composition of an effervescent floating tablet containing metformin hydrochloride regarding tablet hardness, time to dissolve 60% of the embedded drug (t60%), and buoyancy, the floating lag time (FLT). A simplex lattice experimental design has been used comprising different levels of hydroxypropylmethylcellulose (HPMC), stearic acid (SA), sodium bicarbonate (SB) as tablet matrix components, and hardness (H), t60%, FLT as response variables. Two models have been applied to decide which composition will result in Fickian diffusion or in overlapping of two dissolution mechanisms, diffusion and matrix erosion. Three of EFT showed the two dissolution mechanisms but most of EFT showed Fickian diffusion only. Checking the experimental response by a linear, quadratic, special cubic and cubic model using multivariate regression analysis resulted in best fit for the cubic model. Overlaying the results for the cubic model under constraints defined shows the domain of accepted values of response variables. The optimized EFT shall have been included HPMC between 15.6% and 24.2%, SA between 12.8 and 15.6% and SB between 16.1% and 17.5%. The result of this study has been critically evaluated considering analogous EFT described in literature.

The purpose of the study reported by Narasaiah et al [7] was to develop an optimized gastric floating drug delivery system containing Metformin Hydrochloride using Gum Kondagogu and investigate the effect of

formulation and processing parameters. The effervescent granules were prepared by wet granulation technique using Gum Kondagogu as a controlled release natural polymer. Sodium bicarbonate was incorporated as a gas-generating agent. The granules were lubricated with magnesium stearate and talc and compressed. Tablets were characterized for physical properties, floating characteristics (floating lag-time, floating time), swelling index, wetting time, drug content and evaluated for in vitro release characteristics for 10 hrs in 0.1N HCl at 370C. The similarity factor, t50 and t90 were used as parameters for selection of the best formulation compared with commercial product. The tablet erosion, drug diffusion, polymer swelling and the resulting release patterns varied significantly with the type of matrix forming natural polymer used. Comparable release profiles between the commercial product and the designed system (F4) were obtained. Altering the concentration of natural polymer, binding agent and gas-evolving agent were found to have a significant influence on the release rate with accurate control and prolongation of the drug release patterns. The drug release from all the formulations followed zero order kinetics and Korsmeyer-Peppas mechanism.

Preparation of metformin-loaded gum cordia/gellan beads employing ionic-gelation technique was reported by Ahuja et al [8]. The formulation of sustained release beads was optimized using response surface methodology. Effect of various formulation and process variables on % entrapment and % release was screened employing Plackett–Burman screening design. The results revealed that

concentrations of drug and calcium chloride, hardening time and temperature exerted significant effect. Additional batches of beads were prepared utilizing central-composite design for estimating extending effect in a spherical domain. A second-order polynomial equation fitted to the data was used to predict the responses in the optimal region. The optimized formulation provided % entrapment and % release, which were close to the predicted values. The proposed mathematical model was found to be robust and accurate for optimization of controlled release beads of metformin hydrochloride, consistent with the goals of adequate % entrapment and more than 80% release in 24 h.

Chodavarapu et al [9] investigated the effectiveness of the edible gum of *Abelmoschus esculentus* as a polymer in the development of a gastric floating dosage form of Metformin HCl. Abelmoschus esculentus, popularly known as okra, was shown to aid in the formulation of floating tablets. In their study, it was used as a pharmaceutical excipient along with HPMC E15 in the formulation of Metformin HCl floating tablets. The prepared tablets were tested for physicochemical properties,drug content uniformity, in vitro drug release patterns and FT-IR spectral analysis. From the study, it was evident that the formulations which included Abelmoschus esculentus gum (F1, F3, and F4) have lesser floating capacity but show a sustained release of drug where as the formulation (F2) which contained only HPMC has higher floating capacity but poor sustained release of drug. All in all, the formulation F3 (only Okra gum) manifested a prolonged release of the active ingredient.

Development of mucoadhesive microcapsules of Metformin Hcl for controlled release was reported by Kumar et al [10]. Metformin Hcl microcapsules were prepared with a coat consisting of alginate and Gum Karaya by employing Ionotropic Gelation process and Emulsification Ionotropic Gelation process. The microcapsules were evaluated for flow properties, Carr's index, hausner ratio, micro-encapsulation efficiency, drug release characteristics, surface characteristics; compatibility studies and mucoadhesive properties. Sharp endothermic peaks were noticed from the microcapsules formulated with two different techniques at 226ºC indicating the compatibility between the drug and the polymer Gum Karaya. Metformin Hcl release from the microcapsules was slow and followed zero order kinetics ($r > 0.98$) and followed non–fickian (n value 0.5 to 1) release and depended on the coat: core ratio and the method employed in the preparation of microcapsules. Among the two methods Emulsification Ionotropic Gelation method was found to be more suitable for Controlled release of Metformin Hcl over a long period of time. These microcapsules were subjected to in-vitro wash-off test and exhibited good mucoadhesive property.

Formulation and characterization a floating drug delivery system, using Methocel K100M and E50 was reported by Nasa et al [11]. Metformin hydrochloride (Biopharmaceutics Classification System class III) was used as the model drug for the investigation. Effervescent floating tablets of metformin hydrochloride were prepared, employing two different grades of Methocel K100M and E50, by wet

granulation method. The two grades were evaluated for their gel forming properties. The floating tablets were evaluated for pre-compression properties as well as in vitro drug release. The prepared tablets exhibited satisfactory precompression characteristics. The data obtained from the study was fitted in different models viz. zero order, first order, Korsmeyer-Peppas model, Higuchi model and Hixon Crowell model. The drug was found to be released by a combination of diffusion and erosion. The slope from Korsmeyer-Peppas model revealed that the drug release followed non-Fickian-type transport mechanism. It was concluded that the formulation containing 160 mg of Methocel K100M and 40 mg of Methocel E50 was the optimum formulation amongst all the test batches. It was also concluded from the investigation that a combination of Methocel K100M and Methocel E50 in the ratio of 4:1 might be satisfactorily employed in the formulation of a floating drug delivery system.

Salve et al [12] investigated the use of minimum proportions of natural polymers for drug release control by utilizing the advantage of interactions of gums resulting in enhanced matrix strength. They used xanthan and locust bean gum. The xanthan gum component acts to produce a faster gelation of the homopolysaccharide component and the homopolysaccharide acts to cross-link the normally free heteropolysaccharide helices resulting in increased viscosity. The interaction of Xanthan and locust bean gum was confirmed by FT-IR spectroscopy and differential scanning calorimetry. Drug release from optimized batch containing metformin HCl: HPMC K100M in 1:1 and

sodium bicarbonate 5, 10, 15% ratio were found to sustain the drug release for 12 hours.

Meka et al [13] reported preparation and evaluation of a gastroretentive drug delivery system for metformin HCl, using synthetic and semi-synthetic polymers. The floating approach was applied for preparing gastroretentive tablets (GRT) and these tablets were manufactured by the direct compression method. The drug delivery system comprises of synthetic and semi-synthetic polymers such as polyethylene oxide and Carboxymethyl ethyl cellulose (CMEC) as release-retarding polymers. GRT were evaluated for physico-chemical properties like weight variation, hardness, assay friability, in vitro floating behaviour, swelling studies, in vitro dissolution studies and rate order kinetics. Based upon the drug release and floating properties, two formulations were selected as optimized formulations. The two optimized formulations followed zero order rate kinetics, with non-Fickian diffusion and first order rate kinetics with erosion mechanism, respectively. The optimized formulation was characterised with FTIR studies and it was observed that there was no interaction between the drug and polymers.

Preparation of floating matrix tablets containing of Metformin HCL using wet granulation method using HPMC K100M, Eudragit RL 100 as polymer and Sodium Bicarbonate as gas generating agent, was reported by Wadher et al [14]. The prepared formulations were evaluated for hardness, weight variation, friability and drug content, floating time and in vitro drug release characteristics. Comparison between optimized and marketed formulation by

similarity factor ($f2$) divulged similarity in release profile between both. Release kinetic study showed that all batches followed Fickian diffusion.

References:

1. Ali, J., Arora, S., Ahuja, A., Babbar, a. K., Sharma, R. K. Khar, R. K. & Baboota, S. (2007). Formulation and development of hydrodynamically balanced system for metformin: In vitro and in vivo evaluation. *European Journal of Pharmaceutics and Biopharmaceutics 67,* 196–201.

2. Boldhane, S. P., Kuchekar, B. S. (2009). Gastroretentive drug delivery of metformin hydrochloride: formulation and in vitro evaluation using 3^2 full factorial design. *Curr Drug Deliv.* 6;5, 477-85.

3. Nath, B., Nath, L. K., Mazumdar, B., Sharma, N. & Sarkar, M. (2009). Design and Development of Metformin HCl Floating Microcapsules using Two Polymers of Different Permeability Characteristics. *International Journal of Pharmaceutical Sciences and Nanotechnology,* 2(3).

4. Raju, D. B., Sreenivas, R. and Varma, M. M. (2010). Formulation and evaluation of floating drug delivery system of Metformin Hydrochloride. *J. Chem. Pharm. Res.,* 2(2), 274-278.

5. Yellanki, S. K., Deb, S. K., Goranti, S., Nerella, N. K. (2010). Formulation development of mucoadhesive microcapsules of metformin hydrochloride using natural and synthetic polymers and in vitro

characterization. *International Journal of Drug Development & Research,* 2, 2.

6. Rajab, M., Jouma, M., Nubert, R. H., Dittgen, M. (2010). Optimization of a metformin effervescent floating tablet containing hydroxypropylmethylcellulose and stearic acid. *Pharmazie*, 65, 97–101.

7. Narasaiah, L., Reddy, K., Kumar, K., Rao, G., Ramu, Y., Bela, M., Kumar, G., Reddy, V., Rao, S. (2010). Formulation and in vitro evaluation of metformin hydrochloride floating tablets by using Natural Polymer. *J. Chem. Pharm. Res.,* 2(4), 333-342.

8. Ahuja, M., Yadav, M. & Kumar, S. (2010). Application of response surface methodology to formulation of ionotropically gelled gum cordia/gellan beads. *Carbohydrate Polymers, 80,* 161–167.

9. Chodavarapu, N. P., Yendluri, R. B., Suryadevara, H., Reddy, P., Chhatoi, P. (2011). Formulation and evaluation of *Abelmoschus esculentus* mucilage based metformin hydrochloride floating matrix tablets. *International Journal of Pharmacy&Technology*, 3(2), 2725-2745.

10. Kumar, A., Balakrishna, T., Jash, R., Murthy, T., & Sudheer, B.(2011). Formulation and evaluation of mucoadhesive microcapsules of metformin hcl with gum karaya. *International Journal of Pharmacy and Pharmaceutical Sciences.* 3 (3).

11. Nasa, P. & Mahant, S. (2011). Floating drug delivery system using Methocel K100M and E50: Formulation and characterization. *Acta Pharmaceutica Sciencia, 53*, 57 – 65.

12. Salve, P. S. (2011). Development and in vitro evaluation of gas generating floating tablets of metformin hydrochloride. *Asian J. Res. Pharm. Sci.* 1(4), 105-112.

13. Meka, V. S., Gorajana, A., Dharmanlingam, S. R., Kolapalli, V. R. (2013). Design and evaluation of a gastroretentive drug delivery system for metformin HCl using synthetic and semi-synthetic polymers. *Invest Clin.* 54(4), 347-59.

14. Wadher, K. J., Bagde, A., Ailwar, S. Umekar, M. J. (2013). Formulation and evaluation of sustained release gastroretentive dosage form of Metformin HCl. *Der Pharmacia Lettre,* 5 (2), 264-271.

CHAPTER-V

DRUG PROFILE

Drug: Metformin hydrochloride

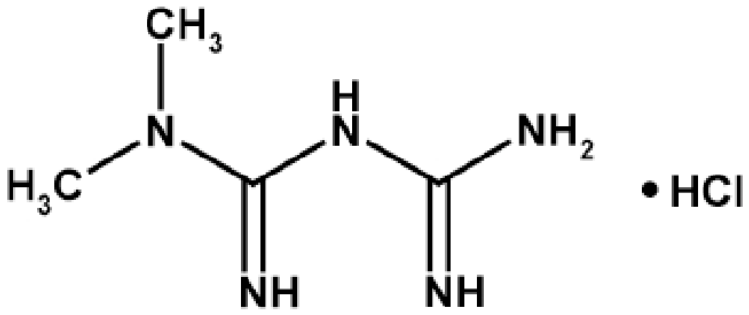

Metformin Hydrochloride

5.1. Chemical name: 1, 1 dimethylbiguanide hydrochloride

5.2. General description: Metformin hydrochloride (N, N dimethylimidodicarbonimidic diamide hydrochloride) is a member of the biguanide class of oral antihyperglycemics and is not chemically or pharmacologically related to any other class of oral antihyperglycemic agents. The empirical formula of metformin hydrochloride is $C_4H_{11}N_5$, HCl and its molecular weight is 165.63.

Metformin hydrochloride is a white to off-white crystalline powder that is freely soluble in water and is practically insoluble in acetone, ether, and chloroform. The pKa of metformin is 12.4. The pH of a 1% aqueous solution of metformin hydrochloride is 6.68.

5.3. Official compendium (Indian Pharmacopoeia, 2007) [1]:

Metformin hydrochloride contains not less than 98.5% and not more than 101.0% of $C_4H_{11}N_5$, HCl, calculated on the dried basis.

Description: a white crystalline powder, hygroscopic.

Identification: A. Determine by infrared absorption spectrophotometry. Compare the spectrum with that obtained with metformin HCl RS or with inference spectrum of metformin HCl.

B. dissolve 25 mg in 5 ml of water, add 1.5ml of 5M sodium hydroxide, 1 ml of napthol solution and, dropwise with shaking, 0.5ml of dilute sodium hypochlorite solution; an orange red colour is produced which darkens on keeping.

C. dissolve 10 mg in 10 ml of water and add 10 ml of solution prepared by miximg equal volume of a 10% w/v solution of sodium nitroprusside, a 10% w/v solution of potassium ferricyanide and a 10% w/v solution of sodium hydroxide and allowing to stand for 20 minutes; a wine red colour developes within 3 mins.

D. gives reaction A of chlorides.

Tests:

Related substance. Determine by liquid chromatography.

Test solution. Dissolve 5 mg of the substance under examination in 10 ml of water.

Reference solution (a). A 0.0005 % w/v solution of substance under examination in water.

Reference solution (b). A 0.0001% w/v solution of dicyandiamide in water.

Chromatographic system

- a stainless steel column 30cm×4mm, packed with octadecylsilane bonded to porous silica (10 µm),

- mobile phase: a solution containing 0.087% w/v of sodium pentanesulphonate and 0.12% w/v of sodium chloride, adjust to pH 3.5 using 1% v/v solution of orthophosphoric acid,

- flow rate. 1 ml/min,

- spectrophotometer set at 218 nm,

-a 20 µl loop injector.

For the test solution record the chromatogram for three times the retention time of the peak. In the chromatogram obtained with the test solution the area of any peak corresponding to dicyandiamide is not greater than that obtained with reference solution (b) and the area of any other secondary peak is not greater than that obtained with reference solution (a).

Heavy metals: 1.0 g complies with the limit test for heavy metals, method B (20 ppm).

Sulphated ash: not more than 0.1%

Loss on drying: not more than 0.5%, determined on 1.0 g by drying in an oven at 105^{o}C.

Assay: weigh accurately about 60 mg, dissolve in 4ml of anhydrous formic acid, add 50 ml of acetic anhydride. Titrate with 0.1M perchloric acid, determining the end point potentiometrically. Carry out a blank titration.

1 ml of 0.1M perchloric acid is equivalent to 0.008281 g of C4H11N5, HCl.

Storage: store protected from light and moisturizer.

Metformin tablets I.P.

Metformin tablets contain not less than 95.0 % and not more than 105.0% of the stated amount of metformin HCl, $C_4H_{11}N_5$, HCl. The tablets may be coated.

Identification:

A. Shake a quantity of the powdered tablets containing 20 mg of metformin HCl with 20 ml of ethanol, filter, evaporate the filtrate to dryness on a water bath and dry the residue at 105^{o}C for 1 h. on the residue, determine by the infrared absorption spectrophotometry. Compare the spectrum with that obtained with *metformin hydrochloride RS* or with the reference spectrum of metformin hydrochloride.

B. Triturate a quantity of the powdered tablets containing 50 mg of metformin HCl with 10 ml water and filter. To 5 ml of the filtrate, add 1.5 ml of 5 M sodium hydroxide, 1 ml of 1-naphthol solution and, dropwise with shaking, 0.5 ml of dilute sodium hypochlorite solution; an orange red colour is produced which darkens on keeping.

C. The filtrate obtained in test B gives reaction A of chlorides.

Tests:

Related substances. Determine by liquid chromatography.

Test solution. Shake a quantity of the powdered tablets containing 0.5 g of metformin HCl with 100 ml of water and filter.

Reference solution (a). Dilute 0.1 ml of the test solution to 100 ml with water.

Reference solution (b). A 0.0001 % w/v solution of dicyandiamide in water.

Chromatographic system

- a stainless steel column 30cm×4mm, packed with octadecylsilane bonded to porous silica (10 µm),

- mobile phase: a solution containing 0.087% w/v of sodium pentanesulphonate and 0.12% w/v of sodium chloride, adjust to pH 3.5 using 1% v/v solution of orthophosphoric acid,

- flow rate. 1 ml/min,

- spectrophotometer set at 218 nm,

-a 20µl loop injector.

For the test solution record the chromatogram for three times the retention time of the principal peak. In the chromatogram obtained with the test solution the area of any peak corresponding to dicyandiamide is not greater than that obtained with reference solution (b) and the area of any other secondary peak is not greater than that obtained with reference solution (a).

Dissolution:

Apparatus. No.2

Medium. 900ml of a 0.68 % w/v solution of potassium dihydrogen phosphate, adjusted to pH 6.8 by the addition of 1M sodium hydroxide.

Speed and time. 100 rpm and 45 mins.

Withdraw a suitable volume of the medium and filter, dilute suitably with water and measure the absorbance of the resulting solution at the maximum at about 233

nm. Calculate the content of $C_4H_{11}N_5$, HCl, in the medium taking 806 as the specific absorbance at 233 nm.

D. Not less than 70 % of the stated amount of $C_4H_{11}N_5$, HCl.

Other tests. Comply with the tests stated under tablets.

Assay. Weigh and powder 20 tablets. Weigh accurately a quantity of the powder containing about 0.1 g of metformin HCl, shake with 70 ml of water for 15 minutes, dilute to 100.0 ml with water and filter. Dilute 10.0 ml of the filtrate to 100.0 ml with water. Further dilute 10.0 ml to 100.0 ml with water and measure the absorbance of the resulting solution at the maximum at about 232 nm. Calculate the content of $C_4H_{11}N_5$, HCl taking 798 as the specific absorbance at 232 nm.

5.4. Metformin Hydrochloride Extended Release Teblets USP [2]

Metformin HCl extended release tablets contain not less than 90.0% and not more than 110.0 % of the labeled amount of metformin HCl ($C_4H_{11}N_5$, HCl).

Dissolution

Test 1:

Medium: pH 6.8 phosphate buffer prepared by dissolving 6.8 g of monobasic potassium phosphate in 1000ml of water and adjusting with 0.2N sodium hydroxide to a pH of 6.8 ± 0.1; 1000 ml.

Apparatus 2: 100 rpm, for tablets labeled to contain 500 mg.

Apparatus 1: 100 rpm, for tablets labeled to contain 750 mg.

Times: 1, 3, and 10 hours.

Time (hours)	500 mg tablet, amount dissolved	750 mg tablet, amount dissolved
1	Between 20% and 40%	Between 22% and 42%
3	Between 45% and 65%	Between 49% and 69%
10	Not less than 85%	Not less than 85%

Test 2:

Medium: pH 6.8 phosphate buffer prepared by dissolving 6.8 g of monobasic potassium phosphate in 1000ml of water and adjusting with 0.2N sodium hydroxide to a pH of 6.8 ± 0.1; 1000 ml.

Apparatus 2: 100 rpm.

Times: 1, 2, 6 and 10 hours.

Time (hours)	Amount dissolved
1	Between 20% and 40%
2	Between 35% and 55%
6	Between 65% and 85%
10	Not less than 85%

5.5. Pharmacokinetic parameters [3]

Oral bioavailability: 52 ± 5 %

Urinary excretion: 99.9 ± 0.5 %

Bound in plasma protein: negligible

Clearance: 7.62 ± 0.30 $ml.min^{-1}kg^{-1}$

Volume of distribution: 1.12± 0.08 lit/kg

Biological half-life: 1.74±0.20 hr

Peak time: 1.9± 0.4 hr

Peak conc.: 1.6± 0.2 µg/ml

5.6. Pharmacology [4]

Metformin HCl causes little or no hypoglycaemia in nondiabetic subjects, and even in diabetics episodes of hypoglycaemia due to metformin are rare. It does not stimulate pancreatic β cells. *Mechanism of action:* it is not clearly understood. It does not cause insulin release, but presence of some insulin is essential for their action. Explanations offered for their hypoglycaemic actions are –

1. Suppress hepatic gluconeogenesis and glucose output from liver (the major action).
2. Enhance insulin-mediated glucose disposal in muscle and fat. Though it does not alter translocation of GLUT4 (the major glucose transporter in sleletal muscle), they enhance GLIT1 transport from intracellular site to plasma membrane. The effect thus differs from that of insulin.
3. Retard intestinal absorption of glucose, other hexose, amino acids and vitamin B_{12}.
4. Interfere with mitochondrial respiratory chain – promote peripheral glucose utilization by enhancing anaerobic glycolysis. However, metformin binds less avidly to mitochondrial membrane.

Actions 3 and 4 appear to contribute little to the therapeutic effect.

Adverse effects: abdominal pain, anorexia, nausea, metallic taste, mild diarrhoea and tiredness are the frequent side effects. Metformin does not cause hypoglycaemia expect in overdose.

Lactic acidosis: small increase in blood lactate occurs with metformin, but lactic acidosis is rare (less than 1 per 10,000 patient years) because it is poorly concentrated in hepatic cells. Alcohol ingestion can precipitate severe lactic acidosis.

Vitamin B_{12} deficiency: due to interference with its absorption can occur with high dose of metformin.

In addition to general restrictions for use of oral hypoglycaemic, biguanides are contraindicated in hypotensive states, cardiovascular, respiratory, hepatic and renal disease and in alcoholics because of increased risk of lactic acidosis.

Special precaution: Patients should not consume alcohol as there is an interaction between metformin and alcohol which could lead to increased risk of lactic acidosis.

Dosage: 250 mg, 500 mg, 750 mg, 850 mg, or 1000mg per day in case of adult.

REFERENCES

1. Indian Pharmacopoeia 2007, volume 2, Govt. of India, Ministry of Health and Family Welfare. Published by Indian Pharmacopoeia Commission, Ghaziabad, India, p. 1358 – 1360.

2. USP NF 2009, Volume 3, p. 2907.

3. Pentikainen, P. J., Neuvonen, P. J. & Penttila, A. (1979). Pharmacokinetics of metformin after intravenous and oral administration to man. *European Journal of Clinical Pharmacology, 16,* 195 – 202.

4. Essentials of Medical Pharmacology, 6th ed. KD Tripathy, Jaypee Brothers Medical Publishers (P) Ltd, New Delhi, India, 2008, p. 267-269.

CHAPTER-VI

EXCIPIENTS PROFILE

6.1. Gellan gum

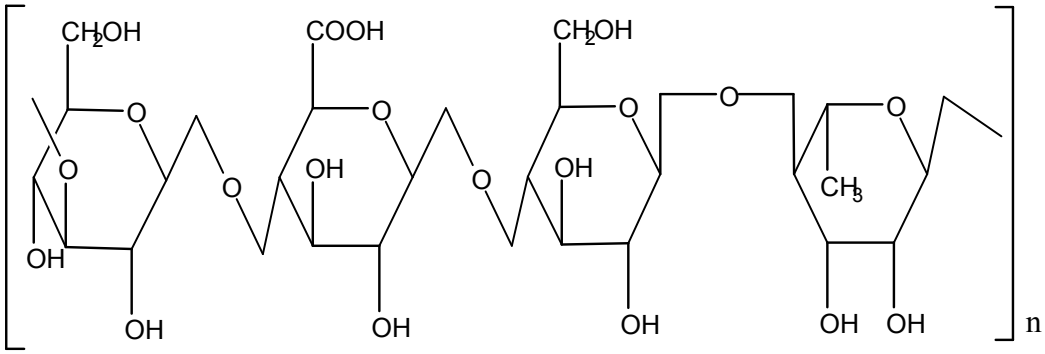

GELLAN GUM

Gellan, is an anionic deacylated exocellular polysaccharide produced by a pure culture of *Pseudomonas elodea* with a tetrasaccharide repeating unit of one α-L-rhamnose, one β-D-glucuronic acid and two β-D-glucose residues [1]. Glucoronic acid is neutralized to mixed potassium, sodium, calcium and magnesium salts. It may contain acyl (glyceryl and acetyl) group as the ortho glycosidically linked esters. It yields not less than 3.3% and not more than 6.8% of carbon di oxide, calculated on the dry basis.

Packaging and storage: preserved in well closed container, and stored at room temperature.

Identification:

A. Prepare a 1% solution of gellan gum by hydrating 1 g in 99 ml of deionised water. Stir the mixture for about 2 hours, using a motorized stirrer and propeller type stirring blade. Draw a small amount of the solution obtained into a wide bore pipet, and transfer it into a 10% $CaCl_2$ solution. A tough, worm like gel will form instantly.

B. To the remaining solution prepared for identification test A, at 0.5 g of NaCl, heat the solution to 80°C, stirring constantly, and hold at 80°C for 1 min. Stop heating and stirring the solution, and allow it to cool to room temperature. A firm gel will form.

Microbial enumeration test: and absence of a specified micro-organism: it meets the requirements of the tests for absence of *Salmonella sp.* and *Escherichia coli.* The total aerobic microbial count is not more than 1000 cfu per gram, and the total combined molds and yeasts count is not more than 100 cfu per gram.

Loss on drying: dry it at 105°C for 2.5 hours. It loses not more than 15.0%.

Total ash: not less than 4.0% and not more than 14.0%, calculated on the dry basis.

Arsenic: method II: not more than 3.0 µg per gram.

Lead: prepare a test preparation as directed, using a 2.0 g portion of gellan gum. Use 4 ml of diluted standard lead solution (4µg of Pb) for the test; the limit is not more than 2.0µg per gram.

Limit of isopropyl alcolhol: proceed as directed under limit of isopropyl alcohol for xanthan gum, using about 5 g of gellan gum, accurately weighed, for the test solution; not more than 750µg per gram is found.

Assay: proceed with gellan gum as directed for procedure under alginates assay, using about 1.2 g of undried gellan gum, accurately weighed [2].

6.2. Tamarind seed gum

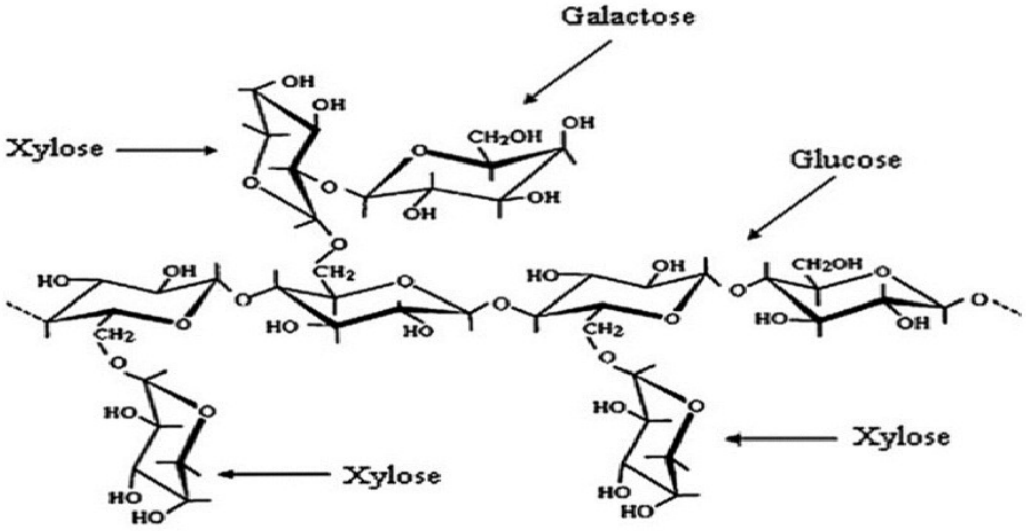

Tamarind seed gum (TSG) is an excellent natural hydrophilic polysaccharide obtained from the endosperm of *Tamarindus indica* Linn (family Leguminosae) having branched structure consisting of a main chain of β-D (1→4) linked glucopyranosyl units, with a side chain consisting of a single xylopyranosyl unit attached to every second, third and fourth D-glucopyranosyl unit through an α-D (1→6) linkage [3]. One D-galacotopyranosyl units is attached to one of the xylopyranosyl unit through a β-D (1→2) linkage. It is widely used as a thickening, stabilizing, emulsifying, mucoadhesive and gelling agent in various pharmaceutical formulations [4] due to possessing of high thermal and chemical stability, non-carcinogenicity, biocompatibility, mucoadhesivity, non-toxicity and high drug holding capacity [5].

TSG has an average molecular weight of 52,350 Dalton and it is also called as a galactoxyloglucan. As per the dry basis analysis, 38.7% of the protein content is

insoluble protein and 61.3% is soluble protein; the soluble protein in TSG is composed of 21.7% salt-soluble protein, 19.6% water-soluble protein, 16.7% alkali-soluble protein and 3.9% alcohol-soluble protein. It has 3.9-7.4% of oil, 0.7-8.2% of crude fibre and 2.45-3.3% ash [6]. The purity of TSG is characterised by various phytochemical tests which show negative results for proteins, steroids, saponins, alkaloids, flavonoids, tannins and phenols; positive results for the presence of carbohydrates, confirmed by the Molisch's test, Barfoed's test and Benedict's test; and also positive results for the presence of mucilage and reducing sugars [7]. TSG is insoluble in organic solvents such as ethanol, methanol, acetone, ether and in cold water, but it gets dissolved completely in hot water at temperatures above 85°C, yielding a highly viscous colloidal solution or a mucilaginous gel showing typical non-Newtonian rheologic behaviour and pseudoplastic properties [8]. TSG possesses various properties like high viscosity, adhesivity, non-carcinogenicity, broad pH tolerance and biocompatibility. It is also found to be a potential emulsifier, nontoxic and non-irritant with haemostatic activity.

Other distinguishable properties of TSG have also been identified, which include the high drug holding capacity, high swelling index and high thermal stability, making it a suitable excipient for drug delivery system. Apart from this, it is an excellent viscosity enhancer showing mucomimetic, mucoadhesive and bioadhesive activities. Recent studies on TSG for various drug formulations revealed other unique properties with wide applications in the pharmaceutical area, which include its potent antidiabetic activity that reduces blood sugar level.

In addition to this, the property of forming films with high tensile strength and flexibility makes it a good excipient for ocular preparations. This film is transparent, nonhygroscopic, non-sticky and retains its form even on rough handling [9]. Acute toxicity and chronic toxicity studies carried out to determine the safety of TSG revealed it to be nontoxic even at high doses. So, the use of TSG in pharmaceutical products is proven to be acceptable as excipients. To establish the carcinogenic properties of TSG, studies were done on both sexes of B6C3F1 mice. Oral toxicity study and carcinogenicity study were carried out for this. The mice were provided with diet containing different percentages of TSG (0, 0.625, 1.25, 2.5 and 5%) for 13 weeks to study subchronic toxicity. This oral toxicity study also helped to determine the dietary level, where it was found that even at maximum level of 5%, the diet showed no toxic effects. Hence, the highest dose of 5% TSG was selected according to the guidelines of carcinogenicity studies. For carcinogenicity study, the blood samples and tissues of various organs were subjected to examination after 98 weeks. The studies proved that there were no signs of carcinogenicity or adverse effects on both the sexes [10]. TSG is a multifunctional polymer, which plays the role of stabiliser, thickener, binder, release retardant, modifier, suspending agent, viscosity enhancer, emulsifying agent, as a carrier for novel drug delivery systems for oral, buccal, colon, ocular systems, nanofabrication, wound dressing, food, cosmetics, confectionery, bakery, etc.

6.3. Polyvinylpyrrolidone [11]

Molecular formula: $(C_6H_9NO)_n$

Density: 1.2 g/cm³

Melting point: 110 - 180 °C

6.3.1. Description:

A homopolymer of vinyl pyrrolidone, manufactured using different initiator systems depending upon the molecular weight. The low molecular weight polymer, having a K-value of 30 or less (K value represents the average molecular weight of soluble povidone grade and is calculated from the relative viscosity in water), is polymerized in water using a hydrogen peroxide initiator system or in isopropanol using an organic peroxide. Higher K value polymer is made by aqueous homopolymerization using an organic azo or peroxide type initiator. When polymerization is carried out in isopropanol, the alcohol solvent is exchanged with water prior to drying.

6.3.2. CAS Number: 9003-39-8

6.3.3. Generic nomenclature: PVP, Polyvinyl pyrrolidone, 1-vinyl-2-pyrrolidinone polymer.

6.3.4. Appearance: Free-flowing, white-yellowish, hygroscopic, tasteless powder or flakes having a slight amine odour.

6.3.5. Solubility: Freely soluble in water and most commonly used pharmaceutical solvents including alcohol and polyglycolated vehicles.

6.3.6. Pharmacopoeial listing: USP, EP, JP, FCC, Codex Alimentarius.

6.3.7. Regulatory: Povidone K-30 (MW 40000) is approved in the US, Code of Federal Regulations.

6.3.8. Health & Safety: Reported impurities in povidone are residual monomer, N-vinyl-2-pyrrolidinone, acetaldehyde, and hydrazine. Limit for residual N-vinyl-2-pyrrolidinone is less than 10 ppm, whereas acetaldehyde content is less than 500 ppm and hydrazine below 1 ppm. Peroxide functionalities are also known to be present, with typical conc. well below 400 ppm. No USP organic volatile impurities should be present. The acceptable daily intake is 0 – 50 mg/kg [12].

Acute oral toxicity: Doses of 300 – 2700 mg/kg were administered with no significant adverse effects (rabbits) [13].

Subchronic oral toxicity: PVP K-90 fed at 2.5 or 5.0% of the diet for 28 days (dogs) demonstrated no toxic, pathological, or histological abnormalities.

Chronic oral toxicity: No toxic effects were observed in a two-year study at 0, 5.0, or 10.0% PVP K-30 and in a 138-week study at 1, 2, 5, and 5% PVP K-90 (rats).

6.3.9. Use: Binder, complexing aid, suspension stabilizer, thickener.

6.4. Magnesium stearate [14]

Magnesium stearate consists mainly of magnesium stearate $(C_{17}H_{35}CO_2)_2Mg$ with variable proportions of Magnesium palmitate, $(C_{15}H_{31}CO_2)_2Mg$ and magnesium oleate, $(C_{17}H_{33}CO_2)_2Mg$. Magnesium stearate contains not less than 3.8% and not more than 5.0% of Mg, calculated on the dried basis.

6.4.1. CAS Number: 557-04-0

6.4.2. Description: A very fine, light, white powder, odourless or with a very faint odour of stearic acid, unctuous and free from gritiness.

6.4.3. Solubility: insoluble in water and ether; slightly soluble in benzene.

6.4.4. Melting point: 150°C

6.4.5. Identification

A. To 5.0 gm add 50 ml of ether, 20 ml of 2 m nitric acid and 20 ml of distilled water and heat under a reflux condenser until dissolution is complete. Allow to cool, separate the aqueous layer and shake the ether layer with two quantities, each 4 ml, of distilled water. Combine the aqueous layers, wash with 15 ml of ether and dilute to 50 ml with distilled water (solution A). Evaporate the ether layer to dryness and dry the residue at 105°C. The freezing point of the residue is not lower than 53°C.

B. 1ml of solution A obtained in test A gives reaction A of magnesium salts.

6.4.6. Tests

6.4.6.1. Appearance of solution: solution A is not more intensely coloured than reference solution YS6.

6.4.6.2 Appearance of solution of the fatty acids: Dissolve 0.5 gm of the residue obtained in the preparation of solution A in 10 ml of chloroform. The solution is clear, and not more intensely coloured than reference solution YS5.

6.4.6.3 Acidity or alkalinity: mix 1.0 g with 20 ml of carbon dioxide-free water, boil for 1 minute, shaking continuously, cool and filter. To 10 ml of filtrate add 0.05 ml of bromothymol blue solution. Not more than 0.05 ml of 0.1 M

Hydrochloric acid or 0.1M sodium hydroxide is required to change the colour of the solution.

6.4.6.4 Acid value of the fatty acids: 195 to 210, determined on 0.2 g of the residue obtained in the preparation of solution A, dissolved in 25 ml of the prescribed mixture of solvents.

6.4.6.5 Free stearic acid: not more than 3%, determined by the following method. Weigh accurately about 1.0 g into a stoppered flask, add 50 ml of chloroform, stopper the flask and shake well. Filter into a beaker through two thicknesses of filter paper taking care to avoid evaporation of the solvent. Wash the filter with 10 ml of chloroform and collect the washings in the beaker. Evaporate the chloroform on a water-bath in a current of air. Dissolve the residue in about 10 ml of ethanol (95%) previously neutralized to phenolphthalein solution and titrate with 0.1 M sodium hydroxide using phenolphthalein solution as indicator.

1 ml of 0.1 M sodium hydroxide is equivalent to 0.0284 g of stearic acid.

6.4.6.6 Zinc stearate: Heat 5.0 g with shaking with a mixture of 50 ml of water and 50 ml of dilute sulphuric acid until the fatty acids separate as an oily layer. Cool, filter the aqueous layer and wash the residue with two successive quantities, each of 5 ml, of hot water, combine the filtrate and the washings and dilute to 100 ml with water. To 5 ml of the resulting solution add 0.5 ml of ammonium mercurithiocyanate solution and 0.05 ml of copper sulphate solution. Scratch the walls of the container with a glass rod and allow to stand for 15 minutes; no violet precipitate is formed.

6.4.6.7 Heavy metals: Heat 5.0 g with 40 ml of 2 M acetic acid and allow to cool. Filter, wash the residue with two quantities, each of 5 ml, of warm water and dilute to 100 ml with water. 12 ml of the resulting solution complies with the limit test for heavy metals, Method D (20 ppm). Use 1.0 ml of lead standard solution (10 ppm Pb) to prepare the standard.

6.4.6.8 Chlorides: 10.0 ml of solution A diluted to 15 ml complies with the limit test for chlorides (250 ppm).

6.4.6.9 Sulphates: Dilute 5.0 ml of solution A to 50.0 ml with water. 2.5 ml of this solution diluted to 15 ml with water complies with the limit test for sulphates (0.6%).

6.4.6.10 Loss on drying: Not more than 6.0%, determined on 1.0 g by drying in an oven at 105°C.

6.4.6.11 Assay: Weigh accurately about 0.75 g, add 50 ml of a mixture of equal volumes of 1-butanol and ethanol, 5 ml of strong ammonia solution, 3 ml of ammonia buffer pH 10.0, 30.0 ml of 0.1 M disodium edentate and 15 mg of mordant black II mixture, heat to 45° to 50° and titrate with 0.1 M zinc sulphate until the colour changes from blue to violet. Repeat the operation without the substance under examination. The difference between the titrations represents the amount of disodium edetate required.

1 ml of 0.1 M disodium edentate is equivalent to 0.002431 g of Mg.

6.4.7 Use: Tablet excipients (lubricant).

6.5. Purified talc [15]

Talc is a powdered, selected natural hydrated magnesium silicate. It may contain varying amounts of aluminium and iron in forms insoluble in 1 M sulphuric acid.

Description: a white or almost white powder, free from grittiness; readily adheres to the skin; unctuous to the touch; odourless.

Identification:

A. when examined microscopically, shows irregular plates, the majority less than 50µm in length. The particles are not notably stained by a 0.1 % w/v solution of methylene blue in ethanol (95%).

B. Melt 0.5 g in a metal crucible with 1 g of potassium nitrate and 3 g of anhydrous sodium carbonate, add 20 ml of boiling water, mix and filter. Wash the residue with 50 ml of water. Mix the residue with a mixture of 0.5 ml of HCl acid and 5 ml of water and filter. To the filtrate add 1 ml of 9 M ammonia and 1 ml of ammonium chloride solution and filter. To the filtrate add 1 ml of disodium hydrogen phosphate solution; a white, crystalline precipitate is produced.

C. Gives the reaction of silicates.

Storage: store protected from moisture.

6.6. References

1. Nitta, Y., & Nishinari (2005). Gelation and gel properties of polysaccharides gellan gum and tamarind xyloglucan. *International Journal of Biological Macromolecules, 5,* 47-52.

2. United States Pharmacopoeia (32)- National Formulary (27), 2009, volume 1, p. 1241.

3. Gidley, M. J., Lillford, P. J., Rowlands, D. W., Lang, P., Dentini, M., Crescenzi, V. (1991). Structure and solution properties of tamarind-seed polysaccharide. *Carbohydrate Research, 214,* 299–314.

4. Nayak, A. K., Pal, D. & Santra, K. (2014). Tamarind seed polysaccharide-gellan mucoadhesive beads for controlled release of metformin HCl. *Carbohydrate Polymers, 103,* 154-163.

5. Saettone, M. F., Burgalassi, S., Giannaccini, B., Boldrini, E., Bianchini, P., & Luciani, G. (2000).Ophthalmic solutions viscosified with tamarind seed polysaccharide. US Patent No. 6056950).

6. Khounvilay K, Sittikijyothin W. (2011). Rheological behaviour of tamarind seed gum in aqueous solutions. *Food Hydrocoll, 30*, 1-5.

7. Phani, G. K., Battu, G., Kotha, N. S. & Raju, L. (2011). Isolation and evaluation of tamarind seed polysaccharide being used as a polymer in pharmaceutical dosage forms. *Res J Pharm Biol Chem Sci, 2,* 274-90.

8. Tattiyakul, J., Muangnapoh, C. & Poommarinvarakul, S. (2010). Isolation and rheological properties of tamarind seed polysaccharide from tamarind kernel

powder using protease enzyme and high-intensity ultrasound. *J Food Sci, 75,* 253-260.

9. Bonferoni, M.C., Rossi, S., Tamayo, M., Pedraz, J. L., Dominguez, G. A. & Caramella, C. (1993). On the employment of l carrageenan in a matrix system. I. Sensitivity to dissolution medium and comparison with Na carboxy methyl cellulose and xanthan gum. *J Control Release, 26,* 119-27.

10. Sano, M., Miyata, E., Tamano, S., Hagiwara, A., Ito, N. & Shirai, T. (1996). Lack of carcinogenicity of tamarind seed, polysaccharide in B6C3F1 mice. Food Chem Toxicol, 34,463-467.

11. H. A. Lieberman, M. M. Rieger, G.S. Banker, Pharmaceutical Dosage Forms: Disperse Systems, volume 3, 2nd edition, Marcel Dekker, Inc., page 282.

12. Evaluation of certain food additives and contaminants. WHO technical report series, No. 751 FAO/WHO Rep. 30th report, 30 – 31, Geneva, 1987.

13. Neumann, A., Leuschener, A., Schwertfeger, W. & Dontenwill, W. (1979). Study on the acute oral toxicity of PVP in rabbits, unpublished report to BASF.

14. Indian Pharmacopoeia, 2007, volume 2, p.1334.

15. Indian Pharmacopoeia, 2007, vol 3, p.1779.

CHAPTER-VII

EXPERIMENTAL WORK

7.1. Materials used:

Gellan gum and Methacrylamide were bought from HiMedia Laboratories private limited, Mumbai, India. Cerric ammonium nitrate was purchased from Qualigens Fine chemicals, Mumbai, India. Metformin HCl (99.57% purity) was received as gift sample from East India Pharmaceutical Works Private Limited, Kolkata, India. Tamarind seed gum was purchased from local market in Kolkata, India and purified. Polyvinyl pyrrolidone (PVP K-30), magnesium stearate, purified talc, acetone and methanol were bought from Merck India Pvt. Ltd., Mumbai, India. All other reagents and chemicals used were of laboratory reagent grade and used without further purification. Triple-distilled water was used throughout the experiment.

7.2. Instrument used:

(i) Domestic microwave oven (Electrolux, C23K101.BB, India)

(ii) Perkin Elmer CHN 2400 microanalyzer for elemental analysis

(iii) FTIR (Bruker, Alpha T, Germany)

(iv) DSC-TGA, Perkin Elmer Pyris Diamond TG/DTA, Singapore

(v) Light microscope (Motic, B_1 series system microscope, India) fitted with camera (Magnus, MITS, India)

(vi) Tablet punching machine (Labpress, 10 station, Remi, Mumbai, India).

(vii) X-ray diffractometer (X-pert Pro, PANalytical, Singapore)

(viii) USP dissolution test apparatus type-II (DS-800; 6+2; SC/TR, Lab India, Mumbai, India)

(ix) Spectrophotometrically (UV-vis double beam spectrophotometer, Pharmaspec-1700, Shimazdu, Japan)

(x) Centrifuge, Remi, Mumbai, India

(xi) Scanning electron microscope (JSM6360, JEOL, UK)

(xii) Digital balance, Satwik Scale Industries, H.P. India

(xiii) Hot air oven, Remi, Mumbai, India

(xiv) Monsanto hardness tester

(xv) Roche Friabilator

(xvi) Magnetic stirrer, Remi, Mumbai, India

(xvii) Digital slide calipers, Digmatic Massschieber, model no-CD-6”CS, Mitutoyo

(xviii) Corp., Japan.

(xix) Digital pH meter, Systronics, India

Volumetric flask, pipette, measuring cylinders, funnel, petridishes etc., made of Borosil glass, Borosil Glass Pvt Ltd, Mumbai. Allglass apparatus used were of "A" class.

7.3. Software used: Design-Expert software (version 9.0.4.1, Stat-Ease Inc., Minneapolis, USA) for statistical analysis and formulation optimization.

7.4. Synthesis and Characterization of polymethacrylamide-grafted-gellan copolymer

7.4.1. Synthesis of polymethacrylamide-grafted-gellan gum

Microwave-promoted free radical initiation method was employed for the synthesis of polymethacrylamide-grafted-gellan gum (PMaa-g-GG) [1]. Amount of methacrylamide (Maa), cerric (IV) ammonium nitrate (CAN) and microwave irradiation time were taken as independent variable synthetic parameters. A total of eight batches of grafted gellan gum with different synthetic conditions were prepared as shown in Table 7.1. 1g gellan gum (GG) was dissolved in 100 mL water (solution A) and specified amount of methacrylamide was dissolved in 25 mL water (solution B). Solution B was then added to solution A and stirred for 1 hour. Specified amount of CAN was dissolved in 25 mL water and mixed with the previous mixture. The mixture was then exposed to microwave in a domestic microwave oven (Electrolux, C23K101.BB, India) at 500 Watt for a specified time (Table 7.1) following one minute heating and one minute cooling cycle. Then it was left for overnight. Acetone was added to it in 1:2 ratios (reaction-mixture: acetone) for precipitation of the grafted gellan gum. The precipitate was

collected and added in 50 mL of 80% v/v aqueous methanol to remove the unreacted free monomer and the homopolymer (polymethacrylamide) formed during graft reaction. After stirring for 1 minute it was allowed to stand for further precipitation. The precipitate was collected and finally washed with distilled water and dried at 40°C to a constant weight. The dried grafted gellan gum was then powdered using pestle and mortar and passed through #100 mesh. Different grafting parameters such as % grafting (%G), grafting efficiency (%GE) and % conversion (%C) were calculated using following formula (Eq. 7.1 to 7.3) to assess the efficiency of the synthesis [2].

$$\% \text{ grafting } (\%G) = (W_1 - W_0) \times 100/W_0 \quad (7.1)$$

$$\% \text{ grafting efficiency } (\%GE) = (W_1 - W_0) \times 100/W_2 \quad (7.2)$$

$$\% \text{ conversion } (\% C) = W_1 \times 100/W_2 \quad (7.3)$$

Where, W_0, W_1 and W_2 are the weight of native gellan gum, grafted gellan gum and methacrylamide, respectively.

Table 7.1

Synthetic conditions, grafting parameters and elemental analysis of polymethacrylamide-grafted-gellan.

Batch no	Amt. of Maa (g)	Amt. of CAN (mg)	MW irradiation time (min)	%G	%GE	%C	Elemental analysis		
							%C	%H	%N
GG	-	-	-	-	-	-	35.55	5.89	0.00
S1	10	400	5	669.58	67.09	77.11	38.81	7.14	10.07
S2	10	400	1	660.16	66.01	76.01	44.77	8.54	11.91
S3	10	150	5	147.68	14.78	24.79	45.05	7.65	8.94
S4	10	150	1	483.73	48.74	58.82	46.10	8.44	11.71
S5	5	400	5	180.60	36.12	56.12	42.44	7.80	9.08
S6	5	400	1	285.93	57.22	77.23	43.69	7.94	10.44
S7	5	150	5	78.09	15.22	35.79	41.36	7.25	6.07
S8	5	150	1	118.54	23.81	43.89	43.70	7.25	7.53

%G, % grafting; %GE, % grafting efficiency; %C, % conversion; %C, carbon percentage; %H, hydrogen percentage; %N, nitrogen percentage.

7.4.2. Characterization of grafted gellan gum

7.4.2.1. Elemental analysis

The elemental analysis of the native gellan gum and eight different batches of Pmaa-g-GG were performed using a Perkin Elmer CHN 2400 microanalyzer to determine the carbon, hydrogen and nitrogen content.

7.4.2.2. Infrared spectral analysis

FTIR spectra of gellan gum and Pmaa-g-GG (S1 batch) were obtained using FTIR (Bruker, Alpha T, Germany) to predict the possible changes of functional groups of grafted gellan gum as compared to its native form. A small amount of each material was mixed with KBr (1%w/w sample) and compressed into tablet. The scanning range selected was 550-4000cm^{-1}.

7.4.2.3. Differential Scanning Calorimetry (DSC) and thermogravimetric analysis (TGA)

DSC and TGA thermograms of gellan gum, Pmaa-g-GG (S1 batch), were recorded under N_2 flow (50 mL/min) using Perkin Elmer Pyris Diamond TG/DTA, Singapore, at a heating rate of 10°C/min and sample mass of 3-5 mg. The heating range was from 30°C to 500°C.

7.4.2.4. Acute oral toxicity study

Acute oral toxicity study of polymethacrylamide grafted gellan gum (Pmaa-g-GG; S1 batch) was performed as per the "Organisation of Economic Co-operation and Development (OECD) guideline for the test of chemicals 425, adopted 17 December 2001". Six nulliparous and non-pregnant eight weeks old female mice

(*Swiss albino species*) were taken for the study, one of which was taken as control. The study protocol was prior approved by the Animal Ethics Committee (CPCSEA approval no: 1682/EO/a/13/CPCSEA) of BCDA College of Pharmacy & Technology, Kolkata, India. Mice were housed in polycarbonate cage with sufficient food and demineralized water was available to them ad libitum at 19°C – 25°C and 40-70% relative humidity in a 12 hour light on/off cycle. A single dose of 2000 mg/kg body weight of Pmaa-g-GG was administered by gavages using a stomach tube to the first test animal. The same dose was administered to the remaining four test animals after survival of the first test animal. No dose was administered to the control animal. The animals were kept under the continuous observation up to 4 h after dosing. The observation was continued up to 14 days occasionally at predetermined intervals. The mortality rate was evaluated by visible observation and reported accordingly.

7.4.2.5. Histopathological study

The control animal and one survived test animal (randomly selected from the five test animals) were euthanized with diethyl ether and sacrificed. Their brain, lung, stomach, kidney, heart and liver were separated and cleaned with 0.9% w/v NaCl solution and then fixed in 10% formalin solution. Each organ was dehydrated serially with 50% alcohol, 80% alcohol and finally with absolute alcohol. It was embedded in melted paraffin and cooled. A thin section of each organ was obtained by cutting the embedded block with a microtome. The sections were then mounted on glass slides and stained with hematoxylin and a counter stain eosin. A cover slip was fixed on each section to obtain a permanent slide.

Finally the slides were examined through a light microscope (Motic, B_1 series system microscope, India) fitted with camera (Magnus, MITS, India) and the fields (40x-view) were captured by the camera to obtain photomicrograph. The photomicrographs of the test organs were compared with that of controls.

7.4.3. Results and discussion

7.4.3.1. Synthesis of polymethacrylamide-g-gellan gum

Graft co-polymerization of methacrylamide onto gellan gum was carried out employing grafting technique by free-radical initiation. In several study, Cerric (IV) ammonium nitrate was used as free-radical initiator [3, 4]. Along with free-radical initiator, microwave-promoted graft-copolymerization has also been reported [5, 6]. Table 7.1 presents the different synthetic conditions of microwave-promoted, cerric (IV) induced graft copolymerization, % grafting, % grafting efficiency, % conversion, % carbon, % hydrogen and % nitrogen of native gellan gum and its grafted forms. For the optimization of the synthetic conditions, amount of CAN, methacrylamide and microwave irradiation time were taken as independent synthetic variables by keeping the other parameters constant. From the values of different grafting parameters shown in Table 7.1, it is clear that amount of CAN has major positive influence on the higher grafting efficiency irrespective of other variables. The anomeric –CHOH on gellan gum-backbone is the reactive vicinal group, where the grafting is initiated. The overall reaction mechanism is that, cerric (IV) ammonium nitrate gets dissociated into Ce^{4+}, ammonium and nitrate ions and then cerric (IV) ion attacks the gellan gum

macrochains resulting formation of a GG-cerric complex. The cerric (IV) ions in the complex get then reduced to cerric (III) ions by oxidizing hydrogen atom and thereby creating a free radical onto GG-backbone. So, a threshold amount of redox initiator is required for the formation of the free radical. The grafting of Maa onto GG was then initiated by the free radical reacting with the monomer. In the presence of Maa, the GG free radical is chemically coupled to the monomer unit, thereby resulting in a covalent bond between Maa and GG to create the chain reaction for propagation. Cerric ions also attack monomer resulting the formation of methacrylamide free radicals which join with another monomer molecule by a covalent bond leading to propagation of homopolymer chains. Finally, termination was achieved through a combination of two propagating chain free radicals initiated from GG-backbone. Termination may also occur by coupling between GG-propagating-free-radical and monomer free radical or between GG-propagating-free-radical and homopolymer-propagating-free radical (composed of only monomers). Homopolymer is formed due to termination by coupling between two homopolymer-free-radicals. A mathematical relation between % grafting and the independent synthetic variables was obtained from the statistical analysis by Design-Expert software which is expressed in Eq. (7.4).

$$\% \text{ grafting} = + 336.39 + 64.89*\text{Maa} + 0.97*\text{CAN} - 29.53*\text{MW} \qquad (R^2 = 0.8600) \tag{7.4}$$

Where, Maa = methacrylamide, CAN = Cerric ammonium nitrate and MW = Microwave irradiation time. This relation indicates the positive effect of Maa and CAN and negative effect of microwave on grafting. The synthetic condition for

the synthetic batch S7 results in lowest grafting whereas the batch S1 and S2 result highest yield. The degree of grafting was shown to increase with the increase in concentration level of methacrylamide at both higher and lower level of two other independent synthetic factors. Similarly, grafting efficiency and other grafting parameters are proportional to the concentration of cerric ammonium nitrate. The microwave irradiation provides rapid transfer of energy in the bulk of the reaction mixture, which reduces reaction time therefore it acts as a catalyst and gives a synergistic activity. This phenomenon substantiates the results of the cerric (IV) initiated microwave-promoted graft copolymerization. In case of batch S1 and S2 the % grafting were nearly same though microwave irradiation time was 5 min (S1) and 1 min (S2), whereas, in case of other batches, % grafting was shown to be inversely proportional to microwave irradiation time. This may be due to the fact that a saturation of free radical points on gellan gum backbone gets generated in a certain time period of microwave irradiation. After that a further irradiation results in the breakage of propagated chains on the free radical sites and premature advance termination [7].The structures of native gellan gum and Pmaa-g-GG have been shown in Fig.7.1. The proposed mechanism of the reaction is as follow:

Initiation:

$Ce(NH_4)_2(NO_3)_6 \rightarrow Ce^{4+} + 2NH_4^+ + 6NO_3^-$

$Ce^{4+} + GG\text{-}OH \rightarrow complex \rightarrow GG\text{-}O^{\bullet} + Ce^{3+} + H^+$

$GG\text{-}O^{\bullet} + M \rightarrow GG\text{-}OM_1^{\bullet}$

$Ce^{4+} + M \rightarrow M^{\bullet} + Ce^{3+} + H^+$

$M^{\bullet} + M \rightarrow M_2^{\bullet}$

Propagation:

$GG\text{-}OM_1^{\bullet} + M \rightarrow GG\text{-}OM_2^{\bullet}$

- - - - - - -   - - -   - - - - - -
- - - - - - -   - - -   - - - - - -

$GG\text{-}OM_{n-1}^{\bullet} + M \rightarrow GG\text{-}OM_n^{\bullet}$

$M_2^{\bullet} + M \rightarrow M_3^{\bullet}$

- - - - - - -   - - -   - - - - - -
- - - - - - -   - - -   - - - - - -

$M_{p-1}^{\bullet} + M \rightarrow M_p^{\bullet}$

Termination:

$GG\text{-}OM_n^{\bullet} + GG\text{-}OM_m^{\bullet} \rightarrow GG\text{-}OM_{(m+n)}$ (graft copolymer)

$GG\text{-}OM_n^{\bullet} + M^{\bullet} \rightarrow GG\text{-}OM_{(n+1)}$ (graft copolymer)

$GG\text{-}OM_n^{\bullet} + M_p^{\bullet} \rightarrow GG\text{-}OM_{(n+p)}$ (graft copolymer)

$M_p^{\bullet} + M_q^{\bullet} \rightarrow M_{(p+q)}$ (homopolymer)

(GG-OH= native gellan gum; M= methacrylamide)

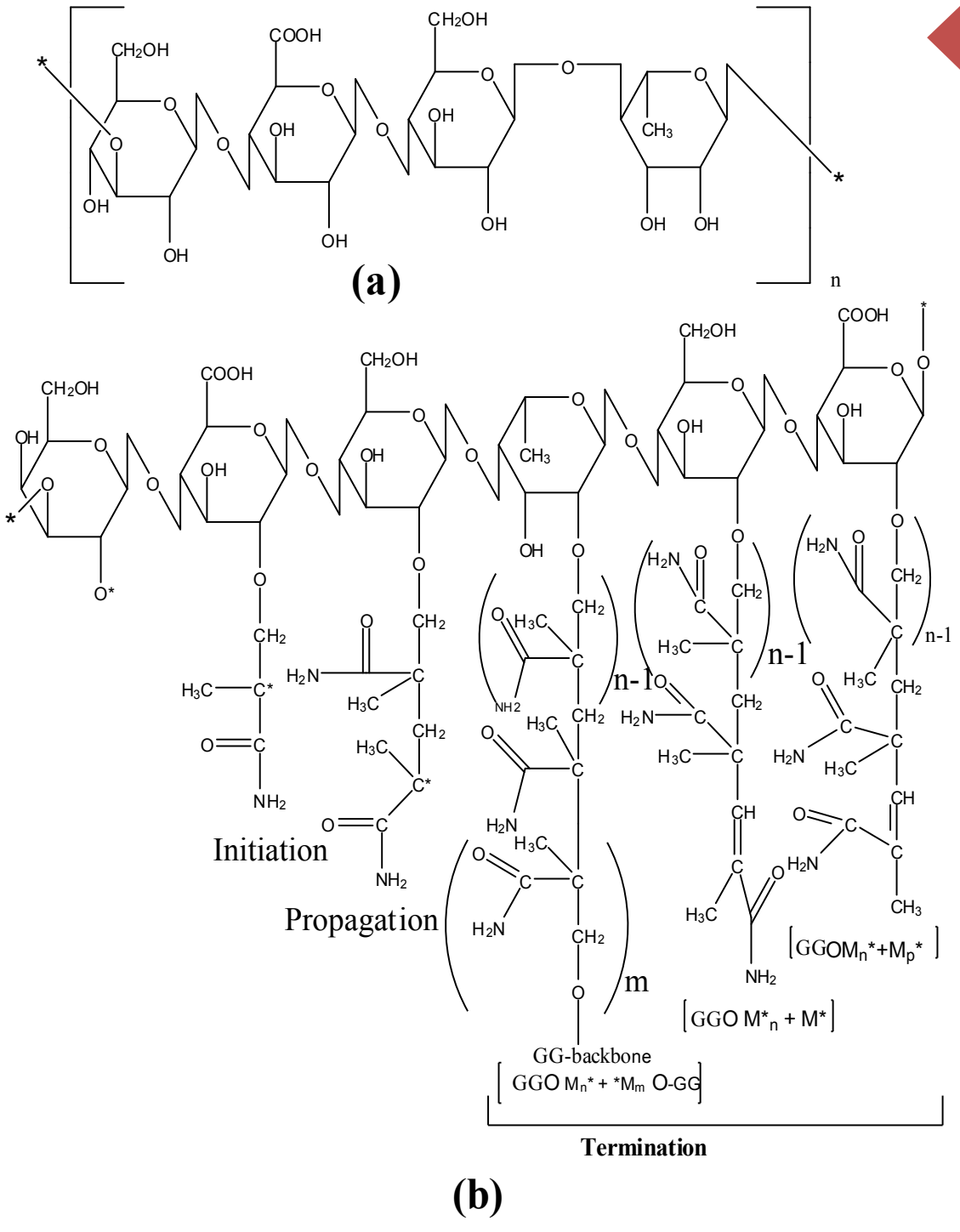

Fig. 7.1: (a) Structure of gellan (b) polymethacrylamide-grafted-gellan (Pmaa-g-GG)

7.4.3.2. Elemental analysis

The results of elemental analysis for GG and eight different synthetic batches of Pmaa-g-GG are shown in Table 7.1. There is no nitrogen content in gellan gum. The values of nitrogen percentage in all eight batches of Pmaa-g-GG estimated in the analysis were significant and these values ratify the grafting of methacrylamide onto gellan gum backbone. The higher values of %N in case of S_1, S_2, S_4 and S_6 accredit the higher % grafting, indicates that the higher values of methacrylamide and cerric ammonium nitrate have positive influence on % grafting whereas microwave irradiation exerts little negative effect on the yield of the grafted gellan gum. This negative effect of microwave irradiation may result from the breakage of propagated chains on the free radical sites and premature advance termination after an optimum time period during irradiation.

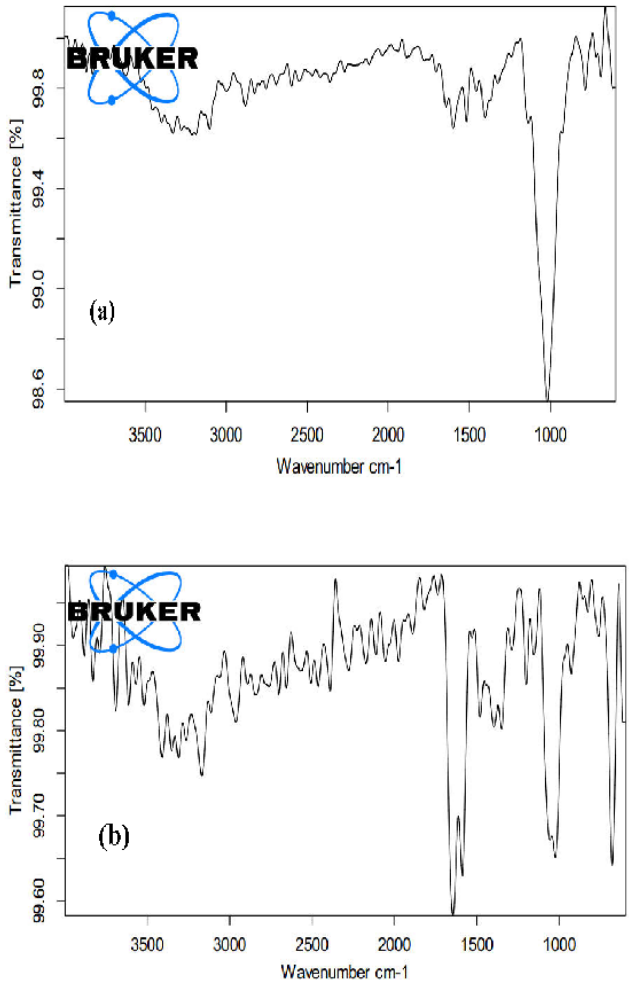

Fig.7.2. FTIR spectrum of (a) gellan, (b) polymethacrylamide-grafted-gellan (Pmaa-g-GG; S1)

7.4.3.3. Infrared spectral analysis

Infrared spectra of gellan gum and grafted gellan gum are shown in Fig. 7.2(a) and 7.2(b) respectively. Gellan gum showed characteristic peaks at 1645.05 cm^{-1} for carbonyl group indicating C=O stretching, at 3212.87 cm^{-1} for –OH group, at 2883.27 cm^{-1} for –COOH group, at 1136.87 cm^{-1} for alcoholic –C-O group, and at 1706.30 cm^{-1} for –C=O group.

Some differences were observed in spectra of grafted gellan gum compared to gellan gum. The infrared spectra of methacrylamide grafted gellan gum shows characteristic peaks at 3829.24 cm^{-1} - 3169.37 cm^{-1} for $–NH_2$ group, due to addition of methacrylamide which was grafted onto gellan gum. An additional peak at 1645.78 cm^{-1} has been observed due to N-H bending. A significant peak is also observed at 1024. 59 cm^{-1} for CH-O-CH_2 group which occurs due to grafting reaction between OH group of C_2 of gellan gum and π bond of methacrylamide.

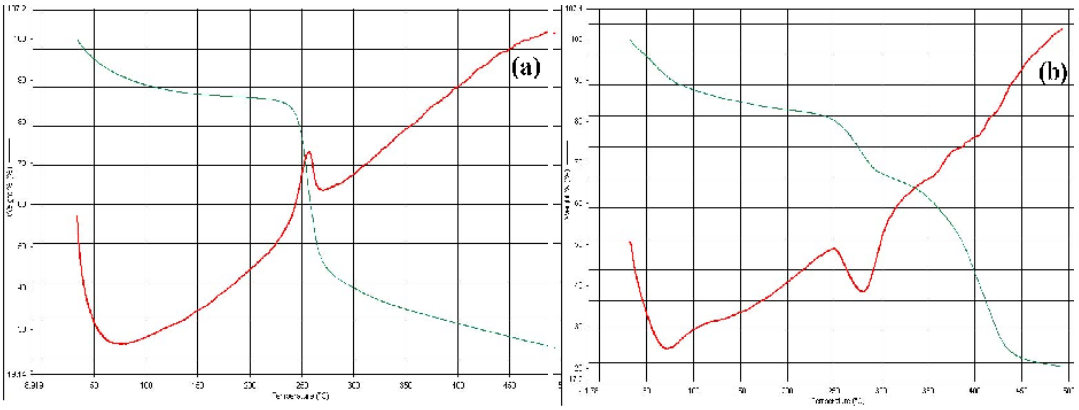

Fig.7.3. DSC thermogram of (a) gellan, (b) polymethacrylamide-grafted-gellan (Pmaa-g-GG; S1)

7.4.3.4. Differential scanning calorimetry and thermogravimetric analysis

DSC and TGA curves of GG and Pmaa-g-GG, are shown in Fig. 7.3(a) and 7.3(b), respectively. An endothermic peak at 70^{o}C and an exothermic peak at around 255^{o}C are recorded in DSC thermogram of GG. TGA thermogram of GG shows a 10% weight loss at 70^{o}C and about 45% weight loss in the temperature

range from 240^{o}C to 300^{o}C. The correlation between endothermic peak and simultaneous reduction in weight at 70^{o}C indicates the loss in moisture present in the gellan gum. The exothermic peak at 255^{o}C and reduction in weight in the temperature range from 240^{o}C to 300^{o}C is probably due to depolymerization with formation of water, carbon monoxide and methane [8]. DSC thermogram of Pmaa-g-GG shows an endothermic peak at 70^{o}C similarly with GG indicating loss in moisture content, which is further established by the 10% reduction in weight at 70^{o}C observed in corresponding TGA curve. Another endothermic peak is recorded at 280^{o}C, which may be due to polymeric chain degradation of the grafted polymers. This fact proves the enhanced thermal stability of the grafted gellan gum compared to its native form because grafted gellan gum undergoes thermal decomposition at 280^{o}C unlike its native form which degrades at 255^{o}C. The specific endothermic peak at 280^{o}C observed in DSC curve for grafted polymer also demonstrates its crystalline nature.

Table 7.2

Mortality rate of animals after a single dose of 2000 mg/kg body weight.

Observation time period	Mortality				
	$Animal_1$	$Animal_2$	$Animal_3$	$Animal_4$	$Animal_5$
30 min	0	0	0	0	0
4hr	0	0	0	0	0
1^{st} day	0	0	0	0	0
3^{rd} day	0	0	0	0	0
7^{th} day	0	0	0	0	0
14^{th} day	0	0	0	0	0

'0', survival and 'X', death.

7.4.3.5. Acute oral toxicity study

The results are shown in Table 7.2. There was no mortality found within the observation period of 14 days after dosing. As per the "organization of Economic Co-operation and Development (OECD) guideline for the test of chemicals" 425, adopted "17 December 2001" Annexure-4, the LD_{50} value is greater than 2000mg/kg dose of Pmaa-g-GG. As per the globally harmonized system (GHS) if LD_{50} value is greater than the 2000 mg/kg dose then the test product will be fallen under the "Category 5" and toxicity rating will be "zero". So, Pmaa-g-GG is under the "category 5" as well as toxicity rating is "zero".

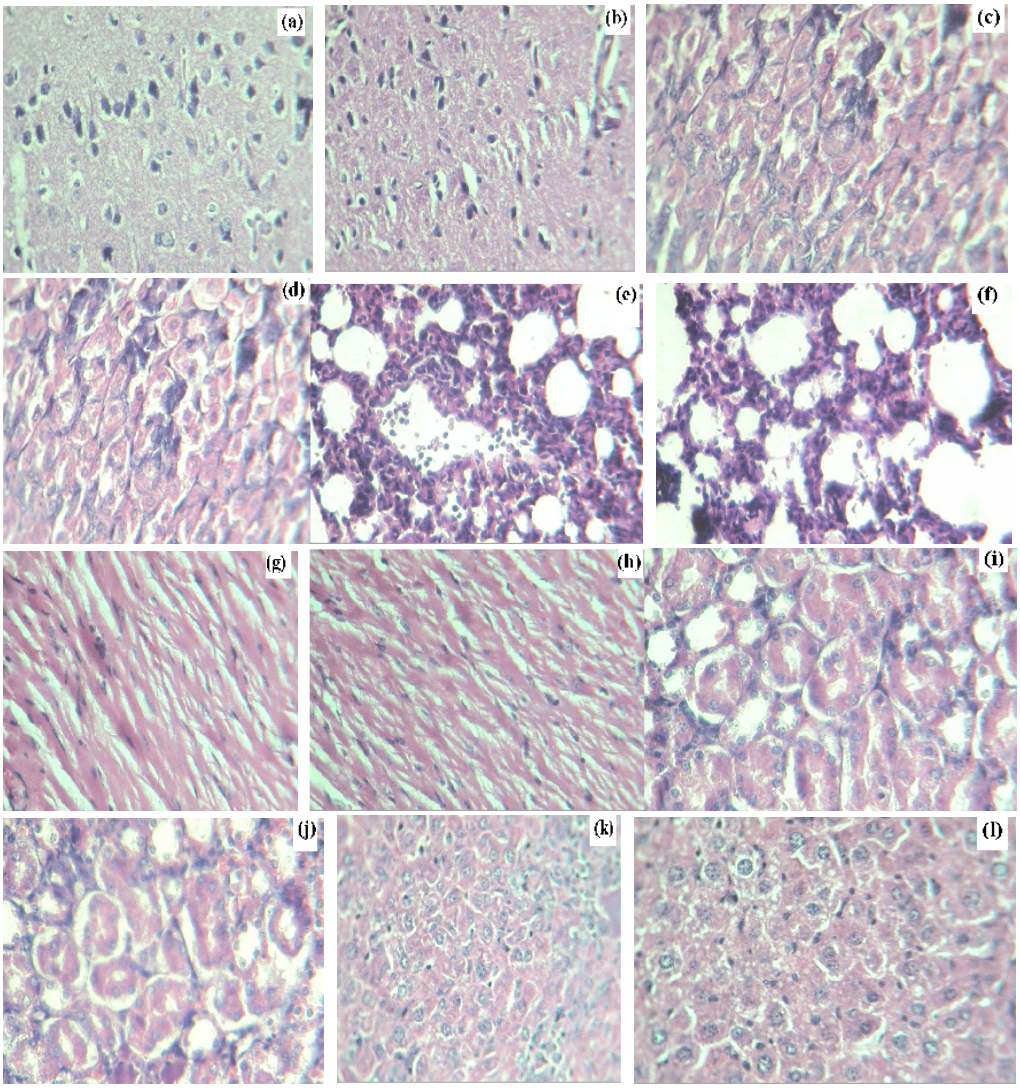

Fig.7.4. Microscopic cross-sectional view (40x) of (a) control-brain (b) test-brain (c) control-stomach (d) test-stomach (e) control-lung (f) test-lung (g) control heart (h) test heart (i) control-kidney (j) test-kidney (k) control liver (l) test-liver.

7.4.3.6. Histopathological study

The 40x micrographs of various organs of control and test animals are shown in the Fig. 7.4. The micrographs of both control and test brain depict morphologically similar granular cells. There is no significant change in

morphology of stratified squamous epithelial cells observed in the micrographs of control and test stomach. Both lung micrographs show alveoli, inter-alveolar septa and connective tissue sheets containing capillary bed clearly without sign of any type of morphological change. The micrograph of control heart provides an overview of cardiac myocytes having a centrally located nucleus, intercalated disks that connect the end of the one cardiac myocyte to the beginning of the next and perkinje fibres. Similar morphological pattern was shown in the micrograph of test heart. 40x micrographs of both control and test kidney show in increasing detail the cuboidal epithelial cells of the loop of Henle and collecting tubules with similar morphology. Both micrographs of test and control liver depict normal hepatocytes, large polygonal cells with central nuclei and Kuppfer cells. Thus histopathological examination establishes the physiological compatibility of the grafted gellan gum.

7.5. Formulation of gastroretentive tablet of metformin hydrochloride based on polymethacrylamide grafted gellan copolymer and tamarind seed gum composite matrix.

7.5.1. Experimental

7.5.1.1. Preparation of Standard curve

100 mg metformin HCl (MFH) was accurately weighed and dissolved in phosphate buffer pH 6.8 (PB) and volume made up to 100 ml (solution 1). 10 ml of solution 1 was diluted with PB to make 100ml (solution 2). Different volumes of solution 2 were taken in five different 25 ml volumetric flasks and volumes were made up with 1ml 0.1N HCl acid and sufficient quantity of PB to produce five different standard solutions with concentrations of 4, 8, 12, 16 and 20µg/ml. One of the standard solutions was then scanned from 190 nm to 1100 nm using UV/ Visible Spectrophotometer (SHIMAZDU, PHARMASPEC 1700, Japan) to obtain λ max. Then absorbances of all standard solutions were measured at observed λ max. This was repeated for three times. Then the average absorbance vs. conc. was plotted and the equation and R^2 value of the curve were obtained. The observed λ max was 230 nm and the equation obtained was y = 0.0798x + 0.0138 and R2 value was 0.9999.

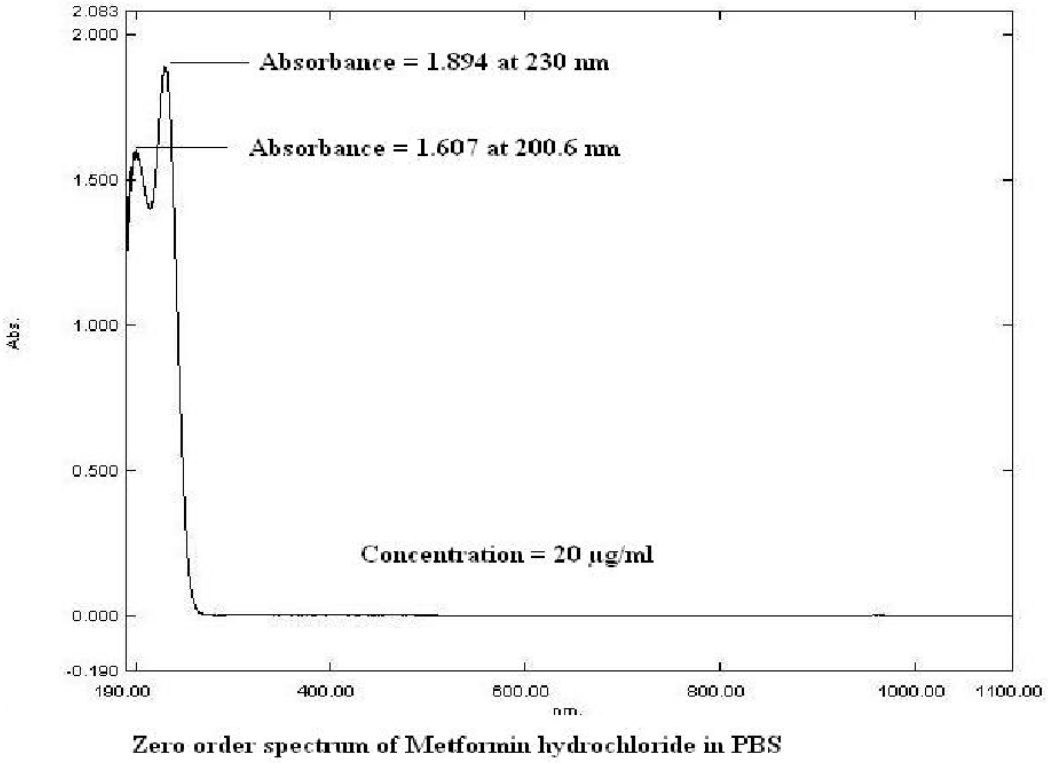

Figure7.5: Zero order spectrum of metformin hydrochloride in phosphate buffer pH 6.8.

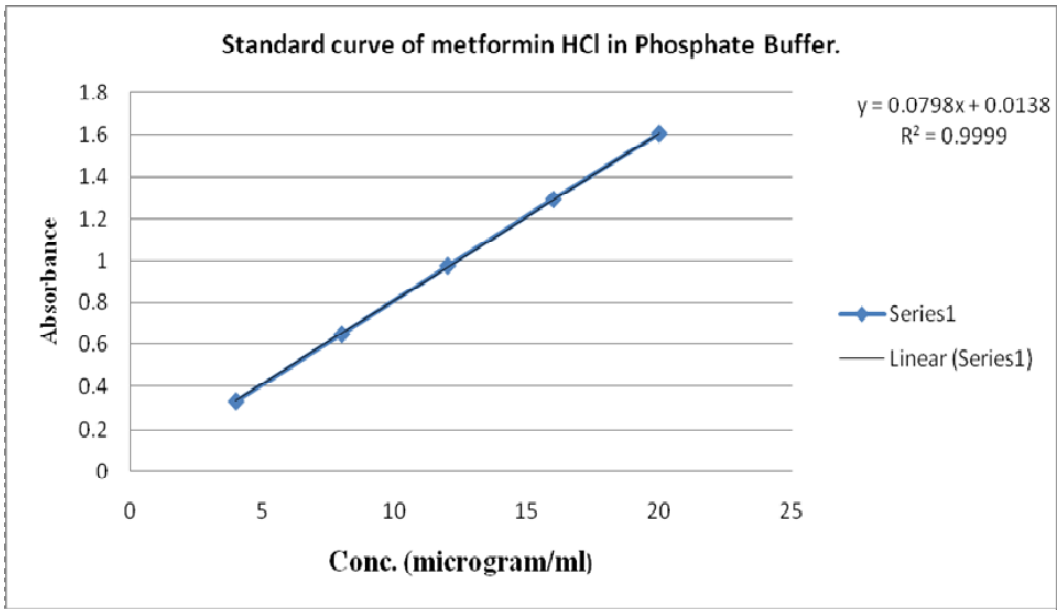

Figure7.6: Standard curve of metformin hydrochloride in phosphate buffer pH 6.8

7.5.1.2. Isolation of tamarind seed gum (TSG)

Tamarind seed gum was purified from commercially available tamarind seed gum purchased from local market in Kolkata, India. Approximately 20 g of the native form was dispersed adding very little amount at a time in 1000 ml distilled water to obtain slurry. The slurry was boiled for 20 min under stirring condition in a water bath. The resulting clear solution was kept overnight so that most of the proteins and fibres settled out. The solution was then centrifuged at 5000 rpm for 20 min. The supernatant was separated and poured into twice the volume of absolute ethanol with continuous stirring for 2 mins. It was allowed to stand for 1h for precipitation of the gum. The precipitate was then washed with distilled water and dried at 60^{0}C to constant weight. The dried gum obtained was crushed to fine powder using domestic mixer and grinder and then it was passed through sieve no. 100. The powder passed through the sieve no.100 was taken for formulation [9].

7.5.1.3. Preparation of polymethacrylamide-grafted-gellan copolymer (Pmaa-g-GG; S2 batch)

Pmaa-g-GG co-polymer having 669.58% grafting (67.09% grafting efficiency) was prepared following the method reported elsewhere [10]**.** Briefly, 1 g gellan gum (GG) was dissolved in 100 mL water (solution A) and 10 g of methacrylamide was dissolved in 25 mL water (solution B). Solution B was then added to solution A and stirred for 1 h. 400 mg of CAN was dissolved in 25 mL water and mixed with the previous mixture. The

mixture was then exposed to microwave in a domestic microwave oven (Electrolux, C23K101.BB, India) at 500 W for 5 min following 1 min heating and 1 min cooling with ice-cold water cycle. Then it was left for overnight. Acetone was added to it in 1:2 ratios (reaction-mixture: acetone) for precipitation of the grafted copolymer. The precipitate was collected and added in 50 mL of 80% (v/v) aqueous methanol to remove the unreacted free monomer and the homopolymer (polymethacrylamide) formed during graft reaction. After stirring for 1 min it was allowed to stand for further precipitation. The precipitate was collected and finally washed with distilled water and dried at 40^{o}C to a constant weight. The dried grafted gellan gum was then powdered using pestle and mortar and passed through #100 mesh. The product was stored in vacuum desiccator until used.

7.5.1.4. Formulation of gastroretentive extended release (GRER) tablet of metformin by 2^3full factorial design

A 2^3 full factorial design was adopted to evaluate the influence of independent factors such as quantity of Pmaa-*g*-GG (X_1), tamarind seed gum (X_2) and sodium bicarbonate (X_3) on the responses (dependent variables) such as buoyancy lag time (BLT), mucoadhesive strength (*F*), cumulative percent drug release at 1h, 2h, 6h and 10h (CPR1h, CPR2h, CPR6h and CPR10h respectively) in simulated gastric fluid (pH 1.2), and drug release rate constant using Design-Expert software (version 9.0.4.1, Stat-Ease Inc., Minneapolis, USA). Three factors were varied at two different levels (high and low) and

the experimental trial was carried out on all eight possible combinations keeping other factors constant (Table 7.3). The low and high level of X_1 , X_2 and X_3 were set at (150 mg; 250mg), (150mg; 250mg) and (80mg; 120mg) respectively.

Table: 7.3

Formula per tablet for each formulation obtained from 2^3 full factorial design.

Formulation code	MFH (mg)	Pmaa-*g*-GG (mg)	TSG(mg)	SBC(mg)	Talc(mg)	Magnesium stearate(mg)	Copolymer : TSG
F1	500	150	150	80	10	10	1:1
F2	500	150	250	80	10	10	3:5
F3	500	250	150	80	10	10	5:3
F4	500	250	250	80	10	10	1:1
F5	500	150	150	120	10	10	1:1
F6	500	150	250	120	10	10	3:5
F7	500	250	150	120	10	10	5:3
F8	500	250	250	120	10	10	1:1
OF	500	158.80	244.99	120	10	10	2.3:3.13

OF, optimized formula; SBC, sodium bicarbonate.

7.5.1.5. Preparation of GRER tablet

Gastroretentive extended release monolithic matrix tablets of metformin HCl were prepared with polymethacrylamide grafted gellan gum, tamarind seed gum and sodium bicarbonate (SBC) of different eight batches employing wet granulation method [10]. A batch of 10 tablets was prepared at a time for each

formulation (Table 7.3). Briefly, semisolid dough was first prepared from the grafted gellan with minimum amount of hot water (50^0C) and then tamarind seed gum, sodium bicarbonate and drug were mixed intimately with it. The mass was then passed through #18 mesh to obtain granules. These granules were dried at 60^0C for 20 mins and passed through # 18 mesh. The granules were lubricated with purified talc (10 mg/tablet) and magnesium stearate (10 mg/tablet). The tablets were compressed in a rotary tablet machine with 12 mm single punch diameter (Labpress, 10 station, Remi, Mumbai, India). Hardness was within the range of 4-5 kg/m^2.

7.5.1.6. Fourier-transform infrared (FTIR) spectroscopy

FTIR spectra of GG, Pmaa-g-GG, TSG, Metformin and tablet formulation (F8) were obtained using FTIR (Bruker, Alpha T, Germany) to predict the possible interactions between drug and polymers. A small amount of each material was mixed with KBr (1%w/w sample) and compressed into tablet. The scanning range selected was 550-4000 cm^{-1}.

7.5.1.7. Differential scanning calorimetry (DSC) study and thermogravimetric analysis (TGA)

DSC and TGA thermograms of drug MFH and tablet formulation (F8) were recorded under N_2 flow (150 mL/min) using Perkin Elmer Pyris Diamond TG/DTA, Singapore, at a heating rate of 10^0C/min in a platinum crucible with alpha alumina powder as reference and sample mass of 3-5 mg to detect possible thermal changes of the drug during tabletting process and interaction between drug and polymers if any. The heating range was from 30^0C to 500^0C.

7.5.1.8. X-ray diffraction (XRD) study

X-ray powder diffractometry of drug metformin HCl and its tablet formulation (F8) were recorded using X-ray diffractometer (Rigaku, Ultima-III, Japan). The diffractometer was run at a scanning speed of 2^0/min with Cu target slit of 10 mm and a chart speed of 2^0/2cm per 2θ and the angular range fixed was from 10^0 to 70^0 to detect possible changes of crystalinity of drug or other interaction with excipients.

7.5.1.9. Determination of drug content of tablet and weight variation

Five tablets were finely powdered; a quantity equivalent to 100 mg of MFH was accurately weighed and transferred into 100 ml volumetric flask containing USP phosphate buffer solution (PB) of pH 6.8. The mixture was allowed to stand for 12 h with an intermittent shaking. The mixture was filtered and the filtrate following suitable dilution was analyzed for MFH content at 230 nm using a UV–Visible spectrophotometer (UV-visible double beam spectrophotometer, Pharmaspec-1700, Shimazdu, Japan). The reliability of the above analytical method was justified by conducting recovery analyses at three levels of spiked drug solution and for three consecutive days in the absence or presence of the polymers. The recovery averaged 99.02 ±1.17%. 10 tablets of each batch were weighed individually and average with % deviation was then calculated.

7.5.1.10. Determination of hardness and friability

Hardness of the prepared tablets was measured to test the mechanical strength. This was carried out using Monsanto hardness tester. The tablet was placed between the two plungers, and a zero reading was taken. The upper plunger

was then forced against the spring by turning a threaded bolt until the tablet fractured. The force of fracture was recorded and the zero force reading was deducted from it. The fracture force in kg was the measurement of the hardness of the tablets. Friability study was carried out using Roche fribilator. A tablet was weighed accurately and placed in the friabilator (mvtex, Kolkata, India). Then it was rotated at 25 rpm for 4 minutes. After that, the tablet was taken out and reweighed. The % friability (f) was calculated using the formula:

$f = (w_1 - w_2) \times 100\% / w_1$

where w_1 is the previous weight and w_2 is the weight after operation.

7.5.1.11. In vitro buoyancy study

The *in vitro* buoyancy of the GRER composite matrix tablets containing metformin HCl was investigated following reported procedure with some modifications [11]. One tablet was placed in the dissolution apparatus type II (DS-800; 6+2; SC/TR, Lab India, Mumbai, India) containing 900 ml of simulated gastric fluid (0.1N HCl with 1.8 g of NaCl; pH 1.2) maintained at 37 ± 0.5^{o}C. The rotation speed of the paddle was set at 50 rpm. The time required for rising to the surface of dissolution medium and the tablet remaining buoyant in acidic medium were recorded to measure the buoyant lag-time (BLT) and total buoyant time (TBT), respectively. The state of the tablets during buoyancy testing were checked visually each hour for 10 h and at the end point of 24 h. buoyancy test for all formulations were performed in triplicate.

7.5.1.12 Tablet density

The density (*D*) of GRER tablets were calculated from tablet height, diameter and weight using the formula expressed in Eq.7.5 [12].

$$D(g/cm^3) = \frac{w}{(m/2)^2 \times \pi \times h} \qquad \text{(Eq.7.5)}$$

Here, *m* is the diameter of a tablet, π is the circular constant, *h* is the height of a tablet, and *w* is the weight of a tablet. All measurements were performed in six replicates. The averages and standard deviations were calculated and reported.

7.5.1.13. Ex-vivo mucoadhesion testing

Mucoadhesive potential of the *GRER* tablets were evaluated by conducting ex vivo mucoadhesion study using a modification of the assembly described earlier [13] with goat gastric mucosa as the model membrane. The mucosal membrane was excised by removing the underlying connective and adipose tissue, and equilibrated at 37^0C±1^0C for 30 minutes in phosphate buffer pH 6.8 before the study. The tablet was lowered onto the mucosa under a constant weight of 5 g for a total contact period of 1 minute. Mucoadhesive strength (*F*) was assessed in terms of the weight in grams required to detach the tablet from the membrane. The tests were repeated in triplicate for each formulation.

7.5.1.14. Surface morphology analysis by scanning electron micrography

The surface morphology of the tablet (F8) before and after the dissolution study were analyzed by a scanning electron microscope (JSM6360, JEOL, UK)

equipped with secondary electron detector. The samples were coated using gold to increase the conductivity of the electron beam. The operating conditions were an accelerating voltage of 17 kV; the working distance was 12 mm at spot size of 45.

7.5.1.15. Determination of equilibrium water uptake (swelling index), swelling-kinetic and water penetration velocity

Drug free composite matrix tablets were weighed and placed in wire baskets and immersed in 200 ml simulated gastric fluid (pH 1.2) at 37^{o}C for 24 h. The baskets were removed from the solution at the end of the period and weighed after removing the surface water with tissue paper in an electronic balance (Electronic Balance, model TP313, Denver Instrument, India). Equilibrium water uptake (swelling index, %) of the tablets was determined from the following relationship (Eq.7.6) :

$$W_E = \frac{(w_1 - w_0) \times 100}{w_0} \qquad \text{(Eq. 7.6)}$$

Where, W_E is the equilibrium water uptake (%), w_0 is the dry weight of tablet plus basket and w_1 is the weight of tablet plus basket after removal from the solution.

The kinetics of swelling of the matrix tablets were studied by measuring the increase in weight of tablet after immersion in simulated gastric fluid (pH 1.2) as a function of time, t [14]. A plot of the weight, W, in grams of the water absorbed per gram of the dry matrix of the tablet against time, t in minutes, gives the swelling isotherm. The horizontal portion of the isotherm corresponds to

equilibrium swelling. To obtain a linear expression, *t/W* is plotted against *t* according to the Eq. 7.7:

$$\frac{t}{W} = A + Bt \qquad \text{(Eq. 7.7)}$$

Rearranging and differentiate the Eq. 7.7, the following expression (Eq. 7.8) can be obtained:

$$\frac{dW}{dt} = \frac{A}{(A + Bt)^2} \qquad \text{(Eq. 7.8)}$$

as $t \rightarrow 0$, the above equation gives the *initial swelling rate*, $dW/dt = 1/A$, which is the reciprocal of the intercept of *t/W* versus *t* plot. The reciprocal of the slope, $1/B = W_\infty$ is the equilibrium swelling, that is, the theoretical maximum uptake of buffer solution at t_∞. The *Matrix Hydration*, *H*, is calculated using the following formula (Eq. 7.9):

$$H = \frac{(w_s - w_0)}{w_s} \qquad \text{(Eq.7.9)}$$

Where, w_s, is the weight of swollen gel at equilibrium and w_0 is the weight of xerogel. The water penetration velocity into the matrices was estimated from the swelling kinetic data using following equation (Eq. 7.10) [15]:

$$V = \frac{1}{2\rho A} \times \frac{dW}{dt} \qquad \text{(Eq.7.10)}$$

where *V* indicates penetration velocity, *dW/dt* represents the slope of *W* versus time curve, ρ is the density of simulated gastric fluid at 37^{0}C and *A* denotes surface area of tablet.

7.5.1.16. Viscoelastic study

The hydrophilic polymers present in the composite matrix tablet forms a hydrogel absorbing water from gastric fluid subsequently after administration and the rheological behavior specially viscoelastic nature which is a function of microstructure of the hydrogel, greatly influence the pattern of drug release from the tablet. Viscoelastic properties are measured mainly by dynamic mechanical tests which evaluate small periodic deformations, structural breakdown or rearrangement [16]. The dynamic mechanical "strain sweep" test examines the microstructural properties of the hydrogel under increased strain. It measures the storage modulus, G', which is an indicator of elastic behavior and reveals the ability of the polymer system to store elastic energy associated with recoverable elastic deformation. The loss modulus, G'', is a measure of the dynamic viscous behavior that relates to the dissipation of energy associated with unrecoverable viscous loss. Viscoelastic study was done on three 10%, w/v, aqueous gel containing PMaa-*g*-GG and TSG in 1:1 (R1), 3:5 (R2) and 5:3 (R3) ratio using Rheometer, Anton Paar, Austria. Storage modulus (G'), loss modulus (G''), and τ (shear stress) were measured at different levels of % strain (γ) and time, separately, and plotted. Viscosity (η) against shear rate was also plotted. In strain-sweep, angular frequency was kept constant at 10 rad/s and in time-sweep, strain and angular frequency were kept constant at 1% and 10 rad/s, respectively.

7.5.1.17. *In vitro drug release study and determination of similarity factor*

In vitro drug dissolution tests from all eight batches of formulated tablets were carried out using USP dissolution test apparatus type-I (DS-800; 6+2; SC/TR, Lab

India, Mumbai, India) in 900 mL simulated gastric fluid (pH 1.2) maintained at 37^0C with a stirrer rotation speed of 50 rpm (USP, 2009, extended release tablet of metformin HCl, method 1). 5 mL of aliquot was withdrawn at predetermined time points and same volume buffer was added to the dissolution medium each time. Drug released from the tablets at different time points were measured spectrophotometrically (UV-vis double beam spectrophotometer, Pharmaspec-1700, Shimazdu, Japan) at the λ_{max} value at 230 nm after suitable dilution with phosphate buffer pH 6.8. The study was repeated in triplicate for each formulation [17]. Similarity factor (f_2) and difference factor (f_1) were calculated to compare the release profile of the tablets of each batch with USP reference release profile for extended release tablet of metformin HCl using Eq. 7.11 and 7.12, respectively.

$$f_2 = 50 \log \left[\left\{ 1 + \left(\frac{1}{n}\right) \sum_{t=1}^{n} (R_t - T_t)^2 \right\}^{-0.5} \times 100 \right] \quad \text{(Eq.7.11)}$$

$$f_1 = \frac{\sum [R_t - T_t]}{\sum R_t} \times 100 \quad \text{(Eq.7.12)}$$

Where, R_t, T_t and t are the reference value, test value and number of replicates respectively.

7.5.1.18. Data treatment

7.5.1.18. 1. Kinetic modeling of drug release

The in vitro drug release data were fitted to various release kinetic models viz. zero order, first order, Higuchi model, Hixson-Crowell and Korsmeyer-Peppas model to understand the mechanism of drug release.

Zero order model: $Q_t = K_0 t$ (Q_t is the amount of drug released in time, t, K_0 is zero order release constant) [18].

Firs order model: $log\ Q_t = log\ Q_0 + K_1 t/2.303$ (Q_0 is the initial amount of drug in solution) [19].

Higuchi model: $Q_t = K_H t^{1/2}$ [20].

Hixson-Crowell model: $(1-f_t)^{1/3} = 1 - K_\beta t$ (f_t is the fraction of drug released at time, t) [21].

Korsmeyer-Peppas model: $f_t = at^n$ (a is a release rate constant incorporating structural and geometric characteristics of the dosage form, n is the release exponent, indicative of the drug release mechanism) [22].

Higuchi model describes drug release as a diffusion process based on the Fick's law, square root time dependent. This relation can be used to describe the drug dissolution from several types of modified release pharmaceutical dosage forms, as in the case of some transdermal systems and matrix tablets with water soluble drugs [23, 24].

Korsmeyer-Peppas model describes the n value in order to characterize different mechanism of drug release, when $n = 0.5$, $0.5 < n < 1$, $n = 1$ and $n > 1$ corresponds to Case-I (Fickian) diffusion or Higuchi kinetic, both diffusion controlled and swelling controlled transport mechanism (anomalous/non-Fickian transport), Case-II transport (zero order which relates to polymer relaxation during polymer swelling) and super Case-II transport, respectively [25, 26]. Finally, times at which 50% ($T_{50\%}$) and 90% ($T_{90\%}$) drug released were calculated from the best fitting kinetic model equation.

Table: 7.4

Independent variables, response variables with their target values and values from numerical formulation optimization.

Sl. No.	Independent variables		Response				
	Parameters	Optimized value	Parameters	USP reference release profile	Target value	Predicted value	Observed value
1.	Pmaa-*g*-GG (X1)	158.8 mg	BLT	-	minimum	2.71 min	2.83 min
2.	TSG (X2)	244.99 mg	Mucoadhesive strength (*F*)	-	maximum	57.28 g	58.68 g
3.	SBC(X3)	120 mg	CPR1h	20-40%	30%	30.0	32.07
4.	-	-	CPR2h	35-55%	45%	41.39	40.16
5.	-	-	CPR6h	65-85%	75%	72.63	71.27
6.	-	-	CPR10h	Not less than 85%	90%	91.47	93.03

7.5.1.18.2. Statistical analysis of the responses and formulation optimization

The independent and response variables considered in this study, are shown in Table 7.4. The responses were analyzed and then numerically optimized using 2^3 full factorial design by Design-Expert software (version 9.0.4.1, Stat-Ease Inc., Minneapolis, USA).

In the analysis, a statistical model (Eq. 7.13) incorporating interactive and polynomial terms was utilized to evaluate the responses:

$$Y_i = b_0 + b_1X_1 + b_2X_2 + b_{12}X_1X_2 + b_{11}X_1^2 + b_{22}X_2^2 \qquad \text{(Eq. 7.13)}$$

Where, Y is the dependent variable (response), b_0 is the arithmetic mean response of the 8 runs, and b_i is the estimated coefficient for the factor X_i. The main effects (X_1 and X_2) represent the average result of changing one factor at a time from its low to high value. The interaction terms ($X_1 X_2$) show how the response changes when two factors are changed simultaneously. The polynomial terms (X_1^2 and X_2^2) are included to investigate nonlinearity. One-way ANOVA was applied to estimate the significance of the model ($p < 0.05$).

In this study, buoyant lag time, mucoadhesive strength (F) and USP reference drug release profile for Metformin HCl extended release tablet were taken as target (Table 7.4). For optimization purpose, buoyant lag time was targeted at minimum, mucoadhesive strength at maximum and the independent formulation variables (amount of Pmaa-*g*-GG, TSG and SBC) were set in the range of low and high level used in the experiment.

After optimization, the matrix tablets were prepared as per the optimized formula and evaluated. Then the observed values of the responses were compared to the predicted and target values.

All measured data are expressed as mean ± standard deviation (S.D.). Each measurement was done in triplicate (n = 3).

7.5.2. Result and discussion

7.5.2.1. Preparation of Pmaa-g-GG copolymer and composite matrix tablet with TSG

The preparation of Pmaa-g-GG copolymer and subsequent formation of composite matrix are schematically presented in Figure 7.7. Graft co-polymerization of methacrylamide onto gellan gum was carried out employing grafting technique by microwave-promoted free-radical initiation using cerric (IV) ammonium nitrate as free-radical initiator. The anomeric –CHOH on gellan gum-backbone is the reactive vicinal group, where the grafting is initiated. The overall reaction mechanism is that, cerric (IV) ammonium nitrate gets dissociated into Ce^{4+}, ammonium and nitrate ions and then cerric (IV) ion attacks the gellan gum macrochains resulting formation of a GG-cerric complex. The cerric (IV) ions in the complex get then reduced to cerric (III) ions by oxidizing hydrogen atom and thereby creating a free radical onto GG-backbone. In the presence of methacrylamide, the GG free radical is chemically coupled to the monomer unit, thereby resulting in a covalent bond between nonomer and GG to create the chain reaction for propagation. Finally, termination occurs through a combination of two propagating chain free radicals initiated from GG-backbone or by coupling between GG-propagating-free-radical and monomer free radical. Finally, Pmaa-g-GG copolymer and tamarind seed gum have been blended along with drug and SBC employing wet granulation method to obtain a polymeric composite matrix.

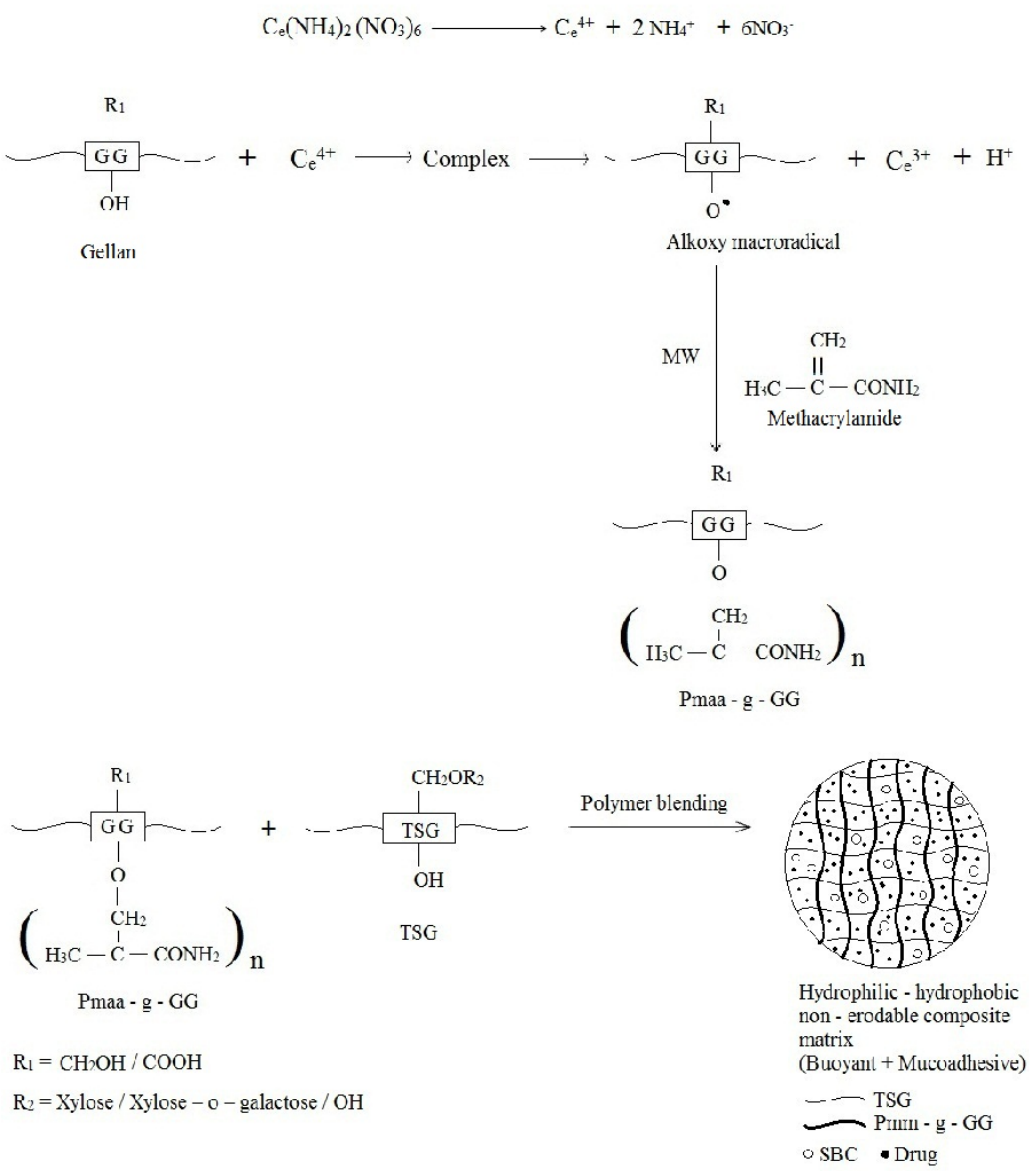

Fig. 7.7: Schematic representation of synthesis of polymethacrylamide grafted gellan (Pmaa-g-GG) and formation of gastroretentive composite matrix tablet.

7.5.2.2. Physical characterization of tablet

The physical characterization of the tablets exhibited the following information: the weight of the tablets was confined within ±4% of the average weight,

thickness varied from 5.07 to 6.18 mm with MSD 0.13% (n= 10), the maximum friability found was 0.46% and the drug content varied within ±5% of the labeled amount. Hardness was within the range of 4-5 kg/m^2. All these variation were found to comply with the requirements of official Compendium.

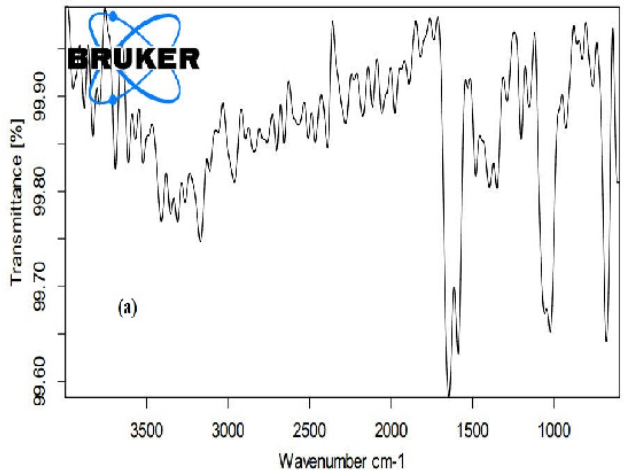

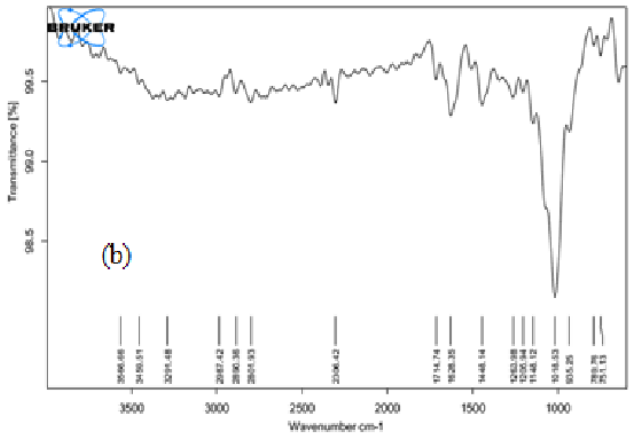

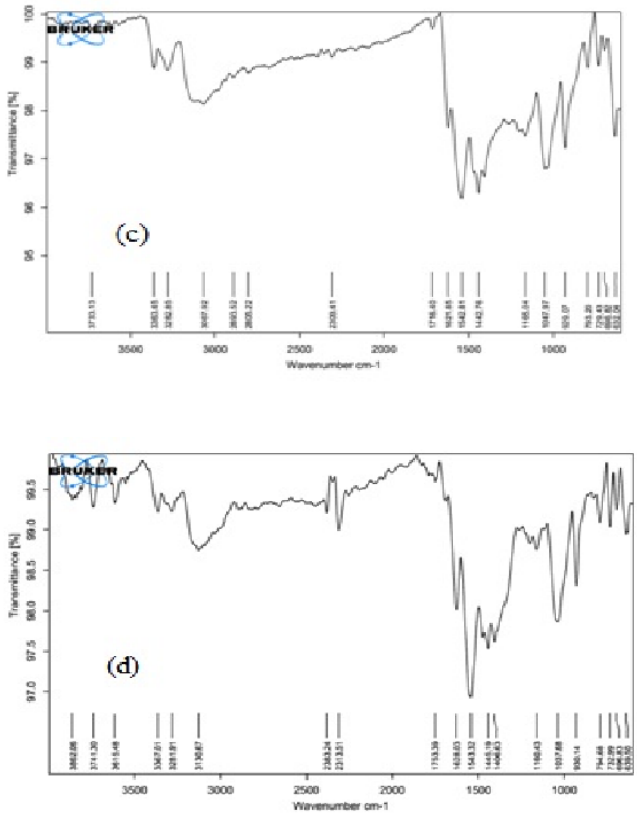

Fig.7.8. FTIR spectrum of (a) polymethacrylamide-grafted-gellan (Pmaa-g-GG), (b) Tamarind seed gum (TSG) (c) metformin hydrochloride and (d) tablet formulation (F8)

7.5.2.3. Fourier-transform infrared (FTIR) spectral analysis

Infrared spectra of Pmaa-g-gellan and TSG are shown in Fig. 7.8. (a) and 7.8.(b) respectively. Pmaa-g-gellan gum shows characteristic peaks at 1647.32 cm^{-1} for carbonyl group indicating C=O stretching, at 3198.43 cm^{-1} for –OH group, at 2883.27 cm^{-1} for –COOH group, at 1159.42 cm^{-1} for alcoholic –C-O group, at 1706.30 cm^{-1} for –C=O group. It also shows characteristic peaks in the range

from 3829.24 cm^{-1} to 3169.37 cm^{-1} for $–NH_2$ group, due to addition of methacrylamide which was grafted onto gellan gum. An additional peak at 1645.78 cm^{-1} has been observed due to N-H bending. A significant peak is also observed at 1024. 59 cm^{-1} for CH-O-CH_2 group which occurs due to grafting reaction between OH group of C_2 of gellan gum and π bond of methacrylamide.

Infrared spectra of tamarind seed gum shows characteristic peaks at 1018.53 cm^{-1}, 1148.12 cm^{-1}, 1448.14 cm^{-1}, 1628.35 cm^{-1}, 2890.36 cm^{-1} and 3291.48 cm^{-1} for – HC=O stretching vibration, - C – O – C - asymmetric stretching vibration of glucopyranosyl and xylopyranosyl units, - CH_2 gr bending vibration, –CH-OH stretching vibration, aliphatic C-H stretching and for the –OH groups, respectively.

Infrared spectra of metformin hydrochloride and tablet formulation are shown in Fig. 7.8 (c) and (d), respectively. Metformin shows the characteristic peaks at 3363.45 cm^{-1} and peaks at 3282.85 cm^{-1} for N – H asymmetric stretching and N - H symmetric stretching, respectively. Peak at 2805.22 cm^{-1} indicates CH_3 symmetric stretching. Peaks at 1621.85 cm^{-1} and 1442.76 cm^{-1} correspond to C = N stretching and CH_3 asymmetric deformation, respectively. All these peaks have been observed in the infrared spectra obtained from tablet formulation, which demonstrates that there is no significant incompatibility between the drug and the other polymers.

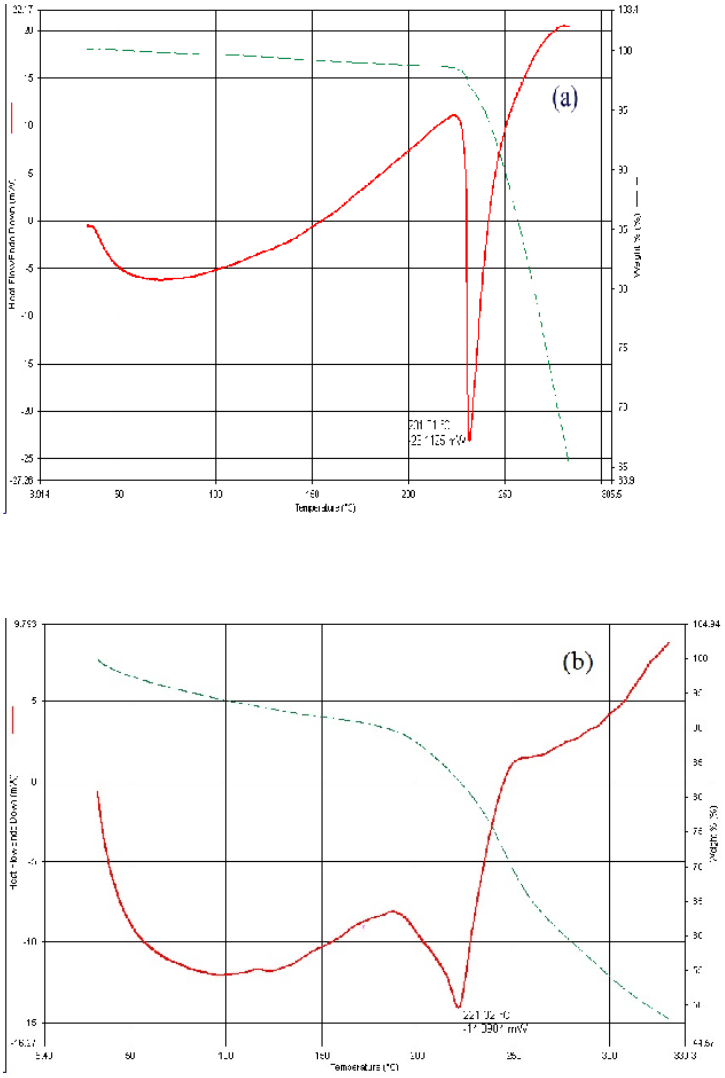

Fig.7.9. DSC-TGA thermogram of (a) metformin hydrochloride (b) tablet formulation (F8)

7.5.2.4. Differential scanning calorimetry (DSC) study and thermogravimetric analysis (TGA)

DSC and TGA curves of metformin HCl (MFH) and tablet formulation are shown in Fig. 7.9(a) and (b), respectively. As shown in Fig. 7.9(a), the DSC-thermogram (red in colour) of MFH shows a broad endothermic peak at 80^{o}C

and an another very sharp endothermic peak at 231.81°C. TGA thermogram (green in colour) of MFH shows only 2% weight loss in the temperature range from 25°C to 226°C, which indicates very little loss in moisture present in the pure drug. Very sharp endothermic peak at 231.81°C indicates narrow melting range and crystalline nature of MTF. Two endothermic peaks at 100°C and at 221.32°C were recorded in DSC thermogram of tablet formulation. TGA thermogram (green in colour) of tablet formulation shows 10% weight loss in the temperature range from 27°C to 175°C. The correlation between endothermic peak at 100°C and simultaneous reduction in weight in the temperature range from 27°C to 175°C indicates the loss in moisture present in the tablet. The sharp endothermic peak at 221.32°C (less in sharpness compared to that of pure drug) indicates the melting point of the drug present in the tablet formulation and partial retention of its crystalinity in the formulation. The significant downward shift in melting point of the drug in the formulation may be due to dilution effect in presence of other excipients.

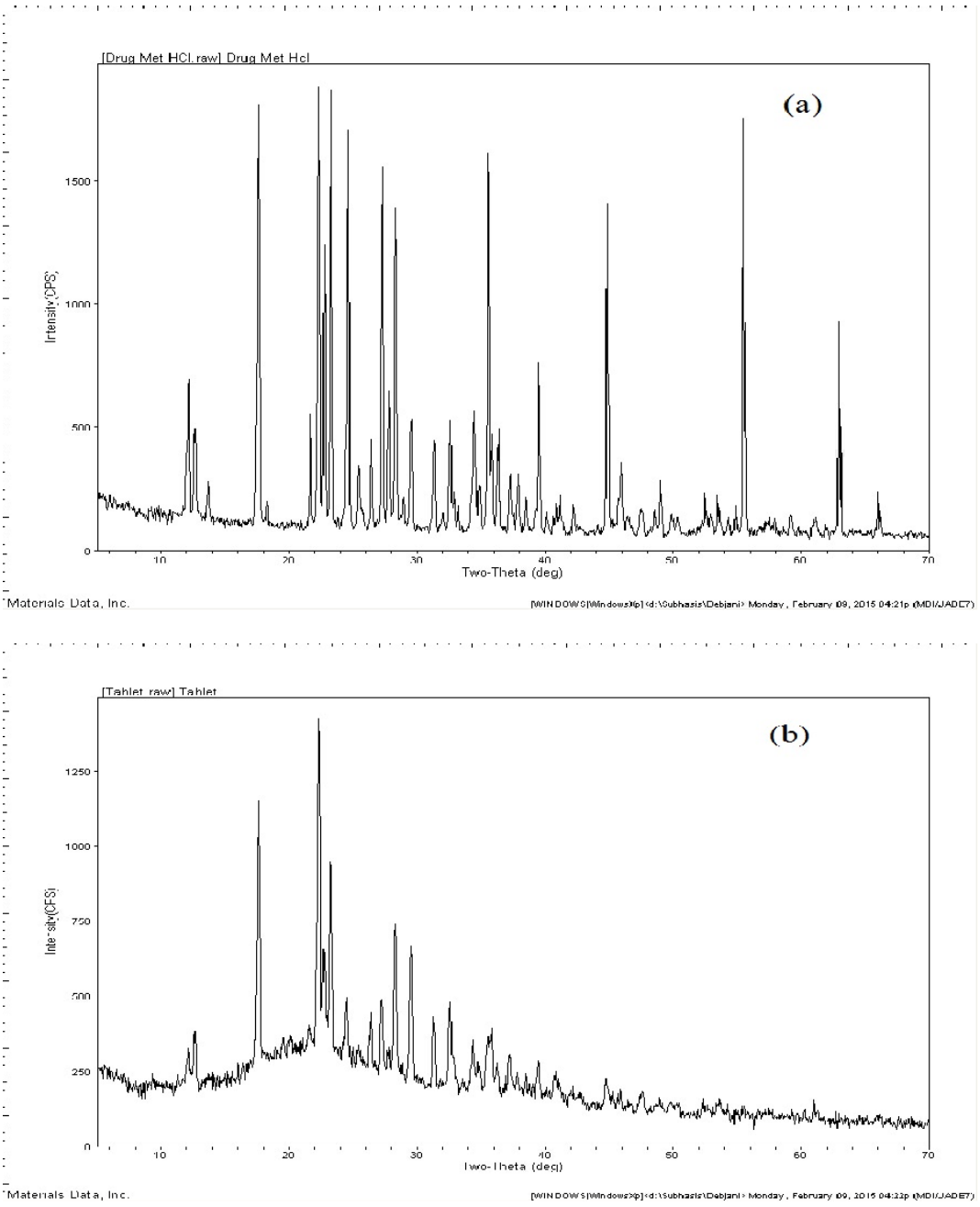

Fig.7.10. X-ray diffractogram of (a) metformine hydrochloride and (b) tablet formulation (F8).

7.5.2.5. X-ray diffraction (XRD) study

X-ray diffractogram of pristine metformin HCl and tablet formulation containing drug were represented in Fig. 7.10 (a) and (b), respectively. Metformin has shown

many characteristic intense peaks at 2θ of 12^0, 17.5^0, 22^0, 23^0, 24.5^0, 28^0, 36^0, 45^0, 55.5^0 and 63^0 along with some peaks with medium intensitiy at 2θ of 21.5^0. 29^0, 31^0, 33^0, 34.5^0 and 39.5^0, that indicate its crystalline nature. The diffractogram obtained from the tablet formulation portray that approximately 80% peaks of pristine drug appeared almost at the same 2θ values in the XRD chart of tablet formulation attributing to the retention of crystalline nature of maximum amount of drug and absence of incompatibility between drug and other formulation components. But the presence of noise to some extent and little decrease in intensities indicate that some amount of drug remain as molecularly dispersed in the composite matrix of the tablet.

Table: 7.5
A summary of ANOVA analysis for the response variables

Response	Sum of square	Degrees of freedom	Mean square	F-value	Press	p-value	R^2	Predicted R^2
BLT	76.56	6	12.76	2314.68	0.35	0.016	0.9999	0.9954
F	996.98	5	199.4	182.93	34.88	0.005	0.9978	0.9651
CPR1h	351.58	5	70.32	38.57	58.34	0.026	0.9897	0.8358
CPR2h	451.45	5	90.29	50.5	57.21	0.019	0.9921	0.8743
CPR6h	978.64	6	163.11	339.66	30.73	0.042	0.9995	0.9686
CPR10h	623.06	5	124.61	386.5	10.32	0.003	0.9990	0.9835
K_H	0.0071	5	0.0014	112.28	0.0004	0.009	0.9965	0.9432

7.5.2.6. Statistical analysis of the responses and formulation optimization

A total eight trial formulations were prepared by employing a 2^3 full factorial design. Different experimental trial formulations are presented in Table 7.3. The results of ANOVA analysis unveiled a statistically significant association between independent and response variables ($p < 0.05$) (Table 7.5). The generated model equations after eliminating insignificant terms ($p > 0.05$) on the basis of ANOVA results were demonstrated in discussion regarding respective responses.

Software generated three-dimensional response surface and corresponding two-dimensional contour plots illustrated the effects of the independent factors on the investigated responses (Fig.7.19 to 7.26). The response surface plots as a function of two independent factors at a time are useful to study their main and interaction effects, simultaneously. Effects of the independent factors on the investigated response were discussed in respective section.

A numerical optimization technique based on the criterion of desirability was adopted to develop the optimized formulation. The primary goal of the optimization process was to find the values of the independent factors that minimize buoyancy lag time, maximize the mucoadhesive strength and comply the USP release reference profile for extended release tablet of metformin HCl (Table 7.4). The desirable ranges of independent factors were restricted to 150mg ≤ Pmaa-g-GG ≤ 250mg, 150mg ≤ TSG ≤250mg and 80mg≤ SBC ≤120mg. An optimal formulation setting having highest desirability (0.858)

was selected among 28 different settings recommended by Design Expert 9.0.4.1 software. The optimal values of Pmaa-g-GG, TSG and SBC selected were 158.80mg, 244.99mg and 120mg, respectively. The confirmation experiments were conducted to test the responses of the optimal formulation (OF). The experimental results and predicted responses are tabulated in Table 7.4. The relative errors ([(predicted value − actual value)/predicted value] × 100) between the predicted and observed values were - 4.43% for BLT, - 2.44% for *F*, - 6.9% for CPR1h, +2.97% for CPR2h, +1.87% for CPR6h and - 1.71% for CPR10h. In short, the experimental findings were within the close agreement to the model-based predictions, which conferred the predictability and validity of the models.

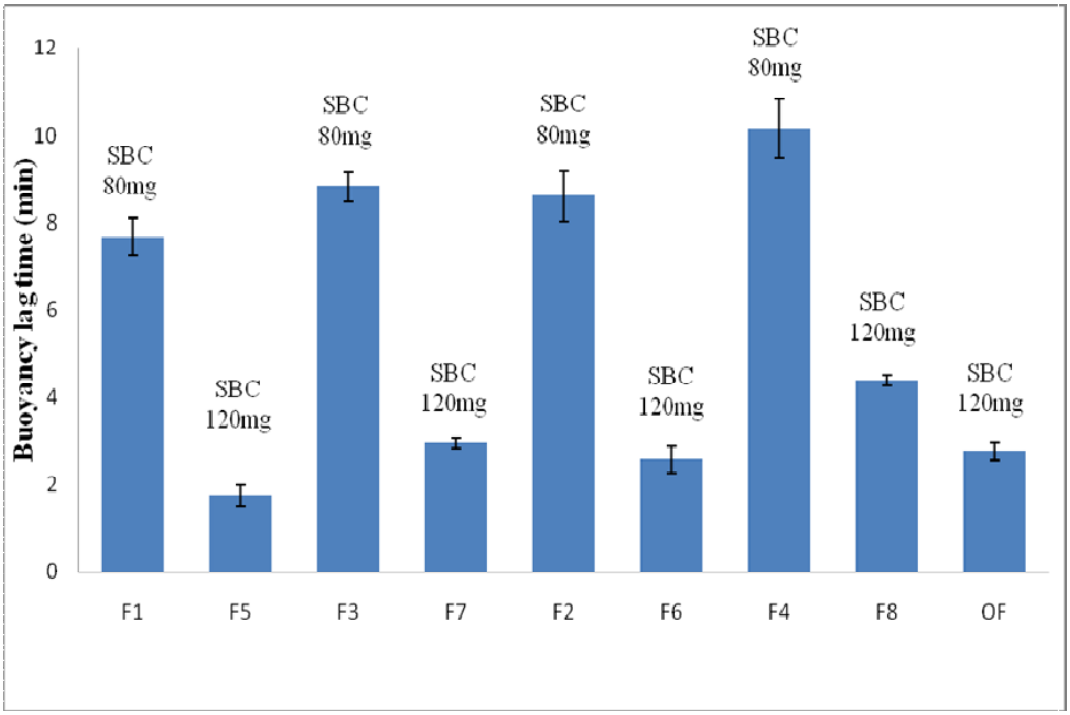

Fig.7.11. Buoyancy lag time exhibited by different batch of composite tablet formulation.

7.5.2.7. In vitro buoyancy study

The buoyancy parameters exhibited by the composite matrix tablet containing metformin HCl are presented in Table 7.6 and Fig. 7.11. The in vitro buoyancy test showed that the average buoyancy lag time (BLT) observed was within the range from 1.74 mins to 10.15 mins and the total buoyancy time (TBT) for all formulations was observed to be greater than 10 hours. The mechanism contributing the buoyancy to the composite matrix involves penetration of HCl acid into the interior of the tablet resulting generation of CO_2 due to the reaction between $NaHCO_3$ of the tablet formulation and HCl acid of the simulated gastric fluid (Eq. 10). Simultaneously, the hydrophilic tamarind seed gum absorbs water and form a continuous barrier gel layer at the outer surface of the tablet resulting subsequent entrapment of CO_2 gas in the matrix. The buoyancy can also be attributed to the swelling and expansion of the matrix volume in aqueous media, leading to significant decrease in tablet density. Thus the resultant effect of the inside upward pressure exerted by CO_2 gas and drop in density due to matrix-swelling leads to the floatation of the tablet in the floating medium.

$$NaHCO_3 + HCl \rightarrow NaCl + CO_2\uparrow + H_2O \qquad \text{(Eq.7.14)}$$

The BLT was considered as response variable in this study as it changes with different formulations whereas TBT remains constant in all designed formulations and hence not taken as response variable. The regression equation for BLT yielded from ANOVA study, is expressed in Eq. 7.15:

$$BLT = +5.87 + 0.71X_1 + 0.56X_2 - 2.95X_3 + 0.13X_1X_2 + 0.044X_1X_3 + 0.00375X_2X_3$$

($R^2 = 0.9999$) (Eq.7.15)

(X_1 = Pmaa-g-GG; X_2 = TSG; X_3 = SBC)

The values of the coefficients of different independent variables in the model equation for BLT indicate that buoyancy lag time is mainly influenced by $NaHCO_3$ and comparatively less influenced by Pmaa-g-GG and TSG. The effect of the $NaHCO_3$ is negative that means increase in the concentration of sodium bicarbonate decreases the buoyancy lag time whereas the effect of other two variables are positive. This may be due to the fact that more $NaHCO_3$ produces more CO_2 that exert more inside upward pressure resulting enhancement in the buoyant efficiency. But on the other hand, increase in the Pmaa-g-GG and TSG results in little increase in BLT. It may be due to the fact that presence of more number of – COOH group of Pmaa-g-GG moiety at its higher level in the matrix, leads to inhibition of penetration of HCl acid in the tablet matrix resulting comparatively slow generation of CO_2. Unlikely, higher level of hydrophilic polymer TSG absorbs more water at initial stage and thus delays floatation by increasing the density temporarily.

Other coefficients in the regression equation indicate very little interactions between the independent variables. Response surface 3 -D plot for BLT (Figure 7.19) showed the effects of independent variables on the buoyancy lag time. The study also showed that the tablet once floated, maintains its buoyancy level over a long period of time (>10 h). The tablets showed to maintain their physical integrity throughout the whole period of dissolution study due to presence of

hydrophilic TSG that forms gel absorbing water in the matrix. This further minimizes the possibility of escape of CO_2 from the interior bulk of the tablet to the outside and finally ensures the continued floatability of the tablet in the floating medium.

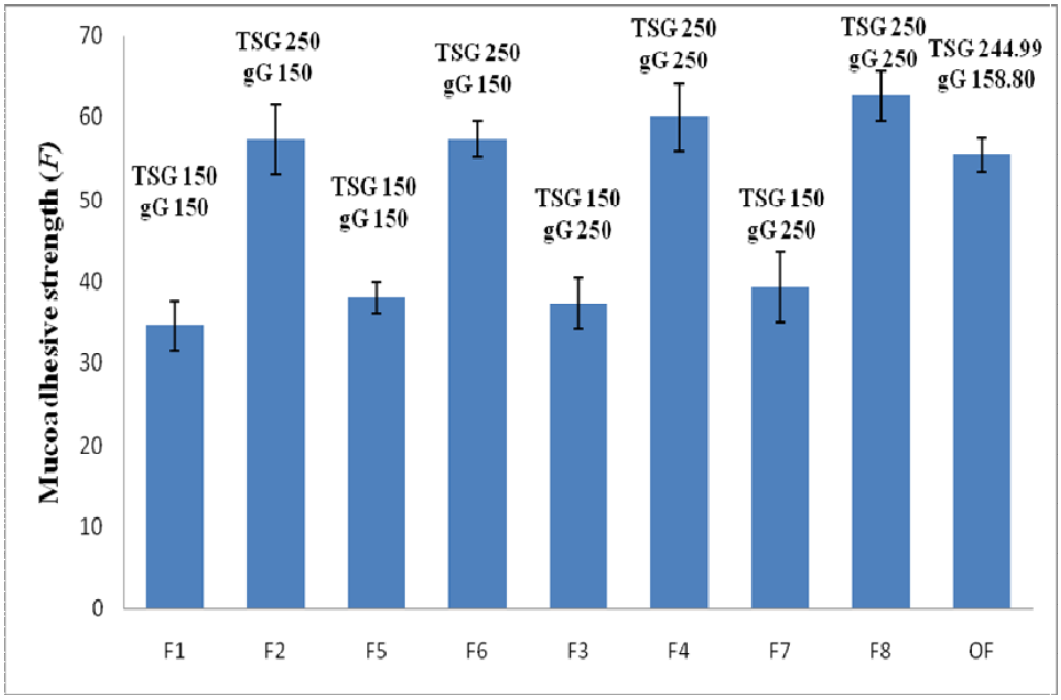

gG, grafted gellan

Fig.7.12. Mucoadhesive strength (*F*) exhibited by different batch of composite tablet formulation.

Table: 7.6

Buoyancy parameters, density, mucoadhesive strength, drug dissolution similarity (f_2) and dissimilarity factors (f_1) of different batches of composite tablets

Formulation code	BLT (min) Mean ± s.d.	TBT (h)	Density (g/cm^3) mean ± s.d.	Mucoadhesive strength (F) Mean ± s.d. (g)	f_1	f_2
F1	7.69 ± 0.431	> 10	1.326±0.014	34.6 ± 3.06	18.36	47.13
F2	8.61± 0.573	> 10	1.263±0.018	57.3 ± 4.16	6.29	67.43
F3	8.83± 0.335	> 10	1.261±0.008	37.3 ± 3.06	6.63	64.01
F4	10.15 ± 0.670	> 10	1.215±0.013	60.0 ± 4.00	21.57	43.89
F5	1.74 ± 0.231	> 10	1.385±0.022	38.0 ± 2.00	20.5	44.79
F6	2.57 ± 0.302	> 10	1.313±0.009	57.5 ± 2.17	4.08	75.84
F7	2.95 ± 0.125	> 10	1.315±0.016	39.3 ± 4.42	7.69	61.09
F8	4.39 ± 0.127	> 10	1.259±0.027	62.6 ± 3.06	14.38	51.94
OF	2.76 ± 0.192	> 10	1.307±0.037	55.46 ± 2.03	5.69	71.58

BLT, buoyancy lag time; TBT, total buoyancy time.

7.5.2.8. Ex-vivo mucoadhesion testing

The results of *ex-vivo* mucoadhesion test of Pmaa-g-GG and tamarind seed gum –composite matrix tablets containing metformin HCl using goat gastric mucosa are presented in Table 7.6 and Fig. 7.12. The value of mucoadhesive strength, *F,* exhibited by different batches of composite tablets ranges from 34.6g to 62.6g. The mucoadhesive property of these tablets could be attributed to the presence of hydroxyl groups in the molecules of hydrophilic TSG and –COOH, $-CH_2OH$ groups in Pmaa-g-GG, which have the ability to form various noncovalent bonds (like hydrogen bonds, Vander Waal's forces and ionic interactions) with mucus molecules [27]. The regression equation for mucoadhesive strength (F) yielded from ANOVA study, is expressed in Eq. 7.16:

$$F = +48.3 + 1.5X_1 + 11.0X_2 + 1.0X_3 + 0.50X_1X_2 - 0.35X_2X_3 \quad (R^2 = 0.9978) \qquad \text{(Eq.7.16)}$$

The values of the coefficients of different independent variables in the model equation for *F* indicate that mucoadhesivity exhibited by composite matrix tablets is mainly influenced by TSG. The value of *F* has shown to increase with increase in the amount of TSG at low and high level of other variables, which may be due to the presence of –OH group (main contributor in mucoadhesivity) in large number in TSG molecules. In case of batch F1, F3, F5 and F7, a little synergistic effect of $NaHCO_3$ on *F* has also been observed at low level of TSG. It may be due to more ionization of –COOH group of Pmaa-g-GG by SBC, which further causes enhancement in formation of noncovalent bond or electrostatic interaction with mucus molecules. But in case of batch F2, F4, F6 and F8, no significant effect of SBC has been observed at high level of TSG, which might be due to domination effect of TSG on chemical activity of $–COO^-$ ions. Pmaa-g-GG has shown to exert a little positive effect in case of F1, F2, F3, F4, F6 and F8 at both level of TSG and SBC which may be due to the presence of $–CH_2OH$ and –COOH groups in the moiety of Pmaa-g-GG. No significant interaction between the variables has been reflected by the regression equation.

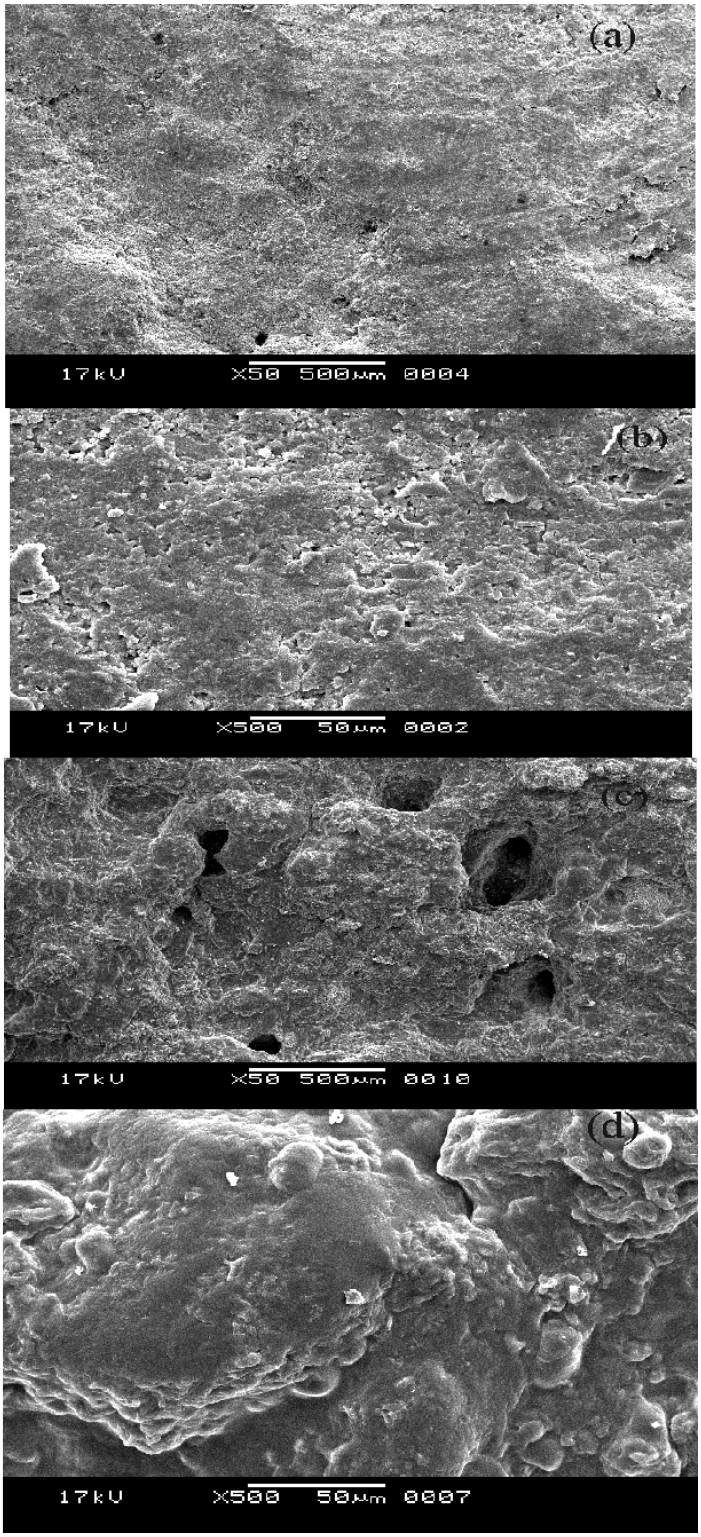

Fig.7.13 Scanning electron micrograph of tablet surface (F8) (a) and (b) before dissolution; (c) and (d) after dissolution

7.5.2.9. Surface morphology analysis

Fig. 7.13 presents the scanning electron micrographs of the tablet surface before and after the drug release study. The micrographs of tablet surface before drug release portray rough, irregular appearance with presence of very thin hair-like cracks. It may be due to difference in solid state crystalline nature of Pmaa-g-GG and TSG, less cold welding at superficial level during consolidation of granules into tablet and shrinkage upon loss of moisture from the tablet surface. The micrographs after dissolution study depict continuous surface with presence of pores and lobules. Continuation of surface and lobule formation may result from the gelation of TSG during dissolution and subsequent drying while pore formation may result from the evolution of CO_2 from the superficial level of the outer gel layer.

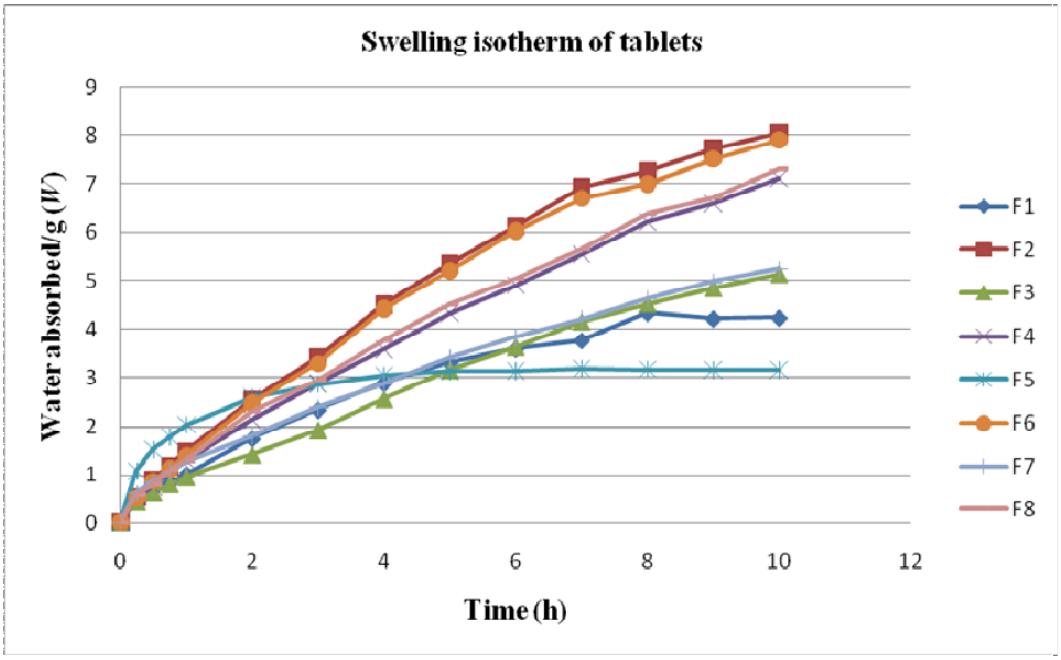

Fig.7.14 Water uptake kinetic profile of different batches of composite tablet.

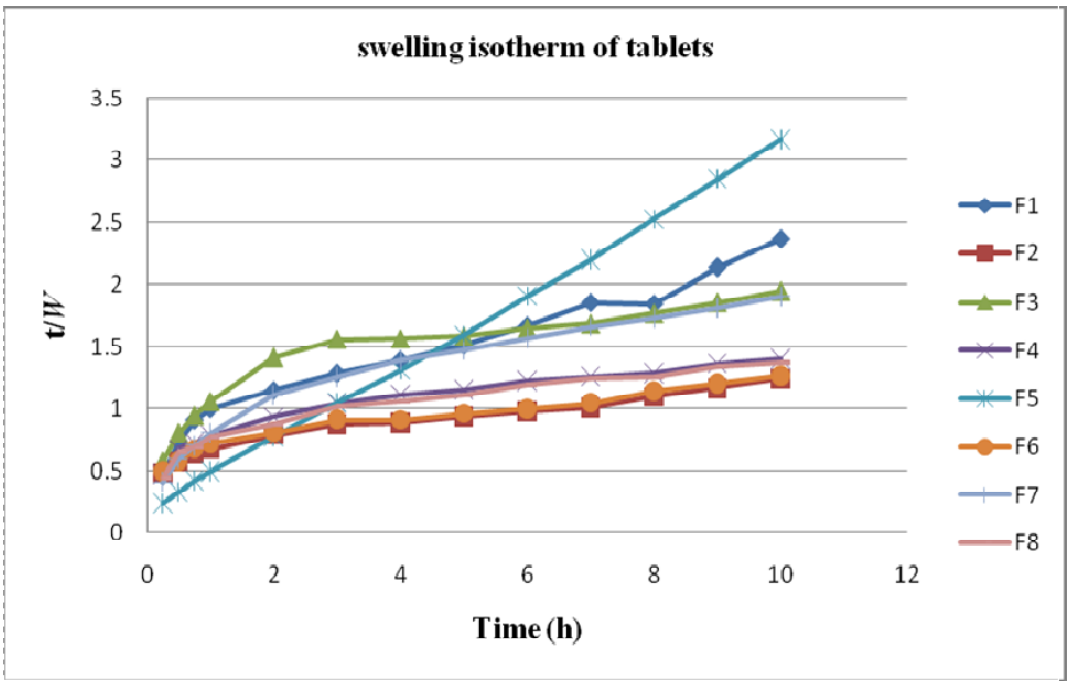

Fig. 7.15. Swelling isotherm (t/W versus time) exhibited by different batches of composite tablets.

Table: 7.7

Swelling parameters and water penetration velocity of different batches of composite tablets

Formulation code	Equilibrium water uptake (%) W_E	Initial swelling rate (dW/dt), h^{-1}	Equilibrium swelling (W_∞), g/g	Matrix hydration, H, (g/g)	Water penetration velocity, V (cm/g.h)
F1	309.46±6.06	1.41	6.25	0.752	0.060
F2	612.44±4.25	1.72	14.92	0.899	0.107
F3	413.35±8.62	1.09	8.77	0.871	0.066
F4	703.91±6.59	1.47	12.33	0.901	0.084
F5	314.49±3.83	5.99	3.39	0.791	0.026
F6	619.33±7.05	1.66	14.93	0.871	0.104
F7	420.09±3.27	1.53	7.19	0.874	0.063
F8	697.23±5.92	1.56	12.35	0.910	0.085

7.5.2.10. Equilibrium water uptake (swelling index), swelling-kinetic and water penetration velocity

Fig.7.14 depicts the kinetic of swelling behavior of composite matrix expressed as W (grams of the water absorbed per gram of the dry matrix of the tablet) as a function of time in simulated gastric fluid (pH 1.2). % equilibrium water uptake, initial swelling rate, equilibrium swelling, matrix hydration and water penetration velocity are presented in Table 7.7. The equilibrium water uptake by the composite matrix tablets observed ranges from 309.46% to 703.91%, which mainly depends upon the amount of tamarind seed gum. Water uptake increased with an increasing amount of TSG in case of all formulations at low and high both level of other two independent variables: Pmaa-g-GG and SBC, which may be due to the presence of different hydrophilic groups in the TSG molecules such as –OH group at 2 and 3 position of first glucopyranosyl unit of the main chain, at 2, 3 and 4 position of xylose unit attached to glucopyranosyl unit of the main chain via $–CH_2O$ at 5 position, at 2 and 3 position of second glucopyranosyl unit, at 2, 3 and 4 position of galactopyranosyl unit in side chain and $–CH_2OH$ group at 5 position of fourth glucopyranosyl unit of the main chain and at 1 position of galactose unit of the side chain. This is also substantiated by the higher values of equilibrium swelling (W_∞) and matrix hydration (H) observed in the formulations with high level of TSG. A little directly-proportional effect of Pmaa-g-GG on water uptake has been observed, which may be due to presence of $–CH_2OH$ group in α-L-rhamnose and third β-D-glucose unit. No significant effect of SBC on water uptake has been found.

Initial swelling rate exhibited by the composite matrix ranges from1.09 h^{-1} (F3) to5.99 h^{-1} (F5) and increases with the increment in the amount of TSG. In case of F5, initial swelling rate has been found to be highest, which may be attributed to the fact that higher amount of SBC generates more CO_2 which evolves at the premature stage of gel formation at the outer surface resulting subsequent formation of more pores at surface. These pores increase the water penetration into the interior of the matrices. But the investigation showed overall water penetration velocity is very low in case of F5, which may be due to presence of low level of both matrix forming polymer Pmaa-g-GG and TSG. In case of F1:F3 and F5:F7, matrix hydration increases with increase in Pmaa-g-GG at low level of TSG whereas no significant change in hydration has been found in case of F2:F4 and F6:F8 at high level of TSG, which may be due to domination of water uptake capacity of poor hydrophilic Pmaa-g-GG by much more hydrophilic TSG. Water penetration velocity exhibited by composite matrices ranges from 0.026 cm/g.h (F5) to 0.107 cm/g.h (F2), which has been observed to increase with increase in TSG and in the formulations with higher values of W_E, dW/dt, W_∞ and H attributing to the greater hydrophilicity of TSG. Second order swelling isotherm (t/W versus t) exhibited by different composite matrices is shown in Fig.7.15.

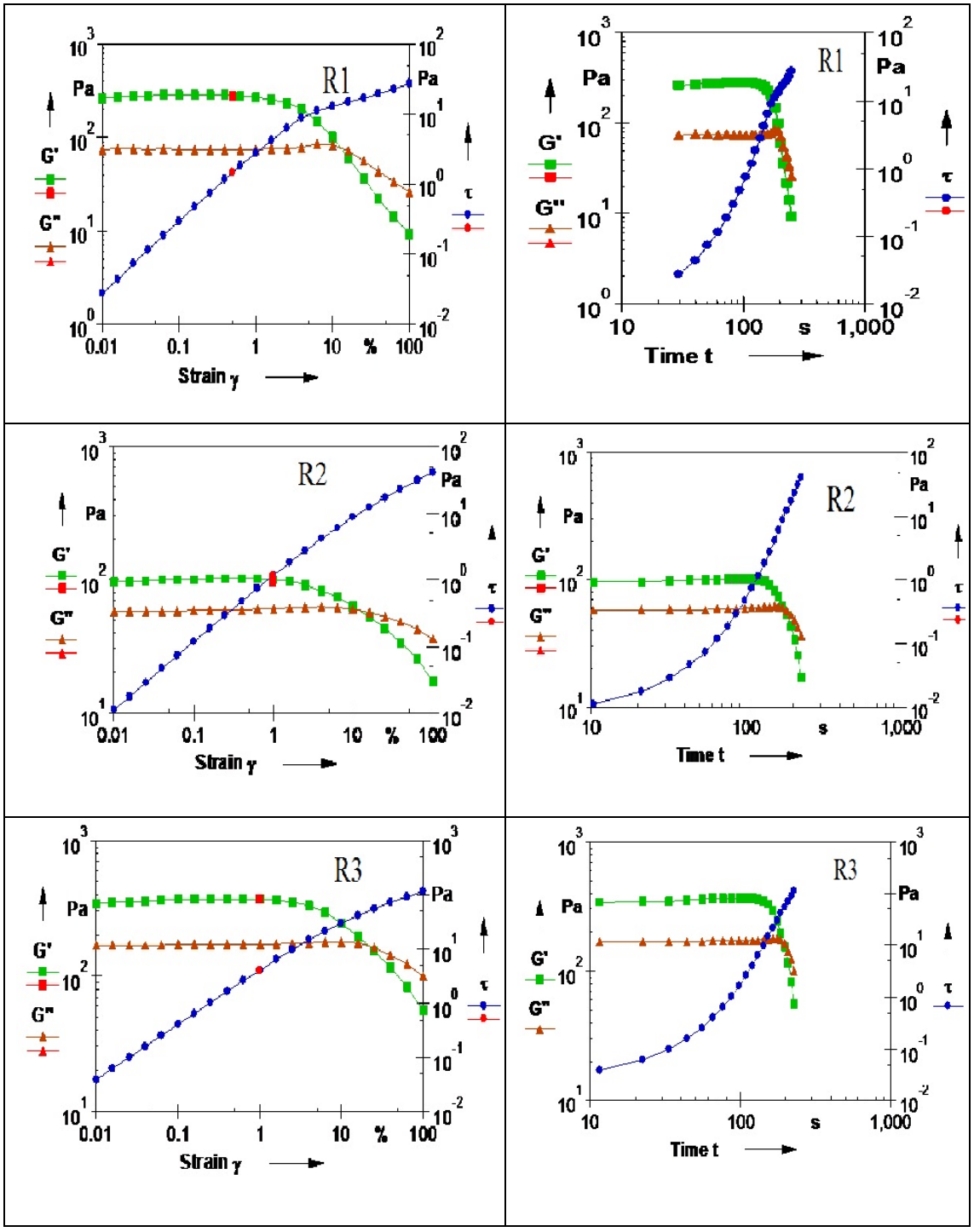

Fig.7.16. Viscoelastic modulus (*G′* and *G″*) profile against strain and time of different ratio of Pmaa-g-GG and TSG [Pmaa-g-GG:TSG = 1:1(R1); 3:5(R2) and 5:3(R3)]

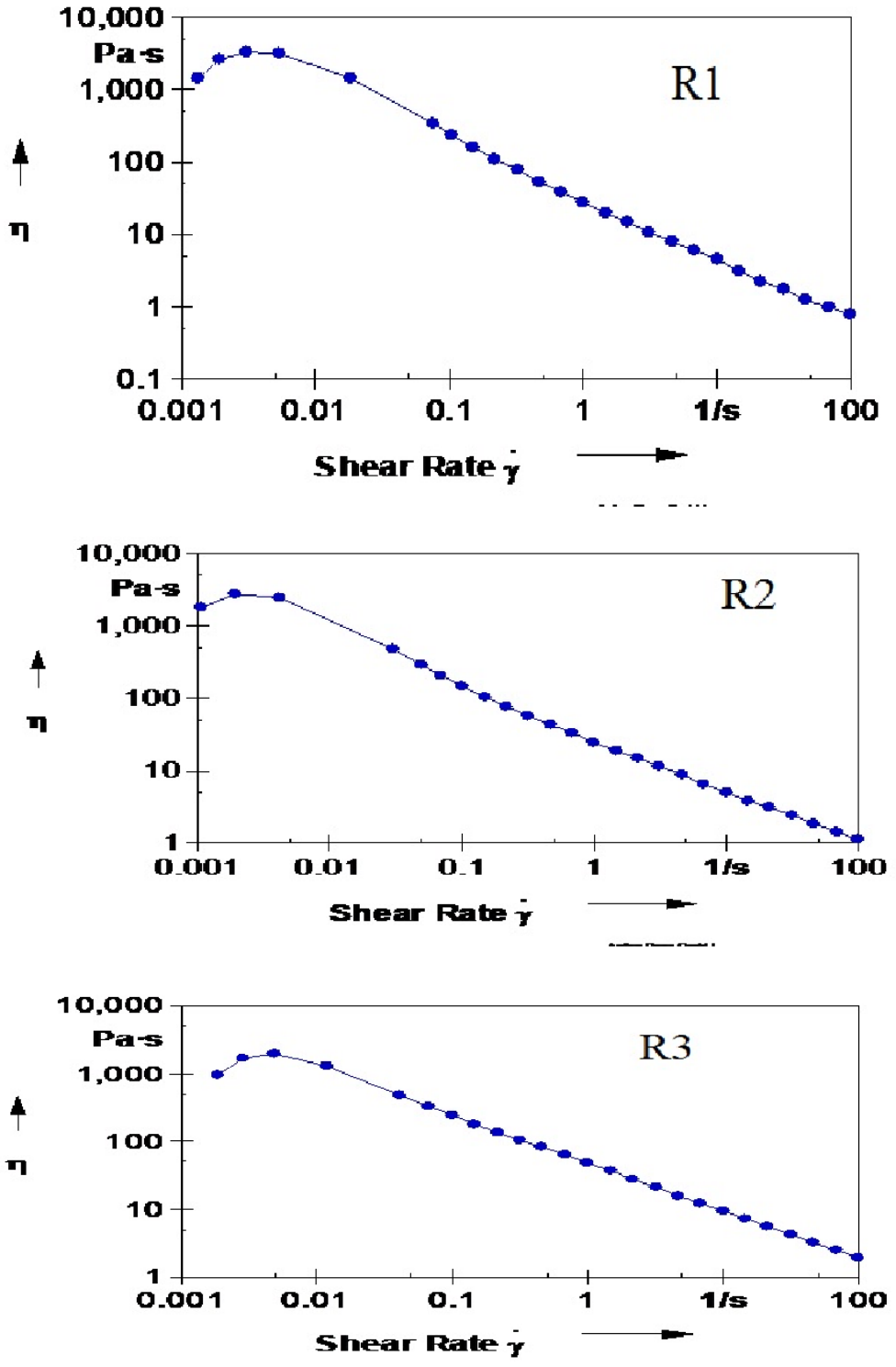

Fig. 7.17. Viscosity against shear rate of different ratio of Pmaa-g-GG and TSG [Pmaa-g-GG:TSG = 1:1(R1); 3:5(R2) and 5:3(R3)]

Table: 7.8

Rheological and viscoelastic parameters of Pmaa-g-GG and TSG composite gel in different ratio used in formulations

Pmaa-g-GG: TSG	Cross-over point				Zero shear viscosity (Pa.s)
	Strain (γ), %	Shear stress (τ), Pa	G' = G'' (Pa)	Cross over time (sec)	
1:1 (R1)	13.04	13.96	0.761	203	2013.3
3:5 (R2)	11.76	9.86	0.593	185	2076.3
5:3 (R3)	22.06	51.62	0.017	190	1256.9

7.5.2.11. Viscoelastic study

Different viscoelastic and rheological parameters are presented in Table 7.8. Fig.7.16 portrays strain sweep curve and time sweep curve and viscosity versus shear rate profiles exhibited by Pmaa-g-GG-TSG composite gel of three different ratios are shown in Fig. 7.17. The gel with ratio R1 (found in F4 and F8) and R2 (found in F2 and F6) exhibit higher zero shear viscosity (2013.3 Pa.s and 2076.3 Pa.s, respectively), which indicates that the particles in the matrices are non-associated having a strong thickened behavior (Rohn, 1987). This high thickness may be attributed to the presence of higher amount of hydrophilic TSG. The gel with ratio R3 (found in F3 and F7) showed highest starting % strain (γ) for structural breakdown at $G' = G''$, which indicates stronger microstructure and high rigidity of the gel matrix. This may attribute to large molecular size of Pmaa-g-GG copolymer with high steric bulkiness due to emanating of numerous side

chains from different points of main polymeric backbone of gellan. This property imparts nonerodability to the composite matrix. Lower zero shear viscosity of R3 may be due to low amount of TSG. In case of R1, higher crossover time observed indicates a strong matrix network of polymer entanglement and possibly better long term stability of the matrix. Higher values of storage modulus (G') observed in R1 and R3 compared to that in R2, indicates more solid like property of the matrix microstructure. Therefore, it can be concluded that the composite gel matrix with ratio R1 showed to have high viscosity and highly rigid strong network. The viscosity versus shear rate profiles (Fig.7.17) depicts that viscosity decreases with increase in shear rate after a very small initial rise. This may be due to penetration of liquid in the void in the polymeric network formed as a result of shearing initially followed by gradual alignment of long axes of polymeric macromolecules in the direction of flow at higher shear rate.

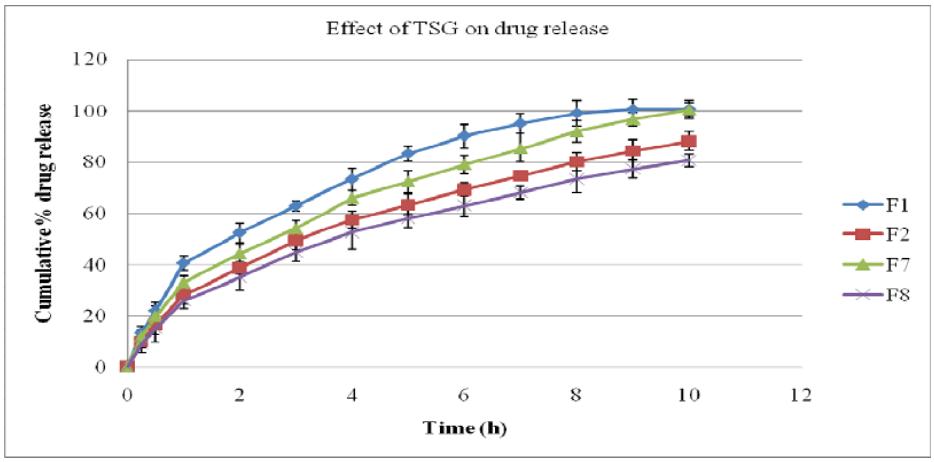

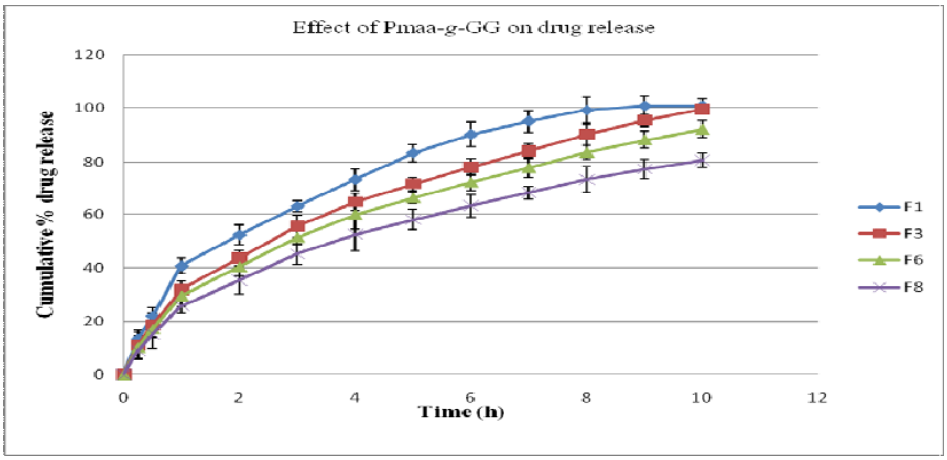

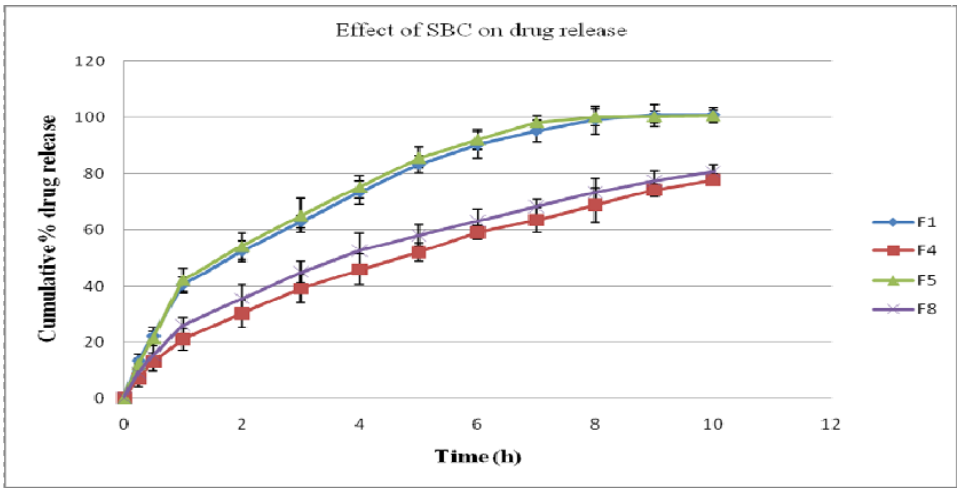

Fig.7.18. Zero order drug release profile (cumulative % release ± SD, n = 3) of metformin HCl from composite tablets (F1 – F8) portraying the effects of independent variables on release.

Table: 7.9

Kinetic modeling of release data from different tablet formulations, release rate constants and $T_{50\%}$, $T_{90\%}$.

Batch	R^2 value						Rate constant (k)					$T_{50\%}$ (h)	$T_{90\%}$ (h)
	Zero order	First order	Higuchi kinetic	HC	KP R^2	KP n	Zero order	First order	Higuchi kinetic	HC	KP		
F1	0.893	0.721	0.978	0.936	0.977	0.540	0.087	0.165	0.340	0.113	0.333	1.94	6.14
F2	0.946	0.769	0.998	0.994	0.991	0.576	0.076	0.180	0.293	0.047	0.249	3.24	10.1
F3	0.946	0.768	0.998	0.967	0.991	0.578	0.086	0.181	0.331	0.070	0.279	2.59	7.97
F4	0.969	0.791	0.999	0.996	0.995	0.627	0.070	0.199	0.265	0.037	0.191	4.51	13.19*
F5	0.869	0.688	0.966	0.955	0.974	0.589	0.087	0.167	0.344	0.121	0.329	1.87	5.84
F6	0.946	0.768	0.998	0.996	0.991	0.579	0.080	0.181	0.307	0.052	0.259	2.99	9.21
F7	0.950	0.780	0.998	0.854	0.992	0.561	0.087	0.177	0.333	0.087	0.291	2.50	7.75
F8	0.946	0.769	0.998	0.989	0.991	0.576	0.071	0.180	0.268	0.039	0.227	3.85	11.93*
OF	0.948	0.776	0.996	0.993	0.989	0.544	0.079	0.170	0.301	0.052	0.276	2.88	9.12

HC, Hixson Crowell; KP, Korsemeyer Peppas; (* extrapolated value from best fitting kinetic model)

Table: 7.10

Cumulative % drug release from different batches of composite tablets at different time points.

Time (h)	Cumulative % drug release ± s.d.								
	F1	F2	F3	F4	F5	F6	F7	F8	OF
0.25	13.32 ± 2.56	9.92 ± 2.41	11.06 ± 5.6	7.03±3.17	12.22± 1.98	10.26 ± 4.23	11.89± 2.6	9.07± 3.33	11.36 ± 4.58
0.5	22.07 ± 3.28	16.53 ± 3.71	18.52 ± 4.7	13.12±2.9	21.41± 2.49	17.17 ± 3.15	19.97± 3.81	15.11 ± 5.32	19.57 ± 3.76
1	40.68 ± 2.89	28.51 ± 3.8	32.03 ± 3.28	21.07±3.8	42.33± 4.17	29.68 ± 4.01	33.23± 2.56	26.05 ± 2.9	32.07 ± 5.56
2	52.33 ± 3.72	38.82 ± 2.29	43.67 ± 2.96	30.18±4.8	54.09± 4.69	40.46 ± 3.45	44.45± 3.67	35.47 ± 5.13	40.16 ± 6.12
3	63.02 ± 2.1	49.4± 3.7	55.62 ± 4.21	39.21±5.1	65.14± 5.98	51.52 ± 2.95	54.03± 3.23	45.14 ± 3.8	52.14 ± 3.09
4	73.21 ± 4.19	57.47 ± 3.41	64.72 ± 3.26	46.05±5.3	75.18± 4.03	59.95 ± 5.53	66.12± 2.69	52.51 ± 6.31	61.32 ± 4.34
5	83.4 ± 3.13	63.54 ± 3.79	71.58 ± 2.58	52.09±3.1	85.82± 3.69	66.3± 2.18	72.31± 4.35	58.06 ± 3.9	67.24 ± 2.18
6	90.25 ± 4.54	69.25 ± 2.45	78.01 ± 3.13	59.2±2.54	92.17± 3.33	72.26 ± 3.09	79.04± 3.76	63.27 ± 4.16	71.27 ± 4.57
7	95.08 ± 3.93	74.62 ± 1.98	84.08 ± 2.76	63.58±4.3	98.24± 2.21	77.88 ± 3.78	85.56± 5.44	68.18 ± 2.55	78.03 ± 3.16
8	99.11 ± 5.18	80.17 ± 3.77	90.34 ± 4.14	68.83±6.1	100.14 ± 3.17	83.67 ± 2.61	92.01± 4.09	73.25 ± 5.07	84.61 ± 2.4
9	100.72± 3.89	84.62 ± 4.12	95.36 ± 2.15	74.08±2.3	100.35 ± 2.19	88.32 ± 3.22	96.77± 2.68	77.31 ± 3.63	88.97 ± 2.78
10	100.8 ± 2.72	88.32 ± 3.64	99.54 ± 1.27	77.79±2.0	100.61 ± 2.14	92.19 ± 3.01	100.63 ± 3.77	80.69 ± 2.67	93.03 ± 3.31

7.5.2.12. In vitro drug release

In case of in vitro drug release study the cumulative percentage of drug release (CPR) from various formulations were correlated with the different independent formulation variables. The regression coefficient (R^2 values), rate constant (k) from different kinetic models, diffusion exponent (n), $T_{50\%}$ and $T_{90\%}$ are shown in Table 7.9 and zero order drug release profile (CPR versus time) is presented in Figure 7.18.

7.5.2.12.1. Statistical analysis of the dependence of release rate on amount of Pmaa-g-GG, TSG and SBC

Mathematical relationship generated using MLRA for the studied response variables are expressed in Eq. 7.17 – 7.21:

$CPR1h = +31.70-3.60X_1 -5.37X_2+1.12X_3+0.83X_1X_2+0.42X_1X_3$ (R^2 = 0.9897) (Eq.7.17)

$CPR2h = +42.44-3.99X_1 -6.20X_2+1.18X_3+0.58X_1X_2+0.55X_2X_3$ (R^2 = 0.9921) (Eq. 7.18)

$CPR6h = +75.43-5.55X_1 - 9.44X_2 +1.25X_3 + 0.79X_1X_2+0.02X_1X_3+ 0.52\ X_2X_3$ (R^2 = 0.9995) (Eq. 7.19)

$CPR10h = +92.57-2.91X_1 -7.82X_2+0.96X_3 - 2.60X_1X_2+0.73X_2X_3$ (R^2 = 0.9990) (Eq. 7.20)

$K = +0.31-0.011X_1 -0.027X_2+2.87E^{-03}X_3-5.87E^{-03}\ X_1X_2 - 0.0016X_1X_3$

(R^2 = 0.9965) (Eq. 7.21)

Where, CPR1h, CPR2h, CPR6h and CPR10h are cumulative % drug release at 1h, 2h, 6h and 10h, respectively in 0.1N HCl, respectively. X_1, X_2 and X_3 are the

amount of Pmaa-g-GG, TSG and SBC, respectively. All the models and the interaction terms were significant as the probability values in all cases were less than 0.05.

7.5.2.12.2. Effect of TSG

The CPR of drug from the composite matrix tablets vs. time profile as shown in Fig. 7.18, indicates that the amount released was mainly dependent on the tamarind seed gum at low and high both level of another two independent variables: Pmaa-g-GG and SBC. When the amount of TSG increases from 150 mg (F1, F3, F5, F7) to 250 mg (F2, F4, F6, F8), the drug release becomes slower, which is also reflected in the regression equations (13-17) and substantiated by the values of release rate constant (K) , $T_{50\%}$ and $T_{90\%}$ presented in Table 7.9. This fact may be due to formation of a continuous compact gel matrix embedded in the rigid 3-D polymeric network of pmaa-g-GG resulting from water uptake by hydrophilic TSG. The contour and 3-D response surface plots showing the effect of TSG on CPR are presented in Fig.7.22, 7.23 and 7.24. A little synergistic effect due to interaction between Pmaa-g-GG and TSG has also been demonstrated by the regression equations corresponding CPR1h, CPR2h and CPR6h.

7.5.2.12.3. Effect of Pmaa-g-GG

The extent of Pmaa-g-GG also showed a significant impact on the CPR of drug from composite matrix (Fig.7.18). As the amount of Pmaa-g-GG was increased from 150 mg (F1, F2, F5, F6) to 250 mg (F3, F4, F7, F8), , the CPR was found to decrease. This may be due to fact that higher Pmaa-g-GG

concentration increased the rigidity of the network, which in turn prevented the imbibition of buffer into the polymer matrix. So there was a reduction in network erosion and loosening leading to reduction in drug release. A significant synergistic effect due to interaction between Pmaa-g-GG and TSG has also been demonstrated by the regression equations corresponding CPR1h, CPR2h and CPR6h. The contour and 3-D response surface plots showing the effect of Pmaa-g-GG on CPR are presented in Fig.7.21 and on rate constant (*K*) in Fig. 7.25.

7.5.2.12.4. Effect of sodium bicarbonate

The amount of SBC showed no such significant impact on drug release as shown in Fig. 7.18, except in case of formulations F4 and F8, in which CPR has been found to increase to some extent with increase in the amount of SBC from 80 mg (F4) to 120 mg (F8) at higher level of another two independent variables: Pmaa-g-GG and TSG . This may happen due to the fact that some portion of unreacted SBC increases the degree of ionization of –COOH groups of β-D-glucuronic acid unit of Pmaa-g-GG moiety resulting more water uptake and subsequent reduction in rigidity of the matrix. This positive interaction effect between Pmaa-g-GG and SBC has also been demonstrated by the regression equation corresponding to CPR1h (Eq.7.17).

7.5.2.12.5. Effect of viscoelasticity

Drug release study revealed that F4 exhibited most sustained drug release compared to others, which is also substantiated by the lowest value of release rate constant and highest value of $T_{50\%}$ and $T_{90\%}$ (Table 7.9). The ratio of Pmaa-g-GG

to TSG found in this formulation (F4) corresponds R1 having high viscosity and highly rigid strong network with higher stability unveiled in viscoelastic investigation, which probably impart the sustaining potential to the matrix. Similar effect has been observed in F8. F2 and F6 corresponding composite ratio R2 exhibit high $T_{50\%}$ and $T_{90\%}$ due to high zero shear viscosity. The formulations F3 and F7 (R3) show lower values of $T_{50\%}$ and $T_{90\%}$, which may be attributed to the fact that the composite gel corresponding ratio R3 possesses a stronger microstructure with higher rigidity but less zero shear viscosity and poor gel-compactness resulting faster drug release.

7.5.2.12.6. Effect of swelling

Comparison of the drug release data with the values of swelling parameters and matrix hydration reveals that values of $T_{50\%}$ and $T_{90\%}$ increase with increase in the values of % W_E, W_∞ and H, indicating the partially swelling controlled mechanism of slower drug release which is further substantiated by the value of release exponent greater than 0.5.

7.5.2.12.7. Kinetics and mechanism of drug release

The regression coefficient (R^2) values, rate constant (k) from different kinetic models, diffusion exponent (n), $T_{50\%}$ and $T_{90\%}$ are shown in Table 7.9. The results demonstrate that most of the formulations follow Higuchi and Korsemeyer-Peppas release kinetic. The diffusion exponent (n) values for all the formulations are within the range of 0.540 (F1) – 0.627 (F4) thus portending the release mechanism is both diffusion controlled and swelling controlled transport (anomalous/non-Fickian transport) based. The lowest values

of rate constant (k) of best fitting kinetic model (Higuchi) resulting from F4 (0.265) and F8 (0.268) establish their sustained release potential. Similarly this fact is also substantiated by the resemblance of the higher values of $T_{50\%}$ and $T_{90\%}$ achieved by these two formulations.

7.5.2.12.8. Release similarity and difference factor

Dissolution similarity (f_2) and difference factor (f_1) were calculated to compare the release profile of each batch with the USP reference release profile (Table 7.4) and shown in the Table 7.6. Highest similarity (75.84) and lowest difference factor (4.08) were exhibited by F6 batch. In order to consider the similar dissolution profiles, the f_1 values should be close to 0 and f_2 values should be close to 100. In general, f_1 values lower than 15 (0 – 15) and f_2 values higher than 50 (50 – 100) show the similarity of the dissolution profiles. FDA and EMEA suggest that two dissolution profiles are declared similar if f_2 is between 50 and 100 [26]. In case of F1:F2 and F5:F6, f_1 has been found to decrease and f_2 to increase with increase in the amount of TSG at low level of Pmaa-g-GG and the reverse effect of TSG has been observed at high level of pmaa-g-GG in case of F3:F4 and F7:F8. Pmaa-g-GG also showed similar effect on f_1 and f_2 values. The values of f_1 and f_2 observed in case of optimized formula (OF) were 5.69 and 71.58, respectively, which indicate good similarity between the release profile of OF and USP reference.

Contour Plots and 3D response surface plots for different response parameters are shown below:

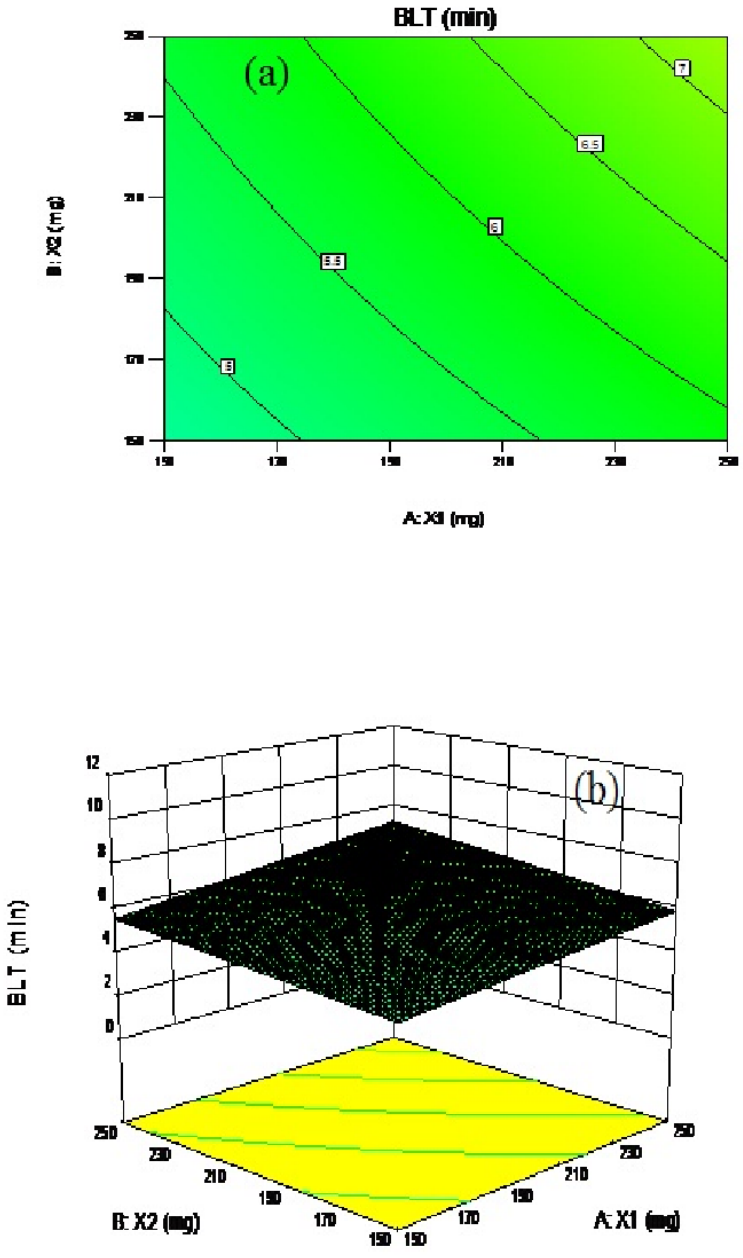

Fig. 7.19. Contour plots (a) response surface 3D plot (b) demonstrating the effect of Pmaa-g-GG (X1) and TSG (X2) on buoyancy lag time (BLT)

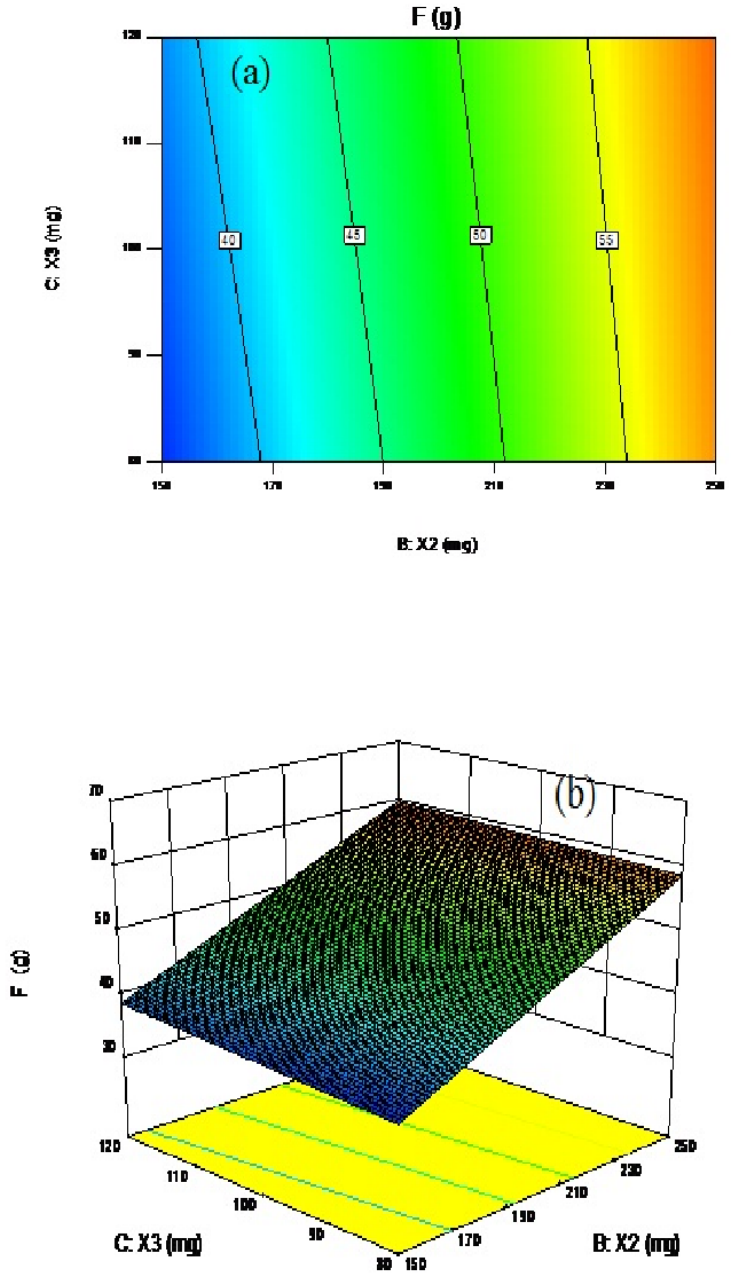

Fig. 7.20. Contour plots (a) response surface 3D plot (b) demonstrating the effect of TSG (X2) and SBC (X3) on mucoadhesive strength (*F*)

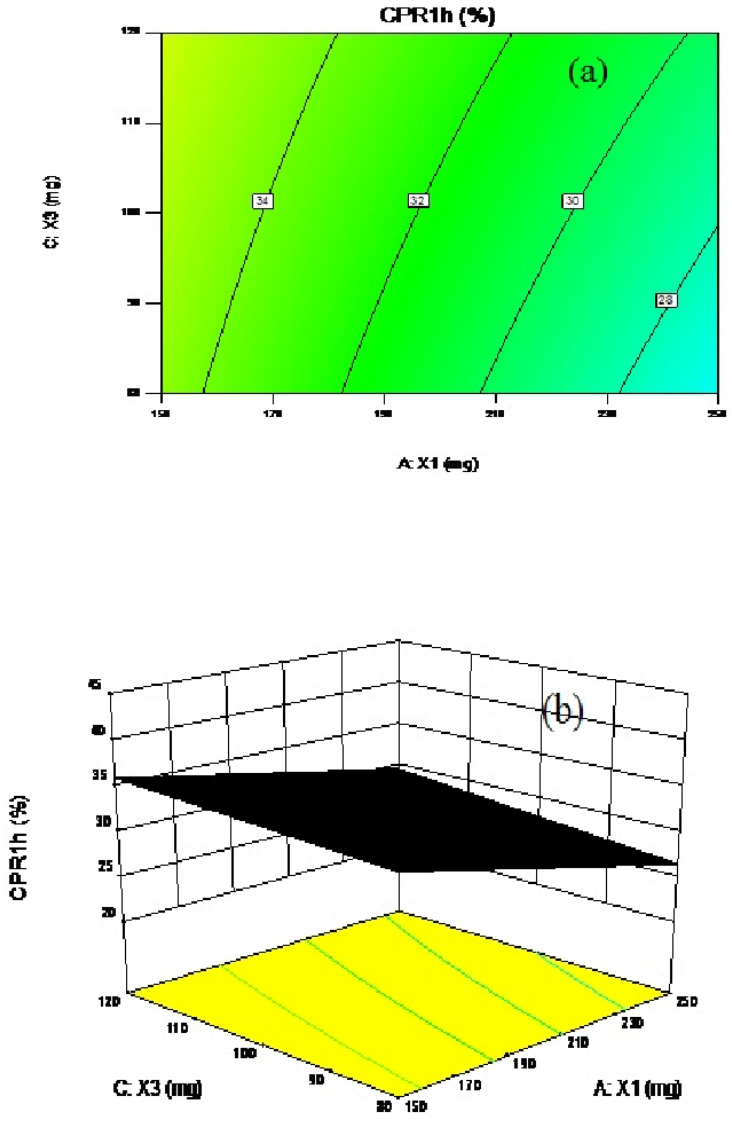

Fig. 7.21. Contour plots (a) response surface 3D plot (b) demonstrating the effect of Pmaa-g-GG (X1) and SBC (X3) on cumulative % release at 1h.

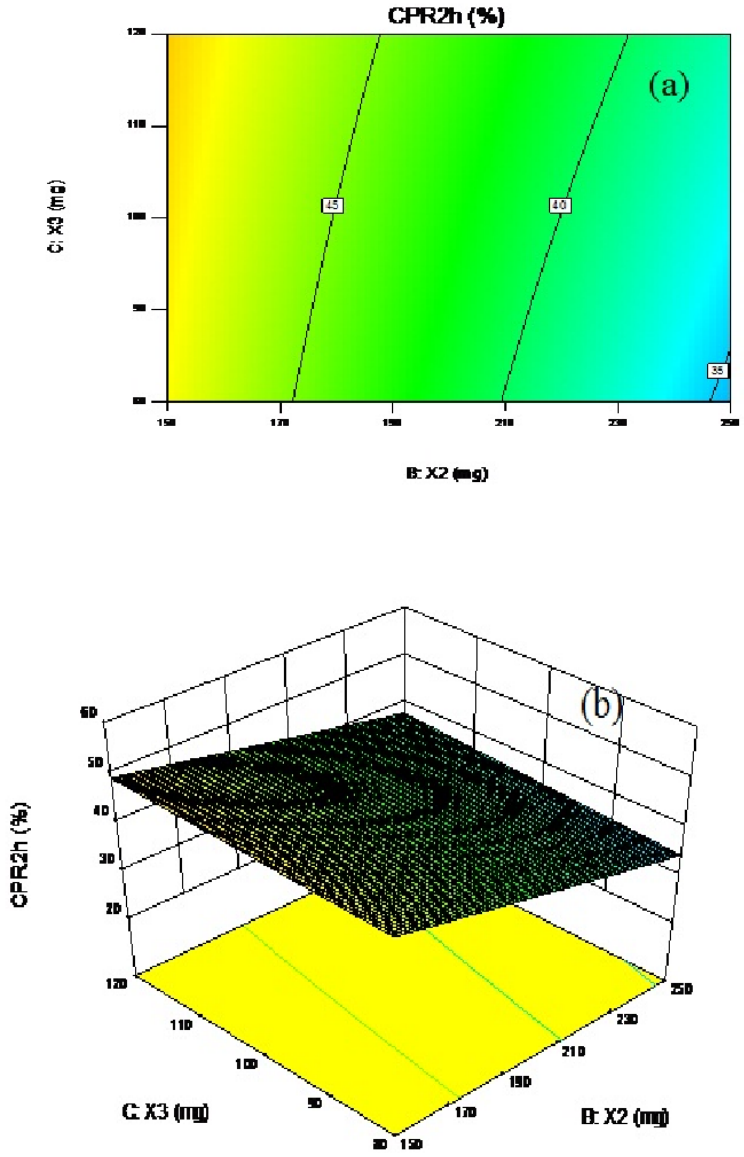

Fig. 7.22. Contour plots (a) response surface 3D plot (b) demonstrating the effect of TSG (X2) and SBC (X3) on cumulative % release at 2h.

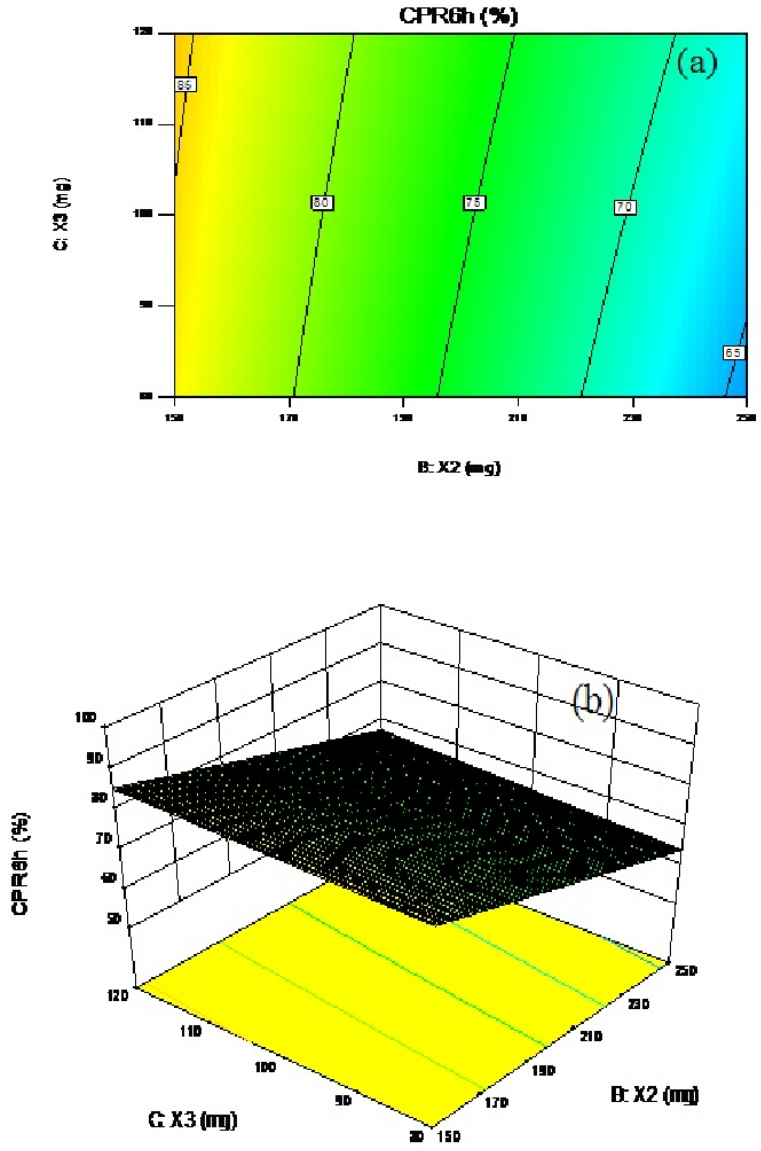

Fig. 7.23. Contour plots (a) response surface 3D plot (b) demonstrating the effect of TSG (X2) and SBC (X3) on cumulative % release at 6h.

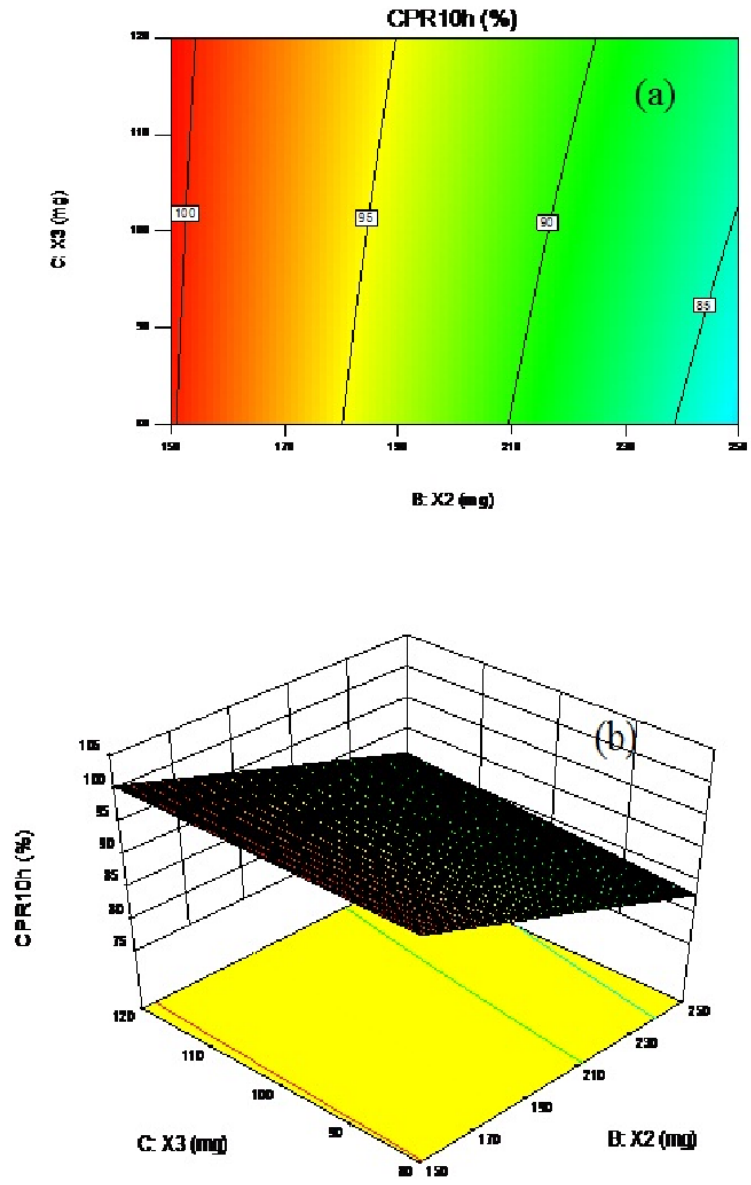

Fig. 7.24. Contour plots (a) response surface 3D plot (b) demonstrating the effect of TSG (X2) and SBC (X3) on cumulative % release at 10h.

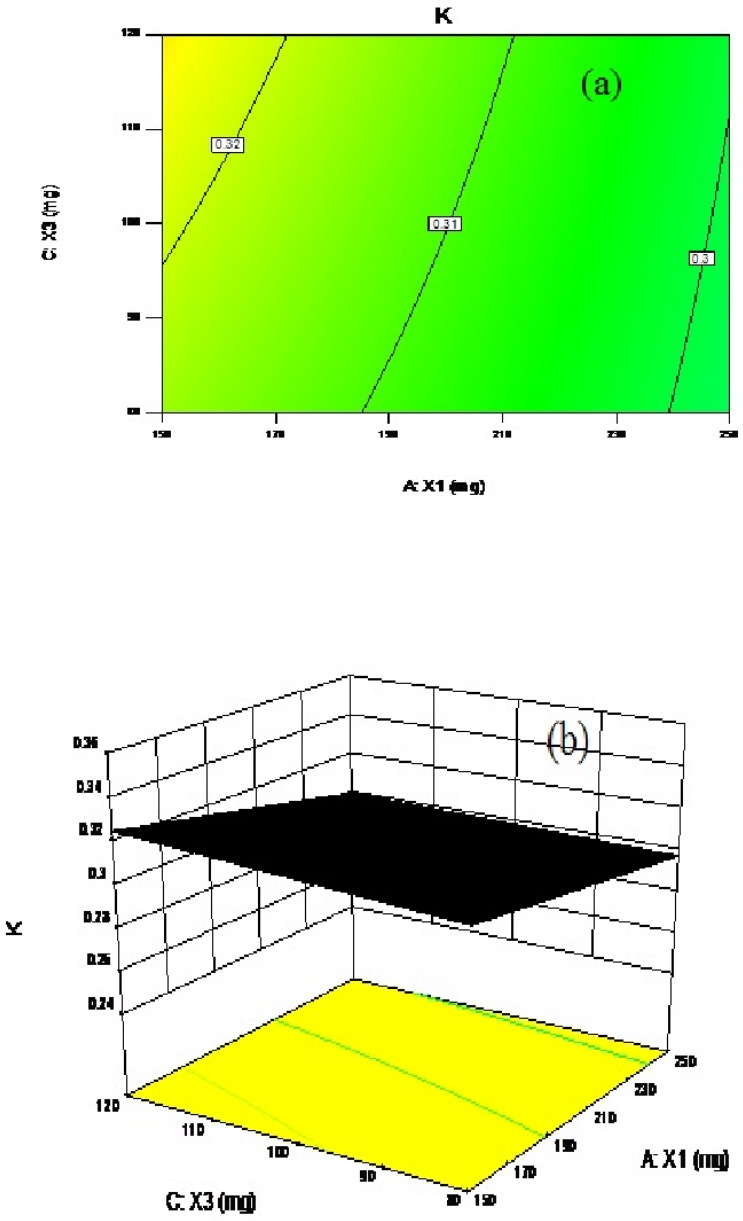

Fig. 7.25. Contour plots (a) response surface 3D plot (b) demonstrating the effect of Pmaa-g-GG (X1) and SBC (X3) on drug release rate constant (K).

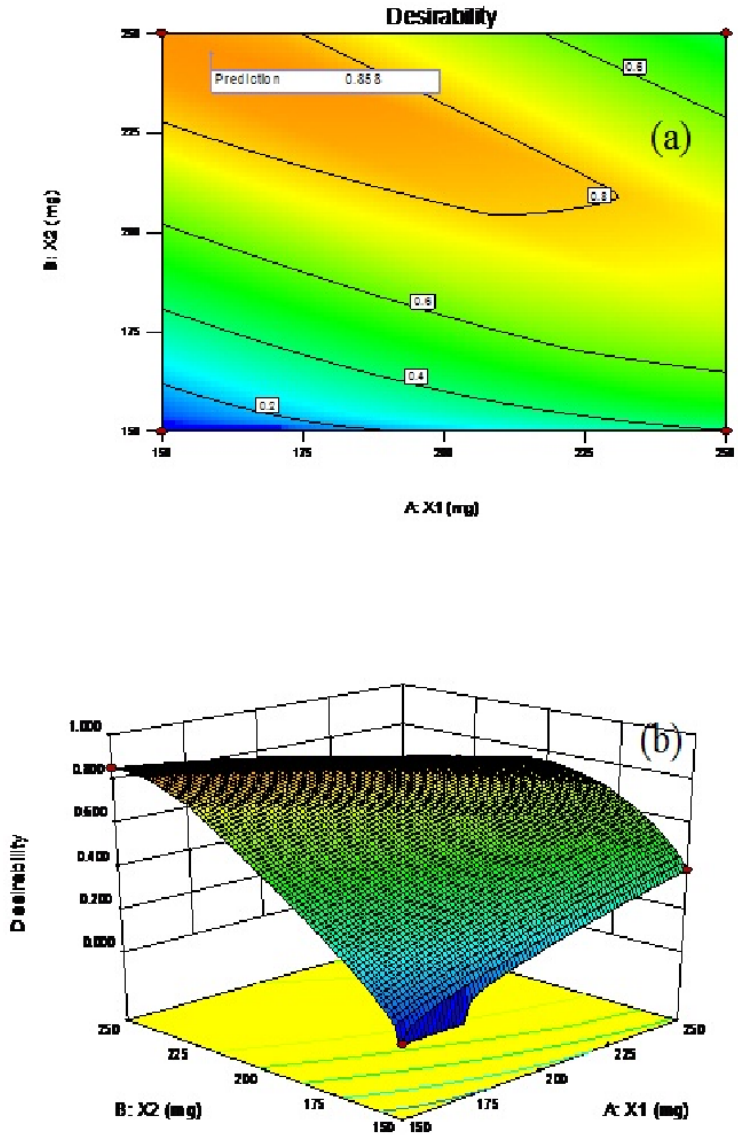

Fig. 7.26. Contour plots (a) response surface 3D plot (b) demonstrating the desirability of the numerical optimization

References:

1. Vijan, V., Kaity, S., Biswas, S., Isaac, J., & Ghosh, A. (2012). Microwave assisted synthesis and characterization of acrylamide grafted gellan, application in drug delivery. *Carbohydrate Polymers, 90,* 496-506.
2. Athawale, V. D., & Lele, V. (1998). Graft co-polymerization onto starch. II: Grafting of acrylic acid and preparation of its hydrogels. *Carbohydrate Polymers, 35,* 21-27.
3. Mishra, A., & Pal, S. (2007). Polyacrylonitrile-grafted okra mucilage: a renewable reservoir to polymeric materials. *Carbohydrate Polymers, 68,* 95 – 100.
4. Fares, M. M., Assaf, S. M., & Abul-Haija, Y. M. (2010). Pectin grafted poly (N-vinyl-pyrrolidone: optimization and in vitro controllable theophylline drug release. *Journal of Applied Polymer Science, 117,* 1945 – 1954.
5. Tiwari, A., & Singh, V. (2008). Microwave-induced synthesis of electrical conducting gum acacia-graft-polyaniline. *Carbohydrate polymers, 74,* 427 – 434.
6. Singh, V., Kumari, P. L., Tiwari, A., & Pandey, S. (2010). Alumina-supported microwave synthesis of *Cassia marginata* seed gum-graft-polyacrylamide. *Journal of Applied Polymer Science, 117,* 3630 – 3638.
7. Anthony, A. A., & Obichukwu, J. N. (2007). Mucuna gum microspheres for oral delivery of glibenclamide: In vitro evaluation. *Acta Pharmaceutica, 57,*161–171.

8. Zohuriaan, M. J., & Shokrolahi, F. (2004). Thermal studies on natural and modified gums. *Polymer Testing, 23,* 575- 579.
9. Nayak, A. K. & Pal, D. (2011). Development of pH-sensitive tamarind seed polysaccharide-alginate composite beads for controlled diclofenac sodium delivery using response surface methodology. *International Journal of Biological Macromolecules, 49,* 784–793.
10. Nandi, G., Patra, P., Priyadarshini, R., Kaity, S. & Ghosh, L. K. (2015). Synthesis, characterization and evaluation of methacrylamide grafted gellan as sustained release tablet matrix. *International Journal of Biological Macromolecules, 72*, 965-974.
11. Fukuda, M., Peppas, N. A. & McGinity, J. W. (2006). Floating hot-melt extruded tablets for gastroretentive controlled drug release system. *Journal of controlled Release, 115,* 121-129.
12. Streubel, A., Siepmann, J. & Bodmeier, R. (2003). Floating matrix tablets based on low density foam powder: effects of formulation and processing parameters on drug release. *European Journal of Pharmaceutical Sciences, 18,* 37-45.
13. Singh, B., Chakkal, S. K. & Ahuja, N. (2006). Formulation and optimization of controlled release mucoadhesive tablets of atenolol using response surface methodology. *AAPS PharmSciTech, 7(1),* article 3.
14. Ofner C. M. III & Schott, H. (1986). Swelling studies of gelatin I: gelatin without additives. *Journal of Pharmaceutical Sciences,* 75, 790.

15. Singh, P., Maity, S., & Sa, B. (2014). Effect of ionic crosslink on the release of metronidazole from partially carboxymethylated guar gum tablet. *Carbohydrate Polymers, 106,* 414–421.

16. Adeyeye, M. C., Jain, A. C., Ghorab, M. K. M. & Reilly, W. J. (2002). Viscoelastic evaluation of topical creams containing microcrystalline cellulose/sodium carboxymethyl cellulose as stabilizer. *AAPS PharmSciTech, 3(2),* article 8.

17. Mondal, N., Nandi, G., Ghosh, L. K. & Gupta, B. K. (2014). Stomach specific sustained delivery of metformin hydrochloride from a novel composite matrix. *International Journal of Drug Formulation and Research, 5,* 140-152.

18. Varelas, C. G., Dixon, D. G., Steiner, C. (1995). Zero order release from biphasic polymer hydrogels. *Journal of Controlled Release, 34,* 185-192.

19. Gibaldi, M., Feldman, S. (1967). Establishment of sink conditions in dissolution rate determinations – theoretical considerations and application to nondisintegrating dosage forms. *Journal of Pharmaceutical Sciences, 56,* 1238-1242.

20. Higuchi, T. (1963). Mechanism of sustained-action medication. Theoretical analysis of rate of release of solid drugs dispersed in solid matrices. *Journal of Pharmaceutical Sciences, 52,* 1145-1149.

21. Niebergall, P. J., Milosovich, G., Goyan, J. E. (1963). Dissolution rate studies. II. Dissolution of particles under conditions of rapid agitation. *Journal of Pharmaceutical sciences, 52,* 236-241.

22. Korsmeyer, R. W., Gurny, R., Doelker, E. M., Buri, P., & Peppas, N. A. (1983). Mechanism of solute release from porous hydrophilic polymers. *International Journal of Pharmaceutics, 15,* 25-35.

23. Desai, S. J., Singh, P., Simonelli, A. P., & Higuchi, W. I. (1966a). Investigation of factors influencing release of solid drug dispersed in inert matrices. III. Quantitative studies involving the polyethylene plastic matrix. *Journal of Pharmaceutical Sciences, 55,* 1230-1234.

24. Desai, S. J., Singh, P., Simonelli, A. P., & Higuchi, W. I. (1966b). Investigation of factors influencing release of solid drug dispersed in inert matrices. IV. Some studies involving the polyvinyl chloride matrix. *Journal of Pharmaceutical Sciences, 55,* 1235-1239.

25. Peppas, N. A. (1985). Analysis of Fickian and non-Fickian drug release from polymers. *Pharmaceutica Acta Helvetica, 60,* 110-111.

26. Costa, P. & Lobo, J. M. S. (2001). Modeling and comparison of dissolution profiles. *European Journal of Pharmaceutical Sciences, 13,* 123-133.

27. Smart, J.D. (2005). The basics and underlying mechanisms of mucoadhesion. *Advanced Drug Delivery Reviews, 57,* 1556–1568.

CHAPTER-VIII

SUMMARY & CONCLUSION

Summary and Conclusion

Metformin HCl is an orally administered biguanide widely used in the management of type-2 diabetes. It is slowly and incompletely absorbed from the stomach and proximal small intestine. The absolute bioavailability is reported to be 50–60% with relatively short plasma elimination half-life of approximately 2 h. This has raised the interest in developing extended-release formulations of metformin. Due to its narrow absorption window, it would be beneficial to develop gastroretentive device through which the gastric residence could be prolonged to release the drug at the absorbing site in a controlled manner for the entire period of drug release from the extended release products to maximize the bioavailability as well as therapeutic benefit along with better patient compliance.

Use of various natural polysaccharides as rate modulator in extended release drug delivery devices is a current trend because of their biocompatibility, low cost, free availability and biodegradability. Gellan, an anionic deacylated exocellular polysaccharide produced by a pure culture of *Pseudomonas elodea* with a tetrasaccharide repeating unit of one α-L- rhamnose, one β-D-glucuronic acid and two β-D-glucose residues, has been used in several types of dosage forms such as stomach-specific controlled release beads, interpenetrating hydrogel microsphere, tablets. However, rapid solubility in water, substantial swelling and rapid erosion of gellan are some of the limitations to make it an ideal matrix material for extended release. One of the powerful methods to modify the various physical, chemical and functional properties of polysaccharides is graft co-polymerization

in which polymers are grafted onto polysaccharides backbone. Graft co-polymerization introduces hydrophobicity and steric bulkiness which considerably protect the matrix and carbohydrate backbone from rapid dissolution and erosion, and provides extended release of drugs. Therefore, firstly, methacrylamide has been grafted onto gellan backbone in order to synthesis gellan graft copolymer and the copolymer has been characterized. The copolymer obtained has been found to possess significant hydrophobicity and capacity to form a rigid erosion proof matrix. However, the matrix is less continuous due to poor gelation. On the other hand, native natural hydrophilic polysaccharides are capable of forming intensively continuous matrix due to high degree of swelling that ensures drug release in more sustained manner but advance erosion is the their main limiting factor. Incorporation of natural hydrophilic polysaccharide into hydrophobic matrix of graft-copolymer is another approach to improve desired functional properties like swelling, drug release kinetic and stability. This composite blending yields a continuous soft but rigid erosion proof hydrated matrix after absorbing water from gastrointestinal fluid, followed by extended drug release over a significantly long period of time.

Tamarind seed gum (TSG) is an excellent natural hydrophilic polysaccharide obtained from the endosperm of *Tamarindus indica* Linn (family Leguminosae) having branched structure consisting of a main chain of β-D (1→4) linked glucopyranosyl units, with a side chain consisting of a single xylopyranosyl unit attached to every second, third and fourth D-glucopyranosyl unit through an α-D (1→6) linkage. One D-galacotopyranosyl units is attached to one of the

xylopyranosyl unit through a β-D (1→2) linkage. It is widely used as a thickening, stabilizing, emulsifying, mucoadhesive and gelling agent in various pharmaceutical formulations due to possessing of high thermal and chemical stability, non-carcinogenicity, biocompatibility, mucoadhesivity, non-toxicity and high drug holding capacity. Numerous oral sustained release gastroretentive drug delivery systems viz., buoyant systems mucoadhesive systems, expandable or swellable systems, high density systems etc. have been reported. Recently, the combined floatation–mucoadhesion approaches for gastroretention have gained importance as these devices exhibit a better gastroretention by virtue of their buoyancy and bio-adhesion properties. Sodium bicarbonate (SBC) has been widely reported as buoyancy contributor in different buoyant systems. Further, TSG has been reported as excellent natural mucoadhesive. Therefore, incorporation of TSG in the matrix of polymethacrylamide-*g*-gellan would impart sustained release as well as mucoadhesion property which can be combined with buoyancy to achieve better gastroretention.

In this study, a novel buoyant-mucoadhesive extended release tablet formulation of metformin HCl based on a hydrophobic polymethacrylamide-g-gellan copolymer and hydrophilic TSG composite matrix has been developed, which is not reported earlier. In this study, SBC and TSG have been used as buoyancy contributor and release modulator-cum-mucoadhesive, respectively. A 2^3 full factorial design was adopted to evaluate the influence of independent factors on the responses (dependent variables) using Design-Expert software (version

9.0.4.1, Stat-Ease Inc., Minneapolis, USA). Tablets were prepared employing wet granulation method and evaluated for *in vitro* drug release, buoyancy, ex-vivo mucoadhesion, hydration kinetic, viscoelastic property and surface morphology. Compatibility between drug and excipients was checked by DSC, FTIR and XRD analysis. The formulation was numerically optimized to obtain USP-reference release profile, minimum buoyancy lag time and maximum mucoadhesive strength.

In the first part, microwave-promoted free radical initiation method was employed for the synthesis of polymethacrylamide-grafted-gellan gum (PMaa-g-GG). Amount of methacrylamide (Maa), cerric (IV) ammonium nitrate (CAN) and microwave irradiation time were taken as independent variable synthetic parameters. A total of eight batches of grafted gellan gum with different synthetic conditions were prepared. The values of different grafting parameters ratify that amount of CAN has major positive influence on the higher grafting efficiency irrespective of other variables. The anova analysis indicates the positive effect of Maa and CAN and negative effect of microwave on grafting. The synthetic condition for the synthetic batch S7 results in lowest grafting whereas the batch S1 and S2 result highest yield. The degree of grafting was shown to increase with the increase in concentration level of methacrylamide at both higher and lower level of two other independent synthetic factors. Similarly, grafting efficiency and other grafting parameters are proportional to the concentration of cerric ammonium nitrate. The microwave irradiation provides rapid transfer of energy in the bulk of the reaction mixture, which reduces reaction time therefore it acts as a

catalyst and gives a synergistic activity. This phenomenon substantiates the results of the cerric (IV) initiated microwave-promoted graft copolymerization. In case of batch S1 and S2 the % grafting were nearly same though microwave irradiation time was 5 min (S1) and 1 min (S2), whereas, in case of other batches, % grafting was shown to be inversely proportional to microwave irradiation time.

The synthesized copolymer was characterized by elemental analysis, FTIR, DSC-TGA and X ray diffraction.

The toxicity study as per the "organization of Economic Co-operation and Development (OECD) guideline for the test of chemicals" 425, adopted "17 December 2001" Annexure-4, revealed the LD_{50} value is greater than 2000mg/kg dose of Pmaa-g-GG. So, Pmaa-g-GG is under the "category 5" as well as toxicity rating is "zero". Histopathological examination establishes the physiological compatibility of the grafted gellan gum.

In second part, gastroretentive extended release monolithic matrix tablets of metformin HCl were prepared with polymethacrylamide grafted gellan gum, tamarind seed gum and sodium bicarbonate (SBC) of different eight batches employing wet granulation method.

The physical characterization of the tablets exhibited the following information: the weight of the tablets was confined within ±4% of the average weight, thickness varied from 5.07 to 6.18 mm with MSD 0.13% (n= 10), the maximum friability found was 0.46% and the drug content varied within ±5% of the labeled amount. Hardness was within the range of 4-5 kg/m^2. All these variation were found to comply with the requirements of official Compendium.

FTIR, DSC and XRD study demonstrates that there is no significant incompatibility between the drug, polymers and other excipients.

A numerical optimization technique based on the criterion of desirability was adopted to develop the optimized formulation. An optimal formulation setting having highest desirability (0.858) was selected among 28 different settings recommended by Design Expert 9.0.4.1 software. The optimal values of Pmaa-g-GG, TSG and SBC selected were 158.80mg, 244.99mg and 120mg, respectively. The confirmation experiments were conducted to test the responses of the optimal formulation (OF). In short, the experimental findings were within the close agreement to the model-based predictions, which conferred the predictability and validity of the models.

The in vitro buoyancy test showed that the average buoyancy lag time (BLT) observed was within the range from 1.74 mins to 10.15 mins and the total buoyancy time (TBT) for all formulations was observed to be greater than 10 hours. The value of mucoadhesive strength, *F,* exhibited by different batches of composite tablets ranges from 34.6g to 62.6g.

The gel with ratio R1 (found in F4 and F8) and R2 (found in F2 and F6) exhibit higher zero shear viscosity (2013.3 Pa.s and 2076.3 Pa.s, respectively), which indicates that the particles in the matrices are non-associated having a strong thickened behavior. The gel with ratio R3 (found in F3 and F7) showed highest starting % strain (γ) for structural breakdown at $G' = G''$, which indicates stronger microstructure and high rigidity of the gel matrix. This property imparts nonerodability to the composite matrix. In case of R1, higher crossover time

observed indicates a strong matrix network of polymer entanglement and possibly better long term stability of the matrix. Higher values of storage modulus (G') observed in R1 and R3 compared to that in R2, indicates more solid like property of the matrix microstructure. Therefore, it can be concluded that the composite gel matrix with ratio R1 showed to have high viscosity and highly rigid strong network. The viscosity versus shear rate profiles depicts that viscosity decreases with increase in shear rate after a very small initial rise.

The CPR of drug from the composite matrix tablets vs. time profile, indicates that the amount released was mainly dependent on the tamarind seed gum at low and high both level of another two independent variables: Pmaa-g-GG and SBC. A little synergistic effect due to interaction between Pmaa-g-GG and TSG has also been demonstrated by the regression equations corresponding CPR1h, CPR2h and CPR6h. The extent of Pmaa-g-GG also showed a significant impact on the CPR of drug from composite matrix . As the amount of Pmaa-g-GG was increased from 150 mg (F1, F2, F5, F6) to 250 mg (F3, F4, F7, F8), , the CPR was found to decrease. This may be due to fact that higher Pmaa-g-GG concentration increased the rigidity of the network, which in turn prevented the imbibition of buffer into the polymer matrix. So there was a reduction in network erosion and loosening leading to reduction in drug release. A significant synergistic effect due to interaction between Pmaa-g-GG and TSG has also been demonstrated by the regression equations corresponding CPR1h, CPR2h and CPR6h. The amount of SBC showed no such significant impact on drug release, except in case of

formulations F4 and F8, in which CPR has been found to increase to some extent with increase in the amount of SBC from 80 mg (F4) to 120 mg (F8) at higher level of another two independent variables: Pmaa-g-GG and TSG . Drug release study revealed that F4 exhibited most sustained drug release compared to others, which is also substantiated by the lowest value of release rate constant and highest value of $T_{50\%}$ and $T_{90\%}$. The ratio of Pmaa-g-GG to TSG found in this formulation (F4) corresponds R1 having high viscosity and highly rigid strong network with higher stability unveiled in viscoelastic investigation, which probably impart the sustaining potential to the matrix. Comparison of the drug release data with the values of swelling parameters and matrix hydration reveals that values of $T_{50\%}$ and $T_{90\%}$ increase with increase in the values of % W_E, W_∞ and H, indicating the partially swelling controlled mechanism of slower drug release which is further substantiated by the value of release exponent greater than 0.5.

Highest dissolution similarity (75.84) and lowest difference factor (4.08) were exhibited by F6 batch. The values of f_1 and f_2 observed in case of optimized formula (OF) were 5.69 and 71.58, respectively, which indicate good similarity between the release profile of OF and USP reference.

The present work was dealt with the development and evaluation of buoyant-mucoadhesive Pmaa-g-GG-TSG composite matrix tablets containing metformin HCl having short elimination half-life (2 h) with an aim to extend the drug release and enhance the bioavailability of the drug through gastroretention over a prolonged period of time. The composite matrix formulation was optimized by employing 2^3 full factorial design. The optimized formulation containing

metformin HCl was further evaluated to establish the robustness of the optimization method. The optimized formulation exhibited excellent buoyancy over a period of 10 h with a very short BLT, good mucoadhesivity and highly similar extended drug release profile with USP reference. Overall, this study provided a simple, reproducible and economical approach for the development of biopolymer based composite matrix tablet for stomach-specific delivery of metformin HCl. In conclusion it needs to be mentioned that this optimized buoyant-mucoadhesive extended release tablet formulation of metformin hydrochloride is so unique in nature and first of its kind that future research workers should evaluate the in vivo gastric retention capacity as well as in vivo drug release profile, pharmacokinetic and pharmacodynamic parameters in human models in order to place it as a marketable product.

Carbohydrate Polymers 137 (2016) 100–110

Contents lists available at ScienceDirect

Carbohydrate Polymers

journal homepage: www.elsevier.com/locate/carbpol

Gastroretentive extended release of metformin from methacrylamide-g-gellan and tamarind seed gum composite matrix

Rosy Priyadarshini[a], Gouranga Nandi[b,*], Abhijit Changder[a], Sailee Chowdhury[b], Sudipta Chakraborty[b], Lakshmi Kanta Ghosh[a]

[a] Department of Pharmaceutical Technology, Jadavpur University, Kolkata 700032, India
[b] BCDA College of Pharmacy and Technology, 78, Jessore Road (S), Hridaypur, Kolkata 700127, India

ARTICLE INFO

Article history:
Received 3 July 2015
Received in revised form 13 October 2015
Accepted 14 October 2015
Available online 19 October 2015

Keywords:
Gastroretentive
Metformin
Polymethacrylamide-g-gellan
Tamarind seed gum
Composite-matrix

ABSTRACT

Formulation of a gastroretentive extended release tablet of metformin based on polymethacrylamide-g-gellan (Pmaa-g-GG)-tamarind seed gum (TSG) composite matrix is the main purpose of this study. Tablets were prepared employing wet granulation method taking amount of Pmaa-g-GG, TSG and $NaHCO_3$ (SBC, buoyancy contributor) as independent formulation variables. The tablets were then evaluated for in vitro drug release, buoyancy, ex vivo mucoadhesion, swelling and surface morphology. Compatibility between drug and excipients was checked by DSC, FTIR and XRD analysis. Buoyancy-lag-time, mucoadhesive strength, % drug release and release-rate constant were statistically analyzed using Design-Expert software (version 9.0.4.1) and the formulation was then numerically optimized to obtain USP-reference release profile. The optimized formulation showed excellent buoyancy over a 10 h period with buoyancy lag time of 2.76 min, significant mucoadhesion and drug release over a period of 10 h with $f_2 = 71.58$. Kinetic modeling unveiled anomalous non-Fickian transport based drug release mechanism.

1. Introduction

Metformin HCl (MFH) is an orally administered biguanide widely used in the management of type-2 diabetes. It is slowly and incompletely absorbed from the stomach and proximal small intestine. The absolute bioavailability is reported to be 50–60% with relatively short plasma elimination half-life of approximately 2 h (Pentikainen, Neuvonen, & Penttila, 1979). This has raised the interest in developing extended-release formulations of metformin (Vijan, Kaity, Biswas, Isaac, & Ghosh, 2012). A significant problem associated with extended release device is that after a short gastric transit period of less than 6 h, the device leaves the upper gastrointestinal tract and the drug release occurs in non-absorbing distal segments of the gastrointestinal tract resulting a short absorption phase accompanied by lesser bioavailability (Chavanpatil, Jain, Chaudhari, Shear, & Vavia, 2005). Therefore, due to its narrow absorption window, it would be beneficial to develop gastroretentive device through which the gastric residence could be prolonged to release the drug at the absorbing site in a controlled manner for the entire period of drug release from the extended release products to maximize the bioavailability as well as therapeutic benefit.

Use of various natural polysaccharides as rate modulator in extended release drug delivery device is a current trend because of their biocompatibility, low cost, free availability and biodegradability (Efentakis & Kouttis, 2001). Gellan, an anionic deacylated exocellular polysaccharide produced by a pure culture of *Pseudomonas elodea* with a tetrasaccharide repeating unit of one α-L-rhamnose, one β-D-glucuronic acid and two β-D-glucose residues, has been used in several types of dosage forms such as stomach-specific controlled release beads (Narkar, Sher, & Pawar, 2010), interpenetrating hydrogel microsphere (Agnihotri & Aminabhavi, 2005), etc. However, rapid solubility in water, substantial swelling and rapid erosion of gellan are some of the limitations to make it an ideal matrix material for extended release. One of the powerful methods to modify the various physical, chemical and functional properties of polysaccharides is graft co-polymerization in which polymers are grafted onto polysaccharides backbone. Graft co-polymerization introduces hydrophobicity and steric bulkiness which considerably protect

Abbreviations: GG, gellan gum; Pmaa, polymethacrylamide; CAN, cerric (IV) ammonium nitrate; Pmaa-g-GG, polymethacrylamide-grafted-gellan gum; SBC, sodium bicarbonate; TSG, tamarind seed gum; BLT, buoyancy lag time; TBT, total buoyancy time; FTIR, Fourier transform infra-red; XRD, X-ray diffraction; DSC, differential scanning calorimetry; TGA, thermogravimetric analysis; KBr, potassium bromide; UV–vis, ultraviolet–visible; CPR1h, CPR2h, CPR6h, CPR10h, cumulative percent drug release at 1 h, 2 h, 6 h and 10 h, respectively; $T_{50\%}$ and $T_{90\%}$, time at which 50% and 90% drug was released, respectively.

* Corresponding author.
E-mail address: nandi_gouranga@yahoo.co.in (G. Nandi).

http://dx.doi.org/10.1016/j.carbpol.2015.10.054
0144-8617/

the matrix and carbohydrate backbone from rapid dissolution and erosion, and provides extended release of drugs. Recently, we have reported synthesis and characterization of methacrylamide grafted gellan (Nandi, Patra, Priyadarshini, Kaity, & Ghosh, 2015), which possesses significant hydrophobicity and capacity to form a rigid erosion proof matrix. However, the matrix is less continuous due to poor gelation. On the other hand, native natural hydrophilic polysaccharides are capable of forming intensively continuous matrix due to high degree of swelling that ensures drug release in more sustained manner but advance erosion is their main limiting factor. Incorporation of natural hydrophilic polysaccharide into hydrophobic matrix of graft-copolymer is another approach to improve desired functional properties like swelling, drug release kinetic and stability (Ahuja, Yadav, & Kumar, 2010). The composite matrix resulted from intimate physical blending of hydrophobic graft-copolymer and hydrophilic natural gum yields a continuous soft erosion proof hydrated matrix after absorbing water from gastrointestinal fluid, followed by extended drug release over a significantly long period of time.

Tamarind seed gum (TSG) is an excellent natural hydrophilic polysaccharide obtained from the endosperm of *Tamarindus indica* Linn; family Leguminosae (Gidley et al., 1991). It is widely used as a thickening, emulsifying, mucoadhesive and gelling agent in various pharmaceutical formulations due to possessing of high thermal and chemical stability, non-carcinogenicity, biocompatibility, mucoadhesivity and non-toxicity (Nayak, Pal, & Santra, 2014). Numerous oral sustained release gastroretentive drug delivery systems viz., buoyant systems (Nayak, Pal, & Malakar, 2013), mucoadhesive systems (Pal & Nayak, 2012), expandable or swellable systems (Klausner, Lavy, Friedman, & Hoffman, 2003), etc. have been reported. Recently, the combined floatation–mucoadhesion approaches for gastroretention have gained importance as these devices exhibit a better gastroretention by virtue of their buoyancy and bio-adhesion properties (Malakar & Nayak, 2013). SBC has been widely reported as buoyancy contributor in different buoyant systems (Fukuda, Peppas, & McGinity, 2006). Further, TSG has been reported as excellent natural mucoadhesive (Nayak et al., 2014). Therefore, incorporation of TSG in the matrix of polymethacrylamide-g-gellan would impart sustained release as well as mucoadhesion property which can be combined with buoyancy to achieve better gastroretention.

In our present attempt, a novel buoyant-mucoadhesive extended release tablet formulation of metformin based on a hydrophobic polymethacrylamide-g-gellan copolymer and hydrophilic TSG composite matrix has been developed, which is not reported earlier. In this study, SBC and TSG have been used as buoyancy contributor and release modulator-cum-mucoadhesive, respectively. A 2^3 full factorial design was adopted to evaluate the influence of independent factors on the responses using Design-Expert software (version 9.0.4.1, Stat-Ease Inc., Minneapolis, USA). Tablets were evaluated for in vitro drug release, buoyancy, ex vivo mucoadhesion, swelling kinetic and surface morphology. Finally, the formulation was numerically optimized.

2. Experimental

2.1. Materials

Gellan gum and Methacrylamide were bought from HiMedia Laboratories Private Limited, Mumbai, India. Cerric ammonium nitrate was purchased from Qualigens Fine Chemicals, Mumbai, India. Metformin hydrochloride (99.57% purity) was received as gift sample from East India Pharmaceutical Works Private Limited, Kolkata, India. TSG was purchased from local market in Kolkata, India and purified. All other reagents and chemicals used were of laboratory reagent grade and used without further purification. Triple-distilled water was used throughout the experiment.

2.2. Isolation of TSG

TSG was purified from its commercially available grade purchased from local market in Kolkata, India. Approximately 20 g was dispersed in 1000 ml distilled water to obtain slurry. The slurry was boiled for 20 min under stirring condition, kept overnight to allow the proteins and fibers to settle out and then centrifuged at 5000 rpm for 20 min. The supernatant was separated, poured into twice the volume of absolute ethanol with continuous stirring for 2 min and allowed to stand for 1 h for precipitation of the gum. The precipitate was then washed with distilled water and dried at 60 °C to constant weight (Nayak & Pal, 2011).

2.3. Preparation of polymethacrylamide-grafted-gellan copolymer

Pmaa-g-GG co-polymer having % grafting value of 669.58 (67.09% grafting efficiency) was prepared following the method reported elsewhere (Nandi et al., 2015). Briefly, 1 g GG was dissolved in 100 ml water and methacrylamide (10 g) and CAN (400 mg) were mixed in it. The mixture was then exposed to microwave in a domestic microwave oven (Electrolux, C23K101.BB, India) at 500 W for 5 min with the process of 1 min exposure to microwave followed by 1 min cooling with ice-cold water outside the oven and repeated for another 4 times. Then it was left for overnight. Acetone was added to it in 1:2 ratios (reaction-mixture: acetone) for precipitation of the grafted copolymer. The precipitate was filtered, washed with 80% (v/v) aqueous methanol to remove the unreacted free monomer and the homopolymer if any, and dried at 40 °C to a constant weight. The product was stored in vacuum desiccator until used.

2.4. Formulation of gastroretentive tablet

A 2^3 full factorial design was adopted to evaluate the influence of independent factors such as quantity of Pmaa-g-GG (X_1), TSG (X_2) and SBC (X_3) on the responses such as BLT, mucoadhesive strength (F), CPR at 1 h, 2 h, 6 h and 10 h in simulated gastric fluid (pH 1.2), rate constant (K), dissolution similarity (f_2) and difference factor (f_1) using Design-Expert software. Three factors were varied at two different levels (high and low) and the experimental trial was carried out on all eight possible combinations keeping other factors constant (Table 1; F1–F8). The low and high level of X_1, X_2 and X_3 were set at (150 mg; 250 mg), (150 mg; 250 mg) and (80 mg; 120 mg), respectively.

2.5. Preparation of tablet

A batch of 10 tablets was prepared at a time for each formulation (Table 1; F1–OF) employing wet granulation method. Briefly, semisolid dough was first prepared from the Pmaa-g-GG with minimum amount of hot water (50 °C) in a deep petridish and then TSG, SBC and drug were mixed intimately with it using spatula. The mass was then passed through #18 mesh to obtain granules. These granules were dried at 60 °C for 20 min in hot-air-oven (Remi, India) and passed through #18 mesh, lubricated with purified talc and magnesium stearate, and compressed in a rotary tablet machine with 12 mm single punch diameter (Labpress, 10 station, Remi, Mumbai, India). F0 batch was prepared by same wet granulation method using microcrystalline cellulose in same punch. Hardness was within the range of 4–5 kg/m^2.

Table 1
Formula per tablet for each formulation obtained from 2^3 full factorial design.

Formulation code	MFH (mg)	Pmaa-g-GG (mg)	TSG (mg)	SBC (mg)	MCC (mg)	PVP (mg)	Talc (mg)	Magnesium stearate (mg)	Copolymer: TSG
F0	500	–	–	–	540	80	10	10	–
F1	500	150	150	80	–	–	10	10	1:1
F2	500	150	250	80	–	–	10	10	3:5
F3	500	250	150	80	–	–	10	10	5:3
F4	500	250	250	80	–	–	10	10	1:1
F5	500	150	150	120	–	–	10	10	1:1
F6	500	150	250	120	–	–	10	10	3:5
F7	500	250	150	120	–	–	10	10	5:3
F8	500	250	250	120	–	–	10	10	1:1
OF	500	158.80	244.9	120	–	–	10	10	2.3:3.13

OF, optimized formula; MCC, microcrystalline cellulose; PVP, polyvinylpyrrolidone K-30.

2.6. FTIR spectroscopy

FTIR spectra of GG, Pmaa-g-GG, TSG, drug and tablet (F8) were obtained using FTIR (Bruker, Alpha T, Germany) to predict the possible interactions between drug and polymers. A small amount of each material was mixed with KBr (1% w/w sample) and compressed into tablet. The scanning range selected was 550–4000 cm^{-1}.

2.7. DSC and TGA study

DSC and TGA thermograms of pristine drug and tablet formulation (F8) were recorded under N_2 flow (150 ml/min) using Perkin Elmer Pyris Diamond TG/DTA, Singapore, at a heating rate of 10 °C/min in a platinum crucible with alpha alumina powder as reference and sample mass of 3–5 mg to detect possible thermal changes of the drug during tabletting process and interaction between drug and polymers if any. The heating range was from 30 °C to 500 °C.

2.8. X-ray diffraction study

X-ray powder diffractometry of drug and its tablet formulation (F8) were recorded using X-ray diffractometer (Rigaku, Ultima-III, Japan). The diffractometer was run at a scanning speed of 2°/min with Cu target slit of 10 mm and a chart speed of 2°/2 cm per 2θ and the angular range fixed was from 10° to 70° to detect possible changes of crystalinity of drug or other interaction with excipients.

2.9. Determination of drug content of tablet

Five tablets were finely powdered; a quantity equivalent to 100 mg of MFH was accurately weighed and transferred into 100 ml volumetric flask containing USP phosphate buffer solution (PB) of pH 6.8. The mixture was allowed to stand for 12 h with an intermittent shaking. The mixture was filtered and the filtrate following suitable dilution was analyzed for MFH content at 230 nm using a UV–visible spectrophotometer (UV–visible double beam spectrophotometer, Pharmaspec-1700, Shimazdu, Japan). The reliability of the above analytical method was justified by conducting recovery analyses at three levels of spiked drug solution and for three consecutive days in the absence or presence of the polymers. The recovery averaged 99.02 ± 1.17%.

2.10. In vitro buoyancy study

The in vitro buoyancy of the tablets was investigated following reported procedure with some modifications (Fukuda et al., 2006). One tablet was placed in the dissolution apparatus type II (DS-800; 6 + 2; SC/TR, Lab India, Mumbai, India) containing 900 ml of simulated gastric fluid (0.1 N HCl with 1.8 g of NaCl; pH 1.2) maintained at 37 ± 0.5 °C with rotational speed of 50 rpm. The time required for rising to the surface of dissolution medium and the tablet remaining buoyant in acidic medium were recorded to measure the buoyant lag-time (BLT) and total buoyant time (TBT), respectively. The state of the tablets during buoyancy testing was checked visually each hour for 10 h and at the end point of 24 h. The test was performed in triplicate.

2.11. Tablet density

The density (D) of the tablet was calculated from tablet height, diameter and weight using the formula expressed in Eq. (1) (Streubel, Siepmann, & Bodmeier, 2003).

$$D(\mathrm{g/cm^3}) = \frac{w}{(m/2)^2 \times \pi \times h} \quad (1)$$

Here, m is the diameter of a tablet, π is the circular constant, h is the height of a tablet, and w is the weight of a tablet. All measurements were performed in six replicates.

2.12. Ex vivo mucoadhesion testing

Mucoadhesive potential of the tablets were evaluated by conducting ex vivo mucoadhesion study using a modification of the assembly described earlier (Singh, Chakkal, & Ahuja, 2006) with goat gastric mucosa as the model membrane. The mucosal membrane was excised by removing the underlying connective and adipose tissue, and equilibrated at 37 ± 1 °C for 30 min in phosphate buffer pH 6.8 before the study. The tablet was lowered onto the mucosa under a constant weight of 5 g for a total contact period of 1 min. Mucoadhesive strength (F) was assessed in terms of the weight in grams required to detach the tablet from the membrane. The tests were repeated in triplicate for each formulation.

2.13. Scanning electron micrography

The surface morphology of the tablet (F8) before and after the dissolution study were analyzed by a scanning electron microscope (JSM6360, JEOL, UK) equipped with secondary electron detector. The samples were coated using gold to increase the conductivity of the electron beam. The operating conditions were an accelerating voltage of 17 kV; the working distance was 12 mm at spot size of 45.

2.14. Swelling study

Drug free tablets were weighed and placed in wire baskets and immersed in 200 ml simulated gastric fluid (pH 1.2) at 37 °C for 24 h. The baskets were removed from the solution at the end of the period and weighed after removing the surface water with tissue

Table 2
Different parameters with their values used in analysis and optimization.

Sl. no.	Independent variables		Response				
	Parameters	Optimized value	Parameters	USP reference release profile	Target value	Predicted value	Observed value
1.	Pmaa-g-GG (X_1)	158.8 mg	BLT	–	Minimum	2.71 min	2.83 min
2.	TSG (X_2)	244.99 mg	Mucoadhesive strength (F)	–	Maximum	57.28 g	58.68 g
3.	SBC(X_3)	120 mg	CPR1h	20–40%	30%	30.0	32.07
4.	–	–	CPR2h	35–55%	45%	41.39	40.16
5.	–	–	CPR6h	65–85%	75%	72.63	71.27
6.	–	–	CPR10h	Not less than 85%	90%	91.47	93.03
7.	–	–	K	–	Minimum	0.302	0.301
8.	–	–	f_1	–	Minimum	4.97	5.69
9.	–	–	f_2	–	Maximum	74.98	71.58

paper. Equilibrium water uptake (swelling index, %) of the tablets was determined from the following relationship (Eq. (2)):

$$W_E = \frac{(w_1 - w_0) \times 100}{w_0} \quad (2)$$

where W_E is the equilibrium water uptake (%), w_0 is the dry weight of tablet plus basket and w_1 is the weight of tablet plus basket after removal from the solution.

The kinetics of swelling of the matrix tablets were studied by measuring the increase in weight of tablet after immersion in simulated gastric fluid (pH 1.2) as a function of time, t (Ofner & Schott, 1986). A plot of the weight, W, in grams of the water absorbed per gram of the dry matrix of the tablet against time, t in minutes, gives the swelling isotherm.

2.15. In vitro drug release study

In vitro drug dissolution tests were carried out using USP dissolution test apparatus type-I (DS-800; 6+2; SC/TR, Lab India, Mumbai, India) in 900 ml simulated gastric fluid (pH 1.2) maintained at 37 °C with a stirrer rotation speed of 50 rpm (USP, 2009, extended release tablet of metformin HCl, method 1). Drug released from the tablets at different time points were measured spectrophotometrically (UV–vis double beam spectrophotometer, Pharmaspec-1700, Shimazdu, Japan) at the λ_{max} value at 230 nm after suitable dilution with phosphate buffer pH 6.8. The study was repeated in triplicate for each formulation. Similarity factor (f_2) and difference factor (f_1) were calculated to compare the release profile of the tablets of each batch with USP reference release profile using Eqs. (3) and (4), respectively.

$$f_2 = 50 \quad \log \left[\left\{ 1 + \left(\frac{1}{n}\right) \sum_{t=1}^{n} (R_t - T_t)^2 \right\}^{-0.5} \times 100 \right] \quad (3)$$

$$f_1 = \frac{\sum [R_t - T_t]}{\sum R_t} \times 100 \quad (4)$$

where R_t, T_t and t are the reference value, test value and number of replicates, respectively. The drug release data were also fitted to various release kinetic models to understand the mechanism of drug release (Costa & Lobo, 2001). Finally, $T_{50\%}$ and $T_{90\%}$ were calculated from the best fitting kinetic model equation.

2.16. Statistical analysis of the responses and formulation optimization

The independent and response variables considered in this study, are shown in Table 2. The responses were analyzed and then numerically optimized using 2^3 full factorial design by Design-Expert software. For optimization purpose, BLT, K and f_1 were targeted at minimum, mucoadhesive strength, f_2 at maximum, drug release to USP reference release profile, and the independent variables were set in the range of low and high level used in the experiment. After optimization, the matrix tablet was prepared as per the optimized formula and evaluated. Then the observed values of the responses were compared to the predicted and target values.

3. Result and discussion

3.1. Preparation of Pmaa-g-GG copolymer and composite matrix tablet with TSG

The preparation of Pmaa-g-GG copolymer and subsequent formation of composite matrix are schematically presented in Fig. 1. The overall reaction mechanism is that, cerric (IV) ammonium nitrate gets dissociated into Ce^{4+}, ammonium and nitrate ions and then cerric (IV) ion attacks the gellan gum macrochains resulting formation of a GG-cerric complex. The cerric (IV) ions in the complex get then reduced to cerric (III) ions by oxidizing hydrogen atom and thereby creating a free radical onto GG-backbone. In the presence of methacrylamide, the GG free radical is chemically coupled to the monomer unit, thereby resulting in a covalent bond between nonomer and GG to create the chain reaction for propagation. Finally, termination occurs through a combination of two propagating chain free radicals initiated from GG-backbone or by coupling between GG-propagating-free-radical and monomer free radical. Finally, Pmaa-g-GG copolymer and TSG have been blended along with drug and SBC employing wet granulation method to obtain a polymeric composite matrix.

3.2. Physical characterization of tablet

The physical characterization of the tablets exhibited the following information: the weight of the tablets was confined within ±4% of the theoretical weight, thickness varied from 5.07 mm to 6.18 mm with MSD 0.13% (n = 10), the maximum friability found was 0.46% and the drug content varied within ±5% of the labeled amount. Hardness was within the range of 4–5 kg/m^2. All these variation were found to comply with the requirements of official Compendium.

3.3. FTIR spectral analysis

Infrared spectra of Pmaa-g-gellan and TSG are shown in Fig. 2(a) and (b), respectively. Pmaa-g-GG shows characteristic peaks at 1647.32 cm^{-1} for carbonyl group indicating C=O stretching, at 3198.43 cm^{-1} for —OH group, at 2883.27 cm^{-1} for —COOH group, at 1159.42 cm^{-1} for alcoholic —C—O group, at 1706.30 cm^{-1} for —C=O group. It also shows characteristic peaks in the range from 3829.24 cm^{-1} to 3169.37 cm^{-1} for —NH_2 group, due to addition of methacrylamide which was grafted onto gellan. An additional peak at 1645.78 cm^{-1} has been observed due to N—H bending. A

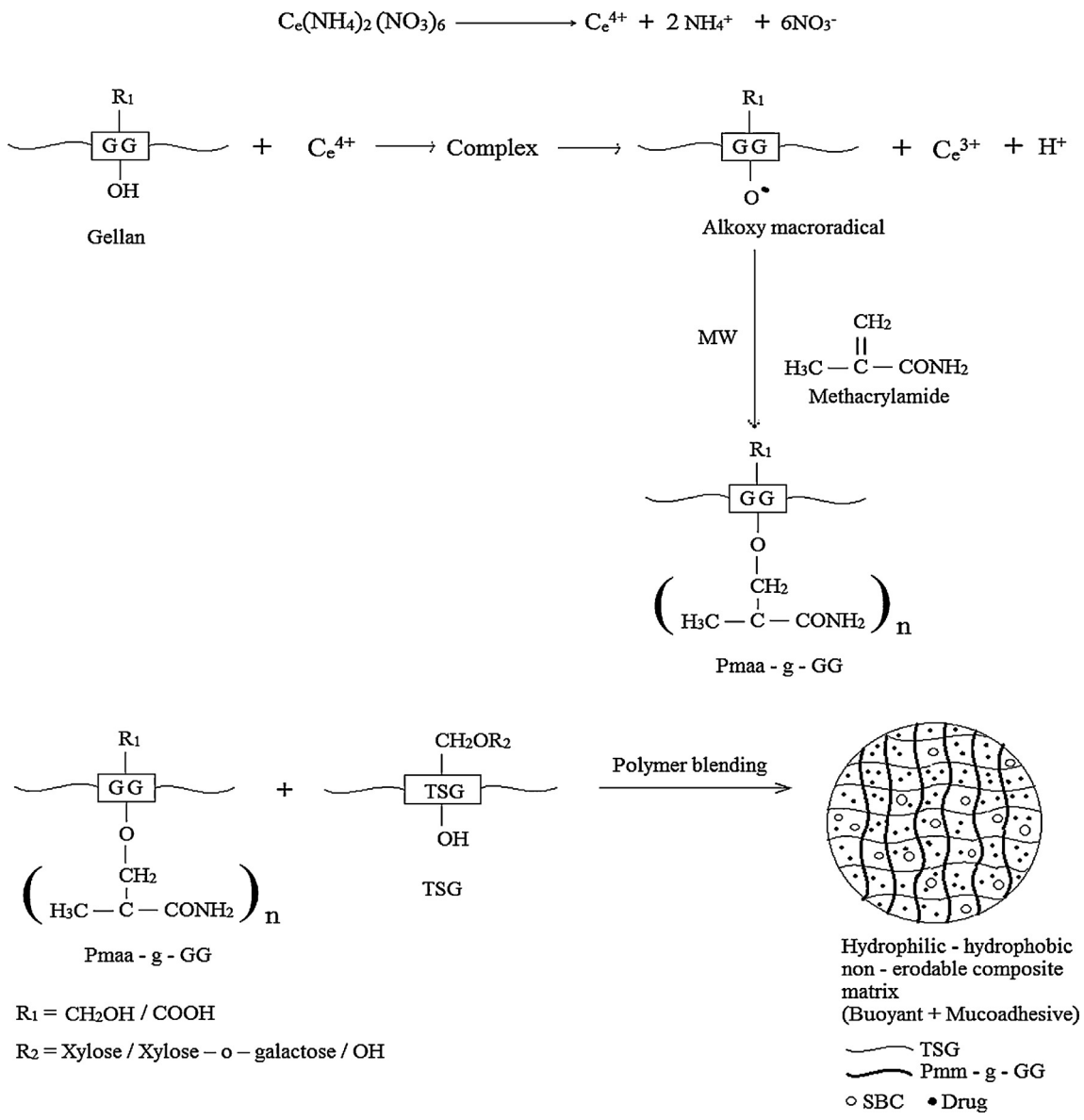

Fig. 1. Schematic representation of synthesis of Pmaa-g-GG and formation of gastroretentive composite matrix tablet.

significant peak is also observed at 1024.59 cm^{-1} for CH—O—CH_2 group which occurs due to grafting reaction between OH group of C_2 of gellan gum and π bond of methacrylamide.

Infrared spectra of TSG shows characteristic peaks at 1018.53 cm^{-1}, 1148.12 cm^{-1}, 1448.14 cm^{-1}, 1628.35 cm^{-1}, 2890.36 cm^{-1} and 3291.48 cm^{-1} for —HC=O stretching vibration, —C—O—C— asymmetric stretching vibration of glucopyranosyl and xylopyranosyl units, —CH_2 gr bending vibration, —CH—OH stretching vibration, aliphatic C—H stretching and for the —OH groups, respectively.

Infrared spectra of metformin and tablet are shown in Fig. 2(c) and (d), respectively. Metformin shows the characteristic peaks at 3363.45 cm^{-1} and peaks at 3282.85 cm^{-1} for N—H asymmetric stretching and N—H symmetric stretching, respectively. Peak at 2805.22 cm^{-1} indicates CH_3 symmetric stretching. Peaks at 1621.85 cm^{-1} and 1442.76 cm^{-1} correspond to C=N stretching and CH_3 asymmetric deformation, respectively. All these peaks have been observed in the infrared spectra obtained from tablet, which demonstrates that there is no significant incompatibility between the drug and the other polymers.

3.4. DSC and TGA study

DSC and TGA curves of metformin and tablet are shown in Fig. 3(a) and (b), respectively. As shown in Fig. 3(a), the DSC-thermogram (red in color) of metformin shows a broad endothermic peak at 80 °C and an another very sharp endothermic peak at 231.81 °C. TGA thermogram (green in color) of metformin shows only 2% weight loss in the temperature range from 25 °C to 226 °C, which indicates very little loss in moisture present in the pure drug. Very sharp endothermic peak at 231.81 °C indicates narrow melting range and crystalline nature of metformin. Two endothermic peaks at 100 °C and at 221.32 °C were recorded in DSC thermogram of tablet formulation. TGA thermogram (green in color) of tablet formulation shows 10% weight loss in the temperature range from 27 °C to 175 °C. The correlation between endothermic peak at 100 °C and simultaneous reduction in weight in the temperature range from 27 °C to 175 °C indicates the loss in moisture present in the tablet. The sharp endothermic peak at 221.32 °C (less in sharpness compared to that of pure drug) indicates the melting point of the drug present in the tablet

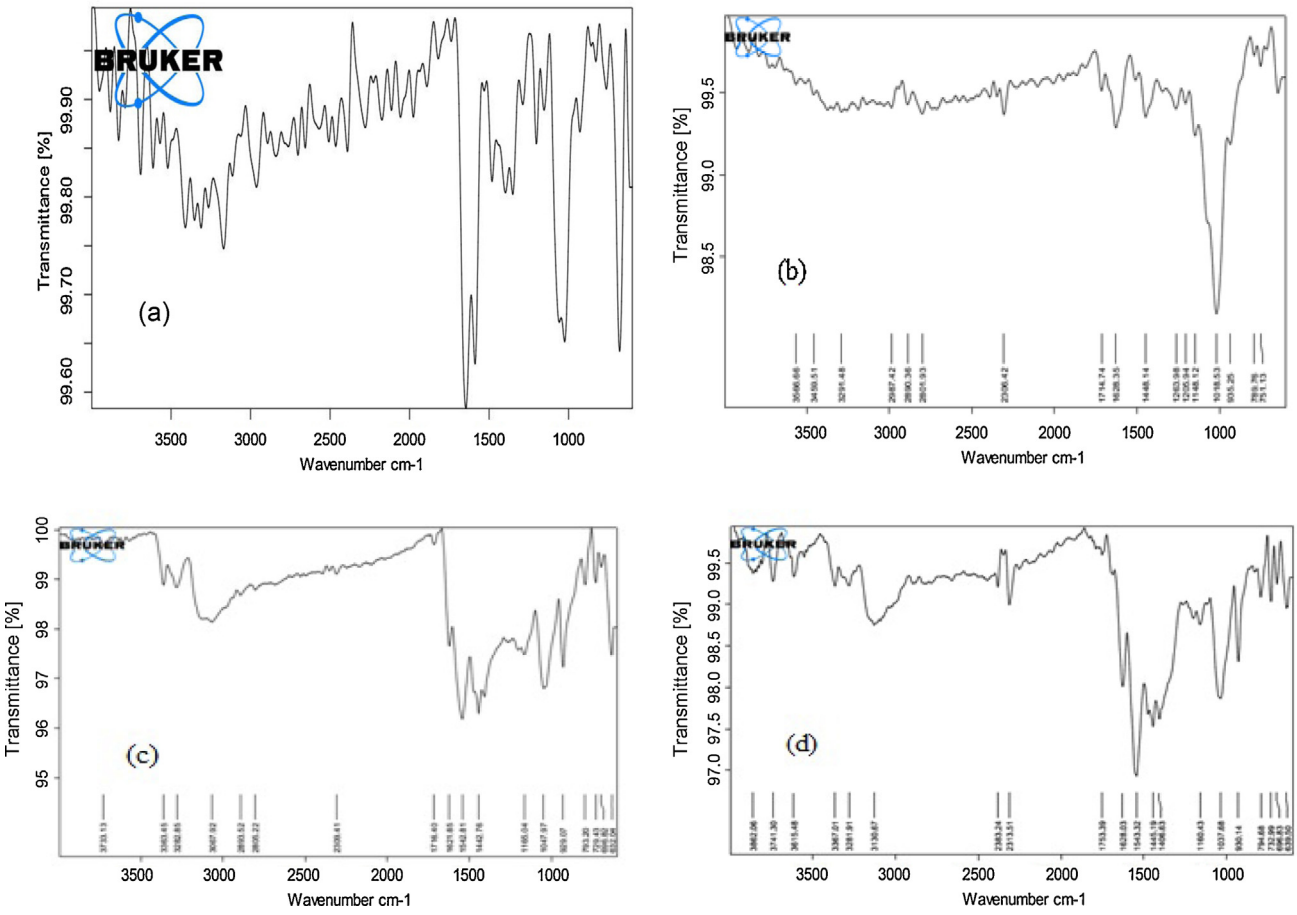

Fig. 2. FTIR spectrum of (a) Pmaa-g-GG, (b) TSG (c) metformin and (d) tablet (F8).

formulation and partial retention of its crystalinity in the formulation. The significant downward shift in melting point of the drug in the formulation may be due to dilution effect in presence of other excipients.

3.5. XRD study

X-ray diffractogram of pristine metformin and tablet containing drug were presented in Fig. 4(a) and (b), respectively. Metformin showed many characteristic intense peaks at 2θ of 12°, 17.5°, 22°, 23°, 24.5°, 28°, 36°, 45°, 55.5° and 63°, that indicate its crystalline nature. The diffractogram obtained from the tablet portray that approximately 80% peaks of pristine drug appeared almost at the same 2θ values in the XRD chart of tablet formulation attributing to the retention of crystalline nature of maximum amount of drug and absence of incompatibility between drug and other formulation components. But the presence of noise to some extent and little decrease in intensities indicate that some

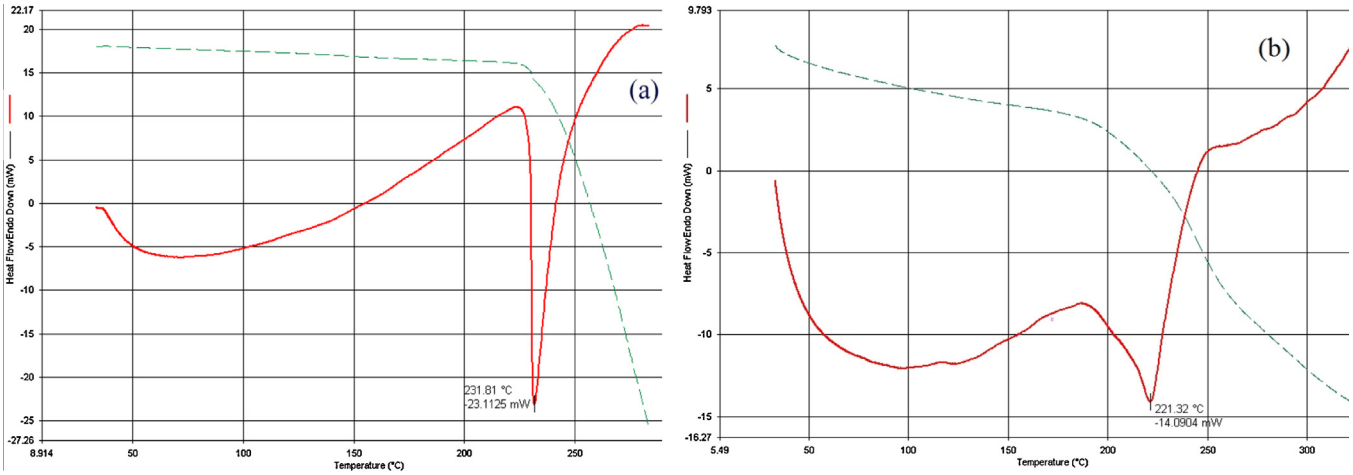

Fig. 3. DSC-TGA thermogram of (a) metformin (b) tablet formulation (F8) (For interpretation of the references to colour in the text, the reader is referred to the web version of this article.).

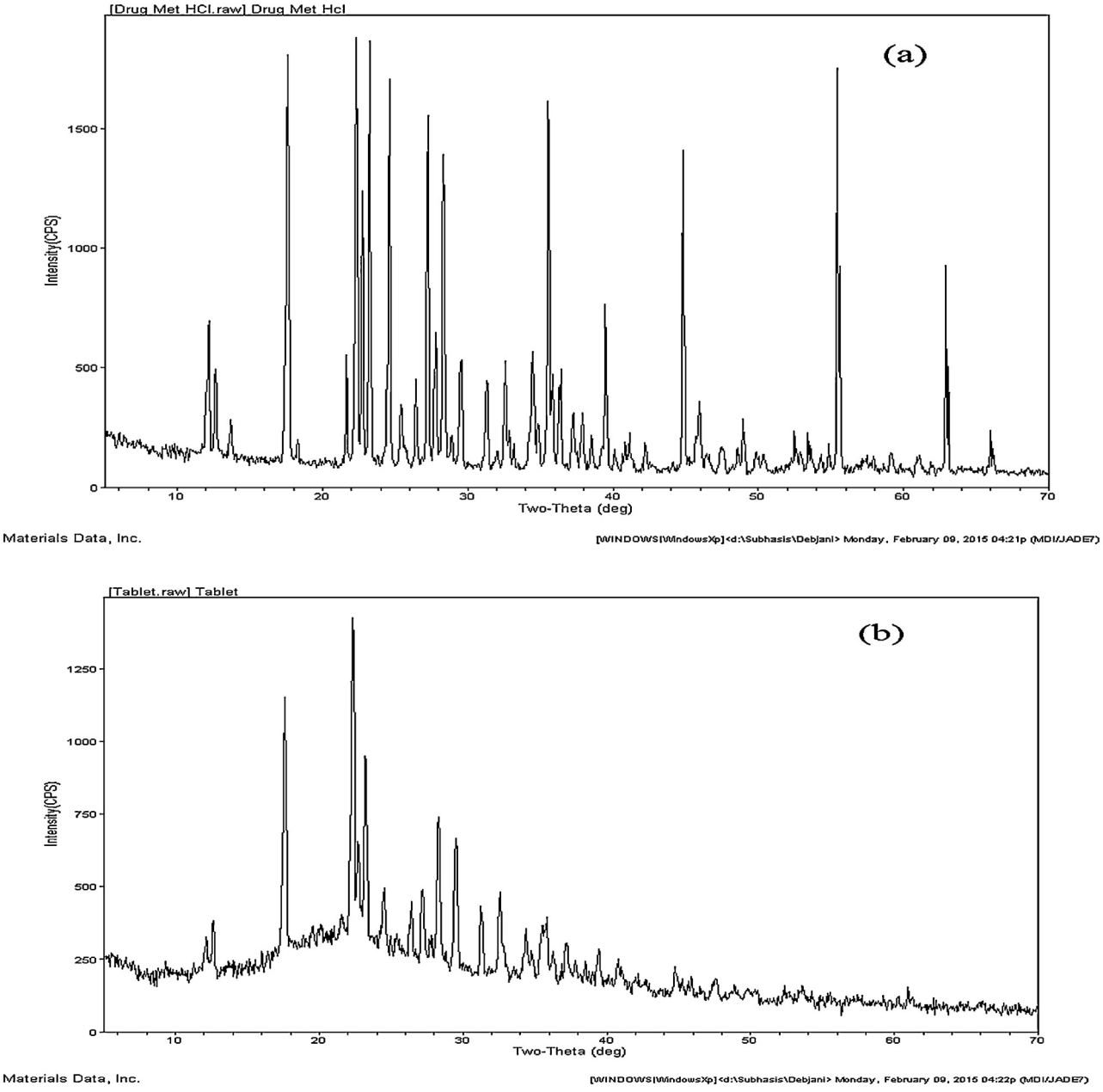

Fig. 4. X-ray diffractogram of (a) metformine and (b) tablet (F8).

amount of drug remain as molecularly dispersed in the composite matrix.

3.6. Statistical analysis of the responses and formulation optimization

The results of ANOVA analysis unveiled a statistically significant association between independent and response variables ($p < 0.05$; Table S1; supplementary file). The generated model equations after eliminating insignificant terms ($p > 0.05$) on the basis of ANOVA results were demonstrated in discussion regarding respective responses. Software generated 3-D response surface and corresponding 2-D contour plots illustrated the effects of the independent factors on the investigated responses (Fig. S2–S11; supplementary file). A numerical optimization technique based on the criterion of desirability was adopted to develop the optimized formulation. The primary goal was to find the values of the independent factors that minimize BLT, maximize the mucoadhesive strength and comply the USP release reference profile for extended release tablet of metformin (Table 2). The desirable ranges of independent factors were restricted to 150 mg ≤ Pmaa-g-GG ≤ 250 mg, 150 mg ≤ TSG ≤ 250 mg and 80 mg ≤ SBC ≤ 120 mg. An optimal formulation setting having highest desirability (0.858) was selected among 28 different settings recommended by the software. The optimal values of Pmaa-g-GG, TSG and SBC selected were 158.80 mg, 244.99 mg and 120 mg, respectively. The confirmation experiments were conducted to test the responses of the optimal formulation (OF). The experimental results and predicted responses are tabulated in Table 2. The relative errors ([(predicted value−actual value)/predicted value] × 100) between the predicted and observed values were −4.43% for BLT, −2.44% for *F*, −6.9% for CPR1h, +2.97% for CPR2h, +1.87% for CPR6h, −1.71% for CPR10h,

Table 3
Buoyancy parameters, density, mucoadhesivity, similarity (f_2), dissimilarity factors (f_1) and swelling index.

Formulation code	BLT (min) Mean ± s.d.	TBT (h)	Density (g/cm^3) mean ± s.d.	Mucoadhesive strength (F) Mean ± s.d. (g)	f_1	f_2	W_E
F1	7.69 ± 0.431	>10	1.326 ± 0.014	34.6 ± 3.06	18.36	47.13	309.5 ± 6.06
F2	8.61 ± 0.573	>10	1.263 ± 0.018	57.3 ± 4.16	6.29	67.43	612.4 ± 4.25
F3	8.83 ± 0.335	>10	1.261 ± 0.008	37.3 ± 3.06	6.63	64.01	413.3 ± 8.62
F4	10.15 ± 0.670	>10	1.215 ± 0.013	60.0 ± 4.00	21.57	43.89	703.9 ± 6.59
F5	1.74 ± 0.231	>10	1.385 ± 0.022	38.0 ± 2.00	20.5	44.79	314.4 ± 3.83
F6	2.57 ± 0.302	>10	1.313 ± 0.009	57.5 ± 2.17	4.08	75.84	619.3 ± 7.05
F7	2.95 ± 0.125	>10	1.315 ± 0.016	39.3 ± 4.42	7.69	61.09	420.1 ± 3.27
F8	4.39 ± 0.127	>10	1.259 ± 0.027	62.6 ± 3.06	14.38	51.94	697.2 ± 5.92
OF	2.76 ± 0.192	>10	1.307 ± 0.037	55.46 ± 2.03	5.69	71.58	616.7 ± 2.45

+0.33% for K, −7.96% for f_1 and +4.54% for f_2. In short, the experimental findings were within the close agreement to the model-based predictions, which conferred the predictability and validity of the models.

3.7. In vitro buoyancy study

The buoyancy parameters exhibited by the tablets are presented in Table 3 and Fig. S12 (supplementary file). The in vitro buoyancy test showed that the average BLT observed was within the range from 1.74 min to 10.15 min and the TBT for all formulations was observed to be greater than 10 h. The mechanism contributing the buoyancy to the composite matrix involves penetration of HCl acid into the interior of the tablet resulting generation of CO_2 due to the reaction between $NaHCO_3$ and HCl acid of the simulated gastric fluid (Eq. (5)). Simultaneously, the hydrophilic TSG absorbs water and form a continuous barrier gel layer at the outer surface of the tablet resulting subsequent entrapment of CO_2 gas in the matrix. The buoyancy can also be attributed to the swelling and expansion of the matrix volume in aqueous media, leading to significant decrease in tablet density. Thus the resultant effect of the inside upward pressure exerted by CO_2 gas and drop in density due to matrix-swelling leads to the floatation of the tablet in the floating medium.

$$NaHCO_3 + HCl \rightarrow NaCl + CO_2\uparrow + H_2O \quad (5)$$

The BLT was considered as response variable in this study as it changes with different formulations whereas TBT remains constant in all designed formulations and hence not taken as response variable. The regression equation for BLT yielded from ANOVA study, is expressed in Eq. (6):

$$BLT = +5.87 + 0.71X_1 + 0.56X_2 - 2.95X_3 + 0.13X_1X_2 + 0.044X_1X_3 + 0.0038X_2X_3 \quad (R^2 = 0.9999) \quad (6)$$

The values of the coefficients of different independent variables in the model equation for BLT indicate that it is mainly influenced by SBC and comparatively less influenced by Pmaa-g-GG and TSG. The effect of the SBC is negative that means increase in the concentration of SBC decreases the BLT whereas the effects of other two variables are positive. This may be due to the fact that more SBC produces more CO_2 that exert more inside upward pressure resulting enhancement in the buoyant efficiency. But on the other hand, increase in the Pmaa-g-GG and TSG results in little increase in BLT. It may be due to the fact that presence of more number of —COOH group of Pmaa-g-GG moiety at its higher level in the matrix, leads to inhibition of penetration of HCl acid in the tablet matrix resulting comparatively slow generation of CO_2. Unlikely, higher level of TSG absorbs more water at initial stage and thus delays floatation by increasing the density temporarily.

Other coefficients in the regression equation indicate very little interactions between the independent variables. It was observed that the tablet once floated, maintained its buoyancy level over a long period of time (>10 h). The tablets showed to maintain their physical integrity throughout the whole period of dissolution study probably due to high binding capacity of TSG.

3.8. Ex vivo mucoadhesion testing

The results of ex vivo mucoadhesion test using goat gastric mucosa are presented in Table 3 and Fig. S13 (supplementary file). The value of mucoadhesive strength, F, exhibited by different batches of tablets ranges from 34.6 g to 62.6 g. The mucoadhesive property of these tablets could be attributed to the presence of hydroxyl groups in the molecules of hydrophilic TSG and —COOH, —CH_2OH groups in Pmaa-g-GG, which have the ability to form various noncovalent bonds (like hydrogen bonds, Vander Waal's forces and ionic interactions) with different groups such as —COOH, —NH_2, —C=O, —OH in mucus molecules (Smart, 2005). The regression equation for F, is expressed in Eq. (7):

$$F = +48.3 + 1.5X_1 + 11.0X_2 + 1.0X_3 + 0.50X_1X_2 - 0.35X_2X_3 \quad (R^2 = 0.9978) \quad (7)$$

The values of the coefficients of different independent variables in the model equation for F indicate that mucoadhesivity is mainly influenced by TSG. The value of F has shown to increase with increase in the amount of TSG, which may be due to the presence of —OH group (main contributor in mucoadhesivity) in large number in TSG molecules. In case of batch F1, F3, F5 and F7, a little synergistic effect of SBC on F has also been observed at low level of TSG. It may be due to more ionization of —COOH group of Pmaa-g-GG by SBC, which further causes enhancement in formation of noncovalent bond or electrostatic interaction with mucus molecules. But in case of batch F2, F4, F6 and F8, no significant effect of SBC has been observed at high level of TSG, which might be due to domination effect of TSG on chemical activity of —COO^- ions. Pmaa-g-GG has shown to exert a little positive effect in case of F1, F2, F3, F4, F6 and F8 at both level of TSG and SBC which may be due to the presence of —CH_2OH and —COOH groups in the moiety of Pmaa-g-GG. No significant interaction between the variables has been reflected by the regression equation.

3.9. Surface morphology analysis

Fig. 5 presents the scanning electron micrographs of the tablet surface before and after the drug release study. The micrographs of tablet surface before drug release portray rough, irregular appearance with presence of very thin hair-like cracks. It may be due to difference in solid state crystalline nature of Pmaa-g-GG and TSG, less cold welding at superficial level during consolidation of granules into tablet and shrinkage upon loss of moisture from the tablet surface. The micrographs after dissolution depict continuous surface with presence of pores and lobules. Continuation of surface and

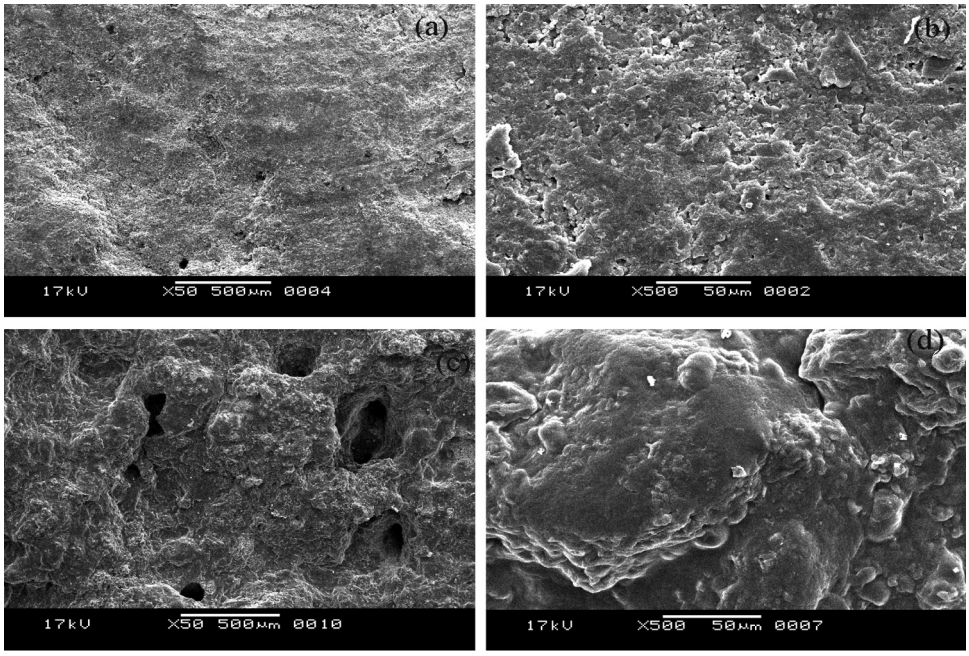

Fig. 5. Scanning electron micrograph of tablet surface (F8) (a) and (b) before dissolution; (c) and (d) after dissolution.

lobule formation may result from the gelation of TSG during dissolution and subsequent drying while pore formation may result from the evolution of CO_2 from the superficial level of the outer gel layer.

3.10. Swelling study

Fig.S1 (supplementary file) depicts the kinetic of swelling behavior of matrix expressed as *W* vs. *t* in simulated gastric fluid (pH 1.2). Swelling index is presented in Table 3. The equilibrium water uptake observed ranges from 309.46% to 703.91%, which is shown to increase with an increasing amount of TSG, which may be due to the presence of different hydrophilic groups in the TSG molecules such as —OH group at 2 and 3 position of first glucopyranosyl unit of the main chain, at 2, 3 and 4 position of xylose unit attached to glucopyranosyl unit of the main chain via $—CH_2O$ at 5 position, at 2 and 3 position of second glucopyranosyl unit, at 2, 3 and 4 position of galactopyranosyl unit in side chain and $—CH_2OH$ group at 5 position of fourth glucopyranosyl unit of the main chain and at 1 position of galactose unit of the side chain. This effect is also demonstrated by the *W* vs. *t* profile. A little directly proportional effect of Pmaa-g-GG on water uptake has been observed, which may be due to presence of $—CH_2OH$ group in α-L-rhamnose and third β-D-glucose unit. No significant effect of SBC on water uptake has been found.

3.11. In vitro drug release

The regression coefficient (R^2), rate constant (k) from different kinetic models, diffusion exponent (n), $T_{50\%}$ and $T_{90\%}$ are shown in Table 4 and drug release profile (CPR versus time) is presented in Fig. 6. The release study on F0 batch was carried out to compare the release of free drug in similar environment with that of extended release formulations. The study revealed 100% drug release within the period of less than 0.5 h.

3.11.1. Statistical analysis of the dependence of release parameters on amount of Pmaa-g-GG, TSG and SBC

Mathematical relationship generated using MLRA for the studied response variables are expressed in Eqs. (8)–(14):

$$\text{CPR1h} = +31.70 - 3.60X_1 - 5.37X_2 + 1.12X_3 + 0.83X_1X_2 + 0.42X_1X_3 \quad (R^2 = 0.9897) \tag{8}$$

Table 4
Kinetic modeling of release data, release rate constants, $T_{50\%}$ and $T_{90\%}$.

Batch	R^2 value						Rate constant (k)					$T_{50\%}$ (h)	$T_{90\%}$ (h)
	Zero order	First order	Higuchi kinetic	HC	KP		Zero order	First order	Higuchi kinetic	HC	KP		
					R^2	n							
F0	–	–	–	–	–	–	–	–	–	–	–	0.17	0.36
F1	0.893	0.721	0.978	0.936	0.977	0.540	0.087	0.165	0.340	0.113	0.333	1.94	6.14
F2	0.946	0.769	0.998	0.994	0.991	0.576	0.076	0.180	0.293	0.047	0.249	3.24	10.1
F3	0.946	0.768	0.998	0.967	0.991	0.578	0.086	0.181	0.331	0.070	0.279	2.59	7.97
F4	0.969	0.791	0.999	0.996	0.995	0.627	0.070	0.199	0.265	0.037	0.191	4.51	13.19
F5	0.869	0.688	0.966	0.955	0.974	0.589	0.087	0.167	0.344	0.121	0.329	1.87	5.84
F6	0.946	0.768	0.998	0.996	0.991	0.579	0.080	0.181	0.307	0.052	0.259	2.99	9.21
F7	0.950	0.780	0.998	0.854	0.992	0.561	0.087	0.177	0.333	0.087	0.291	2.50	7.75
F8	0.946	0.769	0.998	0.989	0.991	0.576	0.071	0.180	0.268	0.039	0.227	3.85	11.93
OF	0.948	0.776	0.996	0.993	0.989	0.544	0.079	0.170	0.301	0.052	0.276	2.88	9.12

HC, Hixson Crowell; KP, Korsemeyer Peppas.

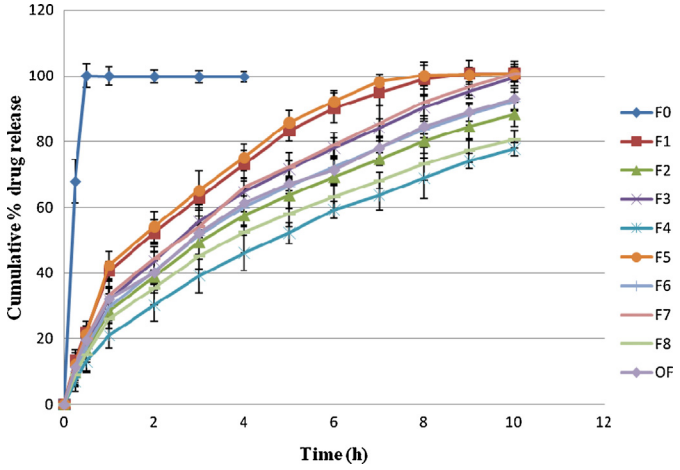

Fig. 6. Drug release profile (cumulative % release ± SD, $n = 3$) from composite tablets.

$$\text{CPR2h} = +42.44 - 3.99X_1 - 6.20X_2 + 1.18X_3 + 0.58X_1X_2 + 0.55X_2X_3 \quad (R^2 = 0.9921) \tag{9}$$

$$\text{CPR6h} = +75.43 - 5.55X_1 - 9.44X_2 + 1.25X_3 + 0.79X_1X_2 + 0.02X_1X_3 + 0.52X_2X_3 \quad (R^2 = 0.9995) \tag{10}$$

$$\text{CPR10h} = +92.57 - 2.91X_1 - 7.82X_2 + 0.96X_3 - 2.60X_1X_2 + 0.73X_2X_3 \quad (R^2 = 0.9990) \tag{11}$$

$$K = +0.31 - 0.011X_1 - 0.027X_2 + 0.003X3 - 0.006X_1X_2 - 0.002X_1X_3 \quad (R^2 = 0.9965) \tag{12}$$

$$f_1 = -11.76 - 0.2X_2 + 0.93X_3 + 0.0017X_1X_2 - 0.003X_1X_3 - 0.0016X_2X_3 \quad (R^2 = 0.9942) \tag{13}$$

$$f_2 = -60.83 + 0.77X_1 + 0.59X_2 - 0.47X_3 - 0.004X_1X_2 + 0.0027X_2X_3 \quad (R^2 = 0.9996) \tag{14}$$

where X_1, X_2 and X_3 are the amount of Pmaa-g-GG, TSG and SBC, respectively.

3.11.2. Effect of TSG, Pmaa-g-GG and SBC

The CPR vs. time profile as shown in Fig. 6, indicates that the amount released was mainly dependent on the TSG. When the amount of TSG increases from 150 mg (F1, F3, F5, F7) to 250 mg (F2, F4, F6, F8), the drug release becomes slower, which is also reflected in the regression Eqs. (8)–(12) and substantiated by the values of release rate constant (K), $T_{50\%}$ and $T_{90\%}$ presented in Table 4. This fact may be due to formation of a continuous compact gel matrix embedded in the rigid 3-D polymeric network of Pmaa-g-GG resulting from water uptake by hydrophilic TSG. A little synergistic effect due to interaction between Pmaa-g-GG and TSG has also been demonstrated by the regression equations corresponding CPR1h, CPR2h and CPR6h. The extent of Pmaa-g-GG also showed a significant impact on the CPR (Fig. 6). As the amount of Pmaa-g-GG was increased from 150 mg (F1, F2, F5, F6) to 250 mg (F3, F4, F7, F8), the CPR was found to decrease. This may be due to fact that higher Pmaa-g-GG concentration increased the rigidity of the network, which in turn prevented the imbibition of buffer into the polymer matrix. So there was a reduction in network erosion and loosening leading to reduction in drug release. The amount of SBC showed no such significant impact on drug release, except in case of formulations F4 and F8, in which CPR has been found to increase to some extent with increase in the amount of SBC from 80 mg (F4) to 120 mg (F8) at higher level of another two independent variables: Pmaa-g-GG and TSG. This may happen due to the fact that some portion of unreacted SBC increases the degree of ionization of —COOH groups of β-D-glucuronic acid unit of Pmaa-g-GG moiety resulting more water uptake and subsequent reduction in rigidity of the matrix. This positive interaction effect between Pmaa-g-GG and SBC has also been demonstrated by the regression equation corresponding to CPR1h (Eq. (8)).

3.11.3. Kinetics and mechanism of drug release

The results demonstrate that most of the formulations follow Higuchi and Korsemeyer-Peppas release kinetic. The diffusion exponent (n) values for all the formulations are within the range of 0.540 (F1)–0.627 (F4) thus portending the release mechanism is both diffusion controlled and swelling controlled transport (anomalous/non-Fickian transport) based.

3.11.4. Release similarity and difference factor

f_1 and f_2 values are shown in Table 3. Highest similarity (75.84) and lowest difference factor (4.08) were exhibited by F6 batch. In order to consider the similar dissolution profiles, the f_1 values should be close to 0 and f_2 values should be close to 100 (Costa & Lobo, 2001). In case of F1:F2 and F5:F6, f_1 has been found to decrease and f_2 to increase with increase in the amount of TSG at low level of Pmaa-g-GG and the reverse effect of TSG has been observed at high level of pmaa-g-GG in case of F3:F4 and F7:F8. Pmaa-g-GG also showed similar effect on f_1 and f_2 values. The values of f_1 and f_2 observed in case of optimized formula (OF) were 5.69 and 71.58, respectively, which indicate good similarity between the release profile of OF and USP reference.

4. Conclusion

The present work was dealt with the development and evaluation of buoyant-mucoadhesive Pmaa-g-GG-TSG composite matrix tablets containing metformin having short elimination half-life (2–4 h) with an aim to extend the drug release and enhance the bioavailability of the drug through gastroretention over a prolonged period of time. The formulation was optimized by employing 2^3 full factorial design. The optimized formulation was further evaluated to establish the robustness of the optimization method. The optimized formulation exhibited excellent buoyancy over a period of 10 h with a very short BLT, good mucoadhesivity and highly similar extended release profile with USP reference. Overall, this study provided a simple, reproducible and economical approach for the development of biopolymer based composite matrix tablet suitable for stomach-specific extended delivery of water soluble drug like metformin.

Conflict of interest

The authors report no conflicts of interest. The authors alone are responsible for the content and writing of the article.

Acknowledgements

One of the authors (R. Priyadarshini) wishes to express thanks to the All India Council for Technical Education (AICTE), New Delhi, India, for financial support. The authors are also thankful to UGC-DSA lab, Department of Pharmaceutical Technology, Jadavpur University, Kolkata, India for providing instrumental support.

Appendix A. Supplementary data

Supplementary data associated with this article can be found, in the online version, at doi:10.1016/j.carbpol.2015.10.054.

References

Agnihotri, S. A., & Aminabhavi, T. M. (2005). Development of novel interpenetrating network gellan-poly (vinyl alcohol) hydrogel microspheres for the controlled release of carvedilol. *Drug Development and Industrial Pharmacy*, *31*, 491–503.

Ahuja, M., Yadav, M., & Kumar, S. (2010). Application of response surface methodology to formulation of ionotropically gelled gum cordial/gellan beads. *Carbohydrate Polymers*, *80*, 161–167.

Chavanpatil, M., Jain, P., Chaudhari, S., Shear, R., & Vavia, P. (2005). Development of sustained release gastroretentive drug delivery system for ofloxacin: In vitro and in vivo evaluation. *International Journal of Pharmaceutics*, *304*, 178–184.

Costa, P., & Lobo, J. M. S. (2001). Modeling and comparison of dissolution profiles. *European Journal of Pharmaceutical Sciences*, *13*, 123–133.

Efentakis, M., & Kouttis, A. (2001). Release of furosemide from multiple unit and single unit preparations containing different viscosity grade of sodium alginate. *Pharmaceutical Development and Technology*, *6*, 91.

Fukuda, M., Peppas, N. A., & McGinity, J. W. (2006). Floating hot-melt extruded tablets for gastroretentive controlled drug release system. *Journal of Controlled Release*, *115*, 121–129.

Gidley, M. J., Lillford, P. J., Rowlands, D. W., Lang, P., Dentini, M., & Crescenzi, V. (1991). Structure and solution properties of tamarind-seed polysaccharide. *Carbohydrate Research*, *214*, 299–314.

Klausner, E. A., Lavy, E., Friedman, M., & Hoffman, A. (2003). Expandable gastroretentive dosage forms. *Journal of Controlled Release*, *90*, 143–162.

Malakar, J., & Nayak, A. K. (2013). Floating bioadhesive matrix tablets of ondansetron HCl: Optimization of hydrophilic polymer-blends. *Asian Journal of Pharmaceutics*, *7*, 174–183.

Nandi, G., Patra, P., Priyadarshini, R., Kaity, S., & Ghosh, L. K. (2015). Synthesis, characterization and evaluation of methacrylamide grafted gellan as sustained release tablet matrix. *International Journal of Biological Macromolecules*, *72*, 965–974.

Narkar, M., Sher, P., & Pawar, A. (2010). Stomach-specific controlled release gellan beads of acid-soluble drug prepared by ionotropic gelation method. *AAPS PharmSciTech*, *11*, 267–277.

Nayak, A. K., & Pal, D. (2011). Development of pH-sensitive tamarind seed polysaccharide-alginate composite beads for controlled diclofenac sodium delivery using response surface methodology. *International Journal of Biological Macromolecules*, *49*, 784–793.

Nayak, A. K., Pal, D., & Malakar, J. (2013). Development, optimization and evaluation of emulsion-gelled floating beads using natural polysaccharide blend for controlled drug release. *Polymer Engineering and Science*, *53*, 338–350.

Nayak, A. K., Pal, D., & Santra, K. (2014). Tamarind seed polysaccharide-gellan mucoadhesive beads for controlled release of metformin HCl. *Carbohydrate Polymers*, *103*, 154–163.

Ofner, C. M., III, & Schott, H. (1986). Swelling studies of gelatin I: Gelatin without additives. *Journal of Pharmaceutical Sciences*, *75*, 790.

Pal, D., & Nayak, A. K. (2012). Novel tamarind seed polysaccharide-alginate mucoadhesive microspheres for oral gliclazide delivery. *Drug Delivery*, *19*, 123–131.

Pentikainen, P. J., Neuvonen, P. J., & Penttila, A. (1979). Pharmacokinetics of metformin after intravenous and oral administration to man. *European Journal of Clinical Pharmacology*, *16*, 195–202.

Singh, B., Chakkal, S. K., & Ahuja, N. (2006). Formulation and optimization of controlled release mucoadhesive tablets of atenolol using response surface methodology. *AAPS PharmSciTech*, *7*(1), article 3

Smart, J. D. (2005). The basics and underlying mechanisms of mucoadhesion. *Advanced Drug Delivery Reviews*, *57*, 1556–1568.

Streubel, A., Siepmann, J., & Bodmeier, R. (2003). Floating matrix tablets based on low density foam powder: Effects of formulation and processing parameters on drug release. *European Journal of Pharmaceutical Sciences*, *18*, 37–45.

Vijan, V., Kaity, S., Biswas, S., Isaac, J., & Ghosh, A. (2012). Microwave assisted synthesis and characterization of acrylamide grafted gellan, application in drug delivery. *Carbohydrate Polymers*, *90*, 496–506.

International Journal of Biological Macromolecules 72 (2015) 965–974

Contents lists available at ScienceDirect

International Journal of Biological Macromolecules

journal homepage: www.elsevier.com/locate/ijbiomac

Synthesis, characterization and evaluation of methacrylamide grafted gellan as sustained release tablet matrix

Gouranga Nandi[a,*], Poushali Patra[b], Rosy Priyadarshini[b], Santanu Kaity[c], Lakshmi Kanta Ghosh[b]

[a] BCDA College of Pharmacy & Technology, 78, Jessore Road (S), Hridaypur, Kolkata 700127, India
[b] Department of Pharmaceutical Technology, Jadavpur University, Kolkata 700032, India
[c] Department of Pharmaceutical Sciences, Birla Institute of Technology, Mesra, Ranchi, Jharkhand 835215, India

ARTICLE INFO

Article history:
Received 13 May 2014
Received in revised form 8 July 2014
Accepted 28 September 2014
Available online 12 October 2014

Keywords:
Gellan
Methacrylamide
Grafting

ABSTRACT

In the present study, the microwave induced synthesis of polymethacrylamide-grafted-gellan gum (PMaa-g-GG) was carried out by free radical initiation using cerric (IV) ammonium nitrate (CAN) as redox initiator. Concentrations of methacrylamide (Maa), CAN and microwave irradiation time were taken as variable synthetic parameters. The modified polysaccharide obtained from different synthetic conditions was then characterized by FTIR, CHN analysis, DSC and powder X-ray diffraction. The yield and extent of grafting were assessed by determining percentage grafting, percentage grafting efficiency, percentage conversion and these were correlated with elemental analysis. The acute oral toxicity study of modified polysaccharide was performed as per OECD guideline. Histological comparison of different organs between control and test animal showed no significant difference. Sustained release tablets of diclofenac sodium (DS) were prepared with modified gellan. In vitro dissolution study showed the tablets were capable of releasing the drug over a period of 8 h.

1. Introduction

In recent years, natural gums have widely explored for their efficiency as potential drug delivery carriers. Natural gums are generally used in controlled release dosage forms as rate modulating polymers [1]. They are preferred over synthetic polymers because of their safety, biocompatibility, low cost, free availability and biodegradability. The native gums pose certain drawbacks like variable chemical composition, variable swelling kinetic, microbial load, microbial growth and change in viscosity upon aging. It can hamper the degree of polymerization, hydration kinetic, viscosity of the hydrated boundary layer and rigidity of polymeric carrier. Therefore, they can be tailored or modified in different ways to not only overcome their drawbacks but also modulate the site of drug release and its kinetic, and makes them parallel or superior than their synthetic counterparts [2]. Tailoring of natural polymers can be done in various ways like carboxymethylation, grafting, blending, crosslinking and so on. Among them, grafting of natural polymer has gained a considerable attention in previous few years. Graft copolymerization is an excellent and fruitful technique to prevent natural polymers from rapid enzymatic degradation in physiological fluids and make them potentially suitable to be used as sustained release matrices [3,4]. Grafting used to introduce hydrophobicity and steric bulkiness, which considerably protects the matrix and carbohydrate backbone to retard the drug release [2]. There are different techniques of grafting viz. grafting initiated by chemical means, grafting initiated by radiation, photochemical grafting, plasma radiation induced grafting, enzymatic grafting. Microwave assisted transitional metal ions such as Ce^{4+} induced polymer grafting is considered as very simple and easier one step method of graft copolymerization [5]. The microwave irradiation provides rapid transfer of fixed energy in the bulk of the reaction mixture resulting very short reaction time with significantly higher yield [6–8].

Abbreviations: GG, gellan gum; PMaa, polymethacrylamide; CAN, cerric (IV) ammonium nitrate; DS, diclofenac sodium; Pmaa-g-GG, polymethacrylamide-grafted-gellan gum; FTIR, Fourier transform infra-red; XRD, X-ray diffraction; DSC, differential scanning calorimetry; TGA, thermogravimetric analysis; KBr, potassium bromide; UV–vis, ultraviolet–visible; C, carbon; H, hydrogen; N, nitrogen; $T_{50\%}$ and $T_{90\%}$, time at which 50% and 90% drug was released respectively; OECD, Organization of Economic Co-operation and Development.

* Corresponding author. Tel.: +91 8442943290; fax: +91 3325842433.
E-mail addresses: nandi.gouranga@yahoo.co.in, gnandi76@gmail.com (G. Nandi).

http://dx.doi.org/10.1016/j.ijbiomac.2014.09.052
0141-8130/

In present study we tried to explore the potentiality of methacrylamide grafted gellan gum as sustained release carrier of diclofenac sodium.

Gellan gum is an anionic, high molecular weight, deacylated exocellular polysaccharide gum produced as a fermentation product by a pure culture of *Pseudomonas elodea* with a tetrasaccharide repeating unit of one α-L-rhamnose, one β-D-glucuronic acid and two β-D-glucose residues [9]. It has been widely used in several types of dosage forms such as stomach-specific controlled release beads [10], interpenetrating hydrogel microsphere [11], tablets [12,13], and ophthalmic solution [14,15]. On the other hand, acrylic acid and its derivative based polymers have occupied a significant position in sustained release matrix forming polymer groups.

Diclofenac sodium is a water soluble aryl-acetic acid derivative nonselective cyclo-oxygenase inhibitor drug having analgesic, antipyretic and anti-inflammatory actions. Its oral bioavailability is 54% with biological half-life of 1–2 h [16]. Extended release tablet of diclofenac sodium is official in USP, 2009 edition.

In the present study, polymethacrylamide (Pmaa) grafted gellan gum (GG) was prepared by microwave assisted redox-initiator-induced graft copolymerization technique. The characterization of polymethacrylamide-grafted-gellan gum was done by FTIR, CHN analysis, and DSC studies. The acute oral toxicity study in *Swiss albino* female mice was carried out according to OECD guideline. The graft copolymer was used to prepare monolithic matrix tablet of a model water-soluble drug, diclofenac sodium. *In vitro* drug release studies and kinetic modeling of release data were performed to understand the potentiality of the modified polymer as a sustained release matrix carrier. Furthermore, tablet formulations were characterized by FTIR, DSC and XRD studies to evaluate the drug polymer compatibility. Statistical analysis and numerical optimization were also done using Design-Expert software.

2. Experimental

2.1. Materials

Gellan gum and methacrylamide were bought from HiMedia Laboratories private limited, Mumbai, India. Cerric ammonium nitrate was purchased from Qualigens Fine chemicals, Mumbai, India. Diclofenac sodium (99.41% purity) was received as gift sample from La-Chemico Private Limited, Kolkata, India. Polyvinyl pyrrolidone (PVP K-30), magnesium stearate, purified talc, acetone and methanol were bought from Merck India Pvt. Ltd., Mumbai, India. All other reagents and chemicals used were of laboratory reagent grade and used without further purification. Triple-distilled water was used throughout the experiment.

2.2. Synthesis of polymethacrylamide-grafted-gellan gum

Microwave-promoted free radical initiation method was employed for the synthesis of polymethacrylamide-grafted-gellan gum (PMaa-g-GG) [2]. Amount of methacrylamide (Maa), cerric (IV) ammonium nitrate (CAN) and microwave irradiation time were taken as independent variable synthetic parameters. A total of eight batches of grafted gellan gum with different synthetic conditions were prepared as shown in Table 1. 1 g gellan gum (GG) was dissolved in 100 mL water (solution A) and specified amount of methacrylamide was dissolved in 25 mL water (solution B). Solution B was then added to solution A and stirred for 1 h. Specified amount of CAN was dissolved in 25 mL water and mixed with the previous mixture. The mixture was then exposed to microwave in a domestic microwave oven (Electrolux, C23K101.BB, India) at 500 W for a specified time (Table 1) following 1 min heating and 1 min cooling cycle. Then it was left for overnight. Acetone was added to it in 1:2 ratios (reaction-mixture:acetone) for precipitation of the grafted gellan gum. The precipitate was collected and added in 50 mL of 80% (v/v) aqueous methanol to remove the unreacted free monomer and the homopolymer (polymethacrylamide) formed during graft reaction. After stirring for 1 min it was allowed to stand for further precipitation. The precipitate was collected and finally washed with distilled water and dried at 40 °C to a constant weight. The dried grafted gellan gum was then powdered using pestle and mortar and passed through #100 mesh. Different grafting parameters such as % grafting (%G), grafting efficiency (%GE) and % conversion (%C) were calculated using following formula (Eqs. (1)–(3)) to assess the efficiency of the synthesis [17]:

$$\%\text{grafting}\,(\%G) = \frac{W_1 - W_0}{W_0} \times 100 \quad (1)$$

$$\%\text{grafting efficiency}\,(\%GE) = \frac{W_1 - W_0}{W_2} \times 100 \quad (2)$$

$$\%\text{conversion}\,(\%C) = \frac{W_1}{W_2} \times 100 \quad (3)$$

where W_0, W_1 and W_2 are the weight of native gellan gum, grafted gellan gum and methacrylamide respectively.

2.3. Characterization of grafted gellan gum

2.3.1. Elemental analysis

The elemental analysis of the native gellan gum and eight different batches of Pmaa-g-GG was performed using a Perkin Elmer CHN 2400 microanalyzer to determine the carbon, hydrogen and nitrogen content.

2.3.2. Infrared spectral analysis

FTIR spectra of gellan gum, Pmaa-g-GG (S1 batch) were obtained using FTIR (Bruker, Alpha T, Germany) to predict the possible

Table 1
Synthetic conditions, grafting parameters and elemental analysis of polymethacrylamide-grafted-gellan.

Batch no	Amt. of Maa (g)	Amt. of CAN (mg)	MW irradiation time (min)	%G	%GE	%C	Elemental analysis		
							%C	%H	%N
GG	–	–	–	–	–	–	35.55	5.89	0.00
S1	10	400	5	669.58	67.09	77.11	38.81	7.14	10.07
S2	10	400	1	660.16	66.01	76.01	44.77	8.54	11.91
S3	10	150	5	147.68	14.78	24.79	45.05	7.65	8.94
S4	10	150	1	483.73	48.74	58.82	46.10	8.44	11.71
S5	5	400	5	180.60	36.12	56.12	42.44	7.80	9.08
S6	5	400	1	285.93	57.22	77.23	43.69	7.94	10.44
S7	5	150	5	78.09	15.22	35.79	41.36	7.25	6.07
S8	5	150	1	118.54	23.81	43.89	43.70	7.25	7.53

%G, % grafting; %GE, % grafting efficiency; %C, % conversion; %C, carbon percentage; %H, hydrogen percentage; %N, nitrogen percentage.

changes of functional groups of grafted gellan gum as compared to its native form. A small amount of each material was mixed with KBr (1%w/w sample) and compressed into tablet. The scanning range selected was 550-4000 cm^{-1}. Diclofenac sodium and its tablet formulation were also analyzed by FTIR to predict the possible interactions between drug and modified polymer by same process.

2.3.3. Differential scanning calorimetry (DSC) and thermogravimetric analysis (TGA)

DSC and TGA thermograms of gellan gum, Pmaa-g-GG (S1 batch), diclofenac sodium and drug formulation (from S1 batch) were recorded under N_2 flow (50 mL/min) using Perkin Elmer Pyris Diamond TG/DTA, Singapore, at a heating rate of 10 °C/min and sample mass of 3–5 mg. The heating range was from 30 °C to 500 °C.

2.3.4. Acute oral toxicity study

Acute oral toxicity study of polymethacrylamide grafted gellan gum (Pmaa-g-GG; S1 batch) was performed as per the "Organization of Economic Co-operation and Development (OECD) guideline for the test of chemicals 425, adopted 17 December 2001". Six nulliparous and non-pregnant eight weeks old female mice (*Swiss albino* species) were taken for the study, one of which was taken as control. The study protocol was prior approved by the Animal Ethics Committee (CPCSEA approval no: 1682/EO/a/13/CPCSEA) of BCDA College of Pharmacy & Technology, Kolkata, India. Mice were housed in polycarbonate cage with sufficient food and demineralized water was available to them ad libitum at 19–25 °C and 40–70% relative humidity in a 12 h light on/off cycle. A single dose of 2000 mg/kg body weight of Pmaa-g-GG was administered by gavages using a stomach tube to the first test animal. The same dose was administered to the remaining four test animals after survival of the first test animal. No dose was administered to the control animal. The animals were kept under the continuous observation up to 4 h after dosing. The observation was continued up to 14 days occasionally at predetermined intervals. The mortality rate was evaluated by visible observation and reported accordingly.

2.3.4.1. Histopathological study. The control animal and one survived test animal (randomly selected from the five test animals) were euthanized with diethyl ether and sacrificed. Their brain, lung, stomach, kidney, heart and liver were separated and cleaned with 0.9% (w/v) NaCl solution and then fixed in 10% formalin solution. Each organ was dehydrated serially with 50% alcohol, 80% alcohol and finally with absolute alcohol. It was embedded in melted paraffin and cooled. A thin section of each organ was obtained by cutting the embedded block with a microtome. The sections were then mounted on glass slides and stained with hematoxylin and a counter stain eosin. A cover slip was fixed on each section to obtain a permanent slide.

Finally the slides were examined through a light microscope (Motic, B_1 series system microscope, India) fitted with camera (Magnus, MITS, India) and the fields (40×-view) were captured by the camera to obtain photomicrograph. The photomicrographs of the test organs were compared with that of controls.

2.4. Preparation of sustained release monolithic matrix tablet of diclofenac sodium

Monolithic matrix tablets of water soluble drug diclofenac sodium were prepared with gellan gum and grafted gellan gum of different nine batches employing wet granulation method. Each tablet contains 100 mg gum, 20 mg polyvinyl pyrrolidone K30 (as binder) and 100 mg drug. A batch of 10 tablets was prepared at a time. Briefly, semisolid dough was first prepared from the gellan gum or grafted gum with minimum amount of hot water (50 °C) and then polyvinyl pyrrolidone K30 and drug were mixed intimately with it. The mass was then passed through #18 mesh to obtain granules. These granules were dried at 60 °C for 20 min and passed through # 18 mesh. The granules were lubricated with purified talc (2.5 mg/tablet) and magnesium stearate (2.5 mg/tablet). The tablets were compressed at an average weight of 225 mg in a rotary tablet machine with 9 mm single punch diameter (Labpress, 10 station, Remi, Mumbai, India). Hardness was within the range of 4–5 kg/m^2.

2.4.1. Powder X-ray diffraction

X-ray powder diffractometry of diclofenac sodium and its tablet formulation (with S1 batch) were recorded using X-ray diffractometer (X-pert Pro, PANalytical, Singapore). The diffractometer was run at a scanning speed of 2°/min and a chart speed of 2°/2 cm per 2θ and the angular range fixed was from 10° to 80°.

2.4.2. In vitro drug release studies and release mechanism

In vitro drug dissolution tests from all nine batches of formulated tablets were carried out using USP dissolution test apparatus type-II (DS-800; 6 + 2; SC/TR, Lab India, Mumbai, India) in 900 mL 0.05 M phosphate buffer (pH 7.5) maintained at 37 °C with a stirrer rotation speed of 50 rpm (USP, 2009, extended release tablet of diclofenac sodium, method 1). 5 mL of aliquot was withdrawn at predetermined time points and same volume buffer was added to the dissolution medium each time. Drug released from the tablets at different time points were measured spectrophotometrically (UV–vis double beam spectrophotometer, Pharmaspec-1700, Shimazdu, Japan) at the λ_{max} value at 276.6 nm. The in vitro drug release data were fitted to various release kinetic models viz. zero order, first order, Higuchi model, Hixson–Crowell and Korsmeyer-Peppas model to understand the mechanism of drug release. The study was repeated in triplicate for each formulation.

Zero order model: $Q_t = K_0 t$ (Q_t is the amount of drug released in time, t, K_0 is zero order release constant) [18].

Firs order model: $\log Q_t = \log Q_0 + K_1 t/2.303$ (Q_0 is the initial amount of drug in solution) [19].

Higuchi model: $Q_t = K_H t^{1/2}$ [20].

Hixson–Crowell model: $(1 - f_t)^{1/3} = 1 - K_\beta t$ (f_t is the fraction of drug released at time, t) [21]. Korsmeyer-Peppas model: $f_t = at^n$ (a is a release rate constant incorporating structural and geometric characteristics of the dosage form, n is the release exponent, indicative of the drug release mechanism) [22].

Higuchi model describes drug release as a diffusion process based on the Fick's law, square root time dependent. This relation can be used to describe the drug dissolution from several types of modified release pharmaceutical dosage forms, as in the case of some transdermal systems and matrix tablets with water soluble drugs [23,24].

Korsmeyer-Peppas model describes the n value in order to characterize different mechanism of drug release, when $n = 0.5$, $0.5 < n < 1$, $n = 1$ and $n > 1$ corresponds to Case-I (Fickian) diffusion or Higuchi kinetic, anomalous (non-Fickian) diffusion, Case-II transport and super Case-II transport respectively [25,26]. Similarity (f_2) and difference factor (f_1) were calculated to compare the release profile of the tablets of each batch with USP reference release profile for extended release diclofenac sodium tablet using Eqs. (4) and (5) respectively.

$$f_2 = 50 \log \left[\left\{ 1 + \left(\frac{1}{n} \right) \sum_{t=1}^{n} (R_t - T_t)^2 \right\}^{-0.5} \times 100 \right] \quad (4)$$

$$f_1 = \frac{\sum [R_t - T_t]}{\sum R_t} \times 100 \quad (5)$$

where R_t, T_t and t are the reference value, test value and number of replicates respectively.

Finally, times at which 50% ($T_{50\%}$) and 90% ($T_{90\%}$) drug released were calculated from the best fitting kinetic model equation.

2.5. Statistical analysis of the responses and optimization of synthetic condition

The independent and response variables considered in this study, are shown in Table 5. The responses were analyzed and then numerically optimized using 2^3 full factorial design by Design-Expert software (version 9.0.3.0, Stat-Ease Inc., Minneapolis, USA). In this study, USP reference release profile for diclofenac sodium extended release tablet was taken as target (Table 5). For optimization purpose, % grafting was targeted at maximum and the independent synthetic factors (methacrylamide, CAN and MW irradiation time) were set in the range of low and high level used in the experiment.

3. Results and discussion

3.1. Synthesis of polymethacrylamide-g-gellan gum

Graft co-polymerization of methacrylamide onto gellan gum was carried out employing grafting technique by free-radical initiation. In several study, cerric (IV) ammonium nitrate was used as free-radical initiator [27,28]. Along with free-radical initiator, microwave-promoted graft-copolymerization have also been reported [7,29]. Table 1 presents the different synthetic conditions of microwave-promoted, cerric (IV) induced graft copolymerization, % grafting, % grafting efficiency, % conversion, % carbon, % hydrogen and % nitrogen of native gellan gum and its grafted forms. For the optimization of the synthetic conditions, amount of CAN, methacrylamide and microwave irradiation time were taken as independent synthetic variables by keeping the other parameters constant. From the values of different grafting parameters shown in Table 1, it is clear that amount of CAN has major positive influence on the higher grafting efficiency irrespective of other variables. The anomeric —CHOH on gellan gum-backbone is the reactive vicinal group, where the grafting is initiated. The overall reaction mechanism is that, cerric (IV) ammonium nitrate gets dissociated into Ce^{4+}, ammonium and nitrate ions and then cerric (IV) ion attacks the gellan gum macrochains resulting formation of a GG–cerric complex. The cerric (IV) ions in the complex get then reduced to cerric (III) ions by oxidizing hydrogen atom and thereby creating a free radical onto GG-backbone. So, a threshold amount of redox initiator is required for the formation of the free radical. The grafting of Maa onto GG was then initiated by the free radical reacting with the monomer. In the presence of Maa, the GG free radical is chemically coupled to the monomer unit, thereby resulting in a covalent bond between Maa and GG to create the chain reaction for propagation. Cerric ions also attack monomer resulting the formation of methacrylamide free radicals which join with another monomer molecule by a covalent bond leading to propagation of homopolymer chains. Finally, termination was achieved through a combination of two propagating chain free radicals initiated from GG-backbone. Termination may occur by coupling between GG-propagating-free-radical and monomer free radical or between GG-propagating-free-radical and homopolymer-propagating-free radical (composed of only monomers). Homopolymer is formed due to termination by coupling between two homopolymer-free-radicals. A mathematical relation between % grafting and the independent synthetic variables was obtained from the statistical analysis by Design-Expert software which is expressed in Eq. (6):

$$\%\,\text{grafting} = +336.39 + 64.89 * \text{Maa} + 0.97 * \text{CAN} - 29.53 * \text{MW}\,(R^2 = 0.8600) \quad (6)$$

where Maa: methacrylamide, CAN: cerric ammonium nitrate and MW: microwave irradiation time. This relation indicates the positive effect of Maa and CAN and negative effect of microwave on grafting. The synthetic condition for the synthetic batch S7 results in lowest grafting whereas the batches S1 and S2 result highest yield. The degree of grafting was shown to increase with the increase in concentration level of methacrylamide at both higher and lower level of two other independent synthetic factors. Similarly, grafting efficiency and other grafting parameters are proportional to the concentration of cerric ammonium nitrate. The microwave irradiation provides rapid transfer of energy in the bulk of the reaction mixture, which reduces reaction time therefore it acts as a catalyst and gives a synergistic activity. This phenomenon substantiates the results of the cerric (IV) initiated microwave-promoted graft copolymerization. In case of batches S1 and S2 the % grafting were nearly same though microwave irradiation time was 5 min (S1) and 1 min (S2), whereas, in case of other batches, % grafting was shown to be inversely proportional to microwave irradiation time. This may be due to the fact that a saturation of free radical points on gellan gum backbone gets generated in a certain time period of microwave irradiation. After that a further irradiation results in the breakage of propagated chains on the free radical sites and premature advance termination [30]. The structures of native gellan gum and Pmaa-g-GG have been shown in Fig. 1. The proposed mechanism of the reaction is as follows:

Initiation:

$$Ce(NH_4)_2(NO_3)_6 \rightarrow Ce^{4+} + 2NH_4^{+} + 6NO_3^{-}$$

$$Ce^{4+} + \text{GG—OH} \rightarrow \text{complex} \rightarrow \text{GG—O}^{\bullet} + Ce^{3+} + H^{+}$$

$$\text{GG—O}^{\bullet} + \text{M} \rightarrow \text{GG—OM}_1^{\bullet}$$

$$Ce^{4+} + \text{M} \rightarrow \text{M}^{\bullet} + Ce^{3+} + H^{+}$$

$$\text{M}^{\bullet} + \text{M} \rightarrow \text{M}_2^{\bullet}$$

Propagation:

$$\text{GG—OM}_1^{\bullet} + \text{M} \rightarrow \text{GG—OM}_2^{\bullet}$$

$$\text{GG—OM}_{n-1}^{\bullet} + \text{M} \rightarrow \text{GG—OM}_n^{\bullet}$$

$$\text{M}_2^{\bullet} + \text{M} \rightarrow \text{M}_3^{\bullet}$$

$$\text{M}_{p-1}^{\bullet} + \text{M} \rightarrow \text{M}_p^{\bullet}$$

Termination:

$$\text{GG—OM}_n^{\bullet} + \text{GG—OM}_m^{\bullet} \rightarrow \text{GG—OM}_{(m+n)} \quad \text{(graftcopolymer)}$$

$$\text{GG—OM}_n^{\bullet} + \text{M}^{\bullet} \rightarrow \text{GG—OM}_{(n+1)} \quad \text{(graftcopolymer)}$$

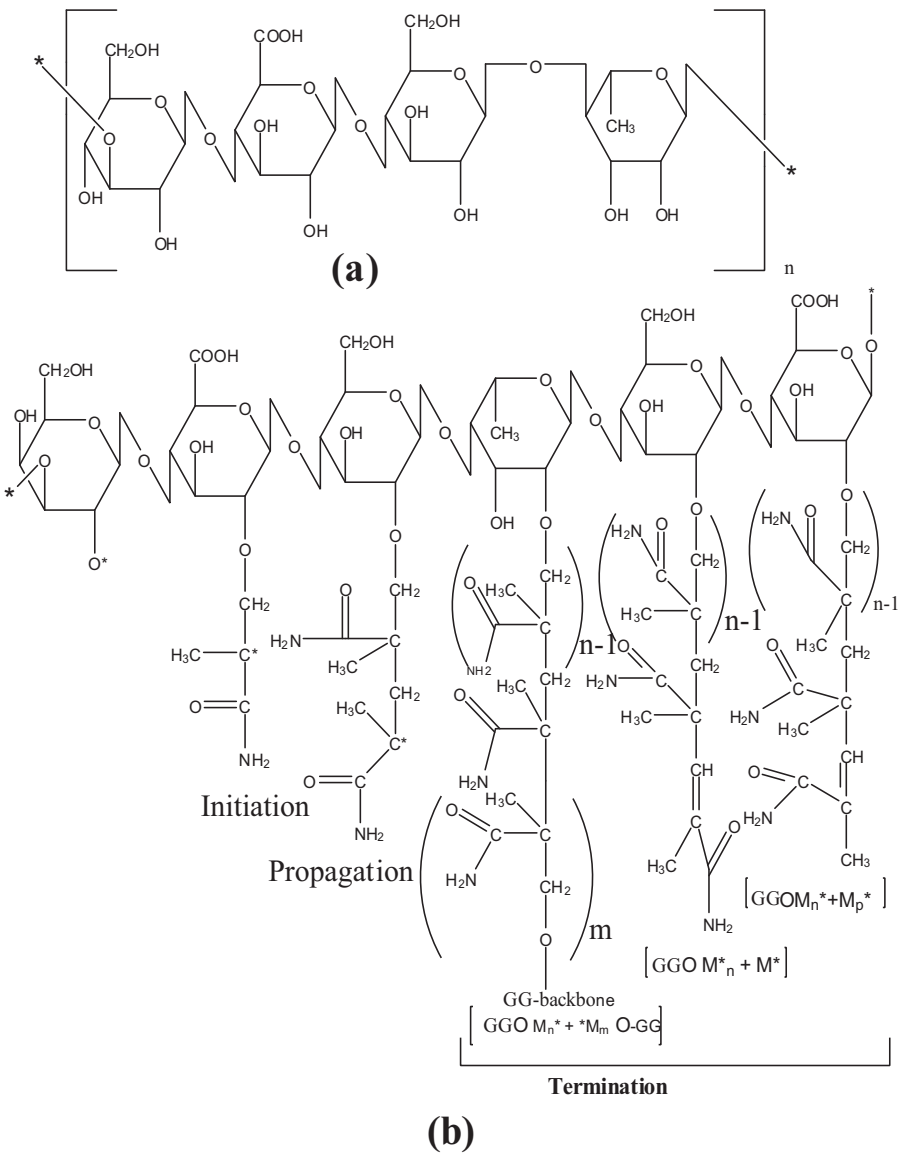

Fig. 1. (a) Structure of gellan gum and (b) polymethacrylamide-grafted-gellan (Pmaa-g-GG).

$$GG{-}OM_n^{\bullet} + M_p^{\bullet} \rightarrow GG{-}OM_{(n+p)} \quad \text{(graftcopolymer)}$$

$$M_p^{\bullet} + M_q^{\bullet} \rightarrow M_{(p+q)} \quad \text{(homopolymer)}$$

(GG—OH = nativegellangum; M = methacrylamide)

3.2. Elemental analysis

The results of elemental analysis for GG and eight different synthetic batches of Pmaa-g-GG are shown in Table 1. There is no nitrogen content in gellan gum. The values of nitrogen percentage in all eight batches of Pmaa-g-GG estimated in the analysis were significant and these values ratify the grafting of methacrylamide onto gellan gum backbone. The higher values of %N in case of S1, S2, S4 and S6 accredit the higher % grafting, indicates that the higher values of methacrylamide and cerric ammonium nitrate have positive influence on % grafting whereas microwave irradiation exerts little negative effect on the yield of the grafted gellan gum. This negative effect of microwave irradiation may result from the breakage of propagated chains on the free radical sites and premature advance termination after an optimum time period during irradiation.

3.3. Infrared spectral analysis

Infrared spectra of gellan gum and grafted gellan gum are shown in Fig. 2(a) and (b) respectively. Gellan gum showed characteristic peaks at 1645.05 cm^{-1} for carbonyl group indicating C=O stretching, at 3212.87 cm^{-1} for —OH group, at 2883.27 cm^{-1} for —COOH group, at 1136.87 cm^{-1} for alcoholic —C—O group, and at 1706.30 cm^{-1} for —C=O group.

Some differences were observed in spectra of grafted gellan gum compared to gellan gum. The infrared spectra of methacrylamide grafted gellan gum shows characteristic peaks at 3829.24–3169.37 cm^{-1} for $-NH_2$ group, due to addition of methacrylamide which was grafted onto gellan gum. An additional peak at 1645.78 cm^{-1} has been observed due to N—H bending. A significant peak is also observed at 1024.59 cm^{-1} for CH—O—CH_2 group which occurs due to grafting reaction between OH group of C_2 of gellan gum and π bond of methacrylamide.

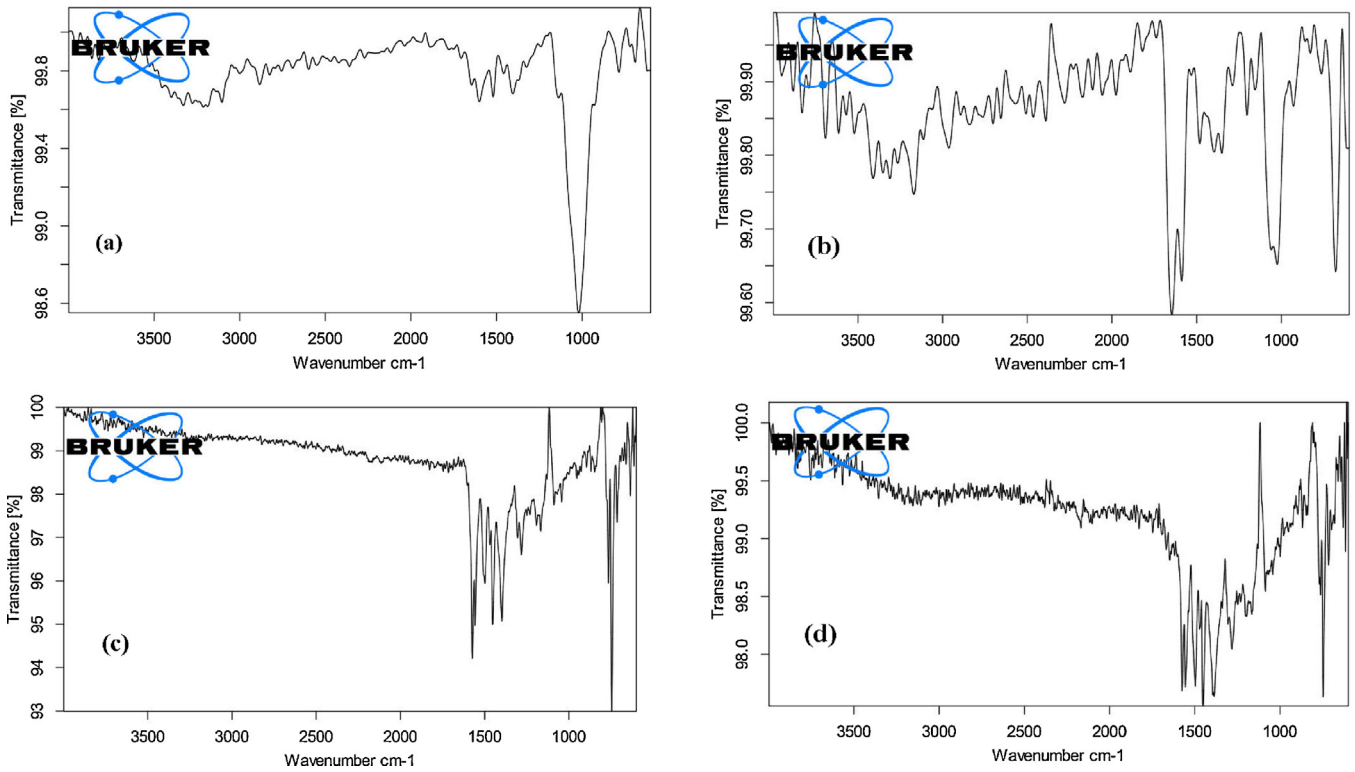

Fig. 2. FTIR spectrum of (a) gellan gum, (b) polymethacrylamide-grafted-gellan (Pmaa-g-GG; S1), (c) diclofenac sodium and (d) tablet formulation (from S1).

Infrared spectra of diclofenac sodium and tablet formulation are shown in Fig. 2(c) and (d) respectively. Diclofenac sodium shows the characteristic peaks at 1573.06 cm^{-1} and 1498.23 cm^{-1} for N—H bending, at 1452.68 cm^{-1} for C—C in aromatic ring. Peaks at 1281.53 cm^{-1} and 1087.97 cm^{-1} indicate C—N stretching and ester C—O group respectively. Peaks at 764.81 cm^{-1} and at 745.82 cm^{-1} indicate C—H bond in aromatic ring and C—Cl stretching respectively. All these peaks have been observed in the infrared spectra obtained from tablet formulation, which demonstrates that there is no significant incompatibility between the drug and the grafted gellan gum.

3.4. Differential scanning calorimetry and thermogravimetric analysis

DSC and TGA curves of GG, Pmaa-g-GG, diclofenac sodium and tablet formulation are shown in Fig. 3(a), (b), (c) and (d) respectively. An endothermic peak at 70 °C and an exothermic peak at around 255 °C are recorded in DSC thermogram of GG. TGA thermogram of GG shows a 10% weight loss at 70 °C and about 45% weight loss in the temperature range from 240 °C to 300 °C. The correlation between endothermic peak and simultaneous reduction in weight at 70 °C indicates the loss in moisture present in the gellan gum. The exothermic peak at 255 °C and reduction in weight in the temperature range from 240 °C to 300 °C is probably due to depolymerization with formation of water, carbon monoxide and methane [31]. DSC thermogram of Pmaa-g-GG shows an endothermic peak at 70 °C similarly with GG indicating loss in moisture content, which is further established by the 10% reduction in weight at 70 °C observed in corresponding TGA curve. Another endothermic peak is recorded at 280 °C, which may be due to polymeric chain degradation of the grafted polymers. This fact proves the enhanced thermal stability of the grafted gellan gum compared to its native form because grafted gellan gum undergoes thermal decomposition at 280 °C unlike its native form which degrades at 255 °C. The specific endothermic peak at 280 °C observed in DSC curve for grafted polymer also demonstrates its crystalline nature.

An endothermic peak at 285.73 °C and an exothermic peak at 310 °C have been seen in DSC thermogram of diclofenac sodium, which indicates melting and subsequent thermal degradation respectively. Approximately 40% weight loss in the temperature range from 290 °C to 340 °C substantiates the thermal degradation of diclofenac sodium in the aforesaid temperature range. Two endothermic peaks at 60 °C and 270 °C observed in DSC curve for tablet formulation demonstrate moisture loss and melting point of diclofenac respectively. The significant change in melting point of drug in the formulation may be due to dilution effect in presence of other excipients.

3.5. Acute oral toxicity study

The results are shown in Table 2. There was no mortality found within the observation period of 14 days after dosing. As per the "Organization of Economic Co-operation and Development (OECD) guideline for the test of chemicals" 425, adopted "17 December 2001" Annexure-4, the LD_{50} value is greater than 2000 mg/kg dose of Pmaa-g-GG. As per the globally harmonized system (GHS) if LD_{50}

Table 2
Mortality rate of animals after a single dose of 2000 mg/kg body weight.

Observation time period	Mortality				
	$Animal_1$	$Animal_2$	$Animal_3$	$Animal_4$	$Animal_5$
30 min	0	0	0	0	0
4 h	0	0	0	0	0
1st day	0	0	0	0	0
3rd day	0	0	0	0	0
7th day	0	0	0	0	0
14th day	0	0	0	0	0

'0', survival and 'X', death.

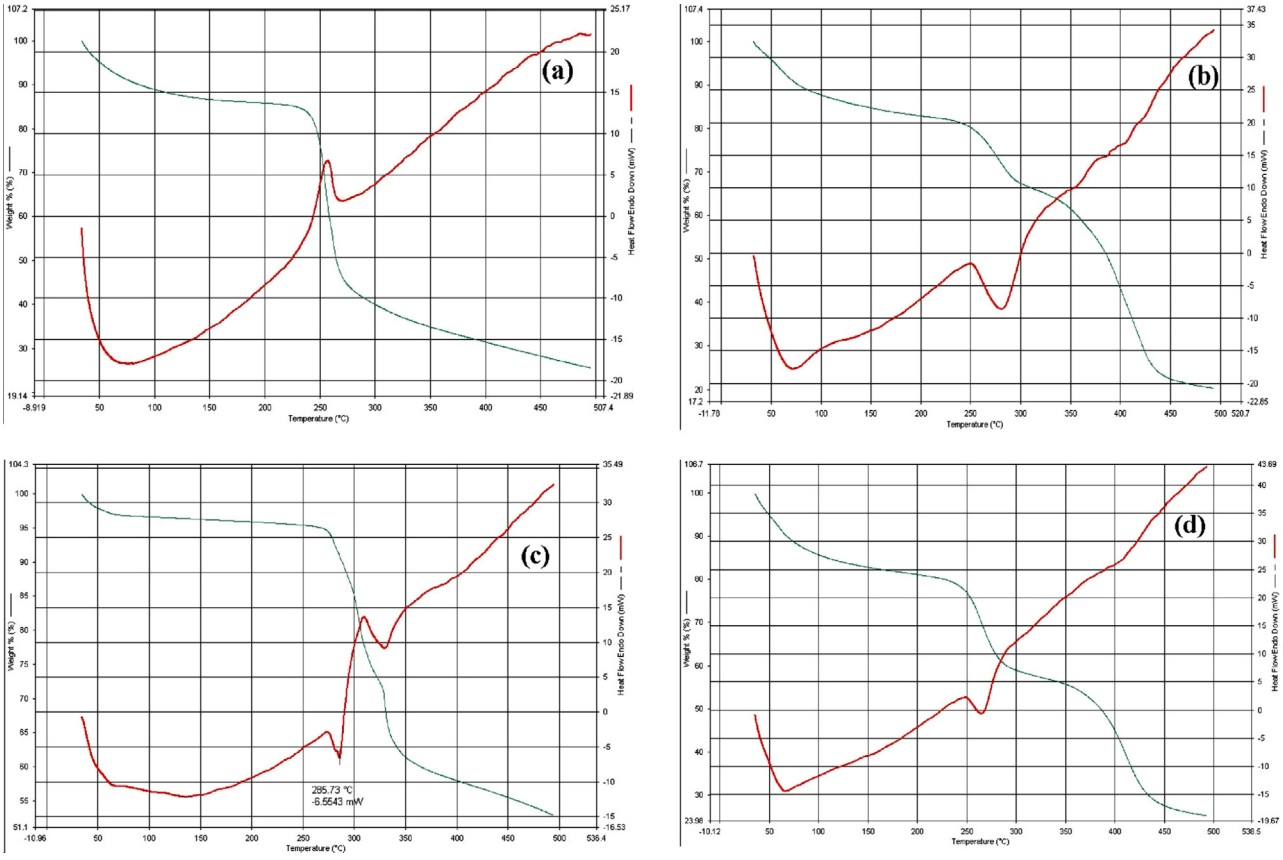

Fig. 3. DSC thermogram of (a) gellan gum, (b) polymethacrylamide-grafted-gellan (Pmaa-g-GG), (c) diclofenac sodium and (d) tablet formulation (S1).

value is greater than the 2000 mg/kg dose then the test product will be fallen under the "Category 5" and toxicity rating will be "zero". So, Pmaa-g-GG is under the "category 5" as well as toxicity rating is "zero".

3.5.1. Histopathological study

The 40× micrographs of various organs of control and test animals are shown in the Fig. 4. The micrographs of both control and test brain depict morphologically similar granular cells. There is no significant change in morphology of stratified squamous epithelial cells observed in the micrographs of control and test stomach. Both lung micrographs show alveoli, inter-alveolar septa and connective tissue sheets containing capillary bed clearly without sign of any type of morphological change. The micrograph of control heart provides an overview of cardiac myocytes having a centrally located nucleus, intercalated disks that connect the end of the one cardiac myocyte to the beginning of the next and perkinje fibers. Similar morphological pattern was shown in the micrograph of test heart. 40× micrographs of both control and test kidney show in increasing detail the cuboidal epithelial cells of the loop of Henle and collecting tubules with similar morphology. Both micrographs of test and control liver depict normal hepatocytes, large polygonal cells with central nuclei and Kuppfer cells. Thus histopathological examination establishes the physiological compatibility of the grafted gellan gum.

3.6. Powder X-ray diffraction

X-ray diffractogram of pure diclofenac sodium and tablet formulation containing drug were represented in Fig. 5. From the diffractogram it can be said that the drug was of crystalline nature in its pure form as well as in tablet because it showed several peaks rather than hump and less noise. The diffractograms portray that the intensities at various 2θ values for pure drug were retained in tablet formulation attributing to the absence of incompatibility between drug and other formulation components.

3.7. In vitro drug release study and release mechanism

The cumulative percentage of drug release (% drug release) versus time curves (zero order profiles) obtained from different formulations is shown in Fig. 6. The curves portray that the release of drug from the monolithic matrix tablet with GG is most rapid (97.5% drug release within 1 h); intermediate in rate (97–100% within 4–5 h) in case of S_3, S_5, S_6, S_7 and S_8 but the rate is seen to be sustained in case of S1, S2 and S4 to a greater extent (80–88% drug release within 8 h). This may be due to the fact that the matrix of the tablets (S3, S5, S6, S7 and S8) is composed of grafted polymers having lower grafting efficiency, thus these less branched network of the polymer leads to rapid water uptake, subsequent swelling and advance network relaxation of the matrix. In case of tablets obtained from S1, S2 and S4, the matrix is composed of comparatively greater branched grafted gellan gum having higher grafting efficiency, which leads to slow water uptake and swelling kinetic resulting sustained drug release over a period of 8 h. The regression coefficient (R^2) values, rate constant (k) from different kinetic models, diffusion exponent (n), $T_{50\%}$ and $T_{90\%}$ are shown in Table 3. The results demonstrate that most of the formulations follow Higuchi and Korsemeyer-Peppas release kinetic. The diffusion exponent (n) values for all the formulations are within the range of 0.436–0.562 thus portending the release mechanism is Case-1 Fickian diffusion or square root of time kinetic based. The lowest values of rate constant (k) of best fitting kinetic models (Higuchi and Korsemeyer-Peppas) resulting from S1, S2 and S4 establish their sustained drug

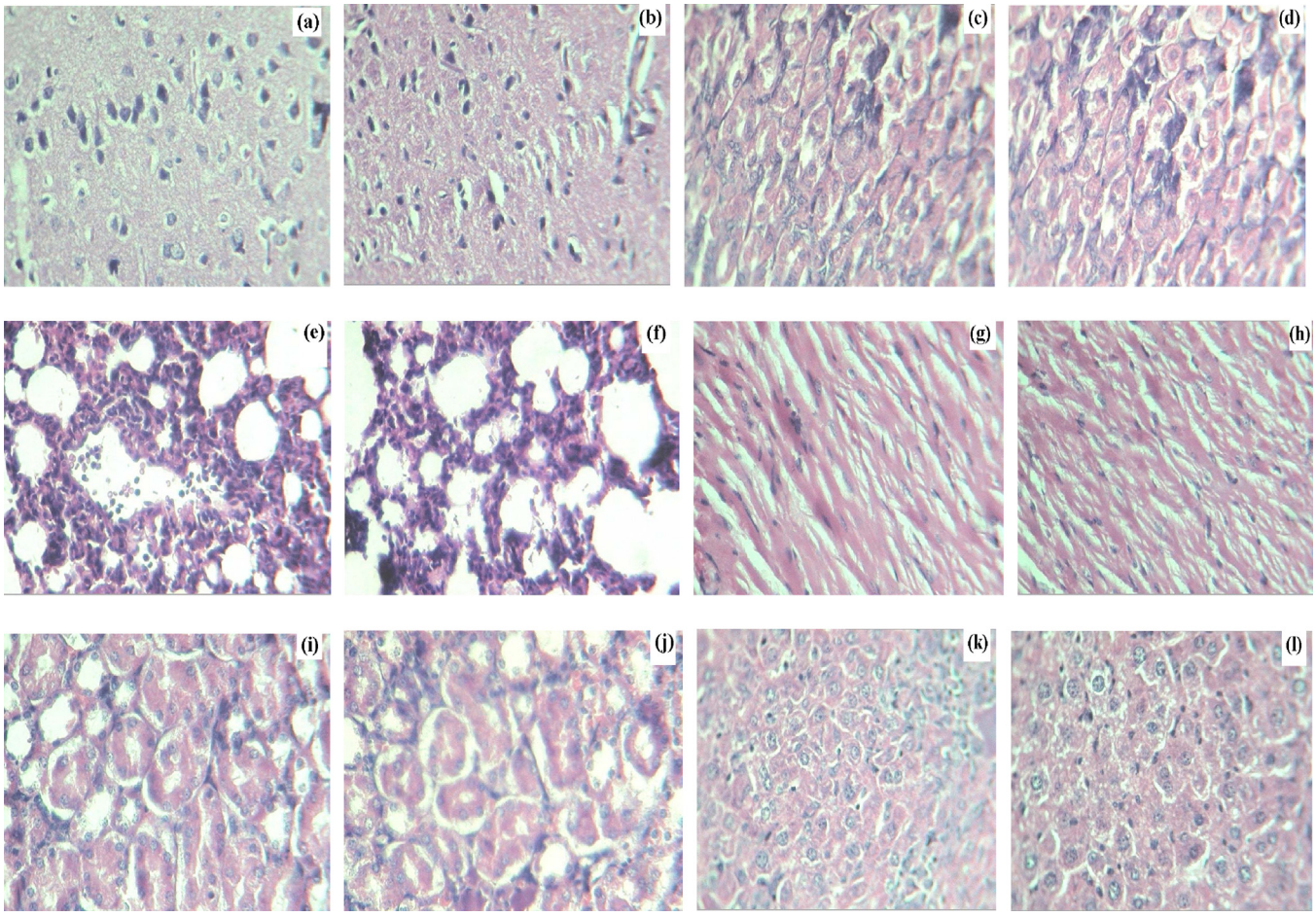

Fig. 4. Microscopic cross-sectional view (40×) of (a) control-brain, (b) test-brain, (c) control-stomach, (d) test-stomach, (e) control-lung, (f) test-lung, (g) control heart, (h) test heart, (i) control-kidney, (j) test-kidney, (k) control liver, and (l) test-liver.

Table 3
Kinetic modeling of release data from different tablet formulations containing gellan and different batches of Pmaa-g-GG, release rate constants and $T_{50\%}$, $T_{90\%}$.

Batch	R^2 value						Rate constant (k)					$T_{50\%}$ (h)	$T_{90\%}$ (h)
	Zero order	First order	Higuchi kinetic	HC	KP		Zero order	First order	Higuchi kinetic	HC	KP		
					R^2	n							
GG	0.734	0.688	0.837	0.876	0.904	0.562	0.363	0.567	0.757	0.443	0.789	0.44	0.95
S1	0.969	0.839	0.999	0.995	0.999	0.552	0.085	0.216	0.293	0.047	0.255	3.31	10.14[a]
S2	0.977	0.869	0.998	0.996	0.998	0.503	0.088	0.201	0.301	0.052	0.291	2.93	9.40[a]
S3	0.908	0.795	0.978	0.997	0.983	0.453	0.150	0.251	0.432	0.148	0.518	0.92	3.15
S4	0.962	0.846	0.999	0.996	0.999	0.488	0.089	0.192	0.309	0.056	0.320	2.49	8.30[a]
S5	0.962	0.845	0.995	0.958	0.989	0.510	0.191	0.342	0.490	0.171	0.495	1.00	3.30
S6	0.945	0.837	0.992	0.907	0.994	0.436	0.127	0.215	0.389	0.155	0.475	1.13	4.33
S7	0.809	0.636	0.911	0.981	0.888	0.533	0.185	0.327	0.497	0.188	0.557	0.65	2.40
S8	0.878	0.739	0.961	0.954	0.958	0.470	0.152	0.255	0.439	0.199	0.524	0.84	3.15

HC, Hixson–Crowell; KP, Korsemeyer Peppas.
[a] Extrapolated value from best fitting kinetic model.

Table 4
Drug release profile comparison: difference factor (f_1) and similarity factor (f_2).

Batch no.	Difference factor (f_1)		Similarity factor (f_2)	
	Comparison with USP release profile	Comparison with S1 batch	Comparison with USP release profile	Comparison with S1 batch
GG	98.7	207.81	13.94	14.14
S1	7.45	0.00	67.47	100.00
S2	4.41	6.92	79.00	72.25
S3	61.65	85.56	25.35	24.18
S4	8.14	15.07	65.86	56.39
S5	59.97	81.67	25.79	24.81
S6	51.24	64.69	29.50	28.21
S7	76.11	113.02	20.53	20.21
S8	65.64	90.21	23.96	22.93

Table 5
Different parameters and their values used in statistical optimization along with optimized value.

Serial no.	Independent variables (synthetic factors)		Response			
	Parameters	Optimized value	Parameters	USP reference release profile	Target value	Predicted value
1.	Methacrylamide(g)	9.94 g	% Grafting (% G)	–	Maxi-mum	666.63
2.	CAN (mg)	399.99 mg	CPR1h	Not more than 28%	Mini-mum below 28%	28.91%
3.	MW irradiation time (min)	1.00 min	CPR2h	20–40%	40%	40.14%
4.	–	–	CPR4h	35–60%	60%	61.41%
5.	–	–	CPR6h	50–80%	75%	74.99%

release potential. Similarly this fact is also substantiated by the resemblance of the higher values of $T_{50\%}$ and $T_{90\%}$ achieved by these three formulations. Dissolution similarity (f_2) and difference factor (f_1) were calculated to compare the release profile of each batch with the release profile of S1 batch and the USP reference release profile (Table 5) and shown in the Table 4. Highest similarity and lowest difference were exhibited by S2 batch.

3.7.1. *Effect of grafting on release parameters: rate-constant, $T_{50\%}$ and $T_{90\%}$*

Fig. 7 depicts the changes in rate constant of best fitting kinetic model (here Koresmeyer-Peppas model), $T_{50\%}$ and $T_{90\%}$ with the changes in % grafting. The curves demonstrate that rate constant decreases with increase in % grafting whereas both of others two parameters increase accordingly indicating slow-release with increment of % grafting. This is also ratified by the slopes of the mathematical relations between release parameters and % grafting expressed in Eqs. (7)–(9):

$$y_1 = -0.004x + 5.894 \ (R^2 = 0.975) \quad (7)$$

$$y_2 = 0.004x + 0.237 \ (R^2 = 0.972) \quad (8)$$

$$y_3 = 0.013x + 1.253 \ (R^2 = 0.979) \quad (9)$$

where y_1, y_2, y_3 and x are (rate constant), $T_{50\%}$, $T_{90\%}$ and % grafting respectively. Higher degree of grafting results a more intensive hydrophobic matrix network (hydrophilic —OH groups of the native gum are involved in the grafting resulting decrease in hydrophilicity and increase in hydrophobicity) which is capable of retarding the drug release.

3.7.2. *Statistical analysis of the dependence of release rate on the synthetic factors*

Mathematical relationship generated by Design-Expert software using 2^3 full factorial design for the studied response variables are expressed in Eq. (10)–(13):

$$\text{CPR1h} = +75.05 - 4.34 * \text{Maa} - 0.007 * \text{CAN} + 6.72 * \text{MW} - 0.017 * \text{CAN} * \text{MW} \ (R^2 = 0.971) \quad (10)$$

$$\text{CPR2h} = +93.18 - 4.87 * \text{Maa} - 0.012 * \text{CAN} + 7.19 * \text{MW} - 0.017 * \text{CAN} * \text{MW} \ (R^2 = 0.9406) \quad (11)$$

$$\text{CPR4h} = +139.67 - 5.59 * \text{Maa} - 0.057 * \text{CAN} \ (R^2 = 0.7187) \quad (12)$$

$$\text{CPR6h} = +130.49 - 4.17 * \text{Maa} - 0.035 * \text{CAN} \ (R^2 = 0.7007) \quad (13)$$

where CPR1h, CPR2h, CPR4h and CPR6h are cumulative drug release at 1, 2, 4 and 6 h respectively.

All the models and the interaction terms were significant as the probability values in all cases were less than 0.05.

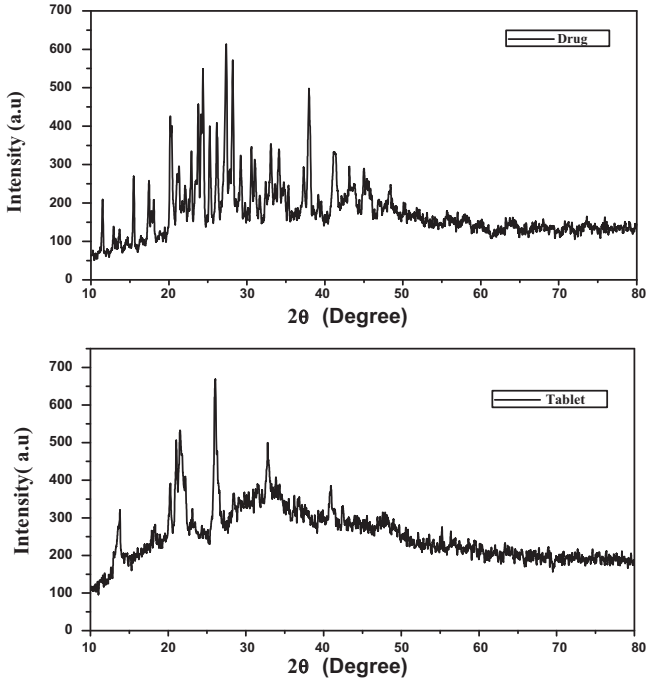

Fig. 5. X-ray diffractogram of pure drug (diclofenac sodium) and tablet formulation (S1).

3.8. *Optimization of synthetic condition*

The optimized synthetic condition with highest desirability (predicted $R^2 = 0.978$) among 69 solutions generated from the numerical optimization using the software and the predicted value of the responses are shown in Table 5. The optimized synthetic condition and predicted value of the responses are shown to be very closer to that of S1 batch. Therefore, in this

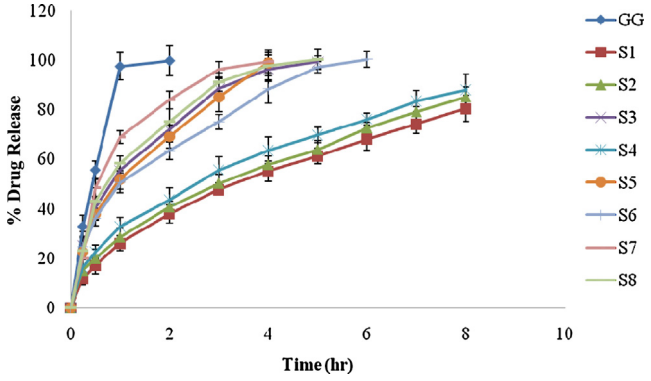

Fig. 6. Release profile (cumulative % release ± SD, $n = 3$) of diclofenac sodium from the tablet formulations containing gellan (GG) and different batches of Pmaa-g-GG (S1–S8).

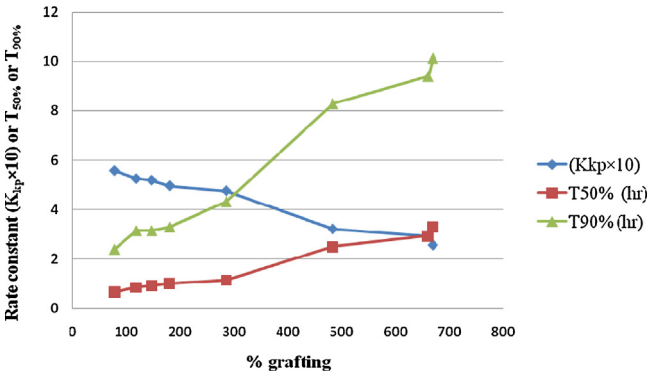

Fig. 7. Different drug release rate parameters versus % grafting curves.

study, S1 can be considered as the best optimized copolymer of polymethacrylamide and gellan gum.

4. Conclusion

Methacrylamide grafted gellan gum (Pmaa-g-GG) was synthesized using microwave-promoted cerric (IV) ion initiated graft copolymerization method. The synthetic conditions were studied by varying three independent process variables: amount of CAN, amount of methacrylamide and microwave irradiation time. Higher levels of CAN and methacrylamide had given higher yield whereas an optimum microwave irradiation time has been seen to be required for higher grafting efficiency. The grafting of methacrylamide onto gellan gum was evidenced by FTIR and elemental analysis. DSC study of the grafted gellan gum revealed its enhanced thermal stability compared to its native form. The monomer (methacrylamide) is toxic in nature but from the toxicity study and histopathological examination in mice it is exhibited that there is no morbidity and histopathological sign in the photomicrograph of different organs at a dose of 2000 mg/kg body weight of Pmaa-g-GG. Sustained release tablet of water soluble drug diclofenac sodium was formulated using the grafted gellan gum as a rate controlling polymer. It exhibited its sustained release potential over a period of 8 h and the release profile followed Higuchi square root kinetic model. The release mechanism was governed by Fickian diffusion. FTIR and XRD studies of drug and grafted gellan gum were carried out to establish compatibility between drug and modified polymer. Thus, microwave-promoted cerric (IV) initiated graft copolymerization is an easy, efficient, less time consuming, reproducible and one-pot synthesis method for the development of graft copolymer which can be fabricated as sustained release polymer in a desired sustained-release drug delivery device.

Conflict of interest

The authors report no conflicts of interest. The authors alone are responsible for the content and writing of the article.

Acknowledgements

The authors acknowledge IICB, Kolkata for CHN analysis, Bengal School of Technology, Chinsura, Hooghly, West Bengal, India for FTIR study, IACS, Kolkata for PXRD study. The authors are also thankful to Deptt. of Pharmaceutical Technology, Jadavpur University, Kolkata, India and the authority of BCDA College of Pharmacy and Technology, Kolkata, India for providing necessary facilities for this work.

References

[1] M. Efentakis, A. Kouttis, Pharm. Dev. Technol. 6 (2001) 91.
[2] V. Vijan, S. Kaity, S. Biswas, J. Isaac, A. Ghosh, Carbohydr. Polym. 90 (2012) 496–506.
[3] K.S. Soppimath, T.M. Aminabhavi, A.M. Dave, S.G. Kumbar, W.E. Rudzinski, Drug Dev. Ind. Pharm. 28 (2002) 957–974.
[4] M.V. Velasco, A. Munoz, M.R. Jimenez-Castellanos, I. Castellano, I. Goni, M. Gurruchaga, Int. J. Pharm. 136 (1996) 107–115.
[5] A. Bhattacharya, B.N. Misra, Progr. Polym. Sci. 29 (2004) 767–814.
[6] V. Singh, D.N. Tripathy, A. Tiwari, R. Sanghi, Carbohydr. Polym. 65 (2006) 35–41.
[7] A. Tiwari, V. Singh, Carbohydr. Polym. 74 (2008) 427–434.
[8] A.V. Singh, L.K. Nath, Int. J. Biol. Macromol. 60 (2013) 62–68.
[9] Y. Nitta, Nishinari, Int. J. Biol. Macromol. 5 (2005) 47–52.
[10] M. Narkar, P. Sher, A. Pawar, AAPS PharmSciTech 11 (2010) 267–277.
[11] S.A. Agnihotri, T.M. Aminabhavi, Drug Dev. Ind. Pharm. 31 (2005) 491–503.
[12] M.O. Emeje, P.I. Franklin-Ude, S.I. Ofoefule, Int. J. Biol. Macromol. 47 (2010) 158–163.
[13] D.P. Shah, G.K. Jani, ARS Pharm. 51 (2010) 28–40.
[14] J. Balasubramaniam, S. Kant, J.K. Pandit, Acta Pharm. 53 (2003) 251–261.
[15] L. Yeujiang, L. Jinpeng, Z. Xiaolin, Z. Ruodan, H. Yongliang, W. Chunjie, AAPS PharmSciTech 11 (2010) 610–620.
[16] J.V. Willis, M.J. Kendall, R.M. Flinn, D.P. Thornhill, P.G. Welling, Eur. J. Clin. Pharmacol. 16 (1979) 405–410.
[17] V.D. Athawale, V. Lele, Carbohydr. Polym. 35 (1998) 21–27.
[18] C.G. Varelas, D.G. Dixon, C. Steiner, J. Control. Release 34 (1995) 185–192.
[19] M. Gibaldi, S. Feldman, J. Pharm. Sci. 56 (1967) 1238–1242.
[20] T. Higuchi, J. Pharm. Sci. 52 (1963) 1145–1149.
[21] P.J. Niebergall, G. Milosovich, J.E. Goyan, J. Pharm. Sci. 52 (1963) 236–241.
[22] R.W. Korsmeyer, R. Gurny, E.M. Doelker, P. Buri, N.A. Peppas, Int. J. Pharm. 15 (1983) 25–35.
[23] S.J. Desai, P. Singh, A.P. Simonelli, W.I. Higuchi, J. Pharm. Sci. 55 (1966) 1230–1234.
[24] S.J. Desai, P. Singh, A.P. Simonelli, W.I. Higuchi, J. Pharm. Sci. 55 (1966) 1235–1239.
[25] N.A. Peppas, Pharm. Acta Helv. 60 (1985) 110–111.
[26] P. Costa, J.M.S. Lobo, Eur. J. Pharm. Sci. 13 (2001) 123–133.
[27] A. Mishra, S. Pal, Carbohydr. Polym. 68 (2007) 95–100.
[28] M.M. Fares, S.M. Assaf, Y.M. Abul-Haija, J. Appl. Polym. Sci. 117 (2010) 1945–1954.
[29] V. Singh, P.L. Kumari, A. Tiwari, S. Pandey, J. Appl. Polym. Sci. 117 (2010) 3630–3638.
[30] A.A. Anthony, J.N. Obichukwu, Acta Pharm. 57 (2007) 161–171.
[31] M.J. Zohuriaan, F. Shokrolahi, Polym. Test. 23 (2004) 575–579.